PROCESSES CONTROLLING CARBON DIOXIDE IN SEAWATER

A DISSERTATION SUBMITTED TO THE GRADUATE DIVISION OF THE
UNIVERSITY OF HAWAII
IN PARTIAL FULFILLMENT OF THE
REQUIREMENTS FOR THE DEGREE OF

DOCTOR OF PHILOSOPHY

IN

OCEANOGRAPHY

May 2002

By

Christopher J. Carrillo

Dissertation Committee:

David M. Karl, Chairperson
Claudia Benitez-Nelson
Edward Laws
Fred Mackenzie
Chris Measures
Edward Ruby

We certify that we have read this dissertation and that, in our opinion, it is satisfactory in scope and quality as a dissertation for the degree of Doctor of Philosophy in Oceanography.

DISSERTATION COMMITTEE

_____

Chairperson

_____

_____

_____

_____

_____

ACKNOWLEDGMENTS

I would like to thank my advisor and committee chair, Dave Karl, Fred Mackenzie, Chris Measures, Ed Laws, Ned Ruby and Claudia Benitez-Nelson for teaching me the art of science. Science is the art of promoting one's own view about perceived truths. Holgar Jannasch (1997) states in Annual Review of Microbiology, "A general distrust of scientists, who have been trained to be guided by their own judgment and priorities, and the suggestion that they become activists. The effect is worse on younger scientists, who are not rewarded for tackling a problem with perseverance, but for hopping from one promising or prioritized subject to another; funding not science being the ultimate goal" (Jannasch 1997). I would like to thank my advisor, Dave Karl for supporting me during the past 7 years and allowing me to pursue my own scientific curiosities.

I would especially like to thank Ron Ogata for giving me my first job in science and turning it into a career. Working was a pleasurable pastime in between my undergraduate classes. I would also like to thank Joris Gieskes for introducing me to the concepts of marine chemistry during my first graduate school class at Scripps Institute of Oceanography. His class taught me how to apply chemistry to the marine environment. The B grade I earned in the class with the comment, " You could have done better" became a motto to live by. And yes, I could have done better.

Many thanks are due to all Palmer Long Term Ecological Research project participants, principal investigators and the captains and crew of the R/V Polar Duke, R/V Laurence M. Gould and the RVIB Nathaniel B. Palmer. These people made the science and all of the hard work enjoyable. Most of the work could not have been accomplished without the help and support of dedicated personal of Antarctic Support

Associates, Raytheon Polar Support and AGUNSA based in Chile. The people who collected and shipped the samples back to Hawaii included Jim Christian, John Dore, Dale Hebel, Dan Sadler, Terry Houlihan, Karin Bjorkman, Dave Karl, Ricardo Letelier, and Georgia Tien. The members of the HOT/COLD group helped in a variety of ways including sample and data analysis. These people included Albert Coleman, Lance Fujieki, Lisa Lum, Ursula Magaard, and Luis Tupas. I appreciate the many CO_2 discussions with former and present students, especially Angie Thomson-Bulldis and Matt Church.

Finally, I would like to thank my family and friends for their personal support. M.J. Pombrakas took care of many bills while I was away on research cruises. My sisters and parents were always there for support. The Thursday night beer/pizza crowd was invaluable in keeping me sane throughout this long period. Financial support for this research was provided by National Science Foundation Grant DPP88-18899 to D. Karl.

ABSTRACT

The oceanic inventory of inorganic carbon is predicted to increase in response to rising atmospheric carbon dioxide (CO_2) concentrations, but the rate is a function of poorly understood interactions of physical, chemical and biological processes. More then half of the CO_2 released by the burning of fossil fuels has been absorbed by the terrestrial and oceanic ecosystems. The mechanisms responsible for these “sinks” are only partially understood and have been observed to vary year to year. With increasing surface ocean CO_2 concentrations, it becomes imperative to understand the CO_2 solution chemistry in seawater and the effect of processes that alter inorganic carbon speciation.

Although the solution chemistry of carbon dioxide (CO_2) in seawater has been extensively studied during the past century, many questions still persist regarding the ecological understanding of the observed variability of the measured CO_2 parameters; pH, fugacity of CO_2 (fCO_2), dissolved inorganic carbon (DIC) and total alkalinity (TA). At equilibrium, these four measurable parameters combined with the proper apparent equilibrium constants for carbonic acid in seawater describe the speciation concentrations of dissolved aqueous CO_2 (CO_2*(aq)), bicarbonate (HCO_3^-) and carbonate (CO_3^{2-}). The observed variability of the measured CO_2 parameters within the environment must be interpreted within the proper framework of assumptions relating the solution chemistry to the physical, chemical and biological processes that alter CO_2 concentrations. This requires a cross disciplinary understanding of the effects of biology and physics on the CO_2 solution chemistry in seawater.

Photosynthesis alters seawater CO_2 chemistry by reducing dissolved aqueous CO_2 to organic matter. This results in a decrease of fCO_2 pressure and DIC concentration. Temperature alters seawater CO_2 chemistry through changes of the equilibrium constants that determine the partitioning of the inorganic carbon species; dissolved aqueous CO_2, bicarbonate and carbonate. The interaction of these two processes on timescales of seconds to years is a major theme of this dissertation. Additionally, the timescale of exchange for CO_2 across an atmosphere-seawater interface can greatly influence the interpretation of observations within natural settings.

The interaction of these processes was studied in three contrasting systems to illustrate the similarities and differences of the interactionsd, and to reveal an unexpected complexity. For instance, the observed decrease of normalized DIC (to a salinity of 35) at Station ALOHA within the North Pacific Subtropical Gyre was the result of the thermodynamic control on the solution chemistry of CO_2 in seawater. In the region west of the Antarctic Peninsula, CO_2 dynamics were a function of temperature changes and dilution due to ice melt, as well as net photosynthesis. Finally, CO_2 chemistry was studied in a temperature-controlled continuous culture. Many results from such studies are applied to open ocean process yet these studies may be flawed because of improper assumptions concerning gas-solution equilibrium and thermodynamic equilibrium.

TABLE OF CONTENTS

LIST OF TABLES

LIST OF FIGURES

CHAPTER I

INTRODUCTION AND RATIONALE

Background

Anthropogenic carbon dioxide (CO_2) in the atmosphere has increased as a result of human-induced changes in global land use and the burning of fossil fuels (Houghton et al. 1987; Marland et al 1994; Sarmiento and Wofsy 1999). The effects of increasing atmospheric CO_2 on the global environment are unknown, but models suggest possible changes in ocean circulation, oceanic primary production and species composition, and widespread changes in global climate (Toggweiler and Sarmiento 1985; Wenk and Siegenthaler 1985; Broecker et al. 1989; Hein and Sand-Jensen 1997). Although the combined oceanic and terrestrial ecosystems have responded by absorbing more then half of the CO_2 released into the atmosphere, the individual mechanisms responsible for absorbing CO_2 are neither well quantified nor understood. Ocean models predict that the rise in atmospheric CO_2 should produce a corresponding increase in surface ocean CO_2 concentrations, but validation of this prediction is often difficult because of natural variability within the oceanic ecosystem and lack of time series data sets (Brewer 1983; Lee et al. 1998; Fancey et al. 1995).

The ocean's role in moderating increasing atmospheric CO_2 levels is uncertain and stems from the inability to constrain and predict the ocean's capacity to absorb CO_2. The ocean's capacity to sequester CO_2 is dependent on the response of the biological (soft tissue and carbonate) and solubility pump processes in altering CO_2 concentrations in the surface ocean (Volk and Hoffert 1985). Accurate estimations of CO_2 within appropriate physical, chemical and biological gradients in a variety of key habitats,

coupled with an understanding of the processes that control these gradients will be required to model ocean and ocean-atmospheric processes. Variability associated with small spatial scales and short temporal scales can give biased estimates when extrapolated to larger areas. Appropriate temporal resolution of these mesoscale processes is needed to lower uncertainties. Consequently, knowledge of the spatial and temporal distributions of the strength and efficiency of each pump is needed to fully understand the ocean's response to increasing atmospheric CO_2 levels.

The North Pacific Subtropical Gyre (NPSG) and Southern Ocean represent two of the largest ecosystems on the globe. The NPSG comprises a surface area of approximately $2x10^7$ km^2 and extends from approximately 15º to 35º N latitude and 135º E to 135º W longitude (Karl 1999). The Southern Ocean comprises an even larger surface area of $7.7x10^7$ km^2 and includes all waters south of 60º South latitude (Tomczak and Godfrey 1994). Both ecosystems are characterized by continuous circulation features (gyre and circumpolar), which isolate them from adjacent habitats. Both regions also have established time-series sites, which have been making high quality measurements of physical, chemical and biological parameters during seasonal and annual time scales.

The U.S. Joint Global Ocean Flux Study-Hawaii Ocean Time-series (JGOFS-HOT) program was established in 1988 as a multi-disciplinary ocean research initiative (Karl and Lukas 1996). The HOT program core measurement component has been making repeat hydrographic, chemical and biological measurements at Station ALOHA (A Long-term Oligotrophic Habitat Assessment) located at 22º 45´ N , 158º W, approximately 100 km north of Oahu, Hawaii. Since October 1988, cruises have been conducted on approximately monthly time scales, each cruise lasting 4 to 5 days. Station

ALOHA is located in deep water (4800 meters), and sampling is restricted to a circle with a 6 nautical mile radius. Specific objectives of the HOT program conform to the goals of U.S. JGOFS and include "measure the time varying concentrations of carbon dioxide in the upper water column and estimate the annual air-to-sea gas flux" (Karl and Lukas 1996).

The Palmer Long-Term Ecological Research (LTER) Program was established in 1990 to study the physical determinants on the Antarctic marine ecosystem (Smith et al. 1995). One component of this multi-disciplinary project is entitled "Microbiology and carbon flux" (D. Karl P.I.), and includes measurements of C and O inventories (dissolved gases and solutes), C and O fluxes (production, particle export and air-to-sea gas exchange) and microbial community structure and function (Karl et al. 1996). The central tenet of the LTER program is that the annual advance and retreat of sea ice is a major physical determinant of spatial and temporal changes in the structure and function of the Antarctic marine ecosystem, from total annual primary production to breeding successes in seabirds (Smith et al. 1995). The LTER grid located off the Antarctic Peninsula covers an area 900 by 200 kilometers (Waters and Smith 1992). This grid, or a portion of it, was sampled once per year during the austral summer (January-February). Additional cruises with specific goals of studying seasonal variations generated by ice processes were conducted during the months of March, June-July and August. A smaller grid, located in Arthur Harbor, is sampled approximately four times throughout each cruise, and other selected coastal stations include Marguerite Bay and Crystal Sound.

Carbon Dioxide Chemistry of Seawater

Inorganic Carbon Speciation

Carbon dioxide gas dissolved in seawater reacts with water to form carbonic acid (H_2CO_3), which is then ionized to bicarbonate (HCO_3^-) and carbonate (CO_3^{2-}).

$$CO_2(g) \leftrightarrow CO_2(aq) \quad (1)$$

$$CO_2(aq) + H_2O \leftrightarrow H_2CO_3 \quad (2)$$

$$H_2CO_3 \leftrightarrow H^+ + HCO_3^- \quad (3)$$

$$HCO_3^- \leftrightarrow H^+ + CO_3^{2-} \quad (4)$$

The notation (g) and (aq) refer to the state of the species as a gas or aqueous solute. $CO_2(aq)$ and H_2CO_3 are combined and expressed as the sum of a hypothetical species labeled $CO_2^*(aq)$ (Department of Energy 1994).

$$CO_2(g) \leftrightarrow CO_2^*(aq) \quad (5)$$

$$CO_2^*(aq) + H_2O \leftrightarrow H^+ + HCO_3^- \quad (6)$$

These reactions can be rewritten in terms of their equilibrium constants:

$$Ko = [CO_2^*(aq)] / CO_2(g) \quad (7)$$

$$K_1 = [H^+][HCO_3^-] / [CO_2^*(aq)] \quad (8)$$

$$K_2 = [H^+][CO_3^{2-}] / [HCO_3^-] \quad (9)$$

Measured Parameters of the Inorganic Carbon System

Within this dissertation, a distinction is made between the carbon species ($CO_2(g)$, $CO_2^*(aq)$, HCO_3^- and CO_3^{2-}) and the "measured" carbon system parameters. They are not

the same except for $CO_2(g)$. Of the four CO_2 species ($CO_2(g)$, CO_2*(aq), HCO_3^- and CO_3^{2-}), only $CO_2(g)$ can be measured directly. The remaining three species must be determined by measuring at least two of four interdependent measurable parameters; total alkalinity (TA), dissolved inorganic carbon (DIC), pH and the fugacity of CO_2 (fCO_2). These four measurable parameters characterize the inorganic carbon system in seawater. A complete description of the inorganic carbon speciation in seawater can, in theory, be obtained with any two carbon parameters, if the appropriate apparent thermodynamic equilibrium constants, temperature, salinity, phosphate and silicate concentrations are also known. Ideally, with an accurate set of measurements and proper apparent thermodynamic constants, only two of the four carbon system parameters should be needed to accurately describe the carbon system at equilibrium. When all four parameters are measured, the thermodynamic relationships describing CO_2 dissolved in seawater can be solved, including the determination of the appropriate set of apparent dissociation constants (K_1 and K_2) for carbonic acid. Or the relative accuracy of each parameter can be determined by solving the thermodynamic relationships using the first and second apparent dissociation constants (K_1 and K_2) for carbonic acid in seawater.

The measurable parameters of the CO_2 system are not direct determinations of the actual carbon speciation except for $CO_2(g)$. $CO_2(g)$ is expressed within this dissertation as a mole fraction, partial pressure and fugacity. The mole fraction is defined as the number of moles of a given substance divided by the total number of moles of all substances. The partial pressure of CO_2 is determined from the mole fraction of CO_2 multiplied by the total atmospheric pressure. It has units of pressure, and within this dissertation the partial pressure and fugacity will be presented in units of μatm. The

fugacity of CO_2 (fCO_2) corrects for the non-ideal nature of the partial pressure of CO_2 (pCO_2) in seawater. Technically the fugacity of CO_2 should be used when calculating CO_2 system parameters, but realistically, it is numerically very close to values of pCO_2; the difference is approximately ± 0.3%. In this dissertation, fCO2 and pCO2 will be assumed to be identical.

$$pCO_2 = X(CO_2)P_{total} \quad (10)$$

$X(CO_2)$ = mole fraction of CO_2 ($\mu M\ M^{-1}$)

P_{total} = Total atmospheric pressure (μatm)

Total alkalinity (TA) of seawater is defined as "the number of moles of hydrogen ion equivalent to the excess of proton acceptors (bases formed from weak acids with a dissociation constant $K \leq 10^{-4.5}$ at 25 °C and zero ionic strength) over proton donors (acids with $K > 10^{-4.5}$) in one kilogram of sample" (Dickson 1981, Rakstraw 1949, Department of Energy 1998). In seawater, the model of TA is defined as:

$$TA=[HCO_3^-]+2[CO_3^{2-}]+[B(OH)_4^-]+[OH^-]+[HPO_4^{2-}]+2[PO_4^{3-}]+[SiO(OH)_3^-]-[H^+]-[HSO_4^-]-[HF]-[H_3PO_4]-\ldots \quad (11)$$

This model may change depending on the chemical constituents and concentrations. For example, within anoxic waters, the concentrations of NH_3^+ and HS may be high enough that they should not be neglected in the representation of seawater.

The pH of seawater is a master variable describing the thermodynamic state of the acid-base equilibria and is defined by three different scales. A review of pH scales and measurements is far beyond the scope of this paragraph and is "one of the more confused areas of marine research" (Dickson 1984). It is important to define a pH scale for

measurements or calculations, and readers are referred to more comprehensive reviews of this subject by Dickson (1984), Dickson (1993) and Culberson (1981). Within this dissertation, pH is defined on the total scale where:

$$[H^+]= [H^+]_F (1+ S_T/Ks) \quad (12)$$

$[H^+]_F$ = Free concentration of hydrogen ion in seawater

S_T = Total sulfate concentration

Ks = Acid dissociation constant for $[HSO_4^-]$

$$=[H^+]_F + [HSO_4^-] \quad (13)$$

The pH is then defined as the negative of the base 10 logarithm of the hydrogen ion concentration:

$$pH = -\log([H^+]) \quad (14)$$

Dissolved inorganic carbon (DIC) is also referred to as total CO_2 (TCO_2 or $\sum CO_2$). During the time that it took to complete this dissertation, many arguments were heard for and against the use of both (DIC versus total CO_2), one or the other term. At this point in time, this author does not care which term is used to describe inorganic solution chemistry in seawater. It is more important to understand the definition and the application. DIC, TCO_2 or $\sum CO_2$ is a measure of the sum of aqueous $[CO_2^*(aq)]$, $[HCO_3^-]$ and $[CO_3^{2-}]$. Generally, I will use the term DIC throughout this dissertation.

$$DIC=[CO_2^*(aq)]+[HCO_3^-]+[CO_3^{2-}] \quad (15)$$

<u>Apparent Equilibrium Constants of the Inorganic Carbon System</u>

There are six sets of measured apparent dissociation constants for carbonic acid in seawater creating a plethora of conflicting discrepancies between the carbon system parameters. Unfortunately, a consensus regarding the proper set of apparent dissociation constants seems unlikely at this time. The determination of the thermodynamic dissociation constants in seawater requires that the activity coefficients of single ions be known. Since these activity coefficients are functions of poorly known ion association, the "true" dissociation constants cannot be determined. Assuming the ion associations are invariable for all types of seawater, the "apparent" thermodynamic dissociation constants can be determined on a representative sample of seawater and applied to all oceanic seawater types. Therefore, if these assumptions are correct, then a single function should relate the apparent thermodynamic dissociation constant in seawater at all temperatures and salinities.

The study of carbonate chemistry in natural waters dates back to the late 19th century. The estimation of carbonic acid in natural waters was determined by titration using indicator dyes (Seyler 1897). Many of the same analytical questions plaguing interpretation of results and cross calibrations encountered then are still valid today. By the early 20th century, a quantitative description of CO_2 had been achieved (Johnston 1916). Buch et al. (1932), and Buch (1938) made the first "modern" determinations of the apparent dissociation constants more than seven decades ago. Since then, "subsequent work on the solution equilibria of the carbon dioxide system in seawater has introduced essentially no new concepts, but has greatly improved the data" (Gieskes 1973).

Approximately five independent measurements have been made since Buch (1932) with the latest by Roy et al. (1993, 1994, 1996); see also (Lyman, 1956; Hansson,

1973; Mehrbach et al., 1973; Goyet and Poisson, 1989). Numerous other determinations have been published based on these five independent data sets by correcting for differences in pH scales (Edmond and Gieskes, 1970; Dickson and Millero, 1987; Lee et al., 1997; Lueker et al., 2000).

Table 1.1 Measurement studies of the apparent constants for the inorganic carbon system in seawater.

Study	Year	Electrode Type	Seawater Type
Buch	1933	Hg/Pt	Natural
Lymann	1956	Glass	Natural
Hannson	1973	Glass	Artificial
Mehrbach	1973	Glass	Natural
Goyet	1989	Glass	Artificial
Roy	1993	H_2	Artificial

Since the first measurements of these apparent thermodynamic constants, a number of field and laboratory studies have investigated the combination of measured parameters and thermodynamic constants that yield the most accurate internal consistency (Table 1.2). Several of these published papers are contradictory, making it difficult for others to reach any reliable conclusions to be adopted on which set of apparent thermodynamic constants should be used. Takahashi (1970) concluded that the GEOSECS data fit best with the constants of Buch (1951). Subsequently, Lee et al. (1995, 1996) concluded that the apparent constants determined by Roy et al. (1993, 1994 1996) and Goyet and Poisson (1989) were most consistent when applied to seawater samples collected from the Gulf Stream. Even more recently, McElligott et al. (1998) concluded there were multiple problems of calibration of the individual measurements of the carbon parameters and apparent constants. Therefore, McElligott et al. (1998) concluded that there was not a single set of apparent constants suitable for all measured

Table 1.2. Recent studies of the apparent constants and measured parameters of the inorganic carbon dioxide system in seawater.

Reference	Best Fit Constants K_1 and K_2	Study	Study Area and/or Water Type	Measured Parameters
Millero et al. 1993	Dickson & Millero[a]	Field	Equatorial Pacific	pH/pCO_2/DIC/TA
Clayton et al. 1995	Dickson & Millero[a]	Field	Equatorial Pacific	pH/DIC/TA
Lee and Millero 1995	Goyet & Poisson Roy	Lab	CRM & Gulf Stream Water	pH/pCO_2/DIC/TA
Lee et al. 1996	Goyet & Poisson Roy	Lab	Gulf Stream Water	pH/fCO_2/DIC/TA
Lee et al. 1997	Mehrbach	Field	North Atlantic	pH/fCO_2/DIC/TA
McElligot et al. 1998	None	Field	Equatorial Pacific	pH/ pCO_2/DIC/TA
Wanninkhof et al. 1999	Mehrbach	Field	Pacific/Atlantic/Indian	DIC/TA/pCO_2
Lee et al. 2000	Mehrbach	Field	Pacific/Atlantic/Indian	pH/fCO_2/DIC/TA
Lueker et al. 2000	Mehrbach	Lab	Pacific & Atlantic Water	fCO_2/DIC/TA
This study	Mehrbach	Field	Pacific & Southern Ocean	pH/fCO_2/DIC/TA

[a] Dickson and Millero refers to Dickson and Millero (1987) and the combined refit of the measured apparent constants of Hasson and Mehrbach.

carbon system parameters. Finally the most recent papers by Lee et al. (2000) and Lueker et al. (2000) concluded from field and laboratory experiments that the constants of Mehrbach et al. (1973), refit by Dickson and Millero (1987) were most consistent for the seawater samples that they analyzed. Although inconsistencies were not listed in earlier papers, Lee et al. (2000) determined that a discrepancy of +0.0047 in spectrophotometric pH values and an overestimation of 8 $\mu eq\ kg^{-1}$ of TA to be the cause of the earlier discrepancies in the Equatorial Pacific. It seems that a whole subdiscipline of oceanography has evolved around the apparent constants and measurements.

Processes Controlling the Carbon Dioxide System of Seawater

Changes in the CO_2 system are caused by mechanisms that fall into three categories; physical, chemical and biological. Physical changes include the vertical and horizontal advection of water. Chemical changes include air-to-sea exchange and any process that alters the chemical speciation of CO_2 in seawater. Biological mechanisms include photosynthesis and respiration. Each process has at a characteristic timescale. For instance, the chemical equilibration of CO_2 happens in seconds (Zeebe et al. 1999). Photosynthesis and respiration can change CO_2 concentrations in seconds to weeks. Air-to-sea exchange of CO_2 occurs on a timescale of 3 to 12 months (Broecker and Peng 1982; Wanninkhof et al. 1992). Therefore, to properly describe and interpret changes within oceanic ecosystems, observations must be made on the proper time scales. For instance, daily rates of primary production cannot be estimated from monthly observations, unless assumptions are made concerning the scaling of the processes.

Because the measurable CO_2 system parameters are interdependent, a change in one will be associated with a change in at least one of the others. This, of course, depends

on the external force or influence. For example, as fCO_2 increases, pH will decrease. As photosynthesis depletes [CO_2^*(aq)], DIC and fCO_2 decrease. In a closed system, an increase in temperature produces an increase in fCO_2 pressure but does not affect DIC. These types of processes will be investigated in this dissertation with respect to the oceanic ecosystem.

Table 1.3 Processes and expected changes in measured carbon system parameters.

Process	fCO_2	DIC	pH	TA
Photosynthesis	↓	↓	↑	↑
Respiration	↑	↑	↓	↓
Heating [a]	↑	–	↓	–
Cooling [a]	↓	–	↑	–
Heating [b]	–	↓	↑	–
Cooling [b]	–	↑	↓	–
$CaCO_3$ precipitation	↑	↓	↓	↓
$CaCO_3$ dissolution	↓	↑	↑	↑

[a] Closed system
[b] Open system

Recently, the "enigma" of apparent uptake and removal of DIC normalized to a salinity of 35 (n35DIC) in the absence of nitrate during the summer warming period was explained by the metabolic activities of N_2 fixing organisms in subtropical waters (Karl et 2001). Although seasonal depletions of n35DIC were observed to occur in tandem with rises in sea surface temperature, it was assumed that net community production dominated the other processes during this period (Michaels et al. 2000; Lee 2001; Karl et al. in press; Karl et al 2001). Although the export production matches the removal of DIC, their results may be a bit fortuitous because there are other processes that could explain these observations. These authors fail to extend their analysis to the complete suite of carbon system measurements and to the annual cycle to determine if the

observations match the mechanism. Many facets of the CO_2 system (i.e. temperature and fCO_2 changes) will be discussed in Chapter 2. For instance, if net community production dominates during the warming period, then fCO_2 should also decrease. On the contrary, observed fCO_2 is highest (supersaturated with respect to the atmosphere) in the summer months. Conversely, if net community production dominates in the summer then does net community respiration dominate in the winter when DIC values increase? Or if mixing from below is an important process, then fCO_2 should increase. On the contrary, fCO_2 decreases during the fall and winter months and are undersaturated with respect to the atmosphere. Finally, if the measurable carbon parameters are interdependent, then how can DIC decrease because of biologically mediated uptake of CO_2 while fCO_2 increases because of changes in temperature?

Table 1.4 DIC, fCO2 and the inorganic carbon speciation concentrations for 4 different scenarios explained in the text. Calculations were performed at a total alkalinity of 2300 µmoles/kg, salinity of 35, 0 umoles kg^{-1} phosphate and 0 umoles kg^{-1} silicate.

	DIC	**fCO_2**	**[CO_2*(aq)]**	**[HCO_3^-]**	**[CO_3^{2-}]**	**Temp**
Initial Conditions	1975	351.9[a]	10.0	1735.4	229.6	25.0
Scenario 1	1965	336.0a	9.5	1719.4	236.1	25.0
Scenario 2	1965	351.9a	9.7	1718.3	236.7	26.2
Scenario 3	1971a	345.0	9.8	1728.6	232.4	25.0
Scenario 4	1960a	345.0	9.5	1711.4	239.5	26.2

a Calculated value

A simple example can illustrate much of the confusion and complexity concerning investigations of CO_2. For instance, assume a decrease of 10 µmole kg^{-1} DIC was observed in surface waters from some set of initial conditions (at a constant salinity and alkalinity; Table 1.4; Initial conditions). If the uptake was biologically mediated and temperature was constant, then calculated fCO_2 values would drop by approximately 15 µatm (Table 1.4, Scenario 1). On the other hand, if temperature rose by 1.2 °C, DIC

concentrations would still drop by 10 μmoles kg^{-1}, but calculated fCO_2 values would remain unchanged from initial values (Scenario 2). The decrease of DIC is the result of changing temperature and not from the removal of inorganic carbon from the system. Matters can be complicated even more by adding a component of air to sea exchange. Air to sea exchange will add or subtract inorganic carbon depending on the fCO_2 saturation state. If half of the fCO_2 were replaced in Scenario 1 by exchange with the atmosphere, then DIC values would only drop approximately 4 μmoles kg^{-1} at a constant temperature (Scenario 3). Finally, if temperature rose 1.2 °C with the same conditions as Scenario 3, then DIC concentrations would drop 15 μmoles kg^{-1}. These examples show the complexity of the CO_2 system and inherent pitfalls of analyzing only one parameter of the system.

Even more interesting are the observed changes in CO_2^*(aq) speciation. In, Scenario 1, the 10 μmole kg^{-1} change in DIC is matched by a 0.5 μmole kg^{-1} change in CO_2*(aq). In Scenario 4, the 15 μmole kg^{-1} change in DIC is again matched by a 0.5 μmole kg^{-1} change in CO_2*(aq). Both temperature and air-to-sea exchange of CO_2 can have a direct effect on the speciation of CO_2 in seawater and should be taken into account when observing biological systems. This again illustrates the differences between the measured carbon system parameters and the carbon speciation.

Within Antarctic waters, processes similar to these observed in subtropical waters also occur. Biologically mediated uptake and removal of DIC occurs concurrently with changes in temperature; albeit, temperature decreases due to ice melt and then warms because of solar radiation. The same types of processes co-occur (photosynthesis and

changes in temperature). The impact of these changes on the CO2 system parameters can only be determined by looking at the whole carbon system over a proper timescale. Chapter 3 and 4 of this dissertation will examine underway fCO_2, DIC, TA and O_2 data to determine controlling processes in surface waters west of the Antarctic Peninsula.

Finally, a chapter was devoted to investigate a process called photorespiration within a continuous culture of phytoplankton. Unfortunately (maybe not), this investigation never proceeded because of complications in the interpretation of the inorganic carbon chemistry within the culture. For example, a culture was allowed to equilibrate (gas bubbled through the culture) with a CO_2 gas concentration of 300 ppm. The CO_2 gas concentration measured after the system had achieved a steady state was 188 ppm. Finally, the CO_2 gas concentration determined from measurements of DIC and alkalinity was 18 ppm. Which value is correct? A steady state model was developed to explain the interaction between chemical interactions, biological uptake of CO_2, and air sea exchange.

Finally, I will conclude this dissertation with an examination of my own data sets in the context of enigmas and unanswered relevant questions regarding CO_2 chemistry in seawater. I will address some of these long-standing and recent problems of variations of CO_2 in natural waters.

CHAPTER II

INORGANIC CARBON SYSTEM DYNAMICS IN THE NORTH PACIFIC SUBTROPICAL GYRE: HAWAII OCEAN TIME-SERIES (HOT) PROGRAM

Abstract

Time-series sites are ideal for studying biogeochemical and ecosystem variability. The processes and subsequent changes governing ecosystem structure and function can only be determined by repeat observations. Observations on proper time scales are imperative to differentiate seasonal and annual variability with respect to long-term trends or stochastic changes. The Hawaii Ocean Time-series (HOT) program was established in 1988 with the intent of documenting and interpreting long term-trends (>20 years) in the context of seasonal to interannual variations of physical, chemical and biological features of the North Pacific Subtropical Gyre (NPSG; Karl and Lukas 1996; Karl 1999). One component of the core measurement program has focused on the measured inorganic carbon system parameters; pH, total alkalinity (TA), dissolved inorganic carbon (DIC) and the fugacity of carbon dioxide (fCO_2). The thermodynamic relationships describing the inorganic carbon system were solved using the constants of Mehrbach et al. (1973) refit by Dickson and Millero (1987) during a 2-year period when the complete set of parameters were measured. A 10-year time-series was then created for all inorganic carbon parameters and analyzed during seasonal, annual and long-term time scales to determine controlling processes. Monthly averaged surface seawater fCO_2 and n35DIC concentrations are correlated to changes in sea surface temperature. Temperature driven changes in the apparent equilibrium constants for carbon dioxide dissolved in

seawater control n35DIC and fCO_2 during a seasonal time scale. Annual variability suggests changes in DIC concentrations control changes of surface ocean fCO_2. Recent literature suggests the rise of surface ocean CO_2 concentrations is caused by an increase of atmospheric CO_2 (Winn et al. 1998). As an alternative, a change in TA could also explain the long-term (20-year) increase of surface ocean fCO_2.

Introduction

Time-series measurements of physical, chemical and biological parameters are needed to observe and understand high frequency variability, daily to sub-seasonal and long-term responses to perturbations in the global climate ecosystem. Repeated measurements at strategic locations are needed to document short-term variability and long-term trends within the marine environment. The fate of increasing anthropogenic carbon dioxide (CO_2) in the atmosphere is unknown, but the oceanic and terrestrial ecosystems are predicted to play major roles in sequestering CO_2. Recent models disagree on the magnitude of the oceanic and terrestrial sinks, and these differences in balancing the global carbon budget are attributed to measurement uncertainties (Cao and Woodward 1998; Fan et al. 1998; Sarmiento and Sunquist 1992; Feely et al. 1998.

Oceanic models suggest rising atmospheric carbon dioxide (CO_2) will produce a corresponding increase in surface ocean CO_2 concentrations, but the interannual variability of the oceanic uptake is predicted to be large (Brewer 1983; Fancey et al. 1995). With increasing surface ocean CO_2 concentrations, it becomes imperative to understand the inorganic carbon system in seawater to determine the controlling processes on proper time scales, for calibrating ocean carbon models with direct measurements and estimating carbon inventory interactions. Validation of these models

with field measurements is imperative to resolve issues of the global inorganic carbon system.

The potential of the NPSG to absorb anthropogenic CO_2 is dependent upon the interactions between the biological, physical and chemical controls (Volk and Hoffert 1885). Processes such as temperature, the photosynthesis-to-respiration balance, calcium carbonate precipitation and dissolution, air-to-sea exchange and organic matter export processes, gyre circulation and vertical mixing can influence inorganic carbon concentrations on various time scales (seasonal and annual), obscuring long-term trends. Analysis of time series data on the proper time scale combined with a thorough understanding of the predicted changes of the measured carbon system parameters is essential to understand processes controlling inorganic carbon concentrations.

Recent analyses of n35DIC at the Hawaii Ocean Time-series (HOT) site suggest the rise of upper ocean CO_2 concentrations during the past decade is a result of rising atmospheric CO_2 and gyre circulation (Winn et al. 1994; Winn et al. 1998). Although, at first glance, this appears to be a plausible explanation, a complete time series analysis of fCO_2, TA and DIC suggests changes in TA and DIC could also affect surface ocean fCO_2. Processes such as temperature, calcium carbonate dissolution and uptake of CO_2 by phototrophic microorganisms also influence the steady state surface seawater fCO_2 pressure. During a seasonal time scale, it has been suggested that the decrease of n35DIC concentrations from winter to summer in certain subtropical regions is a result of net community production driven by N_2 fixation rather then thermodynamic control based on temperature changes (Lee 2001, Karl et al 2001, Karl et al. in press). These analyses failed to explain how a decrease of n35DIC concentrations correlate with an increase of

fCO_2 pressure during the same time period. Before interpreting seasonal variability, the timescales relating the CO_2 equilibration between the atmosphere and ocean with the timescales of the solution chemistry of CO_2 in seawater must be understood.

In this chapter, an analysis of the measured inorganic carbon system will be conducted during seasonal, annual, and decadal time scales to ascertain the dominant processes controlling CO_2 concentrations in the surface ocean at Station ALOHA. Specifically, seasonal changes of n35DIC and fCO_2 will be discussed in terms of temperature-driven solubility changes. Annual changes of n35DIC and fCO_2 will be discussed in terms biological production, temperature, and gyre circulation. Finally, long-term changes (decadal) will be discussed in terms of increasing atmospheric CO_2.

Methods

Program and Field Site

Since October 1988, the HOT program has been conducting studies of the NPSG on approximately monthly intervals (Fig 2.1; Karl and Lukas 1996; Karl 1999). The study site is located at Station ALOHA (A Long Term Oligotrophic Habitat Assessment; 22° 45‘ N 158° W) where samples are taken for a variety of core hydrographic, chemical and biological measurements using a standard set of protocols. Depth profiles (1 to 4700 meters) of DIC and TA have been sampled every cruise (n=2747). Between 1996 and 1998, an underway, semi-continuous fCO_2 measuring system was deployed to map surface seawater fCO_2 at Station ALOHA. Between 1992 and 1998, depth dependent profiles of pH on the total scale (pH_{total}) were sampled and analyzed immediately in

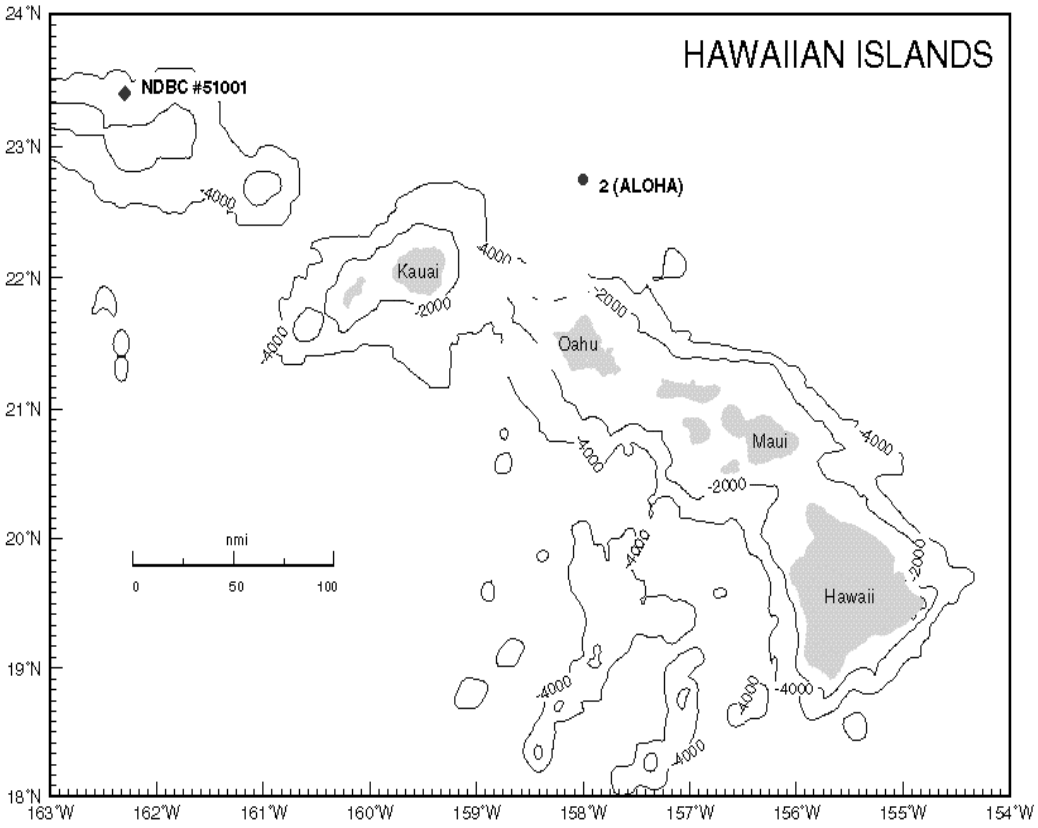

Figure 2.1 Map showing the positions of Station Aloha (22º 45'N, 158º W) and NOAA-NDBC meteorological buoy 51001 (23.4º N, 162.3º W).

shipboard laboratories using a spectrophotometric method. Measurements of wind speed were obtained from the National Data Buoy Center (NDBC) meteorological buoy 51001 at 23.4 ºN, 162.3 ºW, 445 kilometers west of Station ALOHA.

Measurement of DIC and TA

Dissolved inorganic carbon was measured in seawater samples collected during each cruise by coulometric determination of extracted CO_2 (Winn et al. 1994; Winn et al. 1998). Prior to 1993, samples were manually delivered to the coulometer extractor using either a calibrated pipet bulb or gravimetrically using syringes weighed before and after sample injection. Since 1993, sample delivery was automated using a Single Operator Mutiparameter Metabolic Analyzer (SOMMA) system (Johnson et al. 1998). Alkalinity was determined in an open cell using a potentiometric titration with calibrated HCl, and analyzed with a modified Gran plot as recommended by DOE (1994; Winn et al. 1994, 1998). Field precision was determined by an analysis of deep-water reference samples collected between 4250 and 4700 decibars. Assuming the concentration of the deep ocean does not change appreciably during the 10-year time-series, DIC and TA field precision was estimated to be 2-3 μmol kg^{-1} and 3-4 μeq kg^{-1}, respectively. Since 1992, the analytical accuracy and precision of DIC and TA analyses have also been determined by analysis of Certified Reference Materials (CRMs) provided by Andew Dickson. Our analytical DIC precision and accuracy were estimated to be 1 μmol kg^{-1} and less then 2 μmol kg^{-1} respectively. Our analytical TA precision and accuracy were estimated to be 2 μmol kg^{-1} and less then 4 μmol kg^{-1} respectively.

Measurement of the fugacity of CO_2

Between 1996 and 1998, an automated system was deployed to map surface water fCO_2 and measure atmospheric CO_2 concentrations. The mole fraction of CO_2 in surface seawater was measured in water collected from the ship's flow-through underway seawater system. The mole fraction of CO_2 in atmospheric air was measured in air samples collected from the top of the bridge approximately 10-12 meters above the sea surface. Surface seawater was continuously pumped through a shower-head type equilibrator and the CO_2 mole fraction of the equilibrated headspace was measured with a LI-COR model 6252 infrared CO_2 analyzer. Headspace gas was dried using a napthyon® tube drier and a magnesium perchlorate scrubber. The CO_2 mole fraction was converted to fCO_2 using the total pressure and the viral equations of state for CO_2 (DOE 1994). Equilibrator temperature was measured with calibrated thermistors (traceable to NIST thermometers) and system pressure was measured with a Setra pressure transducer. The continuous measurement system was periodically calibrated (every 2 hr) with compressed gas standards with nominal mixing ratios of 278.5, 355.76, and 278.5 parts per million (ppm) by volume. These gas standards were calibrated against World Meteorological Laboratory (WMO) primary standards. A secondary standard reference gas of 350 ppm concentration was also analyzed every 2 hr to provide a check on system stability. Between calibrations, equilibrator and atmospheric samples were measured every 10 min. The entire measurement system was automated using a computer and software written in BASIC. Temperature and salinity were measured with a Sea-Bird thermosalinograph positioned at the intake, which was periodically calibrated by bottle salinity. Calculations were done according to the procedures outlined in DOE (1994).

Measurement of Spectrophotometric pH

Samples for spectrophotometric pH were taken directly into 10 cm spectrophotometric cells. The cells were flushed for 10 to 20 seconds with seawater sampled from the rosette before being capped with PTFE stoppers. The cells are placed in Ziplok® bags and brought to a constant temperature of 25 ºC in a thermostated water bath. The pH was determined on the total scale by measuring the absorbance at 730, 578 and 434 nm on a Perkin Elmer Model 3 dual beam spectrophotometer before and after the addition of 50 µl of m-cresol purple (2 mM). The spectrophotometric cells were kept at a constant temperature of 25 ºC while in the spectrophotometer using a custom made thermostated cell holder. Corrections to the pH values were made for the addition of dye, and all calculations were made according to the procedures outlined in DOE (1994). A computer and software written in QBASIC controlled the entire measurement system.

Carbon System Calculations

The internal consistency of carbon system parameters was calculated using the program CO2SYS of Lewis and Wallace (1995). The program calculates the carbon system parameters based on user-selected apparent constants K_1 and K_2. Any two of the four measurable carbon system parameters (DIC, TA, pH or fCO_2), temperature, salinity, phosphate and silicate are required to calculate the other two carbon system parameters. Calculations can be performed as single input or batch modes. This program can be obtained from the CDIAC website (httpp://www.cdiac.esd.ornl.gov)

Results and Discussion

Solution Chemistry of Carbon Dioxide in Seawater

Variations of CO_2 dissolved in seawater are classified into two categories; open and closed systems. The assumptions inherent in each system determine how to treat the analysis of the measured carbon system parameters. Furthermore, the observed variability cannot be explained without a thorough understanding of the thermodynamic relationships describing the effect of temperature on the solution chemistry of CO_2 in seawater. For example, within an open system, fCO_2 remains constant and DIC varies as a function of temperature (Fig 2.2A and 2.2B). Within a closed system, fCO_2 varies, as a function of temperature and DIC remains constant (Fig 2.2A and 2.2B).

Over appropriate time scales (months to years), the atmospheric-oceanic system is classified as an "open" system. Mixed-layer surface oceanic fCO_2 values are ultimately governed by atmospheric CO_2 concentrations through the physiochemical process of air-to-sea exchange of CO_2. Barring areas where CO_2 concentrations deviate from atmospheric values significantly (i.e. coastal ecosystems where primary production is high), global surface ocean fCO_2 values are closely equilibrated with atmospheric concentrations. Therefore, global variations of temperature do not affect surface ocean fCO_2 concentrations significantly. On the other hand, DIC concentrations will vary as a function of temperature within an open system because of air to sea exchange (Table 2.1). As a sample of water cools at a constant fCO_2 and TA, DIC concentrations increase. High latitude surface waters are 20 to 25 degrees cooler then low latitude tropical surface waters. Therefore, DIC concentrations are greater in colder high latitude waters, in part, because of temperature (Table 2.1).

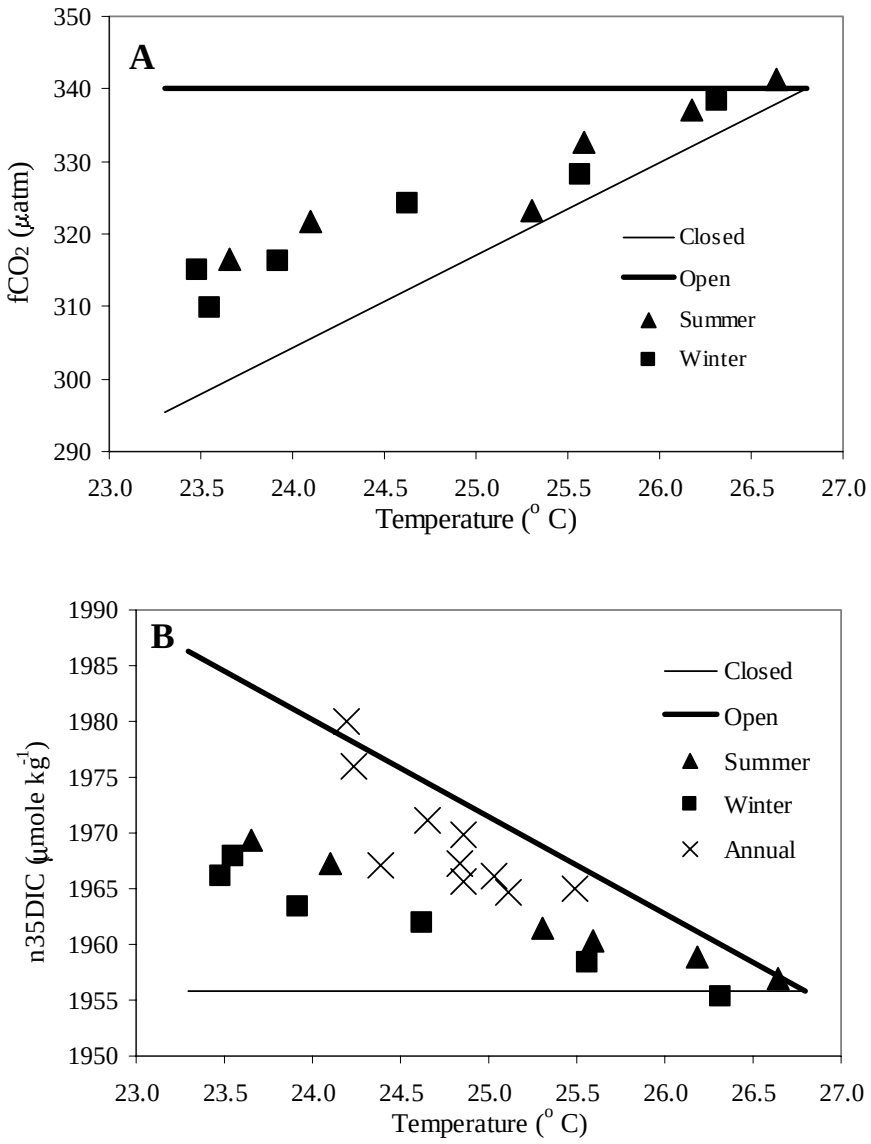

Figure 2.2 A) Temperature versus fCO_2. Thin line represents the change of fCO_2 with temperature in a closed system. Thick line represents the change of fCO_2 with temperature in an open system. Filled triangles represent the spring to summer fCO_2 pressures at Station ALOHA. Filled squares represent fall to winter fCO2 pressures at Station ALOHA. B) n35DIC versus temperature. Thin line represents the change of n35DIC in a closed system. Thick line represents the change of n35DIC in an open system.

Table 2.1 Calculations showing the effect of temperature on the apparent equilibrium constants, CO_2 speciation and DIC within an open system (constant fCO_2 pressure). Calculations were made at a constant alkalinity of 2305 μeq kg^{-1}, 35 salinity, 0 μmol kg^{-1} phosphate and 0 μmol kg^{-1} silicate.

Temp (°C)	Ko (mole m^{-3} atm^{-1})	pK_1 mol kg^{-1}	pK_2 mol kg^{-1}	fCO_2 (μatm)	CO_2*aq (μmol kg^{-1})	HCO_3 (μmol kg^{-1})	CO_3 (μmol kg^{-1})	DIC (μmol kg^{-1})
5	0.0536	6.050	9.299	360.0	18.8	1998.6	119.9	2137.2
25	0.0332	5.847	8.965	360.0	10.2	1743.2	226.5	1979.9

Within a "closed" system, DIC is neither created, nor lost. A change in temperature only re-partitions carbon between the three dissolved inorganic carbon pools (Table 2.2). Hence, DIC concentration is constant. The fCO_2 pressure subsequently becomes a function of the speciation of CO_2 and ultimately the change in temperature. A gas tight glass sample bottle or a gas equilibrator is an example of a "closed" system. When seawater in a "closed" container is heated, fCO_2 increases while DIC remains constant (Table 2.2).

Table 2.2 Calculations showing the effect of temperature on the apparent equilibrium constants, CO_2 speciation and DIC within a closed system (constant DIC concentration). Calculations were made at a constant alkalinity of 2305 μeq kg^{-1}, 35 salinity, 0 μmol kg^{-1} phosphate and 0 μmol kg^{-1} silicate.

Temp (°C)	Ko (mole m^{-3} atm^{-1})	PK_1	PK_2	fCO_2 (μatm)	CO_2 (μmol kg^{-1})	HCO_3 (μmol kg^{-1})	CO_3 (μmol kg^{-1})	DIC (μmol kg^{-1})
20	.02908	5.891	9.044	287.1	9.3	1737.8	227.9	1975.0
25	.03324	5.847	8.965	351.9	10.0	1735.4	229.6	1975.0

Ultimately, variations in the carbonate, bicarbonate and aqueous carbon dioxide concentrations determine the observed DIC concentration and are controlled by a set of reactions and apparent equilibrium constants relating the concentrations of individual dissolved CO_2 species (Chapter 1). Therefore, understanding how the individual carbon species vary as a function of temperature will explain changes of fCO_2 and DIC within each system (open and closed; Figure 2.3A,B, and C). The effect of temperature on the

speciation is manifest through changes in the apparent equilibrium constants (Ko, K_1 and K_2) for carbonic acid in seawater, which are functions of temperature, salinity and pressure. Solving the thermodynamic relationships shows the link between fCO_2 and the dissolved inorganic carbon species. At a constant salinity, pressure and alkalinity, bicarbonate concentrations decrease with increasing temperature for both open and closed systems (Fig 2.3B). Likewise, carbonate concentrations increase with increasing temperature in both open and closed systems (Fig 2.3C). Differences are observed in $CO_2{}^*_{(aq)}$ concentrations. Within a closed system, CO_2*(aq) concentrations increase with increasing temperature, and within an open system CO_2*(aq) decreases with increasing temperature (Fig 2.3A). This difference is explained through the following analysis.

The assumption, within an open system, of constant fCO_2 pressure determines the partitioning of dissolved inorganic carbon as a function of temperature. The pressure of CO_2(g) is related to the dissolved species through Henry's Law. Based on Henry's Law, a change in temperature driven gas solubility (Ko) determines the change of $[CO_{2(aq)}]$ at a constant CO_2(g) pressure . For example, as temperature rises in an open system, gas solubility (Ko) decreases (Table 2.1). Therefore, $[CO_2$*(aq)] must also decrease (Fig 2.3A). Subsequently, the concentrations of HCO_3^- and CO_3^{2-} ultimately become a function of CO_2(g), Ko, K_1 and K_2. The system can then be solved showing that HCO_3^- decreases with increasing temperature and CO_3^{2-} increases with increasing temperature (Fig 2.3A and B).

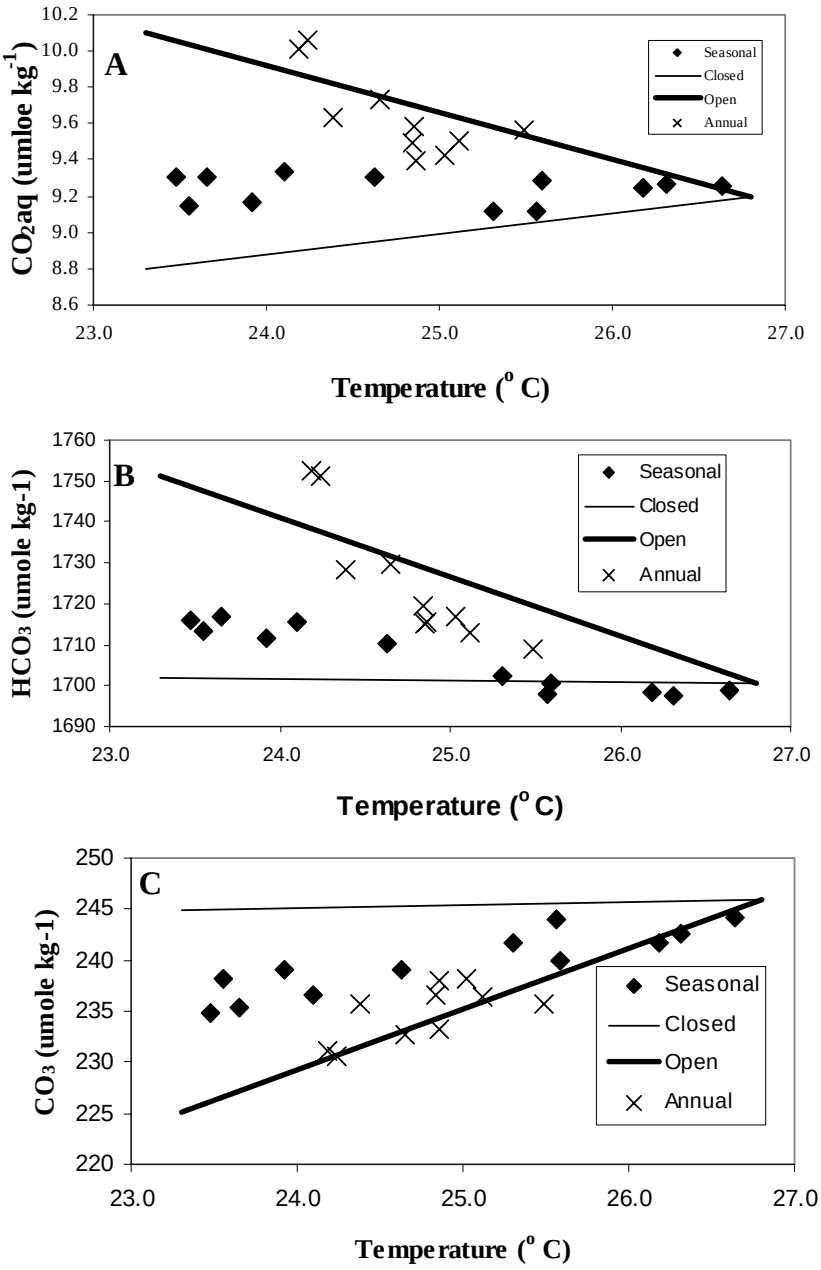

Figure 2.3 Changes of carbon system speciation (CO_2*(aq), HCO_3^- and CO_3^{2-} with respect to temperature. Thick lines represent changes in open systems and thin lines represent changes in closed systems. Filled triangles represent seasonal values at Station ALOHA. Crosses represent annual values at Station ALOHA. A) CO_2*(aq). B) HCO_3^-. C) CO_3^{2-}

$$pCO_2 * Ko = CO_{2(aq)} \quad (1)$$

$$[HCO3] = \frac{-KKof(CO2)}{2} + \frac{\sqrt{KKof(CO2))^2 - 4(KKof(CO2))(Kof(CO2) - DIC}}{2} \quad (2)$$

where $K=K_1/K_2$.

$[CO_3^{2-}] = DIC - [CO_2*(aq)] - [HCO_3^-]$ (3)

Within a closed system, variations of temperature alter CO_2(g) pressure without changing DIC concentration (Fig 2.2A and B). Both the first and second apparent constants change as a function of temperature. Bicarbonate concentrations subsequently decrease. The decrease in HCO_3^- is matched exactly by increases in CO_2(aq) and CO_3^{2-}. Hence, DIC remains constant. Henry's Law then relates [CO_2(aq)] and CO_2(g) through the gas solubility constant (Ko). As temperature increases, gas solubility (Ko) decreases. Therefore CO_2(g) pressure increases because of both the lower gas solubility (Ko) and the increase of [CO_2*aq]. Changes of CO_2(g) as a function of temperature are 3.8 to 4.23% per °C (Millero 1995).

Seasonal Variability

In order to minimize effects of precipitation and evaporation between cruises, DIC and TA were normalized to a constant salinity of 35 (n35DIC=DIC *35/salinity**;** n35TA=TA*35/salinity). Additionally, seasonal cycles were normalized to the year 1989 by subtracting long-term trends through a linear fit of the data. The fugacity of CO_2, sea surface temperature and n35DIC show clear seasonal patterns (Fig. 2.4 A and B).

Maximum fCO_2 of 345 μatm occur during the summer between August and October and minimum fCO_2 of 310 μatm occur during the winter between February and April (Fig 2.4A). Maximum sea surface temperatures of 26.4 ºC occur between September and October and minimum sea surface temperatures of 23.3 ºC occur between February and April (Table 2.3; Fig 2.4A). Maximum n35DIC concentrations of 1970 μmol kg^{-1} occur between February and March. Minimum concentrations of approximately 1955 μmol kg^{-1} occur between September and November (Table 2.3; Fig. 2.4B). The fugacity of CO_2 drives the flux of CO_2 from the atmosphere. Maximum fluxes (into the ocean) of 0.15 mol m^{-2} $month^{-1}$ (approximately 3.0 μmol kg^{-1} $month^{-1}$ for a mixed layer depth of 50 meters) occur between February and March and minimum fluxes (out of the ocean) of 0.05 mol m^{-2} $month^{-1}$(approximately -0.5 μmol kg^{-1} $month^{-1}$ for a mixed layer depth of 50 meters) occur between August and October (Fig 2.4C).

The seasonal cycle of monthly averaged fCO_2 pressures show a clear pattern positively correlated with seasonal temperature changes (r^2=0.88; Fig 2.2A). The seasonal cycle of monthly averaged n35DIC concentrations show a clear pattern negatively correlated (r^2 = -0.88) with seasonal temperature and fCO_2 pressures (Fig2.2B). Although fCO_2 and SST are positively correlated, the linear model of 2.60± 0.67% per °C ($pCO_2(T_1) = pCO_2(T_2)$ x exp(0.0423 ($T_1 – T_2$)) is statistically lower then that estimated for a closed system of 3.80 to 4.23% per °C ($pCO_2(T_1) = pCO_2(T_2)$ x exp(0.0423 ($T_1 – T_2$); Fig 2.2A; Millero et al. 1993; Goyet et al. 1993 Takahashi et al 1993; Millero 1995)

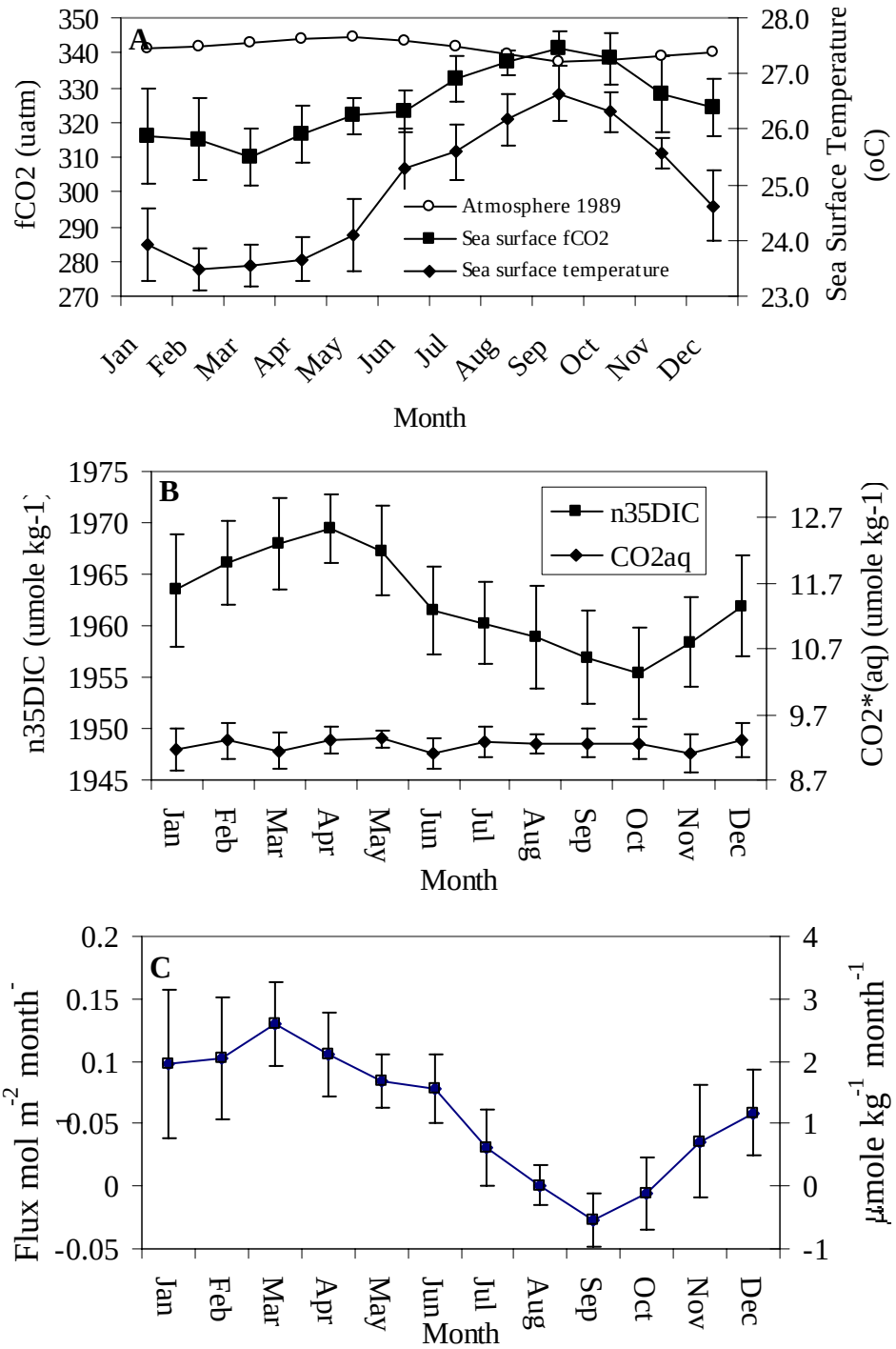

Figure 2.4 Monthly average and standard deviations of A) fCO_2 and sea surface temperature. Atmospheric CO_2 B) n35DIC and CO_2*(aq) .C) Air sea flux of CO_2. Positive values represent a flux from the atmosphere to the ocean and negative values represent a flux from the ocean to the atmosphere. Secondary axis represent the flux in units of µmol kg^{-1} assuming a mixed layer of 50 meters.

Table 2.3 Inorganic carbon system properties of surface seawater at Station ALOHA.

Property		Winter/Spring (Dec – Apr)	Summer/Fall (Jul – Oct)
Temperature (°C)		23.54 ± 0.51	26.02 ± 0.48
Salinity		34.99 ± 0.21	35.00 ± 0.19
DIC	**(μmol kg^{-1})**	1974.0 ± 14.6	1965.4 ± 15.2
N35DIC	**(μmol kg^{-1})**	1974.4 ± 5.5	1965.6 ± 5.9
TA	**(μeq kg^{-1})**	2303.4 ± 17.2	2302.8 ± 12.0
N35TA	**(μeq kg^{-1})**	2303.7 ± 6.5	2301.4 ± 3.3
Silicate	**(μM)**	1.4 ± 0.3	1.3 ± 0.3
Phosphate	**(μM)**	0.09 ± 0.03	0.07 ± 0.02

The underlying basis describing changes in sea surface temperature, fCO_2 and n35DIC concentrations is not initially obvious. The decrease of n35DIC concentrations in subtropical regions has been suggested to be a result of the apparent uptake and removal by phytoplankton through export production (Lee 2001; Karl et al 2001; Feely et al. 2001; Karl et al in press). It has also been suggested that the seasonal cycle of n35DIC (removal during the spring and summer seasons and replacement during the fall and winter seasons) is a consequence of air-sea exchange of CO_2 driven by changes in upper ocean temperature and the advection of warm DIC-poor waters (Winn et al. 1994, 1998). What are the relationships between temperature, primary production, fCO_2, n35DIC, advection and air-sea exchange? Does sea surface temperature control surface ocean fCO_2 pressure while the biologically mediated uptake of inorganic carbon controls n35DIC concentrations? Can a one-dimensional analysis adequately describe the changes observed?

The positive correlation of fCO_2 with temperature implies a closed-like system driven by the seasonal cycle of sea surface temperature. The negative correlation of n35DIC and sea surface temperature suggests these changes are part of an open-like

system. The observed variability of n35DIC and fCO_2 in surface seawater at Station ALOHA must be interpreted within the proper framework of assumptions and during the proper timescales relating the CO_2 equilibration between the atmosphere and surface-ocean. Furthermore, the interdependency of the measured carbon system parameters demands that the mechanisms explaining the changes in one CO_2 system parameter must be consistent with changes in the other measured CO_2 system parameters (Chapter 1).

Can seasonal variability of fCO_2 and n35DIC be explained by temperature-driven changes in the apparent CO_2 equilibrium constants as opposed to uptake and removal by phytoplankton, and/or from the exchange with the atmosphere (Lee 2001, Winn et al. 1998; Appendix B end of dissertation)? The discussion will be limited to the spring season, when sea surface temperatures increase but the analysis can also apply to the fall season, when sea surface temperatures decrease. During the spring, sea surface temperature increases 2.9 °C (during approximately 5 months) from a minimum in winter to a summer maximum (Fig 2.4A). The sea surface temperature increase drives surface ocean fCO_2 upwards from a winter minimum (approximately 30 μatm below atmospheric pressure) to a summer maximum (approximately 2-3 μatm above atmospheric pressure). As fCO_2 increases, the flux of CO_2 from the atmosphere decreases. Based on the direction of the flux (from the atmosphere to the ocean), n35DIC should increase from the spring to summer because CO_2 is being added from the atmosphere. This is not observed. Therefore, the change in n35DIC cannot be a function of air-sea exchange driven by sea surface temperature. The air-sea flux is in the wrong direction.

Because of the interdependency of the measured CO_2 system parameters, processes affect the CO_2 system and not just one parameter of the system. The

interdependency of n35DIC and fCO_2 is determined by the assumptions inherent in an open or closed system. The assumptions pertaining to whether a system is open or closed will depend on the timescale of air-sea equilibrium (constant fCO_2). The exchange of CO_2 between the ocean and atmosphere is defined as open system if the timescale of exchange is sufficiently long-lasting to establish gas-solution equilibrium (constant fCO_2). Otherwise, the system displays characteristics of a closed system or somewhere in between. Since the timescale for air-sea exchange is 3 months to a year, equilibrium with respect to fCO_2 is never fully achieved between the surface ocean and overlying atmosphere; especially if sea surface temperature is changing on timescales of weeks to months (Broecker and Peng 1982). Therefore, as sea surface temperature drives fCO_2 up, it also drives n35DIC down through the apparent equilibrium constants and partitioning of the CO_2 species. This difference is attributed to the dissimilar timescales of seasonal heating and cooling and flux of CO_2 from air-sea exchange.

Correcting n35DIC concentrations for air-sea exchange must be done on the proper timescales to correct for air-to-sea fluxes. The saturation state of fCO_2 with respect to the atmosphere and solubility represent the potential amount of CO_2 needed to re-establish equilibrium with the atmosphere. The piston velocity coefficient represents the rate at which equilibrium will be established (units of cm hr^{-1}). The rate or timescale of air-sea exchange is on the order of 3 months to a year (Broecker and Peng 1982). Therefore, "correcting" DIC concentrations on monthly timescales only corrects for a fraction of the carbon needed to establish equilibrium with the atmosphere. Typically, this is at most, 20% of the total change. Since equilibrium is not re-established, the CO_2 system behaves more like a closed system.

It is imperative to emphasize that phytoplankton do not utilize n35DIC, but CO_2*(aq) (and maybe HCO_3^-) which would cause fCO_2 and DIC to change in-phase over a seasonal cycle. Although the drawdown of n35DIC is equal to export production (Appendix B end of dissertation), the removal is counter-intuitive to the out of phase cycle of fCO_2. fCO_2 increases during the period of stratification when net community production should be lowering values. Additionally, high supersaturated fCO_2 is observed during the summer when export production is at its highest. Low, undersaturated fCO_2 is observed during the winter when biological production is at its lowest. The ”biological signal” is reflected in the mean fCO_2 undersaturation observed during 75% of the year (Appendix B end of dissertation).

Annual Variability

Annual averages of surface water fCO_2 pressure and n35DIC show an increasing trend between 1989 and 1999 (Fig 2.5 A & B). Normalized 35DIC increases from 1965 to 1977 μmol kg^{-1}. The fugacity of CO_2 increases from 320 to 340 μatm and is approximately 13 μatm below atmospheric concentrations on average. Atmospheric concentrations also increase from 341 to 352 μatm during the same time period. Annual averages, maximum and minimum sea surface temperature shows no statistically significant increasing trend between 1989 and 1999 (Fig 2.5C). Between 1996 and 1999 the trend of n35DIC increases. Normalized 35DIC concentrations increases from 1965 to 1979.9 μmol kg^{-1} in 4 years. Between 1989 and 1999, the trend of maximum SST and mean SST decreased. Mean temperature decreased from 25.5 to 24.2 °C.

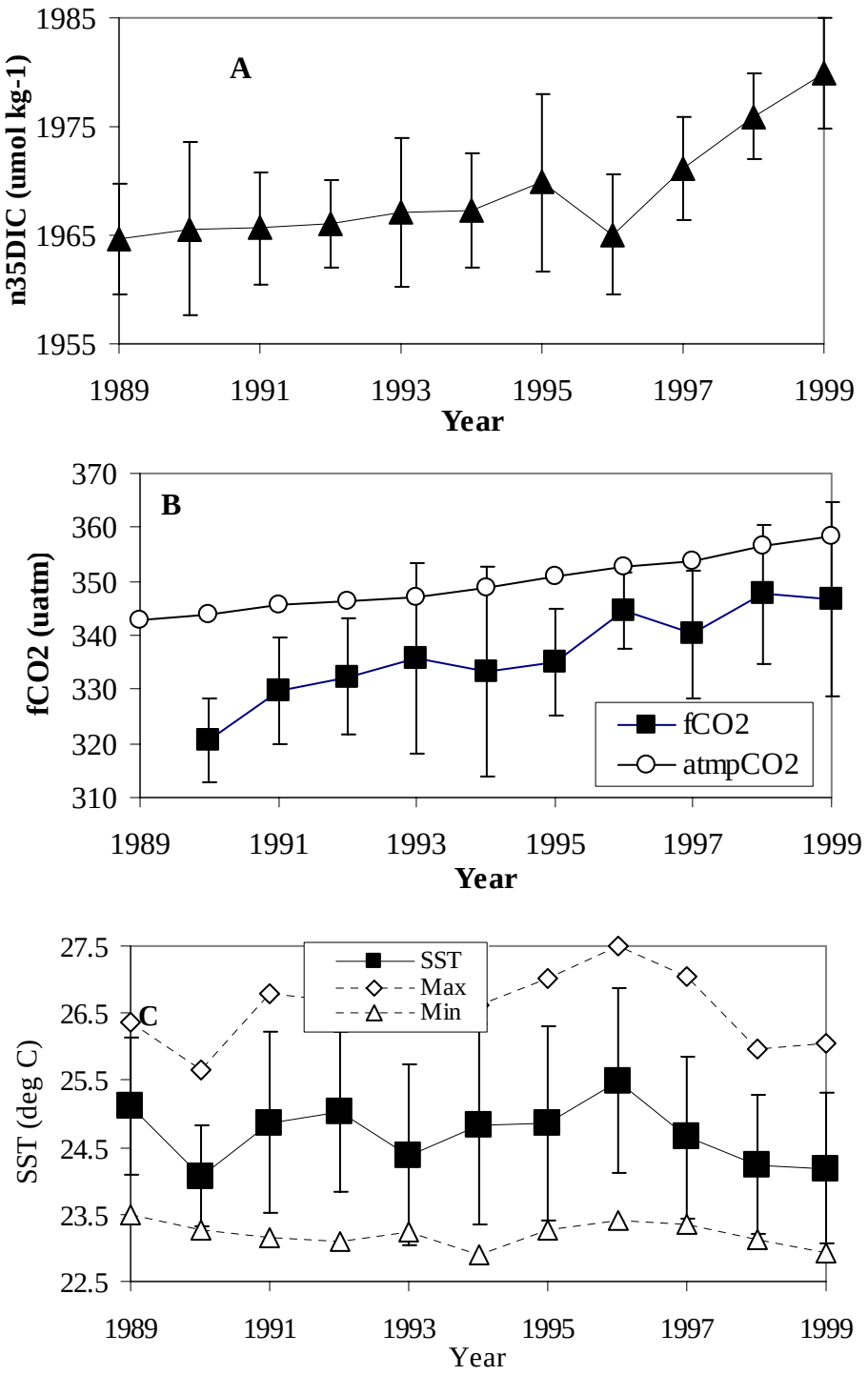

Figure 2.5 Annual averages of A) n35DIC B) fCO_2 and atmospheric CO_2 C) maximum, minimum and mean sea surface temperature

The discussion of overall upward trend of fCO_2 and n35DIC is deferred until the next section on decadel variability. Winn et al. (1994, 1998) concluded that the advection of low n35DIC water from the southeast and exchange of CO_2 between the atmosphere and surface ocean were responsible for the increase of n35DIC (0.8 μmol kg^{-1} yr^{-1}) between 1988 and 1995 at Station ALOHA. Between 1996 and 1999, annual n35DIC concentrations have increased dramatically from 0.8 μmol kg^{-1} yr^{-1} to approximately 3.7 μmol kg^{-1} yr^{-1}, which implies a change in horizontal advection (movement of water north or south) and/or a change in air-sea flux (Fig 2.5A). Although n35DIC concentrations show a discernible increase between 1996 and 1999, surface water fCO_2 pressure has not increased dramatically between 1996 and 1999 (Fig 2.5B). This would imply that there has not been a significant change in the air-to-sea flux of CO_2. Why does the trend of surface ocean n35DIC deviate from the trend of fCO_2.

Once again, it can be shown that the increasing trend of n35DIC is a result of the effect of temperature on the CO_2 system. Although one can explain the n35DIC increase between 1996 and 1999 by involking shifts in surface waters north or south, it still remains a valid exercise to understand processes in one dimension. Ultimately, temperature effects on n35DIC must be understood for waters north and south of Station ALOHA. A complete analysis of the carbon speciation can help determine the temperature effect on CO_2 concentrations. CO_2*aq displays an increasing trend with a slightly greater increase between 1996 and 1999 (Fig 2.6A). Bicarbonate also shows an increasing trend but with a discernible increase between 1996 and 1998 (Fig 2.6 B). Carbonate shows a decreasing trend with a slightly greater decrease between 1996 and

1999 (Fig 2.6 C). The variations of the inorganic carbon speciation are consistent with the effect of temperature through changes in the apparent equilibrium constants within an open system (Fig 2.3 and Fig 2.6). These temperature variations are most apparent between 1996 and 1999. Between 1996 and 1999 the annual sea surface temperature shows a decreases relative to the mean annual temperatures (Fig 2.5 C). This temperature anomaly is driven by maximum temperatures observed during the summer season.

During annual timescales, the atmosphere-ocean system behaves as an open system because CO_2 exchange with the atmosphere occurs on a shorter timescale. As water cools, fCO_2 pressures decrease, driving a flux from the atmosphere to the surface ocean (Takahashi 1993). Subsequently, n35DIC concentrations will increase because of higher solubility at lower temperatures and exchange of CO_2 with the atmosphere (description of an open system). Therefore, observed increasing trend between 1996 and 1999 of n35DIC at Station ALOHA is determined by the sea surface temperature and fCO_2.

Even though the annual timescale is sufficiently long that fCO_2 should equilibrate with the atmosphere, it is, on average 13 μatm below atmospheric values. This steady state undersaturation of fCO_2 with respect to the atmosphere can be explained in one of two ways. First, this observation is the result of the movement of surface water past station ALOHA. As relatively warmer, surface waters from the southeast move north and cool, fCO_2 decreases. This implies that the rate of water movement

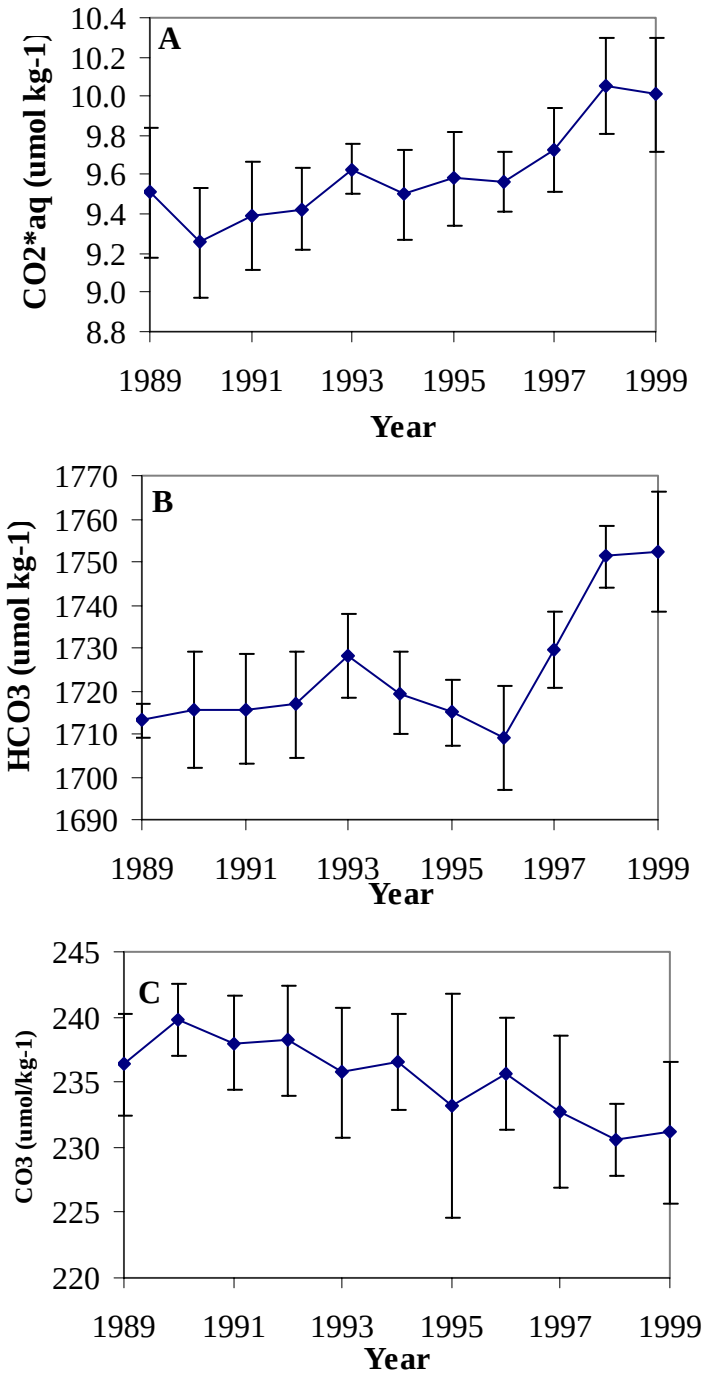

Figure 2.6 Annual averages and standard deviations of A) CO_2*(aq) B) HCO_3^- C) CO_3^{2-}

north is greater then air-sea exchange. If this is the case, CO_2 system properties are a function of annual variations of gyre circulation, advective processes, sea surface temperature and air-sea exchange (Fig 2.6 A,B and C).

Second, the consistent annual undersaturation of fCO_2 with respect to the atmosphere can also be explained through the uptake of CO_2*(aq) by phytoplankton (Appendix B). The second hypothesis entails changes in primary production controlling the inorganic carbon chemistry of surface waters through the removal of CO_2*(aq) by phytoplankton. The removal of CO_2*(aq) causes a reduction in fCO_2 pressure and n35DIC concentration. Therefore, mean annual fCO_2 undersaturation of approximately 13 μatm is a result of the removal of CO_2*(aq) on annual timescales. Determining which process controls the fCO_2 undersaturation will require spatial resolution of fCO_2 gradients north and south of Station ALOHA. A detailed model was developed to illustrate these interactions and is explained in Appendix B (end of dissertation).

The fCO_2 time-series also has relevance in estimating the net rate of carbon dioxide exchange between the atmosphere and surface ocean. The flux of CO_2 is a function of gas transfer coefficient, the solubility and the difference between CO_2 partial pressure in the surface water and atmosphere. The variability intrinsic in calculating fluxes is critical in understanding reported values. Functions describing the gas transfer coefficient are derived from measurements of wind speed, the invasion rate of bomb ^{14}C into the oceans, and rates of evasion or invasion of tracers released into the ocean. Depending on the function and wind speed, differences of calculated gas transfer can vary three-fold. Another source of error derives from the use of either bulk mixed-layer

temperature or skin temperature to calculate solubility of CO_2. Corrections can range from 5 to 15% in the winter to 39 to 56% in the summer (Wong et al. 1995).

The piston velocity coefficient was estimated using average wind speeds of 5, 7 and 10 meters sec^{-1} to represent the minimum, average and maximum wind speeds recorded near Station ALOHA (Wanninkhof 1992). The solubility of CO_2 was estimated using mixed-layer temperatures (Weiss 1974). The annual net fluxes were -0.41 ± 0.06, -0.67 ± 0.11 and -1.22 ± 0.14 mol C m^{-2} yr^{-1} between 1991 and 1999 using the minimum, mean and maximum wind speeds, respectively (Table 2.4). Between 1991 and 1999 there is a slight downward trend in the calculated fluxes (Table 2.4). Although the flux of CO_2 has shown a slight decrease (i.e., the ocean is a smaller implied sink for atmospheric CO_2) in the past ten years (1991-1999), the longer term trend since 1979 has actually been just the opposite (i.e., the ocean is a greater implied sink for atmospheric CO_2). Weiss et al. (1982) determined the area between 15-20° N to be a net source of CO_2 to the atmosphere of 0.1 mol m^{-2} yr^{-1} (Table 2.4). Wong et al. (1995) determined that although their data was in general agreement with Weiss et al. (1982), the variations could not be explained by changes in sea surface temperature alone as Weiss et al.(1982) had described. The calculated flux from the HOT program data set clearly shows Station ALOHA to be a net sink of approximately of -0.67 mol CO_2 m^{-2} yr^{-1}, suggesting a change from a weak source to a stronger sink in the two decades between 1979 and 1999. This stronger sink may be the result of a change in the net ecosystem metabolism driven by changes in ecosystem structure (Smith 1985). The annual variations may ultimately be controlled by the interactions, strengths and efficiencies of the soft tissue pump and physical controls (Volk and Hoffert 1985).

Table 2.4 Net annual fluxes in mol m^{-2} yr^{-1}

Wind Speed m s^{-1}	Flux 1979[a]	1985[b]	1991	1992	1993	1994	1995	1996[c]	1997	1998	1999	Mean
	+0.10	-0.07 to -0.17	***	***	***	***	***	***	***	***	***	
5	***	***	-0.43	-0.43	-0.44	-0.41	-0.49	-0.42	-0.41	-0.30	-0.31	-0.41 (±0.06)
7	***	***	-0.80	-0.72	-0.74	-0.69	-0.83	-0.54	-0.66	-0.51	-0.52	-0.67 (±0.11)
10	***	***	-1.49	-1.34	-1.36	-1.29	-1.54	-0.80	-1.21	-0.96	-0.97	-1.22 (±0.24)

a Weiss et al. 1982.
b Wong et al. 1995
[c] Gap in data from February to April.

Decadal Variability

Superimposed on the seasonal and annual signals of fCO_2 and n35DIC are positive interannual trends (Table 2.5). Between 1979 and 1999, surface ocean fCO_2 increases 1.15 μatm yr^{-1} ranging from 0.61 to 1.69 at the 95% confidence level (Table 2.5). Between 1985 and 1999, surface ocean fCO_2 shows an even larger increase of 1.52 μatm yr^{-1} ranging from 0.86 to 2.18 at the 95% confidence level (Table 2.5). Finally, between 1989 and 1999, surface ocean fCO_2 increases 2.46 μatm yr^{-1} ranging from 1.56 to 3.36 at the 95% confidence level (Table 2.5). The rise of fCO_2 for the different time periods (excluding the period from 1989 to 1999) is equivalent to the rise of atmospheric CO_2 of 1.48 to 1.58 μatm yr^{-1} at the 95% confidence interval estimated between 1979 and 1999 (Table 2.5). Overall, sea surface temperature changes range from –0.07 to –0.03 ºC yr^{-1} with the 95% confidence level ranging from –0.12 to 0.6 for the same time periods as fCO_2. Normalized DIC shows an increase of 1.18 μmol kg^{-1} yr^{-1} ($p<0.0005$) between 1989 and 1999 and an increase of 3.98 μmol kg^{-1} yr^{-1} ($p<0.0005$) between 1996 and 1999. (Table 2.5)

Table 2.5 Linear least squares fit with lower and upper confidence intervals at the 95% confidence level.

	Slope	95% lower	95% higher	p-value
Mauna Loa Atm. CO_2 1979-1999	1.53	1.48	1.58	<<0.0005
fCO_2 1979-1999 (μatm yr^{-1})	1.15	0.61	1.69	<0.0005
fCO_2 1985-1999 (μatm yr^{-1})	1.52	0.86	2.18	<0.0005
fCO_2 1989-1999 (μatm yr^{-1})	2.46	1.56	3.36	<0.0005
Temperature (^{o}C yr^{-1}) 1979-1999	-0.07	-0.12	-0.02	<<0.0005
Temperature (^{o}C yr^{-1}) 1985-1999	-0.06	-0.12	0.01	=0.08
Temperature (^{o}C yr^{-1}) 1989-1999	-0.03	-0.12	0.06	=0.51
n35DIC (μmol/kg yr^{-1}) 1989-1999	1.18	0.79	1.57	<0.0005
n35DIC (μmol/kg yr^{-1}) 1996-1999	3.98	2.36	5.61	<0.0005

The response of the surface ocean to rising atmospheric CO_2 can only be inferred by comparing the rise in CO_2 between the surface ocean and atmosphere. Superimposed on the seasonal signal is a positive upward trend of fCO_2 and n35DIC, which is consistent with a long-term rise in atmospheric CO_2 (Fig 2.7A & B). Between August 1979 and June 1980, fCO_2, DIC, sea surface temperature and salinity were measured between 15-20° N Latitude as part of the North Pacific Experiment (NORPAX) Equatorial Experiment (Fig 2.4; Weiss et al. 1982). Between 1985 and 1988 fCO_2, temperature and salinity were also measured on 12 cruises in the vicinity of Station ALOHA (± 3° latitude and ± 2° longitude) on the German container-carrier *M/V Lillooet* by C. S. Wong et al.(1995; Fig 2.7A) as part of the Oceanic CO_2 Monitoring Project. Neither time-series is long enough to determine any meaningful interannual trend, but the combined Weiss-Wong-HOT time-series covers a 20-year period (1979-1999) and shows a statistically

significant ($p<<0.005$) linear increase of 1.15 μatm yr^{-1} in fCO_2. This increase is slightly lower then the calculated increase of atmospheric CO_2 for the same time period but the 95% confidence intervals of 0.61 to 1.69 μatm yr^{-1} is statistically indistinguishable from measured 20 year increase in atmospheric CO_2 (Table 2.4). These results are consistent with studies in the North Atlantic and equatorial Pacific showing surface waters equilibrating with the atmosphere at a rate of approximately1.5 μatm yr^{-1} (Takahashi et al. 1993; Feely et al. 1999).

Imprinted on these signals is a long-term trend consistent with the increase of atmospheric CO_2. Although the long-term trend is consistent with the increase of atmospheric CO2, an alternate hypothesis can be invoked using the same data that involve changes in both the soft tissue and carbonate pumps (Volk and Hoffert 1985).

A n35DIC concentration of approximately 1954 μmol kg^{-1} is derived (Jan,1979) using the more conservative estimation of 0.8 μmol kg^{-1} yr^{-1} from Winn et al. (1998) and hindcasting back to January 1980 (Fig 2.7B). Using data from Weiss et al. (1982) and calculating predicts n35DIC concentrations in the range of 1965 to 1975 μmol kg^{-1} (Jan, 1979); a 10 to 20 μmol kg^{-1} difference. The difference is just outside the range predicted by the reported accuracy of 0.5%. Although the accuracy and location of Weiss data can be questioned, the implications suggest long term changes of TA (carbonate pump) controlling fCO_2 and not DIC or atmospheric CO_2. Total alkalinity values reported in

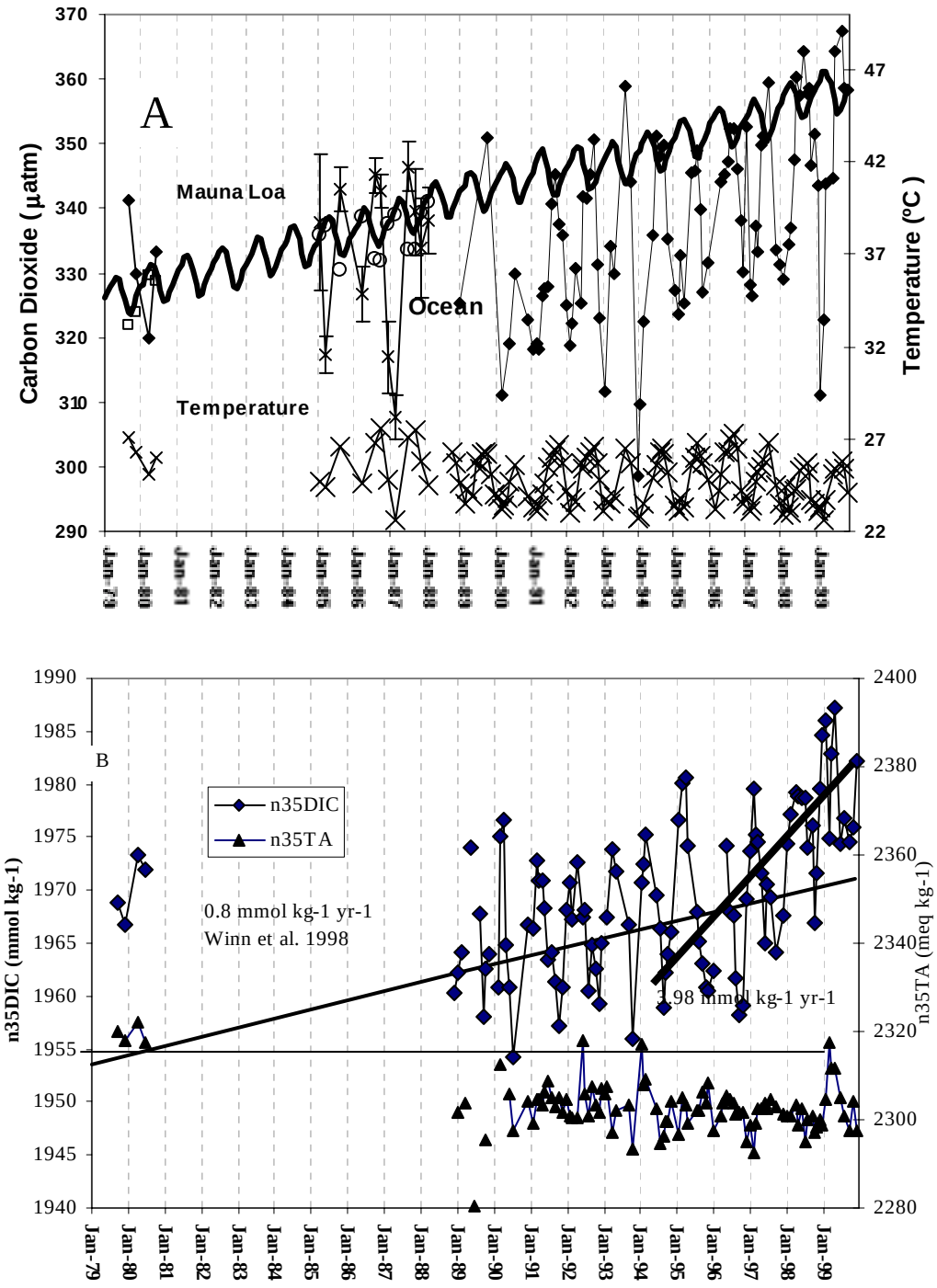

Figure 2.7 A) Time series of fCO_2 and sea surface temperature and B) n35DIC and n35TA at Station ALOHA.

Weiss et al. 1982 are within the range of n35TA measured at Station ALOHA. Although mean n35TA at Station ALOHA is 2305 ± 7 μeq kg^{-1}, there are periods when n35TA are observed to be as high as 2319 μeq kg^{-1} (Fig 2.9B). These three periods are correlated to the lowest fCO_2 values observed, highlighting the effect of total alkalinity on fCO_2.

fCO_2 pressures can be constructed from the fCO_2 temperature relationship (Takahashi et al. 1993). Additionally, the rise in atmospheric CO_2 can be added to the fCO_2 values to simulate changes in surface water fCO_2. A 20-year time series of sea surface temperature was created using the HOT sea surface temperature climatology (Fig 2.5). A fCO_2 value of 341 μatm was used to initialize the calculation starting January 1979. This "baseline" run describes the seasonal cycle of fCO_2 for the 20-year period but does not recreate the positive 20-year upward trend (Fig 2.5). The positive 20-year trend can be created in one of two ways; by increasing sea surface temperature or by adding in the rise in atmospheric CO_2. Based on the 1.51 μatm yr^{-1} increase in atmospheric CO_2, 0.1 μatm $month^{-1}$ is added to each time step (of 1 month) to simulate the increase predicted from atmospheric equilibration. The comparison between model and fCO_2 from Weiss-Wong-HOT time series shows a reasonable match (residuals =2 ± 11 μatm; Fig 2.5) . On the other hand, if atmospheric concentrations are held constant, the rise of fCO_2 can be explained by an increase of sea surface temperature of 0.06 to 0.08 ºC yr^{-1}; a rise predicted from coupled atmosphere-ocean model simulations (Haywood et al. 1997).

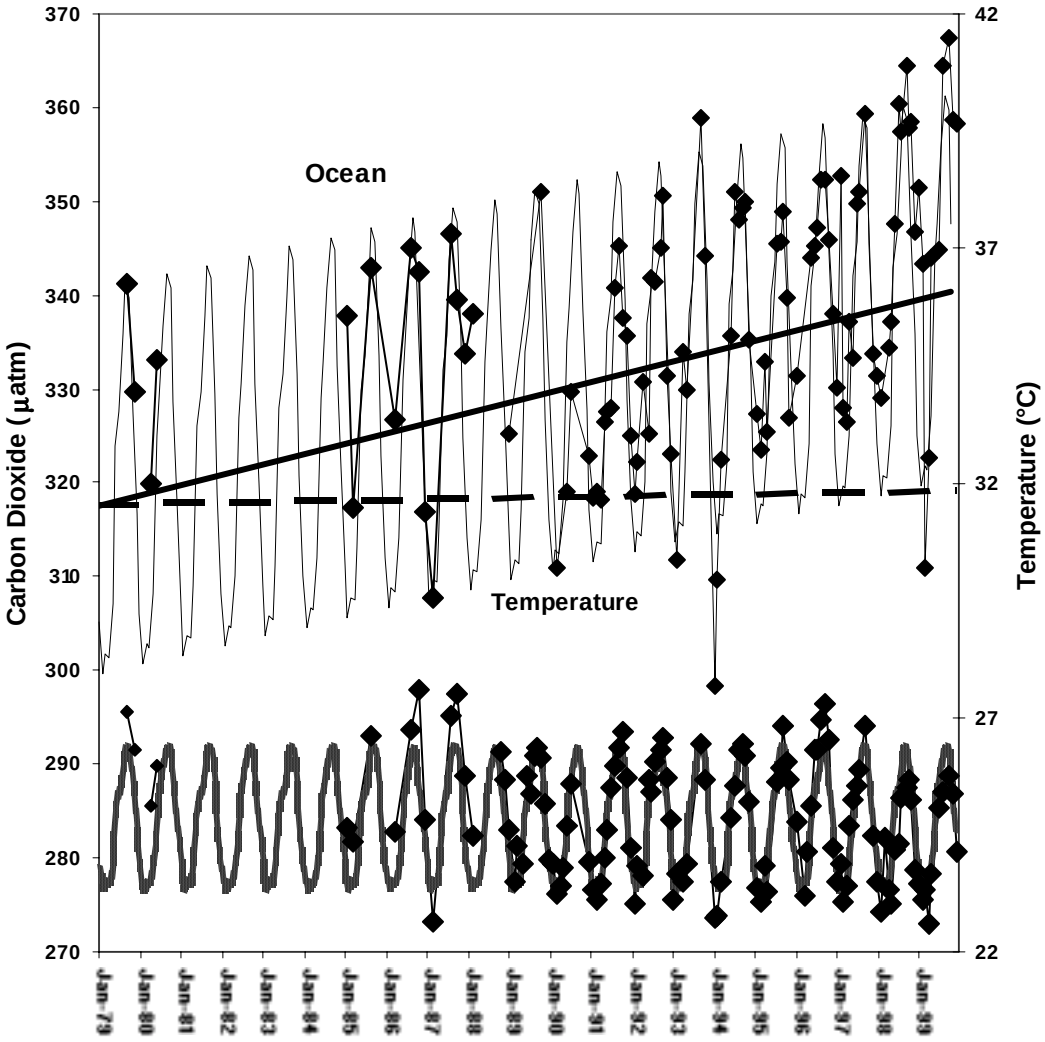

Figure 2.8 Model fit of fCO_2. Solid line represents model slope. Dashed line represents model slope without atmospheric increase.

Many scenarios can be imagined to explain the increase of surface seawater fCO_2 as a function of temperature and atmospheric CO_2. For instance, if sea surface temperatures showed a long term cooling trend, an increase of fCO_2 greater then that observed in the atmosphere is needed to counter the decrease attributed to the temperature change. Although the data supports the latter example, the scenario is probably incorrect. Sea surface temperatures reported during the NORPAX Equatorial Experiment were measured between 15-20ºN Latitude, 2 to 7 º further south of Station ALOHA. These values are on average 0.8 ºC warmer because of the more southern location.

Conclusions

Sea surface temperature correlates with fCO_2 and n35DIC during seasonal time scales. This correlation is the result of the interaction between air-sea exchange, mean annual undersaturation of fCO_2 with respect to the atmosphere, and mostly the thermodynamic control on the solution chemistry of CO_2 in seawater. During annual timescales, the marked increase of n35DIC between 1995 and 1999 is not observed for n35TA and fCO_2. This increase is correlated to a marked decrease of annual sea surface temperature, illustrating the thermodynamic control of the solution chemistry in seawater. The mean annual 13 μatm fCO_2 undersaturation can be explained by cooler waters advected past Station ALOHA or by primary production. An analysis of depth dependent profiles of n35DIC suggests primary production as the control (Chapter 5). Long term (20-year) trends of fCO_2 are consistent with the rise of atmospheric CO_2. Although the long-term trends suggest the changes of fCO_2 are controlled by atmospheric input of CO_2,

variability of n35DIC suggest that changes in the TA pool may actually control fCO_2 over long-term timescales. Overall, the NPSG is a sink for atmospheric CO_2 but the magnitude and consistency of the sink may depend on factors controlling DIC and TA.

Appendix A

I will compare the internal consistency between two estimates of apparent dissociation constants, K_1 and K_2, for carbonic acid in seawater using inorganic carbon field data from the HOT program. With the appropriate apparent dissociation constants, DIC, TA, salinity, temperature, phosphate and silicate concentrations, a time series of fCO_2 will be created with data from the HOT program. Between 1996 and 1998, pH_{total}, DIC, TA and fCO_2 were measured at Station ALOHA allowing for the closure of the inorganic carbon system (Table 2.6 & 2.7). Using the constants of Roy et al. (1993; 1994; 1996), calculated internal consistency between parameters is -4.1 ± 0.3% fCO2, 0.6 ± 0.2% DIC, -0.5 ±0.4% TA and 0.08 ±0.02% pH (Table 2.6). Using the constants of Mehrbach et al. (1973) refit by Dickson and Millero (1987), calculated internal consistency between parameters is -0.8 ± 0.4% fCO_2, 0.3 ± 0.2% DIC, 0.3 ± 0.2% TA and -0.01 ± 0.2% pH (Table 2.7; Lewis and Wallace 1995).

Table 2.6 Internal Consistency of carbon system parameters measured at Station ALOHA using the apparent thermodynamic constants of Roy et al. (1993, 1994, 1996).

Parameter Pair	**ΔpH**	**ΔTA**	**ΔDIC**	**ΔfCO_2**
pH-TA			-1.0%	-0.7%
pH-DIC		-0.9%		-1.7%
pH-fCO_2		0.5%	1.7%	
fCO_2-TA	-0.03%		1.0%	
fCO_2-DIC	-0.08%	-1.1%		
DIC-TA	0.36%			-9.7%
Mean	**0.08 ±0.02%**	**-0.5 ±0.4%**	**0.6±0.2%**	**-4.1 ±0.3%**

Table 2.7 Internal Consistency of carbon system parameters measured at Station ALOHA using the apparent thermodynamic constants of Mehrbach et al. (1973), refit by Dickson and Millero (1987).

Parameter Pair	**ΔpH**	**ΔTA**	**ΔDIC**	**ΔfCO_2**
pH-TA			-0.1%	-0.6%
pH-DIC		-0.1%		-0.7%
pH-fCO_2		0.7%	0.8%	
fCO_2-TA	-0.03%		0.1%	
fCO_2-DIC	-0.03%	0.1%		
DIC-TA	0.02%			-1.2%
Mean	**-0.01 ±0.02%**	**0.3 ±0.2%**	**0.3±0.2%**	**-0.8±0.4%**

Although there are a number of determinations, for simplicity, I only compare the more commonly used constants of Roy et al. (1993;1994;1996) with those of Mehrbach et al. (1973) as refit by Dickson and Millero (1987). Overall, the comparison between measured versus calculated values supports using the apparent constants of Mehrbach et al. (1973) refit by Dickson and Millero (1987). Our results agree with the recent experiments of Lueker et al. (2000), who studied Station ALOHA surface seawater to examine the internal consistency between fCO_2, DIC and TA. Although former studies at Station ALOHA utilized the apparent constants of Roy et al. (1993; 1994; 1996), this is

the first time all four carbon system parameters were measured and compared to access the complete carbon system. Sabine et al. (1995) used the constants of Roy et al. (1993; 1994; 1996) with measurements of DIC, TA and pH. Measurements of pH were made on the NBS scale and converted to the total seawater scale (Bates and Culberson (1977). Winn et al. (1998) also used the constants of Roy et al. (1993, 1994 1996) to calculate fCO_2 from DIC and TA, but fCO_2 values were not reported.

Apparent constants can be a function of the parameters used. For example, the constants of Roy et al. (1993, 1994 1996) were found to fit pH, DIC and TA data, while the constants of Mehrbach et al. (1976) were found to work with fCO_2, DIC and TA (Lee et al. 1997). Significant differences occur in those combinations of parameters (pH and fCO_2 from DIC and TA) in which K_2 is used in the calculation.

For example, using fCO_2 and TA to calculate pH is contingent upon the measurement uncertainties, and uncertainties in K_1. On the other hand, calculated DIC removed measurement uncertainties, and uncertainties in K_1, K_2 and the ratio of TA/DIC. It has been suggested that certain pairs are less desirable to calculate parameters of the CO_2 system (Millero et al. 1993). Of these, the combinations of TA and DIC should not be used to calculate pH and fCO_2, and pH and fCO_2 should not be used to calculate TA and DIC. Unfortunately, many oceanographic expeditions measure only DIC and TA.

Appendix B Data

n35DIC

	1989	1990	1991	1992	1993	1994	1995	1996	1997	1998	1999	n	Avg	sd
Jan	1962.3			1968.2		1970.66		1962.31	1973.8	1974.3	1984.6	**7**	**1970.8**	**7.8**
Feb	1964.1	1960.8	1966.3	1970.8	1967.4	1972.54	1976.6		1979.6	1977.2	1986	**10**	**1972.1**	**7.8**
Mar		1975	1972.8	1967.2		1975.23	1980.1		1975.2		1974.9	**7**	**1974.3**	**3.8**
Apr		1976.7	1971	1972.6	1973.8		1980.6		1974.6	1979.3	1982.8	**8**	**1976.4**	**4.2**
May	1974.1	1964.9	1970.9		1971.8		1974.2	1974.2	1971.5	1978.9	1987.1	**9**	**1974.2**	**6.1**
Jun		1960.9	1968.2	1967.5		1969.44		1968.03	1965.1	1978.6		**7**	**1968.2**	**5.4**
Jul		1954.3	1963.5	1968.1		1966.34	1967.9	1967.61	1970.6	1978.7	1974.3	**9**	**1967.9**	**6.8**
Aug	1967.8		1964.2	1960.6		1958.97	1965.1	1961.77	1969.3	1974	1976.7	**9**	**1966.5**	**6.0**
Sep	1958.0		1961.3	1964.9	1966.7	1962.18	1963	1958.16	1964.1	1976.2		**9**	**1963.8**	**5.5**
Oct	1962.6		1957.2	1962.6	1956	1963.98	1960.8	1959.11		1967	1974.5	**9**	**1962.6**	**5.6**
Nov	1963.9			1959.2		1966.11	1960.5			1971.6	1976	**6**	**1966.2**	**6.5**
Dec		1966.7	1960.8	1965				1969.14	1967.6	1979.7	1982.2	**7**	**1970.2**	**7.8**
n	**7**	**7**	**10**	**11**	**5**	**9**	**9**	**8**	**10**	**11**	**10**			
Avg	**1964.7**	**1965.6**	**1965.6**	**1966.1**	**1967.1**	**1967.3**	**1969.9**	**1965.0**	**1971.1**	**1976.0**	**1979.9**			
sd	**5.1**	**8.0**	**5.1**	**4.1**	**6.9**	**5.2**	**8.1**	**5.6**	**4.8**	**3.9**	**5.1**			

fCO_2

	1989	1990	1991	1992	1993	1994	1995	1996	1997	1998	1999	n	Avg	sd
Jan	325.3			325.0		298.4		331.5	330.1	331.4	351.5	**7**	**327.6**	**15.7**
Feb			318.3	318.8	311.7	309.6	327.3		352.7	329.0	343.4	**8**	**326.4**	**15.2**
Mar		311.0	319.0	322.2		322.4	323.6		328.1		311.0	**7**	**319.6**	**6.5**
Apr			318.1	330.7	334.0		332.8		326.4	334.3	322.6	**7**	**328.4**	**6.3**
May			326.5		329.9		325.4	344.0	337.2	337.1	343.9	**7**	**334.9**	**7.7**
Jun		319.1	327.6	325.2		335.7		345.2	333.4	347.6		**7**	**333.4**	**10.4**
Jul		329.8	328.0	341.9		351.1	345.4	347.2	349.7	360.4	344.8	**9**	**344.3**	**10.2**
Aug			340.8	341.4		348.1	345.7	352.4	351.1	357.4	364.4	**8**	**350.2**	**8.0**
Sep			345.3	345.1	359.0	349.4	348.8	352.4	359.4	364.4		**8**	**353.0**	**7.2**
Oct	351.0		337.6	350.5	344.1	349.9	339.8	346.0		357.9	367.5	**9**	**349.4**	**9.2**
Nov				331.4		335.2	327.0			358.5	358.6	**5**	**342.1**	**15.3**
Dec		322.8	335.7	323.0				338.0	333.7	346.7	358.3	**7**	**336.9**	**12.6**
n	**2**	**4**	**10**	**11**	**5**	**9**	**9**	**8**	**10**	**11**	**10**			
Avg	**338.2**	**320.7**	**329.7**	**332.3**	**335.7**	**333.3**	**335.1**	**344.6**	**340.2**	**347.7**	**346.6**			
sd	**18.2**	**7.8**	**9.8**	**10.7**	**17.5**	**19.3**	**9.9**	**7.0**	**11.9**	**12.9**	**18.0**			

CO_2*(aq)

	1989	1990	1991	1992	1993	1994	1995	1996	1997	1998	1999	n	Avg	sd
Jan	9.3			9.5		8.9		9.4	9.7	9.8	10.3	**7**	**9.5**	**0.4**
Feb			9.4	9.5	9.2	9.3	9.8		10.3	9.9	10.2	**8**	**9.7**	**0.4**
Mar		9.2	9.5	9.4		9.6	9.7		9.7		9.2	**7**	**9.5**	**0.2**
Apr			9.4	9.7	9.9		9.7		9.6	9.9	9.7	**7**	**9.7**	**0.2**
May			9.5		9.7		9.7	9.8	9.6	10.1	10.1	**7**	**9.8**	**0.2**
Jun		9.1	9.5	9.0		9.5		9.5	9.5	10.1		**7**	**9.5**	**0.3**
Jul		9.2	9.2	9.5		9.9	9.7	9.6	9.8	10.4	9.8	**9**	**9.7**	**0.4**
Aug			9.4	9.4		9.6	9.6	9.5	9.7	10.1	10.2	**8**	**9.7**	**0.3**
Sep			9.5	9.5	9.8	9.6	9.5	9.4	9.8	10.2		**8**	**9.7**	**0.3**
Oct	9.7		9.2	9.6	9.6	9.6	9.4	9.5		9.9	10.2	**9**	**9.6**	**0.3**
Nov				9.3		9.5	9.1			10.0	10.0	**5**	**9.6**	**0.4**
Dec		9.4	9.3	9.3				9.8	9.6	10.2	10.4	**7**	**9.7**	**0.4**
n	**2**	**4**	**10**	**11**	**5**	**9**	**9**	**8**	**10**	**11**	**10**			
Avg	**9.5**	**9.3**	**9.4**	**9.4**	**9.6**	**9.5**	**9.6**	**9.6**	**9.7**	**10.1**	**10.0**			
sd	**0.3**	**0.1**	**0.1**	**0.2**	**0.3**	**0.3**	**0.2**	**0.2**	**0.2**	**0.2**	**0.4**			

HCO_3

	1989	1990	1991	1992	1993	1994	1995	1996	1997	1998	1999	n	Avg	sd
Jan	1715.9			1722.1		1726.9		1715	1732.4	1741.2	1764.4	**7**	**1731.1**	**17.3**
Feb			1728.1	1733	1713.7	1729.6	1711.2		1744.6	1751.5	1768.9	**8**	**1735.1**	**19.3**
Mar		1720.5	1735.9	1718.4		1735.6	1727.2		1738.8		1733.2	**7**	**1729.9**	**8.0**
Apr			1723.6	1736.3	1739.1		1718.1		1732.4	1751.3	1758.7	**7**	**1737.1**	**14.4**
May			1723.1		1732.5		1724.5		1722.4	1757.6	1766.3	**6**	**1737.7**	**19.3**
Jun		1711.3	1719.3	1702.9		1717.5		1723.1	1711.5	1754		**7**	**1719.9**	**16.4**
Jul		1699.5	1704.6	1727.5		1720	1717.2	1695.3	1728.9	1763.4	1728.7	**9**	**1720.6**	**20.5**
Aug			1711.5	1708.4		1707.2	1714.8	1700.9	1728.7	1742.1	1751.3	**8**	**1720.6**	**18.1**
Sep			1712.2	1716.2	1732.5	1707	1706.4	1699.9	1726.1	1750.9		**8**	**1718.9**	**16.8**
Oct	1710.2		1691.8	1715.6	1722.7	1714.2	1711.5	1699.9		1741.3	1742.1	**9**	**1716.6**	**16.8**
Nov				1698.2		1717.7	1703.8	1709.9		1752.5	1750.2	**6**	**1722.1**	**23.6**
Dec		1731.2	1707.4	1706.7				1728.2	1730.5	1758.2	1759.2	**7**	**1731.6**	**21.2**
n	**2**	**4**	**10**	**11**	**5**	**9**	**9**	**8**	**10**	**11**	**10**			
Avg	**1713.1**	**1715.6**	**1715.8**	**1716.8**	**1728.1**	**1719.5**	**1715.0**	**1709.0**	**1729.6**	**1751.3**	**1752.3**			
sd	**4.0**	**13.5**	**12.8**	**12.3**	**10.0**	**9.7**	**7.7**	**12.1**	**8.9**	**7.3**	**13.9**			

CO_3

	1989	1990	1991	1992	1993	1994	1995	1996	1997	1998	1999	n	Avg	sd
Jan	239.1			236.9		244.6		235.5	228.5	231.1	223.8	**7**	**234.2**	**7.0**
Feb			234.9	232.7	238.4	236.1	221.3		220.7	229.6	227.3	**8**	**230.1**	**6.6**
Mar		236.3	234.3	233.6		236	226.8		228.5		242.5	**7**	**234.0**	**5.2**
Apr			234.2	231.5	228.2		224.2		230.7	230.1	234.1	**7**	**230.4**	**3.5**
May			233.4		233.1		227.1	232.5	232.5	227.7	231.8	**7**	**231.2**	**2.6**
Jun		243	237.9	245.5		233.5		233.6	237.6	230.7		**7**	**237.4**	**5.4**
Jul		240.5	242	239.1		230.8	234.8	234	234.6	226.3	232.9	**9**	**235.0**	**4.9**
Aug			239.7	239.4		236.8	237.1	237.3	237.4	231.4	231	**8**	**236.3**	**3.3**
Sep			241	242.1	239.6	236.8	241.1	241.2	240.8	231.8		**8**	**239.3**	**3.4**
Oct	233.6		243.1	240.7	239.5	236.2	241.9	241.7		235.6	229.2	**9**	**237.9**	**4.6**
Nov				239.3		238.1	244.6			234.1	234.3	**5**	**238.1**	**4.3**
Dec		239.2	239.5	239.5				229.4	236	228.2	224.3	**7**	**233.7**	**6.3**
n	**2**	**4**	**10**	**11**	**5**	**9**	**9**	**8**	**10**	**11**	**10**			
Avg	**236.4**	**239.8**	**238.0**	**238.2**	**235.8**	**236.5**	**233.2**	**235.7**	**232.7**	**230.6**	**231.1**			
sd	**3.9**	**2.8**	**3.6**	**4.2**	**5.0**	**3.7**	**8.6**	**4.2**	**5.9**	**2.7**	**5.5**			

CHAPTER III

PROCESSES REGULATING OXYGEN AND CARBON DIOXIDE IN SURFACE WATERS WEST OF THE ANTARCTIC PENINSULA

Abstract

Geographic surveys of O_2 and CO_2 concentrations in surface waters west of the Antarctic Peninsula show large temporal and spatial variability as predicted for polar regions with winter ice cover and vernal phytoplankton blooms. The saturation states of surface seawater fugacity of carbon dioxide ($fCO_{2\{Sat\}}$) range from 27 to 112% relative to the atmosphere, and oxygen saturation states ($O_{2\{Sat\}}$) range from 80 to 157% of the corresponding air-saturated values. Areas of O_2 supersaturation and fCO_2 undersaturation occurred mostly in coastal waters and were correlated with increases in chlorophyll *a*, suggesting a biological control. Net community production (NCP) showed offshore to onshore gradients with O_2 production as high as 25 μmol O_2 m^{-3} day^{-1} and CO_2 consumption as high as 15 μmol C m^{-3} day^{-1} in coastal areas. Areas of surface water O_2 and fCO_2 supersaturation were found off-shelf, suggesting heating as a locally significant process. Areas of fCO_2 supersaturation and O_2 undersaturation were also found in selected off-shelf, regions suggesting upwelling as a source of the CO_2-enriched waters. Finally, within selected coastal areas O_2 and fCO_2 undersaturations were found, suggesting cooling as a locally significant process. The magnitude and seasonal cycle of biological, chemical and physical processes can explain the temporal and regional variability that is observed.

Introduction

The Southern Ocean comprises 22% ($77x10^6$ km^2) of the total global ocean surface, but remains poorly sampled relative to more accessible oceanic habitats (Tomczak and Godfrey, 1994). Open ocean areas in the Southern Ocean have high nutrient concentrations but relatively low standing stocks of phytoplankton and low rates of primary production (Holm-Hansen and Mitchell, 1991). In sharp contrast to these high nutrient, low productivity oceanic habitats, coastal regions of Antarctica exposed to the annual advance and retreat of sea ice support seasonal phytoplankton blooms with high rates of primary production (Smith, 1985; Holm-Hansen et al., 1989; Moore et al., 1999). The Antarctic marine habitat experiences extreme seasonal cycles. The summer season is characterized by nearly continuous solar radiation, relatively warm temperatures and sea ice ablation; all of these processes contribute to a decrease in mixed-layer depth. The fall and winter seasons are characterized by decreased solar radiation, decreasing temperature and sea ice formation, which all contribute to deeper mixed-layer depths.

The capacity of the world's ocean to sequester CO_2 is dependent on the response of the biological and solubility pumps in altering CO_2 concentrations in the surface waters (Volk and Hoffert, 1985). The Southern Ocean's role in moderating increasing atmospheric CO_2 levels is uncertain because of unpredictable spatial and temporal heterogeneity of the biological and solubility pumps and the previously mentioned undersampling in critical regions. Although the flux of CO_2 into the Southern ocean is predicted to be high, the long-term storage is low (Sabine et al. 1999; Calderia and Philip 2000). Predicting future concentrations and estimating fluxes in data-poor regions will

require accurate, predictive ecosystem models and an understanding of the processes controlling CO_2 variations temporally and spatially.

Measurements of atmospheric O_2/N_2 ratios may help constrain the contribution of biological processes to the oceanic uptake of atmospheric CO_2 (Keeling and Shertz, 1992; Bender et al., 1996; Sherr and Sherr, 1996). Seasonal changes in the O_2/N_2 ratio in air result from variations in net terrestrial and oceanic primary production and oceanic heating and cooling. In the Southern Hemisphere (especially the Southern Ocean), models predict marine autotrophic production and heterotrophic respiration to be the primary controls of seasonal variations of the O_2/N_2 ratio in air (Keeling et al., 1993; Sherr and Sherr, 1996). Coupling atmospheric changes of O_2/N_2 ratios to oceanic biological production and consumption will require an understanding of the links between organic and inorganic carbon cycling in the ocean and O_2 fluxes at the air-sea interface. Additionally, the interaction between the physical, chemical and biological controls on O_2 and CO_2 concentrations must be understood to predict future changes of the ecosystem in response to climate change.

The marine environment west of the Antarctic Peninsula is situated in a climatically sensitive region and is an ideal location to investigate the interaction between biological, chemical and physical processes. (Smith et al., 1999b). The environment includes a temporally variable (interseasonal and interannual) sea ice zone, open ocean areas, shelf water and coastal embayments. The Palmer Long-Term Ecological Research (LTER) Program was established in 1990 to study the physical determinants on the Antarctic marine ecosystem, especially the interconnections between climate variability

and habitat variability, and the response of the marine ecosystem to change. The central tenet of the LTER program is that the annual advance and retreat of sea ice is a major physical determinant of spatial and temporal changes in the structure and function of the Antarctic marine ecosystem, from annual primary production and particle export to breeding successes in seabirds (Smith 1995). The timing of the bloom in the region west of the Antarctic Peninsula may depend on a variety of interconnected factors including water column stability induced by seasonal ice melt, light, temperature and nutrients (Smith et al., 1996). Even though phytoplankton blooms can be transient events that follow the ice edge in open waters, they may have significant impacts on the annual fluxes of CO_2.

The use of ship-based underway systems has become prevalent in studies to map and understand CO_2 dynamics in open ocean and near shore areas (Sabine and Key, 1998; van Geen et al., 2000). Interpretation of these data is often difficult because CO_2 variability is a function of the spatiotemporal scales of the controlling process(es) (Simpson 1985). Often, more than one process is responsible for controlling CO_2 concentrations. Simultaneous measurements of dissolved O_2 concentrations can help identify the processes that control seawater CO_2 (DeGrandpre et al., 1997; DeGrandpre et al., 1998). For instance, simultaneous measurements of fCO_2 undersaturation and O_2 supersaturation both with respect to the atmosphere would implicate net photosynthesis as a controlling process since no other means could produce this effect. Additionally the only possible source of simultaneous fCO_2 supersaturation and O_2 undersaturation would be net respiration. The use of property-property relationships between $fCO_{2\{Sat\}}$, $O_{2\{Sat\}}$,

temperature, salinity and chlorophyll *a* can help elucidate the relative role of physical, chemical and biological controls on CO_2 distributions.

The goal of this research was to determine the spatial and temporal O_2 and CO_2 distributions and the major processes regulating their concentrations in Southern Ocean surface waters west of the Antarctic Peninsula. The ratio of $O_{2\{Sat\}}$ to $fCO_{2\{Sat\}}$ will be used to elucidate processes controlling fCO_2 and O_2 distributions. Specific examples will be taken from smaller subsets of the underway data to quantify changes in fCO_2 and O_2 pressures and concentrations.

Materials and Methods

Setting

The LTER program conducts annual oceanographic research cruises over a geographically defined grid west of the Antarctic Peninsula (Waters and Smith, 1992). The entire LTER study region covers an area 900 by 200 kilometers. The grid consists of ten lines 100 km apart, roughly perpendicular to the coast, extending 200 km off-shore. The "grid lines" are labeled depending on the distance from the first line located just south of Marguerite Bay. For example, the "200 line" is the grid line 200 km north of the 0 gridline, and this line extends perpendicular to Marguerite Bay. Station locations are 20 km apart along each line. Portions of this grid are sampled at least once per year in the months of January and February during the annual LTER cruise. During the 1997 austral summer field season, the 200 to 600 lines were sampled (Fig. 3.1). During austral winter 1999, a cruise was conducted to specifically study the formation of sea ice, and the 200 and 600 lines were sampled. These lines are located just off Marguerite Bay and Anvers

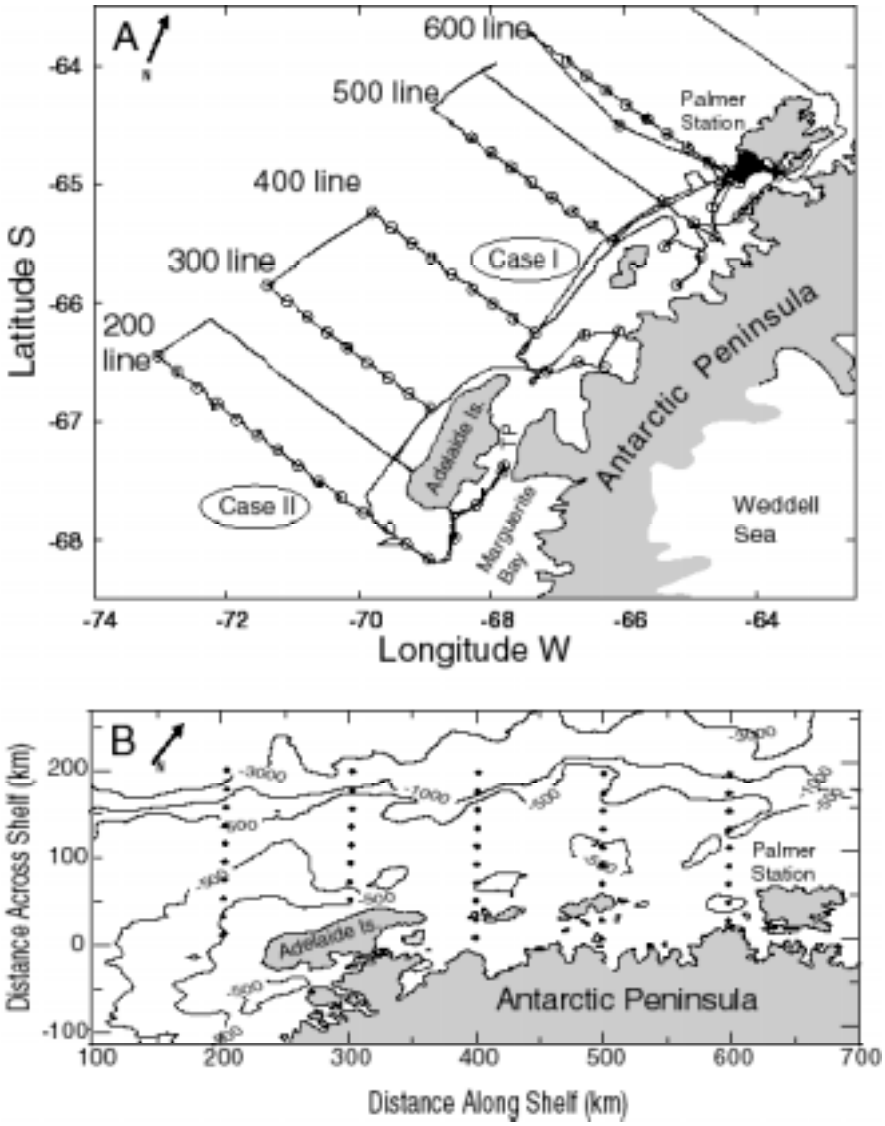

Figure. 3.1. (A) Long Term Ecological Research (LTER) program study area in the region west of the Antarctic Peninsula. Station locations are represented with open circles, and the cruise track is represented by a solid line. Stations are located approximately 20 km apart perpendicular to the Peninsula and aligned in transects 100 km apart, parallel to the Peninsula. Tickle Passage is represented with a TP. (B) Map of the LTER study area showing the bathymetric contours. Stations are represented by solid circles.

Island. A smaller grid, located in Arthur Harbor was also sampled approximately four times throughout each cruise. Other selected coastal areas where studies were conducted included Marguerite Bay and Crystal Sound (Fig 3.1).

Continuous Underway Sampling System

During the 1997 austral summer LTER field season, an automated underway fCO_2, pH and O_2 measurement system was deployed on the *Research Vessel Polar Duke*. The underway system acquired seawater from the ship's bow intake located approximately 5 meters below the sea surface, and atmospheric air collected from the top of the ship's bridge approximately 10-12 meters above the sea surface. Surface seawater fCO_2 was determined by continuously pumping water through a counter flow rotating disk type equilibrator (Bjork, 1948; Cross et al., 1956; Schink et al., 1970; Sabine and Key, 1998) as described previously by Carrillo and Karl (1999). The mole fractions of CO_2 and water vapor were measured with a LICOR model 6262 infrared CO_2 and H_2O analyzer. The CO_2 mole fraction was converted to fCO_2 using the total pressure and the viral equations of state for CO_2 (DOE, 1994). The saturation state, $fCO_{2\{Sat\}}$, was calculated using the equation:

$$fCO_{2\{Sat\}} = (\text{Measured } fCO_2 / \text{ Atmospheric } CO_2)*100$$

where atmospheric fCO_2 is 358 μatm. The continuous measurement system was periodically calibrated (every 2.5 hr) using compressed gas standards with nominal mixing ratios of 259.28, 303.86, and 373.19 parts per million (ppm by volume). These gas standards were calibrated with World Meteorological Laboratory (WMO) primary standards obtained and certified by the NOAA Climate Monitoring and Diagnostics

Laboratory (CMDL). Equilibrator temperature was measured with an Omega RTD, and system pressure was measured with a Setra pressure transducer. Between calibrations, equilibrator and atmospheric samples were measured every 5 minutes. The entire measurement system was automated using a PC computer and LabVIEW® software. Temperature and salinity were measured with a Sea-Bird thermosalinograph positioned at the intake that was periodically calibrated by bottle salinity.

Oxygen concentration was monitored with 3 Endeco type 1125 pulsed oxygen electrodes. Electrode output was calibrated daily to bottle oxygen samples taken from CTD casts and with water collected from the underway system just downstream from the electrodes. The overall mean and standard deviation between electrodes after calibration with discrete samples was 4.8 ± 5.4 μM (n=8198). Oxygen saturation was calculated using the equations of Weiss (1970).

Net Community Production and Respiration

Net community production (NCP) was estimated by variations in O_2 and CO_2 during light incubation experiments, and dark community respiration (DCR) was estimated by variations in O_2 and CO_2 during dark incubation experiments. Net community production is defined as gross primary production minus algal and heterotrophic respiration (Williams 1993). Oxygen incubation experiments were conducted in 140 ml iodine flasks at surface seawater temperature. For each measurement, the whole flask was fixed and titrated potentiometrically with a standardized solution of soduim thiosulfate (HOT Program Protocols; http://www.hahana.soest. hawaii.edu/hot/protocols/protocols.html). Changes in CO_2 were

determined by direct measurements of DIC following either light or dark incubations. Incubation experiments were conducted in 300 ml Pyrex bottles at surface seawater temperatures and were terminated by the addition of $HgCl_2$. DIC was determined coulometrically using a Single Operator Metabolic Multi-parameter Analyzer (SOMMA) system (Johnson et al., 1987). Oxygen and DIC measurements have analytical precision of approximately 0.05% over the concentration ranges observed in this study.

Ancillary Data

Water samples were obtained from discrete water depths at hydrographic stations using a Bio-optical Profiling System (BOPS; (Smith et al., 1984). This system includes a Sea Bird conductivity-temperature-depth (CTD) mounted on a rosette with Go Flo bottles. Chlorophyll *a* samples were collected during the cruise from the underway surface seawater system and from the BOPS. Chlorophyll a was extracted and analyzed using fluorometer standard methodology (Smith et al., 1981). Nutrients (nitrate plus nitrite) were collected and analyzed using a Technicon Autoanalyzer.

Results

Data Overview

Analysis of the underway system data shows that surface seawater fCO_2 in 1997 ranges from 100 μatm to 390 μatm compared to a mean atmospheric value of 358 ± 3 μatm for the LTER region (Fig 3.2A). Surface seawater O_2 concentrations range from 300 to 550 mmol m^{-3} (Fig 3.2B). Temperature ranged from -1.8 to 2.7º C, and salinity ranged from 29.5 to 33.8 (Fig 3.2C & 3.2D). All parameters show a high degree of variability occurring on or after year day 35. This period corresponds to a time during transit into Marguerite Bay and the northbound transit near the coast.

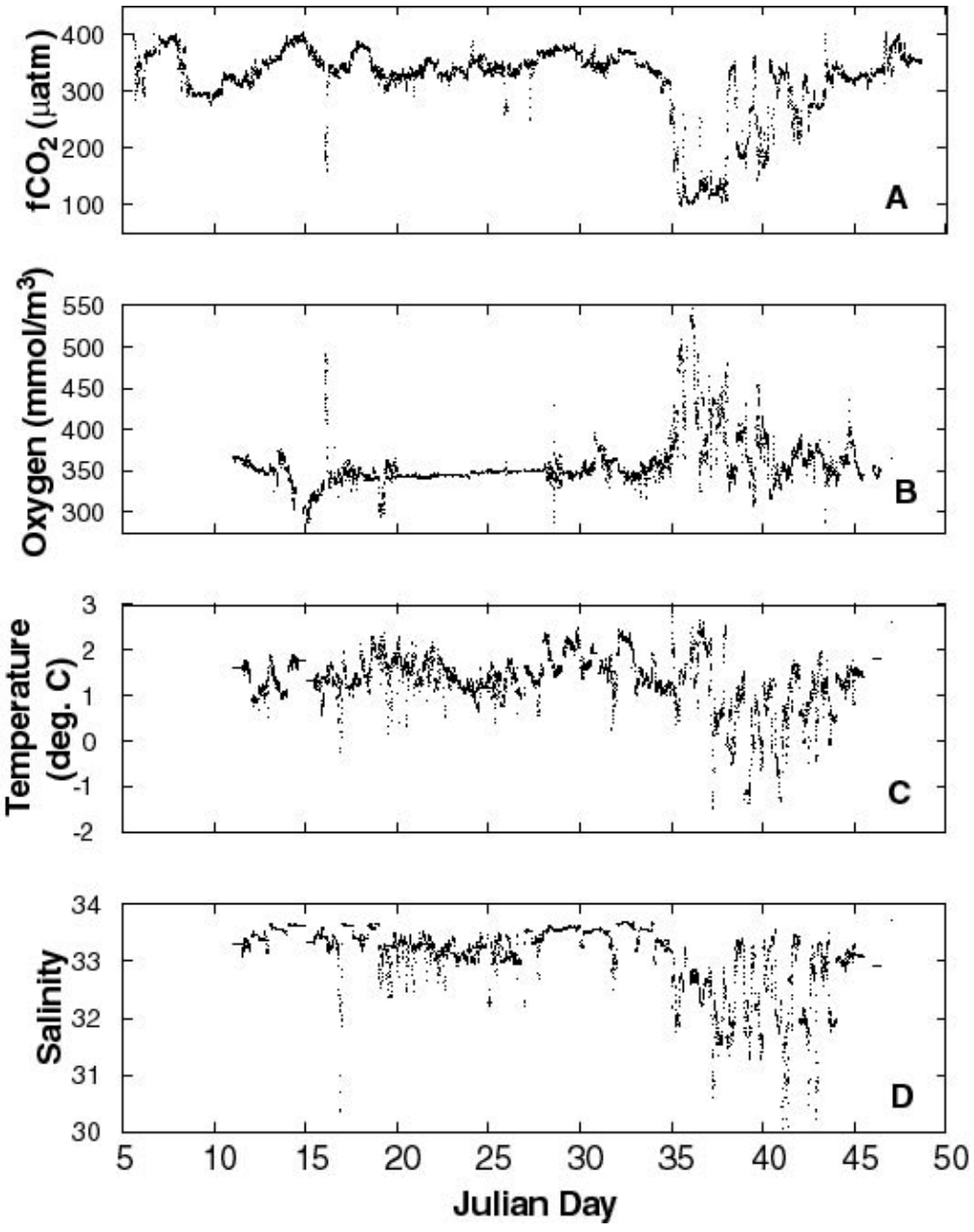

Figure 3.2. Year day versus (A) fCO_2 (µatm), (B) Oxygen concentration (mmol m^3), (C) temperature and (D) salinity.

Plots of $fCO_{2\{Sat\}}$ versus temperature or salinity show little correlation. However, $fCO_{2\{Sat\}}$ and $O_{2\{Sat\}}$ show a much better linkage. (Fig 3.3A, 3.3B & 3.3C). Typically, areas of surface ocean fCO_2 supersaturation were found at the outer shelf, and areas of undersaturation were encountered in coastal waters, so $fCO_{2\{Sat\}}$ typically increased with increasing distance from shore (Fig 3.4A). Generally, colder, fresher waters were encountered near the coast and warmer, saltier waters were found off-shelf (Fig 3.4B & 3.4C).

These underway data segregate into one of four quadrants on a graph of $O_{2\{sat\}}$ versus $fCO_{2\{Sat\}}$, with the origin at 100% $O_{2\{Sat\}}$ and 100% $fCO_{2\{Sat\}}$ (Fig 3.3C). Plotting the

spatial distribution of points based on their quadrant location from Fig 3.3C shows that most points in quadrant I are located in Marguerite Bay and near the coast. The maximum $O_{2\{Sat\}}$ (155%; 550 mmol m^{-3}) and minimum $fCO_{2\{Sat\}}$ (35%; 90 μatm) are found in Marguerite Bay. Generally, data in quadrant II are found in the southern offshore region of the LTER grid between the 200 and 400 line (Fig 3.3D). These values represent slight O_2 and fCO_2 supersaturations and are correlated with the warmest (2.5º C) surface waters encountered (Fig 3.4B). Data in quadrant III are located in the northern offshore region between the 500 and 600 line. These values are slightly supersaturated with respect to fCO_2 and undersaturated with respect to O_2. Data collected during the austral winter, Jul 1999, are represented by a rectangle located in quadrant III. Winter data show an undersaturation of O_2 (85%) and supersaturation of fCO_2 (115%). The horizontal and

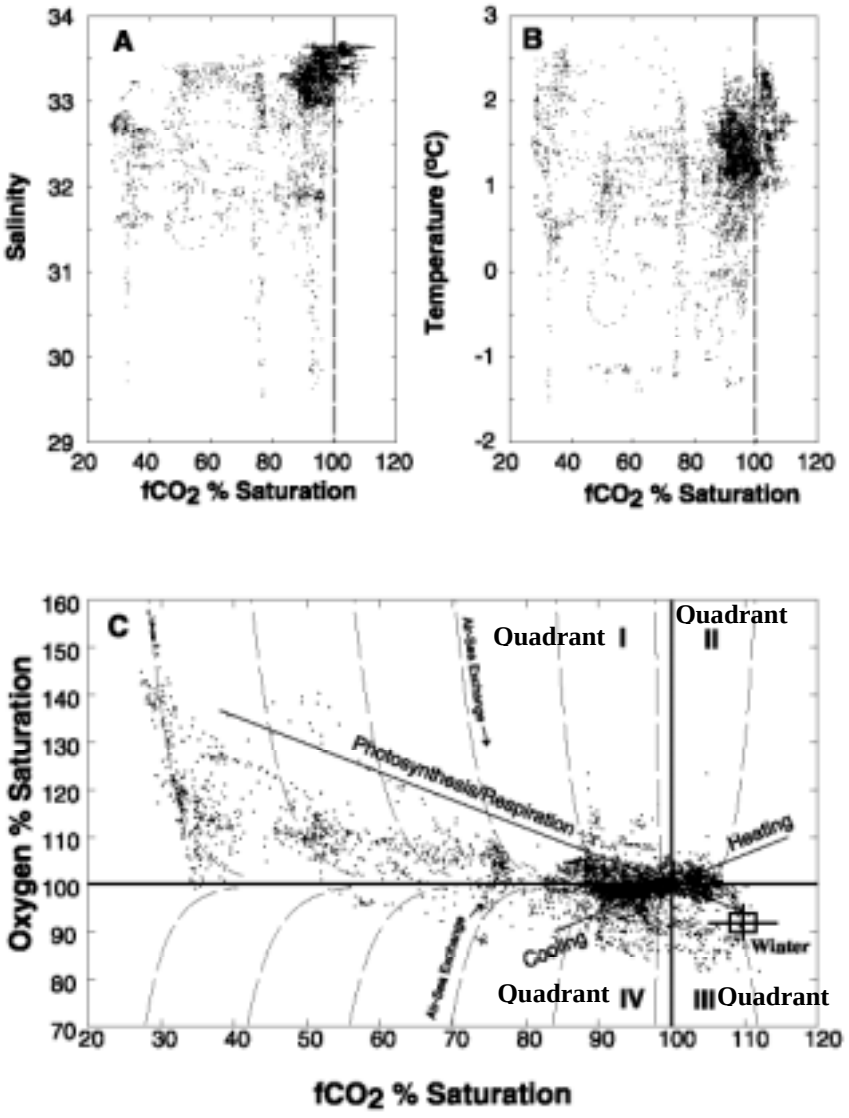

Figure 3.3 The fugacity of CO_2 versus (A) salinity and (B) temperature. The vertical dashed lines represent 100% $fCO_{2\{Sat\}}$. (C) The fugacity of CO_2 versus O_2 saturation. Vertical and horizontal solid lines represent 100% saturation levels of O_2 and fCO_2. The intersection of these lines in the lower right corner denotes the origin and represents 100% O_2 and fCO_2 air-saturation. Based on these lines, the figure is separated into 4 quadrants. Quadrant I is located in the upper left corner. Quadrant II is located in the upper right corner. Quadrant III is located in the lower right corner. Quadrant IV is located in the lower left corner. The open rectangle in quadrant III represents the mean of data collected during the austral winter, July 1999. The standard deviations are represented by the horizontal and vertical lines. The solid line that extends from the origin into quadrant I represents net organic matter production of O_2 and consumption of CO_2 at a theoretical PQ of 1.3. The solid line that extends from the origin into quadrant II represents heating with a temperature change of +4.0 ° C. The dashed line that extends from the origin into quadrant IV represents cooling with a temperature change of -4.0 °C. Dashed lines represent the $O_{2\{Sat\}}$:$fCO_{2\{Sat\}}$ values based on a model of air-to-sea exchange.

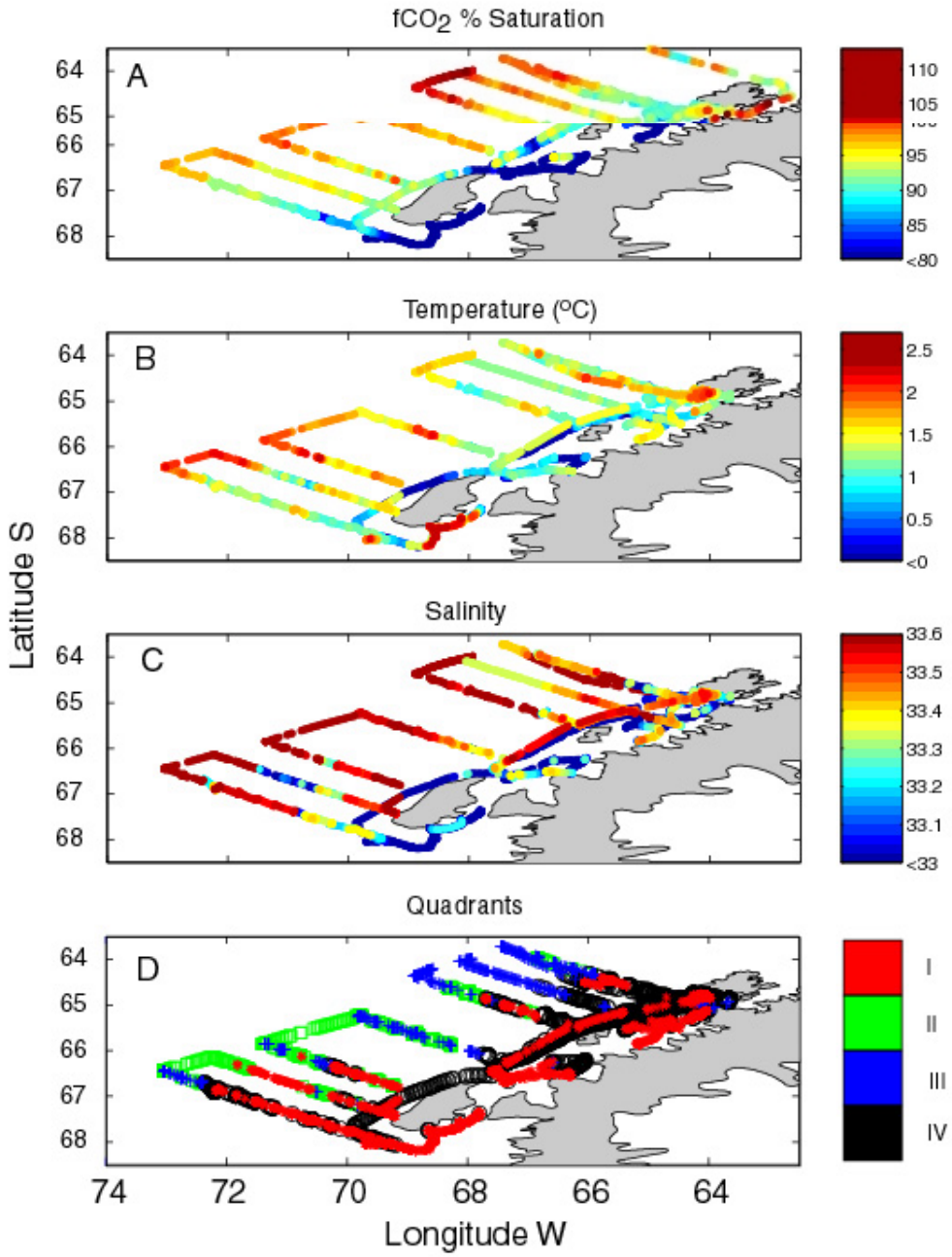

Figure 3.4 Spatial distribution of (A) fCO_2 saturation, (B) temperature, (C) salinity and (D) quadrants as defined in Figure 3C.

vertical bars represent the standard deviation of all measured values. Finally, data in quadrant IV are located generally near the coast. These values represent fCO_2 and O_2 undersaturation states. Two case studies are presented to illustrate the time and space variability of CO_2 and O_2 inventories.

Case Study I: Effect of Cooling and Net Organic Matter Production

The effects of cooling and net organic matter production on $O_{2\{Sat\}}$ and $fCO_{2\{Sat\}}$ will be illustrated using a subset of the underway data. On Jan 27, a 159 km transect was conducted parallel to the Antarctic Peninsula approximately 50 km offshore between 67.5° and 65.5° W (400 to 550 line; Fig 3.1A). Approximately two weeks later (Feb 9-10), this area was resampled from south to north. The initial survey on Jan 27 showed that temperature, salinity and $O_{2\{Sat\}}$ were relatively constant at 1.5 ± 0.1^{o} C, 33.5 ±0.1 and 100.0% respectively (Fig 3.5A, 3.5B & 3.5C). The fugacity of CO_2 was nearly constant at $97.0 \pm 1.1\%$, with the exception of an anomalously low spike (70% saturation) at approximately 67.0° W (Fig 3.5D). Chlorophyll *a* concentrations at stations 400.040 and 500.040 during the Jan 27 transect were 0.6 mg/m^3 (Fig 3.5E).

On Feb 9-10, during the second survey of this area, temperature and salinity showed an overall cooling and a freshening. In the southern portion of the transect, temperature ranged from 0 to -1.5^{o} C and salinity ranged from 31.9 to 32.1 (Fig 3.5A & 3.5B). In the northern portion of the transect, temperatures ranged from 0 to 0.5^{o} C, and salinity ranged from 29.5 to 31.5. Oxygen saturation decreased overall with values ranging from 86 to 95% in the southern portion of the transect to 95 to 99% in the north (Fig 3.5C).

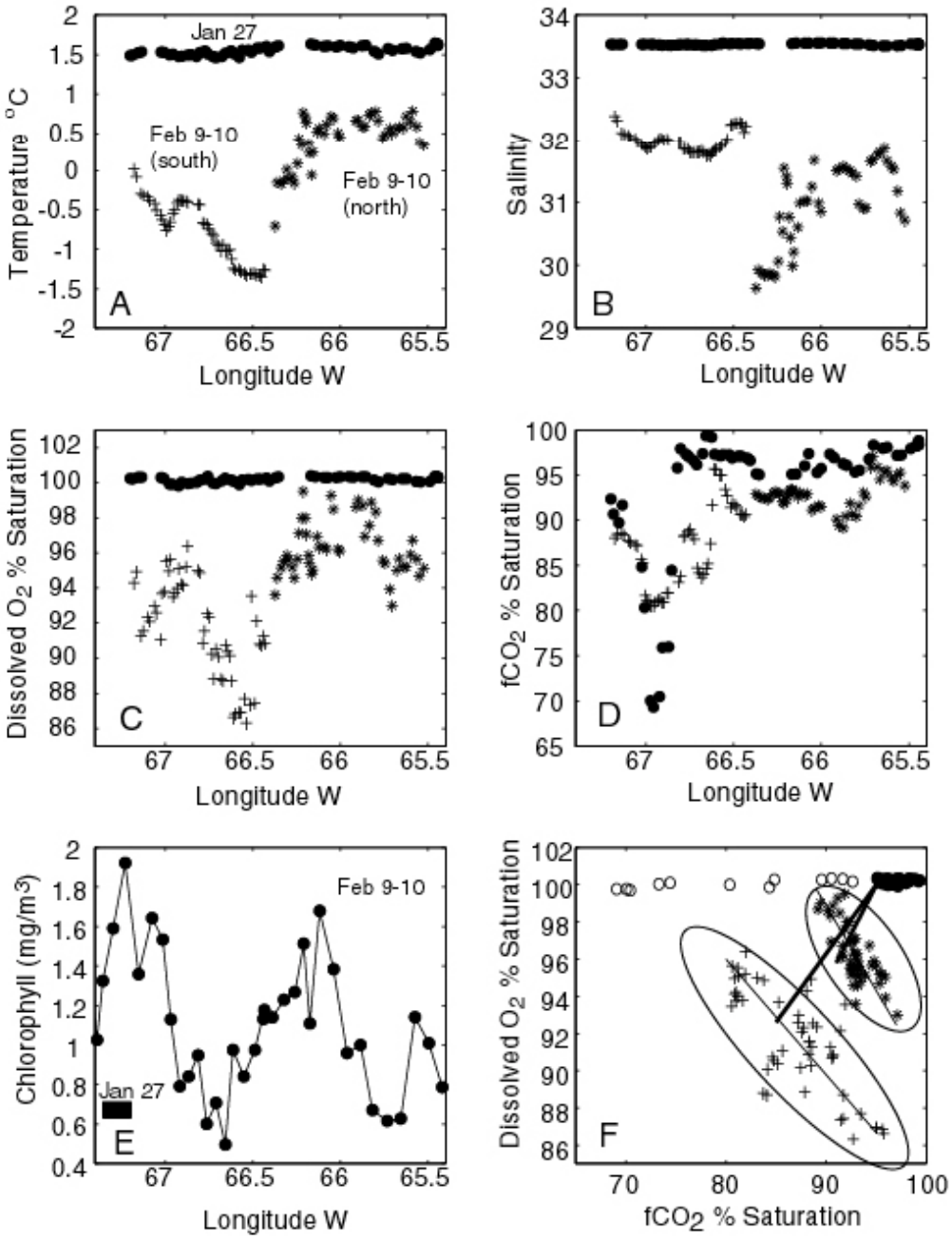

Figure 3.5 Longitude W versus (A) temperature, (B) salinity, (C) O_2 saturation, (D) fCO_2 saturation and (E) Chlorophyll (mg/m^3). (F) The fugacity of CO_2 saturation versus O_2 saturation. Filled circles represent values from the Jan 27 transect. Plus signs represent values from the southern half of the Feb 9-10 transect. Asterisks represent values from the northern half of the Feb 9-10 transect.

The fugacity of CO_2 generally showed a decrease in saturation except for the area that had a relatively low fCO_2 value on Jan 27 (Fig 3.5D). In the northern portion of the transect, values ranged from 90 to 97% saturation. In the south, values ranged from 80 to 96 % saturation. Chlorophyll samples were taken from the underway system during the transect north (Feb 9-10), and values ranged from a maximum of 1.9 to a minimum of 0.5 mg m^{-3} (Fig 3.5E).

A graph of $O_{2\{Sat\}}$ versus $fCO_{2\{Sat\}}$ can be described by three clusters (I, II and III; Fig 3.5F). A positive correlation is shown between cluster I (representing Jan 27 data) and clusters II and III (representing the north and south components the Feb 9-10 data). The anomalous 12 circles were not used in the correlation analysis and represent the low $fCO_{2\{Sat\}}$ spike (Fig 3.5F). Fitted lines show the predicted values of fCO_2 and O_2 based on a cooling of –2.5 and –1 deg C and freshening of 1.5 and 2.5 as described by the changes in temperature and salinity. A model II linear regression (geometric mean) was fit for the northern and southern cluster of points with slopes of -0.6 (0.5 to 0.8 at the 95% confidence interval) and -0.9 (0.7 to 1.2 at the 95% confidence interval), respectively.

Case Study II Organic Matter Production, Respiration and Air-to-Sea Exchange

A second case study illustrates the effect of net organic matter production, respiration and air-sea exchange in determining the $O_{2\{Sat\}}$:$fCO_{2\{Sat\}}$ of surface waters. Between Feb 1 and Feb 3, a 300 km offshore-to-onshore transect was conducted into Marguerite Bay. Oxygen saturation increased off to onshore into Marguerite Bay, with values ranging from 95 to 158% (Fig. 3.6A). In contrast, the fugacity of $CO_{2\{Sat\}}$ decreased from offshore to onshore, with values ranging from 105 to 27% (Fig. 3.6A).

Salinity decreased offshore to onshore with values ranging from 33.6 to 30.5 (Fig. 3.6C). Temperature generally decreases from offshore to onshore (with values ranging from 2.5 to 0.5º C), except within Marguerite Bay where temperatures were relatively warm at 1.7º C (Fig. 3.6B).

Net community production increased from offshore to onshore with the exception of one station in Marguerite Bay. Estimates based on changes of oxygen in light bottles ranged from 0.5 to 23.8 mmol O_2 m^{-3} d^{-1} (Table 3.1; Fig 3.6B). Within Marguerite Bay, estimates of NCP based on changes of DIC in light bottles ranged from 9.0 to 19.2 mmol C m^{-3} d^{-1}. Dark community respiration (DCR) also increased from off to onshore. Estimates based on changes of O_2 in dark bottles range from 0.9 to 23.7 mmol O_2 m^{-3} d^{-1} (Fig 3.6B). Within Marguerite Bay estimates of DCR based on changes of DIC in dark bottles ranged from 0.3 to 5.1 mmol C m^{-3} d^{-1}. Chlorophyll *a* concentrations increased offshore to onshore with values ranging from 0.1 to 20.7 mg m^{-3} (Table 3.1; Fig 3.6C). Nitrate plus nitrite concentrations decreased from offshore to onshore with concentrations ranging from 0.29 to 27.33 mmol m^{-3} (Table 3.1; Fig 3.6C).

Discussion

The discussion is divided into three sections. The first is devoted to describing the processes that change $O_{2\{Sat\}}$ and $fCO_{2\{Sat\}}$. The second section describes and analyzes the spatial and seasonal distributions of $O_{2\{Sat\}}$:$fCO_{2\{Sat\}}$. The last two sections use subsets of the data as specific examples of the processes that can change $O_{2\{Sat\}}$:$fCO_{2\{Sat\}}$.

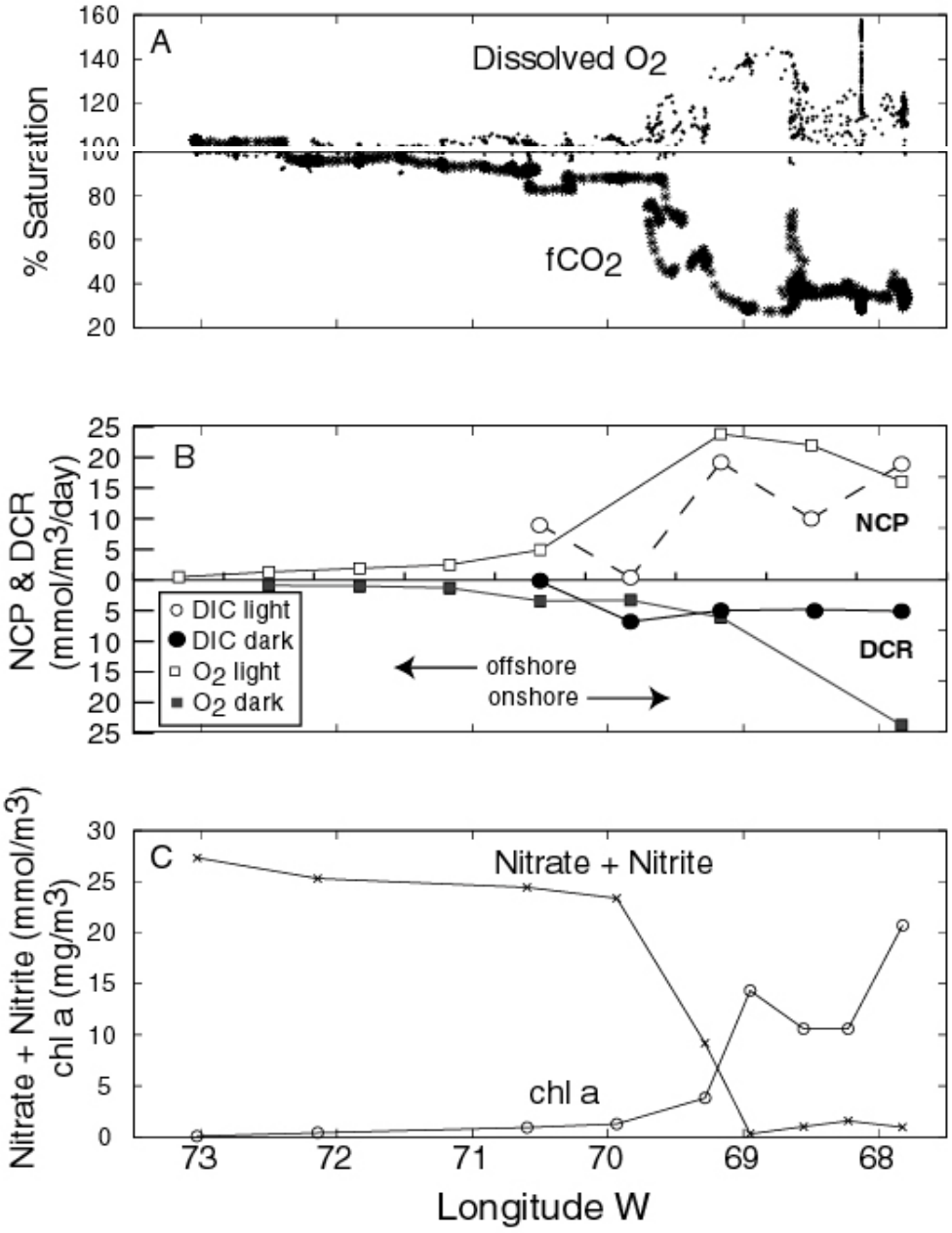

Figure 3.6 Longitude versus (A) fCO_2 and O_2 saturation (B) Net community production and dark community respiration measured by DIC and O_2 light dark bottle incubations (C) [Nitrate + Nitrite] and chlorophyll *a* concentrations.

Table 3.1. Net community production and dark community respiration estimated by the oxygen and dissolved inorganic carbon light/dark bottle incubation method.

	DIC (μmol l^{-1} d^{-1})				O_2 (μmol l^{-1} d^{-1})							
Station	**Gross**	**NCP**	**DCR**	**P/R**	**Gross**	**NCP**	**DCR**	**P/R**	**PQ**	**RQ**	**NO_3+NO_2 μM**	**Chl a mg m^{-3}**
200.200	***	***	***	***	***	0.5	***	***	***	***	27.33	0.1
200.140	***	***	***	***	***	1.3	0.9	1.4	***	***	25.30	0.4
200.040	***	***	***	***	***	1.9	1.0	1.9	***	***	24.43	0.9
200.000	***	***	***	***	***	2.5	1.3	2.0	***	***	23.37	1.3
200.-040	9.3	9.0	0.3	26.1	8.3	4.9	3.4	1.4	0.9	0.1	9.17	3.8
200.-060	7.2	0.4	6.8	0.1	2.3	-0.9	3.3	-0.3	0.3	2.1	0.29	14.3
mb1[a]	24.2	19.2	5.0	3.9	30.0	23.8	6.1	3.9	1.2	0.8	1.00	10.6
mb2	14.8	10.0	4.8	2.1	19.9	22.0	***	***	1.3	***	1.57	10.6
tp[b]	24.0	18.9	5.1	3.7	39.8	16.1	23.7	0.7	1.7	0.2	0.94	20.7

*** No data
a Marguerite Bay
b Tickle Passage

Background

An understanding of how net organic matter production/respiration, temperature-driven solubility changes and air-sea gas fluxes affect $O_{2\{Sat\}}$:$fCO_{2\{Sat\}}$ is essential to interpret measured data. Within this section, an overview of the basic chemistry, physics and biology will be discussed. The variability shown by the underway measurements (Fig 3.2) reflects a combination of the above mentioned processes controlling O_2 and fCO_2 (Table 3.2). Except for air-sea gas exchange, all of these processes drive O_2 and fCO_2 away from air-saturated equilibrium values at fairly well constrained stoichiometric proportions (Table 3.2). Generally, air-sea gas exchange will drive saturation back to atmospheric equilibrium concentrations at stoichiometric proportions that are dependent on the air-sea O_2 and fCO_2 gas fluxes.

Table 3.2. Summary of processes affecting upper ocean O_2 and fCO_2

Process	O_2 % Saturation	fCO_2 % Saturation
Increase Temp.	+2.5%/ºC	+4%/ºC
Decrease Temp.	-2.5%/ºC	-4%/ºC
Production	+1% $O_{2\{Sat\}}$/2% $fCO_{2\{Sat\}}$	-1% $O_{2\{Sat\}}$/2% $fCO_{2\{Sat\}}$
Respiration	-1% $O_{2\{Sat\}}$/2% $fCO_{2\{Sat\}}$	+1% $O_{2\{Sat\}}$/2% $fCO_{2\{Sat\}}$

Temperature affects O_2 and fCO_2 through changes in solubility. A fundamental difference between the behavior of O_2 and CO_2 is the chemical reactivity or solubility in seawater. Carbon dioxide gas reacts with water to form carbonic acid, which dissociates to form bicarbonate and carbonate ions. Most of the total dissolved inorganic carbon in seawater (typically >99%) exists as bicarbonate and carbonate ions at the pH of seawater (7.45 to 8.25; Wallace 2001).

Oxygen and fCO_2 saturation is affected by temperature and salinity. An increase in temperature produces an increase in the O_2 and fCO_2 saturation states, and a decrease in temperature produces a decrease in both the O_2 and fCO_2 saturation states. Salinity has less of an effect than temperature. The range of salinity encountered over the cruise produces only a 2.5% range in $O_{2\{Sat\}}$, while the range of observed temperatures produces a 11.2% range in $O_{2\{Sat\}}$. The $\Delta fCO_{2\{Sat\}}$:$\Delta O_{2\{Sat\}}$ ratio for heating and cooling is 1.7.

Air-sea exchange rates differ for O_2 and fCO_2. Timescales range from days to weeks for O_2 and months for fCO_2 (Appendix A; Broecker and Peng 1985). In surface seawater, the disequilibrium between the partial pressure of a gas in the overlying atmosphere and that in surface water drives a bi-directional flux across the air-sea interface in the direction towards equilibrium (Kanwisher, 1963). The net flux is a function of the gas transfer

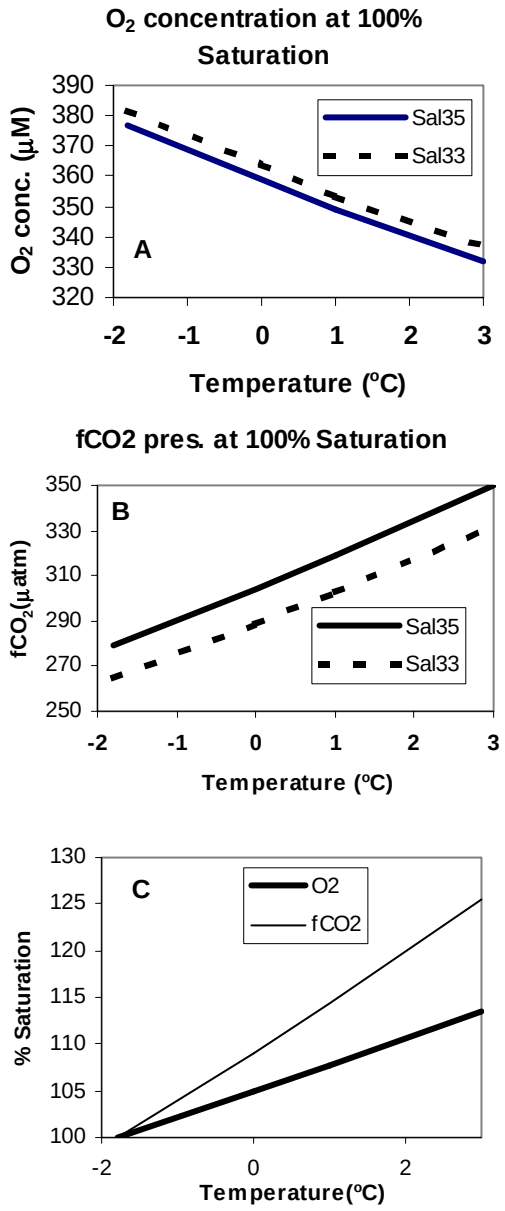

Figure 3.7 A) Temperature versus oxygen concentration at 100% saturation at salinities of 33 and 35. B) The change of fCO_2 as a function of temperature at salinities of 33 and 35. C) Changes of O_2 and fCO_2 % Saturation as a function of temperature

coefficient (also referred to as the piston velocity coefficient), and the difference in gas partial pressure of the gas between the atmosphere and ocean. The gas transfer coefficient is a function of gas diffusion and stagnant film thickness but is usually parameterized by wind speed (Smith, 1985; Liss and Merlivat, 1986; Wanninkhof, 1992).

Over large time and space scales organic matter production and remineralization are defined by the chemical reaction:

$$\mathbf{CO_2} + \mathbf{H_2O} + \overset{\text{light}}{\leftrightarrow} \mathbf{(CH_2O)} + \mathbf{O_2} \quad (1)$$

The forward reaction describes photosynthetic production of organic matter, where CO_2 and water (H_2O) combine to form reduced carbon and O_2. The reverse reaction describes the metabolic process of respiration. Compared to the more restrictive, light dependent photosynthetic production, a broad range of auto- and heterotrophic organisms contribute to the respiration rate in any given ecosystem. Photosynthesis is the only process that increases O_2 concentrations while concurrently decreasing CO_2 concentrations. Respiration is the only process that decreases O_2 concentrations while concurrently increasing CO_2 concentrations. Biological oxygen production is coupled to biological organic carbon production through the photosynthetic quotient (i.e. PQ). The gross photosynthetic quotient is the molar ratio of oxygen production to the rate of inorganic carbon utilization; PQ values are generally in the range of 1.3 ±0.1, depending upon the source of N (NH_4^+ versus NO_3^-; Laws et al. 1991). If the PQ is expressed in terms of O_2 and fCO_2 saturation states, PQ is 0.5 (i.e .$\Delta\ O_{2\{Sat\}} / \Delta fCO_{2\{Sat\}}$ = P.Q. = 0.5)

Spatial and Seasonal Variations of Gas Saturation States

Oxygen and fCO_2 vary from air-saturated equilibrium states, suggesting a

combination of processes controlling O_2 and fCO_2 distributions within the LTER study region (Fig. 3.2). The relationship between $O_{2\{Sat\}}$ and $fCO_{2\{Sat\}}$ has not been used extensively but may be a useful way to study ecosystem dynamics. For example, in the LTER study region, the maximum $fCO_{2\{Sat\}}$ of 112% is associated with a minimum $O_{2\{Sat\}}$ of 81%. The maximum $O_{2\{Sat\}}$ of 157% is associated with the minimum $fCO_{2\{Sat\}}$ of 27%. The only possible cause of simultaneous fCO_2 undersaturation and O_2 supersaturation is photosynthesis, and the only possible source of simultaneous fCO_2 supersaturation and O_2 undersaturation is net respiration. Consequently, over relevant time and space scales, the correlation between $O_{2\{Sat\}}$ and $fCO_{2\{Sat\}}$ can help constrain the net autotrophic:heterotrophic balance of the ecosystem.

Overall, the strongest correlation observed is the negative correlation between $O_{2\{Sat\}}$ and $fCO_{2\{Sat\}}$ (Fig. 3.3C). The model II linear regression (geometric mean) slope is -0.4 which is more than 5 times larger than the calculated slope of -0.5 describing net organic matter production. This is most likely a result of the competing processes of organic matter production and differential air-sea gas exchange affecting the O_2:fCO_2 ratios. As photosynthesis produces O_2 and depletes CO_2 concentrations in surface seawater, air-sea gas exchange will ventilate the supersaturated O_2 more rapidly then it will replenish the undersaturated CO_2 (Appendix A). At high O_2 concentrations (>120% saturation) the$\Delta O_{2\{Sat\}}$:$\Delta fCO_{2\{Sat\}}$ratio for air-sea gas exchange is approximately 3. As O_2 concentrations approach atmospheric equilibrium, the ratio of $O_{2\{Sat\}}$:$fCO_{2\{Sat\}}$ decreases. The overall effect is a decrease in the slope of the $O_{2\{Sat\}}$ versus $fCO_{2\{Sat\}}$ regression.

Changes in fCO_2 concentrations cannot be explained by temperature variations

alone. The range of temperatures encountered for the grid was approximately 4º C. The solubility change calculated for a warming or cooling of 4º C is approximately 48 μatm (Weiss, 1974). Therefore temperature variations can only account for at most 20% of the full range of measured fCO_2 concentrations.

Klinck (1998) presented a physical description of the seasonal changes of heat and salt in the LTER study area. During the winter, surface waters are near freezing (-1.8º C) and have a salinity range from 33.8 to 34.1. During the transition from fall to winter, surface seawaters are cooled by decreasing air temperatures and wind-driven heat exchange. As surface water densities increase, surface stratification decreases and waters are mixed with deeper waters of lower O_2 and higher CO_2. This is reflected by the relatively constant fCO_2 supersaturation and O_2 undersaturation observed during the winter (Fig. 4.4). The depth of the winter mixed-layer will determine the O_2 and CO_2 winter surface concentrations through changes in the mixed layer depth (Gordon and Huber, 1990; Smith et al., 1999a).

Between winter and summer, the topmost 10 to 30 meters warm and freshen as solar insolation increases and sea ice melts; air-sea exchange will drive gas pressure towards air-saturated equilibrium values. Warming and freshening will therefore increase O_2 and fCO_2 saturation. In areas of net organic matter production, net photosynthesis decreases fCO_2 and increases O_2 concentrations. In localized areas, especially near the coast, glacial ice cools and freshen surface waters, which would decrease O_2 and fCO_2 saturation states.

The spatial distribution of values clustered between 90 and 110% $fCO_{2\{Sat\}}$ and 85

to 110% $O_{2\{Sat\}}$ implies surface seawater within the LTER region remains close to atmospheric equilibrium during January. This cluster accounts for > 80% of the total area surveyed in the LTER grid. The remaining $O_{2\{Sat\}}$:$fCO_{2\{Sat\}}$ values represent a large disequilibrium and are found primarily in Marguerite Bay and other isolated coastal areas. These isolated coastal areas represent a large biological signal but account for a smaller fraction of the area surveyed.

The spatial distribution of $O_{2\{sat\}}$:$fCO_{2\{Sat\}}$ values within the LTER grid is the result of a variety of competing ecosystem processes that affect fCO_2 and O_2. Quadrant I data depict areas of fCO_2 undersaturation and O_2 supersaturation implying a biological source (net photosynthesis). These conditions were most often located in protected coastal waters where near surface stratification is typically enhanced by glacial and sea ice melt.

Quadrant II data are representative of outer stations along the 200 line and correlate well with warmer (>2.5 ºC) offshore waters. These local warm waters may be the result of localized heating since mixed layer depths were relatively shallow (10 meters), but may also derive from the southern edge of the Antarctic circumpolar current (Hofmann et al., 1996).

Quadrant III data derive from the offshore stations along the 600 line where relatively cooler surface water temperatures prevail. In contrast to the offshore waters in the southern region, the off-shelf region to the north shows slight fCO_2 supersaturations and O_2 undersaturations (Quadrant III; Fig. 3.3) that intrude onto the shelf. Surface water temperatures were somewhat cooler in the northern then in the southern region, with a

deeper mixed layer to the north. One prominent deep channel (500 m) extends to the northwest of Anvers Island. These canyons can act as conduits for water to move onto the shelf as inferred from temperature and salinity changes over deeper areas of the shelf (Klinck, 1998). The northern region gas characteristics, fCO_2 supersaturation and O_2 undersaturation, imply upwelling as a potential source for the CO_2-enriched and O_2-depleted subsurface waters. Alternatively, in the southern region, we hypothesize that localized stratification and heating may be responsible for the fCO_2- and O_2-enriched waters. Local warming of surface waters has previously been reported for Antarctic Peninsula habitats (Huntely

Areas of fCO_2 undersaturation and O_2 undersaturation (Quadrant IV) were generally encountered in coastal and on-shelf waters. Data within quadrant IV derive from samples along the coast where glacial melt may continuously freshen and cool the surface waters through the summer months. The freshening and cooling may drive local sinks for O_2 and fCO_2 throughout the spring and summer seasons. Additionally, areas of ice melt are potential sites for phytoplankton bloom formations, which can further decrease fCO_2 undersaturations. Ecosystem processes resulting in the quadrant I and IV data sets are discussed more thoroughly in the following two case study sections.

Case Study I: Effects of Cooling and Net Organic Matter Production

An unexpected result of our analysis of the underway system data was the positive correlation of $fCO_{2\{Sat\}}$ and $O_{2\{Sat\}}$ for a repeat transect separated by 14 days. This result is consistent with surface water cooling. Correlation of fCO_2 with temperature is generally found only in open ocean oligotrophic environments and is not expected for

more eutrophic coastal environments where biological processes dominate (Takahashi et al. 1993). However, Antarctic coastal waters are a variable mosaic in both time and space due to patchy plankton blooms and the effect of glacial and sea ice melt on surface waters close to the continent.

In the LTER study region, fresher waters are typically found close to the continent, where glacial and sea ice meltwaters can affect the local heat and salt budgets compared to saltier waters found offshore (Klinck, 1998). Variations in temperature and salinity between transects are consistent with the advection and melting of ice (Ohshima et al., 1998). Ice is advected into an ice-free area that has been previously warmed by solar radiation. The advection of ice overwhelms the local balance of heat and salt, causing both a decrease in temperature and salinity.

During the Jan 27, southbound transit, temperature, salinity and $O_{2\{Sat\}}$ were spatially invariant, suggesting a relatively homogenous water mass. The fugacity of $CO_{2\{Sat\}}$ was also spatially invariant except for an anomalous low spike in fCO_2 saturation at approximately 66° S and 67° W. Because the surface exposure history of this water mass is unknown, we can only speculate about the anomalous signal. It may be a remnant of an earlier bloom where carbon dioxide was removed but not yet replenished by gas exchange with the atmosphere or respiration.

The positive regression shown between cluster I, Jan 27, southbound transit, and clusters II and III, Feb 9-10 northbound transit imply cooling had lowered $O_{2\{Sat\}}$ and $fCO_{2\{Sat\}}$. Predicted changes of O_2 and fCO_2 based on cooling and freshening trends match observed values reasonably well (Table 3.3; Fig. 3.5). A comparison of calculated

and measured values shows differences no greater then 2% for either fCO_2 or O_2 saturation states.

Table 3.3. Transect properties.

Date	Temp.	Salinity	Chl a	$O_{2\{Sat\}}$ calc[a]	$O_{2\{Sat\}}$ meas.	$fCO_{2\{Sat\}}$ calc.[b]	$fCO_{2\{Sat\}}$ meas.
Jan 27	1.5 ± 0.1	33.5 ± 0.1	0.6	100.4	100.2 ± 0.1	95.0	97.0 ± 1.1
Feb 9-10 (south)	-1.0± 0.3	32.0± 0.2	1.2	92.7	91.6 ± 2.8	85.3	87.1 ± 4.5
Feb 9-10 (north)	0.5± 0.2	31.0± 0.4	1.2	95.8	96.3 ± -1.6	91.1	92.8 ± 1.7

[a] Calculated dissolved O_2 saturation based on Weiss (1970).
[b] Calculated fCO_2 based on Goyet et al.(1993).

Superimposed on the temporal physical signal is a spatially variable biological signal. Comparison of O_2 and fCO_2 saturation shows a positive correlation if the values are grouped according to the temperature and salinity characteristics. Surface waters located south are colder and saltier relative to surface waters in the north. Three scenarios may help to explain these T-S characteristics. First, a different water mass may have advected into the area with different temperature and salinity characteristics. Second, differential ice melting with more ice ablation in the northern than in the southern sector may have contributed to the different temperature and salinity characteristics. Third, differential mixing or upwelling of colder saltier waters in the southern section may have contributed to the different temperature and salinity characteristics. Unfortunately we cannot distinguish among these possibilities, and the T-S characteristics may be a combination of any of the three.

The negative regression between $O_{2\{Sat\}}$ and $fCO_{2\{Sat\}}$ in clusters II and III indicates that net organic matter production and net community respiration are first-order controlling factors. The negative correlation between $O_{2\{Sat\}}$ and $fCO_{2\{Sat\}}$ also correlates

with a two-fold increase in chl *a* concentration, from 0.6 to 1.2 mg/m^3. Overall, this case study is an example where the physical process of cooling has the effect of lowering O_2 and fCO_2 saturation in a coastal area. A spatial biological signal was then superimposed onto the temporally varying temperature signal. Quantification of both processes in space and in time will be required to constrain CO_2 budgets in this area.

Case Study II: Organic Matter Production, Respiration and Air-to-Sea Exchange

Biological production of organic matter can have a significant effect on O_2 and CO_2 concentrations on small spatial scales (< 10 km) and short time scales (< 1 week; Holm-Hansen and Mitchell, 1991; Karl et al., 1991; Carrillo and Karl, 1999). The effect of biological production on the ambient $O_{2\{Sat\}}$:$fCO_{2\{Sat\}}$ is seen in the offshore to onshore transect into Marguerite Bay (Fig. 3.6). Offshore waters are characteristic of high nutrient, low chlorophyll surface waters with low rates of NCP and DCR. Corresponding O_2 and fCO_2 saturation states are very close to equilibrium with the atmosphere, which also suggests very low biological activity and very little heating or cooling. Net community production increased with decreasing distance from shore. Nitrate, nitrite and fCO_2 saturation show corresponding decreases, suggesting the overall effect of NCP over DCR in controlling fCO_2 values. Areas of fCO_2 undersaturation (30%) and O_2 supersaturation (155%) were encountered in Marguerite Bay and were associated with accumulations of chlorophyll *a*, implying a biological source. Within Marguerite Bay, the effects of net organic matter production on O_2 and fCO_2 are clearly shown. Increases in O_2 and chlorophyll *a* concentrations are correlated with a decrease in $[NO_3 + NO_2]$ and fCO_2. Marguerite Bay is near the head of a submarine canyon that may sustain large

phytoplankton blooms by an enhanced macro and micro-nutrient supply via topographic routing of deep waters (Hofmann et al., 1996; Klinck, 1998). These biological hotspots may also facilitate carbon and energy transfer to higher trophic levels.

The effect of respiration on O_2 and CO_2 is less obvious. The importance of heterotrophic microbes (bacteria and protozoans) within the marine food web has been recognized for several decades (Pomeroy, 1974). Bacterioplankton may account for a large sink of organic matter produced by primary producers. The role of these microbes in determining the fate of organic carbon remains undetermined (Jahnke and Craven, 1995). In temperate coastal ecosystems, heterotrophic respiration may be decoupled from autotrophic production by a temporal lag (Blight et al., 1995; Robinson et al., 1999). Since Antarctic ecosystems are dominated by extreme seasonal cycles of light and heat, heterotrophic respiration may be temporally and, therefore, spatially decoupled from photosynthesis. Atmospheric O_2 measurements support the seasonal phasing of autotrophic versus heterotrophic plankton metabolism but provide no mechanism to explain the phenomenon (Sherr and Sherr, 1996). In contrast to current dogma stating that heterotrophic respiration is coupled to photosynthetic production, bacterial abundance has been shown to decrease with increasing chlorophyll *a* concentration in Southern Ocean ecosystems (Karl and Bird, 1993; Bird and Karl, 1999). Recent studies showing a significant positive correlation between respiratory activity and chlorophyll *a* suggested that community respiration is dominated by photoautotrophs during the spring and summer seasons (Karl et al., 1991; Aristegui and Montero, 1995).

A potential consequence of the high O_2 and low fCO_2 condition is the premature

demise of the bloom via algal photorespiration (Karl et al., 1996). Photorespiration is a light dependent respiratory process of photoautotrophs and involves a light dependent oxygen uptake and release of CO_2. There are very few, if any, estimates of photorespiration in Antarctic marine phytoplankton. The effects of photorespiration may often be obscured by a net decrease in photosynthesis and therefore ignored as an important process in oxygen and carbon flow. Photorespiration and photosynthesis are closely coupled processes because both metabolic pathways draw from the same pools of carbon and oxygen (Anderson and Beardall, 1991; Karl et al., 1996; Tolbert, 1997). During the summer season, photoautotrophic respiration may account for a larger fraction of O_2 consumption and CO_2 production then heterotrophic respiration in oxygen supersaturated regions. Direct evidence for this process in Antarctic coastal waters is not available, but all indications suggest that it could be an important process (Karl et al., 1996).

Generally, DCR within Marguerite Bay remained low compared to NCP (Fig. 4.4). The exception to this trend occurs at station within Marguerite Bay where NCP had essentially ceased. Although measured O_2 concentrations were above 450 μM and fCO_2 values were approximately 100 μatm, rates of DCR were greater than estimates of NCP, implying net heterotrophy. Another anomalous station sampled in the ice-covered area of Tickle Passage shows high rates of DCR based on O_2 consumption but low rates based on production of CO_2.

At O_2 concentrations above 120% saturation, differential exchange of O_2 and CO_2 across the atmosphere-ocean interface can decouple O and C dynamics. Oxygen produced

is quickly ventilated relative to CO_2. The slope of $O_{2\{Sat\}}$ and $fCO_{2\{Sat\}}$ within Marguerite Bay has a significantly steeper slope of –3.8 (model II linear regression geometric mean) than was calculated for the entire LTER region. This regression matches the ratio of $O_{2\{Sat\}}$:$fCO_{2\{Sat\}}$ for air-sea exchange at high O_2 concentrations (>400 μM). Because of air-to-sea exchange, O_2 concentrations decrease from 156% saturation to equilibrium (100% saturation) in approximately 30 days. The corresponding $fCO_{2\{Sat\}}$ increases only 9% within the same period. These differences (56% for $O_{2\{Sat\}}$ versus 9% for CO_2) are largely a function of gas solubility. Consequently, we suggest that air-to-sea exchange is a major factor in returning O_2 values to their respective atmospheric equilibrium values in spite of measurable respiration. Due to differences in the behavior of these two biogenic gases, the same is not true for fCO_2 thus causing a decoupling in $O_{2\{Sat\}}$:$fCO_{2\{Sat\}}$ dynamics.

Conclusions

Heating and cooling of surface waters are relatively small sources and sinks (±10 –15%) of O_2 and CO_2 in the region west of the Antarctic Peninsula. The spatial distribution of $O_{2\{Sat\}}$:$fCO_{2\{Sat\}}$ values centered around atmospheric equilibrium account for 80% of the LTER grid surveyed in January. Net organic matter production is a large source of O_2 and sink for CO_2, yet occurs in only a small portion of the LTER grid surveyed. The relative magnitude of net biological processes in changing O_2 and fCO_2 saturation states is approximately four-fold greater than for heating and cooling. Austral winter data confirm that surface waters west of the Antarctic Peninsula are a local sink for

O_2 and source of CO_2.

Appendix A: Air-Sea Flux Model

The difference between the air-to-sea exchange rates of O_2 and CO_2 can be illustrated by comparing modeled flux estimates. This is a model calculation and illustrates the different time scales of O_2 and fCO_2 air-sea exchange. Air-sea fCO_2 gas flux estimates were calculated by multiplying the atmosphere (358 μatm) and surface ocean fCO_2 difference by the gas transfer coefficient and solubility of CO_2 in seawater. The gas transfer coefficient was calculated using the equation of Wanninkhof (1992) with a constant wind speed of 3 m sec^{-1}. The solubility of CO_2 in seawater was calculated from Weiss (1974). At each time step, fCO_2 is calculated from DIC using a Revelle factor of 15 which is a representative value for water at these latitudes (Broecker and Peng 1982). Air-sea O_2 flux estimates were calculated using the equations of Weiss (1970) and the gas transfer coefficient. Model calculations were initiated with values of 1º C, 33 salinity and concentrations of O_2, DIC and fCO_2 of 500 μM, 1900 μM and 100 μatm, respectively. These values represent a phytoplankton bloom situation as observed in Marguerite Bay. The air-sea flux is calculated for every time step and incremented on a daily timescale. The change in the stoichiometric proportions of $O_{2\{Sat\}}$ and $fCO_{2\{Sat\}}$ decreases as O_2 and fCO_2 approach atmospheric equilibrium values (Fig 3.3C). Oxygen concentrations approach atmospheric equilibrium concentrations much more quickly then CO_2 because of the lower solubility of O_2 versus fCO_2.

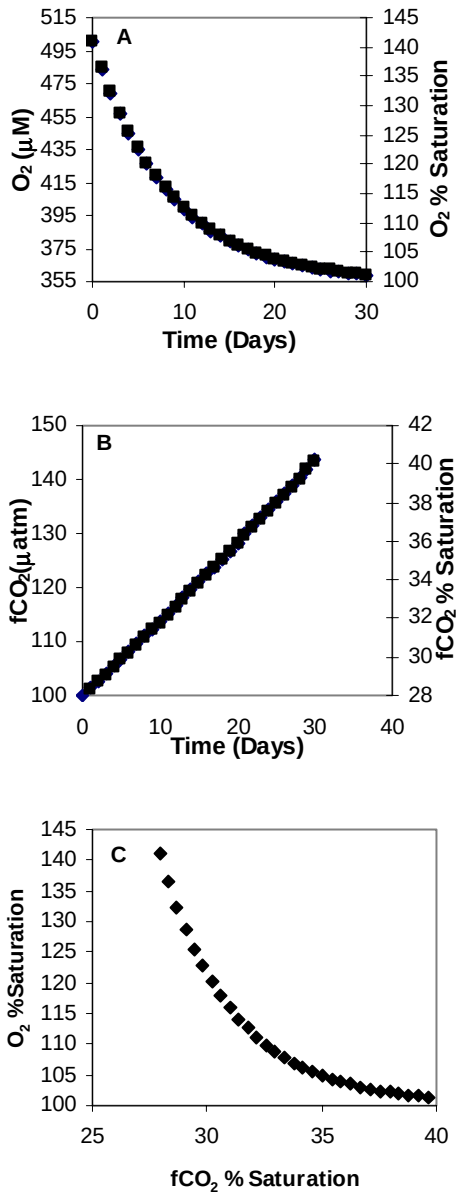

Fig 3.8 A) Changes in O_2 concentrations a function of time based on air-to-sea gas exchange estimation , assuming constant temperature and salinity. B) Changes in fCO_2 pressure as a function of time based on air-to-sea exchange assuming constant temperature and salinity. C) Changes of % Saturation of O_2 and fCO_2 based on air-to-sea exchange

CHAPTER IV

DISSOLVED INORGANIC CARBON SYSTEM DYNAMICS IN THE REGION WEST OF THE ANTARCTIC PENINSULA: PALMER LONG-TERM ECOLOGICAL RESEARCH PROGRAM

Abstract

Geographic, seasonal and annual studies of dissolved inorganic carbon (DIC) and total alkalinity (TA) show spatial and temporal variability resulting from interactions of hydrographic, chemical and biological variations west of the Antarctic Peninsula. The Palmer Long-Term Ecological Research (Pal-LTER) Program was established in 1990 to study the Antarctic marine ecosystem in the area west of the Antarctic Peninsula, especially habitat change and response to climate variability. Geographic surveys of dissolved inorganic carbon concentrations in surface waters exhibited a wide range of values relative to seasonal and annual variations. Areas of relatively low DIC concentrations (2110 μmol kg^{-1}) were found in coastal fjords and bays when compared to areas of higher DIC concentrations (2150 μmol kg^{-1}) seaward. In contrast, areas of relatively higher n35DIC (n35DIC=DIC*35/salinity) concentrations (2240 μmol kg^{-1}) were found inshore when compared to areas of lower n35DIC concentrations (2220 μmol kg^{-1}) offshore. Seasonal depletions of n35DIC, normalized [nitrate+ nitrite] (n35N) and normalized phosphate (n35P) were correlated in coastal areas. Molar uptake ratios of C:N:P were 94:15:1. In areas further offshore (40 to 200 kilometers compared to 0 to 40 kilometers), n35DIC dynamics were decoupled from nutrient dynamics, suggesting a separation of inventories and fluxes between coastal and offshore regions. During the winter, a combination of photosynthesis, respiration, and

calcium carbonate precipitation and dissolution control n35DIC and n35TA concentrations. The spatial distributions of these processes produce winter conditions that are as heterogeneous as summer conditions. Finally, annual trends are difficult to estimate at this time because of large geographical and seasonal variability.

Introduction

The role of Antarctic marine environments in regulating the global climate system is uncertain, in part because of the strong seasonal forcing and general undersampling of south polar habitats. Data on seasonally resolved time-scales are needed to fully understand the mechanisms controlling ecosystem variability. Because of the remoteness and, therefore, inaccessibility of Antarctic waters, geographical, seasonal and annual time-series data are sparse. The Antarctic marine ecosystem undergoes one of the largest seasonally phased transformations on the globe. During the austral fall and winter seasons, solar radiation decreases, surface seawater temperatures decline, and sea ice covers surface ocean waters, suspending atmospheric and surface ocean interactions. During the austral spring and summer seasons, solar radiation increases, temperatures rise, and sea ice ablates, creating a shallow fresher stratified mixed layer leading to the spring-summer bloom of phytoplankton.

The seasonal advance and retreat of Southern Ocean sea ice impacts the whole ecosystem structure and increases habitat variability both temporally and spatially. Sea ice formation induces calcium carbonate precipitation and colonization by microorganisms as an over-wintering strategy (Richardson 1976; Ackely and Sullivan 1994). During the transition from spring to summer, sea ice melt water increases water column stability and decreases gas solubility. Sea ice extent and thickness influence

plankton populations and, indirectly, the carbon system dynamics (Gleitz et al. 1995; Hoppema et al. 1995). The timing of the annual advance and retreat of sea ice is an important factor controlling the timing of bloom event(s) and the determination of air-to-sea exchange of dissolved gases with the atmosphere (Carrillo and Karl 1999). Interannual variability may be as important as seasonal variability if the timing, magnitude, and duration of ice coverage determine the extent and persistence of bloom events and seasonal venting of ocean gases.

The marine environment contained within the Palmer Long-Term Ecological Research (Pal-LTER) study area is situated in a climatically sensitive region and is an ideal location to investigate the interaction between biological, chemical, and physical processes in regulating marine habitats (Smith et al. 1999). This region includes a variable seasonal ice zone, open ocean areas, shelf water, and coastal regions. The Pal-LTER Program was established in 1990 to study the physical determinants of the Antarctic marine ecosystem (Smith et al. 1995). Within the Pal-LTER program, the Hawaii-based group "Coupled Ocean-ice Linkages and Dynamics" (COLD) has focused research on the topics of microbiology and carbon flux. The central tenet of the Pal-LTER program is that the annual advance and retreat of sea ice is a major physical determinant of spatial and temporal changes in the structure and function of the Antarctic marine ecosystem, from inorganic carbon system dynamics to total annual primary production to the breeding successes of seabirds (Smith et al. 1995).

Since 1986, measurements of DIC and TA have been made in the region west of the Antarctic Peninsula. Between 1986 and 1992, these measurements were confined to coastal areas (0 to 40 kilometers from the Antarctic Peninsula) within the Gerlache Strait.

After 1992, the study area expanded to offshore areas located 40 to 200 kilometers west of the Antarctic Peninsula. In this chapter, an analysis of the distributions of DIC, [nitrate+ nitrite] (N), and phosphate (P) within these areas will provide information on the spatial variability and coupling of nutrient dynamics. This analysis will be extended to a seasonally resolved time-series to determine whether the spatial coupling of nutrients can be extended temporally. Finally, annual trends will be scrutinized in terms of geographical and seasonal variability.

Methods

Since 1987, two time-series programs have sampled various marine regions on seasonal and annual time-scales. The Research on Antarctic Coastal Ecosystem Rates (RACER) program investigated physical and biological processes causing high productivity within the Gerlache Strait between 1987 and 1992. Information concerning the first of 4 field program projects can be found in Deep-Sea Research volume 38, 1991. The Palmer Long Term Ecological Research Program (Pal-LTER) has expanded the investigations started during the RACER program within a larger defined research grid located off the Antarctic Peninsula. Data from these two programs will be used in this chapter.

Programs and Field Sites

The Research on Antarctic Coastal Ecosystem Rates (RACER) program was designed to study living and non-living carbon pool dynamics in several representative coastal regions of the western portion of the Antarctic Peninsula (Fig 4.1). The RACER data sets consist of biological and physical parameters, including meteorological data

during winter and summer seasons. An initial 4-month field study (RACER I) conducted in a 25,000 km^2 region of the Western Bransfield Strait during the 1986-87 austral summer documented phytoplankton blooms of >750 mg chl a m^{-2} (0-30 m) and sustained daily photosynthetic production rates as large as 2-5 g C m^{-2} (Huntley et al. 1991). These blooms resulted in significant inorganic nutrient depletions and a seasonal depletion of dissolved inorganic carbon (DIC normalized to 35 salinity) in excess of 100 μmol kg^{-1} in selected regions of Gerlache Strait (Karl et al. 1991a). Subsequent studies (RACER II and III) were confined to a 4,000 km^2 area of Gerlache Strait to study the factors involved in the formation and demise of phytoplankton blooms during the austral summers of 1989-90 and 1991-92. A final study (RACER IV) was conducted in the same area as RACER II and III but during austral winter (July 1992). During each RACER cruise, the area was studied on one of two timescales. First, the predetermined array of stations was occupied on a short time scale (less than three hours per station) to obtain a synoptic view of the area with respect to the measured parameters. Typically, the grid of stations was sampled during a period of 3 to 5 days. Selected stations within this grid were also occupied for longer time periods to record the daily variability and to conduct process-oriented experiments. One such location, station A (i.e., RACER I station 43) located in Gerlache Strait (64° 14.00' S and 61° 17.00' W) was occupied during all four RACER cruises.

The Palmer Long-Term Ecological Research (LTER) Program was established in 1990 to study the physical determinants of the Antarctic marine ecosystem. The Pal-LTER grid located off the Antarctic Peninsula covers an area 900 by 200 kilometers (Fig 4.1; Waters and Smith 1992, Chapter 3). This grid or sub-component is sampled during a

17 to 45 day cruise centered in mid-January. The grid consists of ten lines 100 km apart, roughly perpendicular to the coast, extending 200 km off-shore. The "grid lines" are labeled depending on the distance from the first line located just south of Marguerite Bay. For example, the "200 line" is the grid line 200 km from the 0 gridline, and this line extends perpendicular to Marguerite Bay. Station locations are 20 km apart along each line. During each field season, spatial surveys are conducted. Generally, gridlines 200 through 600 are sampled during the austral summer cruises. At each station, a Bio-optical profiling system (BOPS) was utilized to obtain a variety of physical, chemical and biological samples. These samples include salinity, temperature, pressure, nutrients, oxygen, CO_2, primary production and bacterial production. Additionally, net tows are conducted at each station to identify and determine macrozooplankton abundance. During 1993, two cruises were conducted in the austral fall (March) and winter (August) to obtain seasonal data and to study the effect of ice processes on the marine ecosystem.

DIC, Total Alkalinity and fCO_2 Measurements

A description of DIC and total alkalinity analysis during the RACER project is found in Carrillo and Karl (1999) and Karl et al (1991). Generally, the same methods were used for RACER and LTER inorganic carbon analyses. DIC was measured on seawater samples collected during each cruise by coulometric determination of extracted CO_2 (Johnson et al 1985, 1987). Prior to 1998, samples were delivered to the coulometer extractor using syringes weighed before and after sample injection. Since 1998, sample delivery has been automated using a Single Operator Mutiparameter Metabolic Analyzer (SOMMA) system (Johnson et al. 1998). TA is

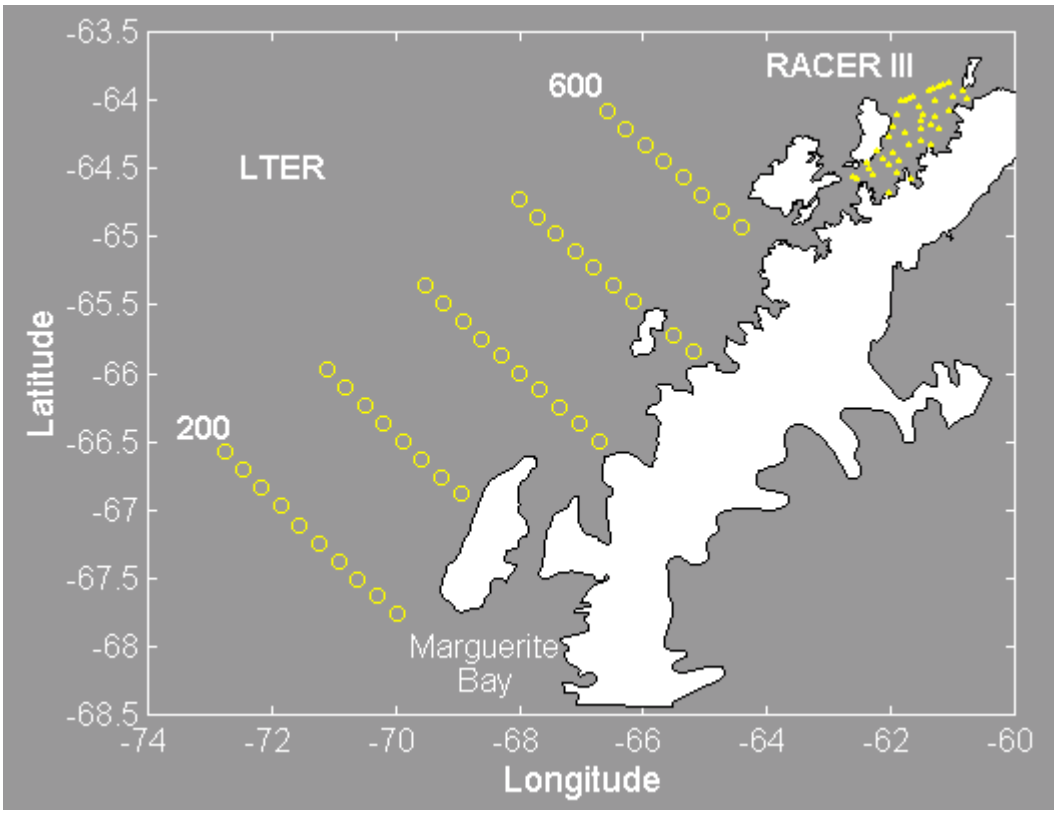

Figure 4.1 Map of the RACER and LTER study areas. LTER station locations are represented with open circles and RACER station locations are represented with small filled circles. The LTER grid consists of 10 lines extending 200 km on to off-shore and 900 km along the western coast of the Antarctic Peninsula. Station locations are approximately 20m km apart. The 200 and 600 “grid lines” are labeled in the figure. Stations within Marguerite Bay and the Palmer Basin are also sampled but are not shown. This grid is sampled once per year in the months of January and February during the annual LTER cruise.

determined in an open cell by a potentiometric titration with calibrated HCl and analyzed using a modified Gran plot as recommended by DOE (1994). Since 1998, the accuracy and precision of DIC and TA analyses have also been determined by analysis of certified reference materials (CRMs) provided by Andrew Dickson. Our analytical DIC precision and accuracy based on CRMs is estimated to be 1 μmol kg^{-1} and less then 2 μmol kg^{-1}, respectively. Our analytical TA precision and accuracy is estimated to be 2 μeq kg^{-1} and less then 4 μeq kg^{-1}, respectively.

During the 1996 to 1998 austral summer LTER field seasons, an automated underway fCO_2 measurement system was deployed on the *R/V Polar Duke* and *R/V Laurence M. Gould.* The underway system acquires seawater from the ship's bow intake located approximately 5 meters below the sea surface, and atmospheric air from the top of the bridge approximately 10-12 meters above the sea surface. Surface seawater fCO_2 was determined by continuously pumping water through a counter flow rotating disk type equilibrator (Bjork et al. 1948; Cross et al. 1956; Schink 1970; Sabine et al. 1998) as described previously by Carrillo and Karl (1999). The CO_2 and water vapor mole fractions were measured with a LI-COR model 6262 infrared CO_2 analyzer. The CO_2 mole fraction was converted to fCO_2 using the total pressure and the viral equations of state for CO_2 (DOE 1994). The continuous measurement system was periodically calibrated (every 2.5 hr) with compressed gas standards with nominal mixing ratios of 259.28, 303.86, and 373.19 parts per million. These gas standards were calibrated with World Meteorological Laboratory (WMO) primary standards obtained and certified by the NOAA Climate Monitoring and Diagnostics Laboratory (CMDL). Equilibrator

temperature was measured with an Omega RTD, and system pressure was measured with a Setra pressure transducer. Between calibrations, equilibrator and atmospheric samples were measured every 5 min. The entire measurement system was computer automated using LabVIEW® software. Temperature and salinity were measured with a Sea-Bird thermosalinograph system positioned at the seawater intake and periodically calibrated by bottle salinity.

Temperature, Salinity and Dissolved Inorganic Nutrients

Temperature and salinity were measured using a standard Seabird conductivity-temperature-depth (CTD) package with dual sensors, which was part of the Bio-Optical Profiling System. A description of the dissolved nutrient analysis during the RACER program is found in Karl et al. (1991). Water samples were drawn from a CTD/rosette system and measured on a Technican Autoanalyzer system. Values were obtained from the Pal-LTER database. (www.crseo.ucsb.edu/lter/lter.html). Values for [nitrate + nitrite] and phosphate were normalized to a constant salinity of 35 (n35N and n35P, respectively) and expressed as μmol kg^{-1}.

Results

During the Pal-LTER 1993 field cruises, DIC and n35DIC exhibited a wide range of concentrations within the Pal-LTER grid area. During the austral summer cruise, DIC concentrations ranged from 2110 to 2160 μmol kg^{-1} in the region 40 to 50 kilometers from shore (Fig 4.2A). The lowest concentrations (2110 to 2120 μmol kg^{-1}) were observed at inshore stations on the southern half of the grid area (200 to 400 lines; Fig 4.2A). In offshore areas, 180 to 200 km from shore, DIC concentrations range from 2140

to 2166 μmol kg^{-1}. Fresher surface waters were observed inshore compared to offshore regions on the same gridline. For example, salinities ranged from 33.0 to 33.2, 40 to 50 kilometers from shore on the 200 to 400 lines (Fig 4.2B). Offshore (190 to 200 kilometers from shore), salinities ranged from 33.7 to 33.8 (Fig 4.2B).

Variations in DIC concentrations resulting from the addition or removal of fresh water are removed by normalizing to a constant salinity (n35DIC = DIC *35/salinity). Normalized-35DIC concentrations ranged from 2233 to 2245 μmol kg^{-1} 40 to 50 kilometers from shoreline and 2213 to 2256 μmol kg^{-1} 180 to 200 kilometers from shore (Fig 4.3A). Normalized-35DIC concentrations were relatively higher at stations located 40 kilometers from shore than compared to stations located 200 kilometers from shore on the 200, 400 and 600 lines (Fig 4.3A). During the austral winter cruise (August 1994), n35DIC concentrations ranged from 2228 to 2259 μmol kg^{-1} 40 to 50 kilometers from shore and 2212 to 2220 μmol kg^{-1} 180 to 200 kilometers from shore. At select stations on the 200 line, n35DIC concentrations were as low as 2134 to 2152 μmol kg^{-1} (Fig 4.3B).

During the 1993 annual austral summer cruise, the median and mean n35DIC concentrations were 2130 and 2240 μmol kg^{-1} respectively (Fig 4.4A). Overall, concentrations were within the range of 2150 to 2278 μmol kg^{-1}. During the February to March 1993 cruise, the median and mean n35DIC concentrations were 2222 and 2232 μmol kg^{-1} respectively (Fig 4.4A). Values were within the range of 2219 to 2289 μmol kg^{-1}. During the August 1993 austral winter cruise, the mean and median n35 DIC concentrations

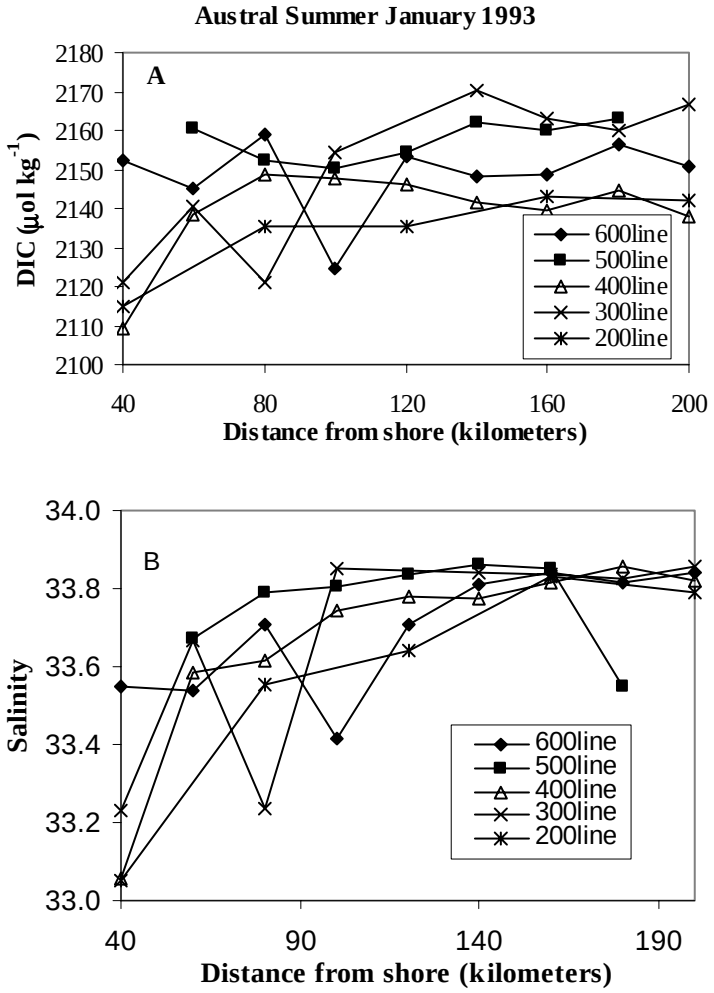

Figure 4.2 A) DIC µmol kg^{-1} versus distance from shore within the Pal-LTER grid area for gridlines 200 through 600. B) Salinity versus distance from shore within the Pal-LTER grid area for gridlines 200 through 600.

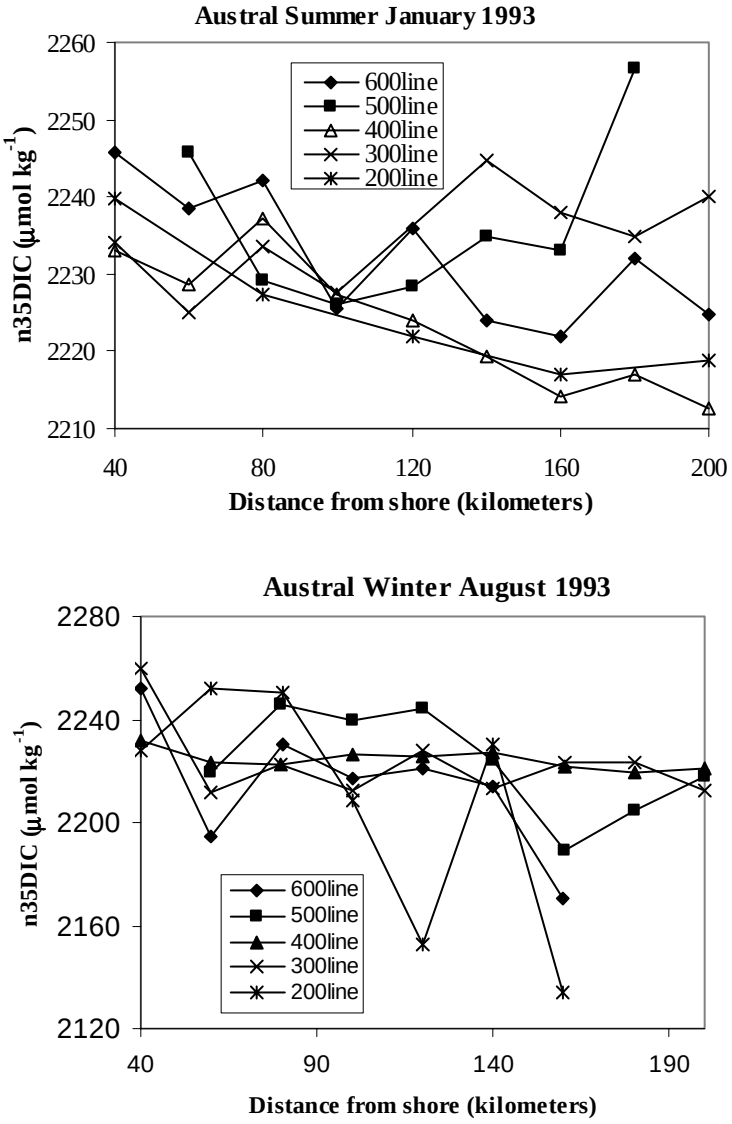

Figure 4.3 A) n35DIC µmol kg^{-1} versus distance from shore within the Pal-LTER grid area for gridlines 200 through 600. B) n35DIC µmol kg^{-1} versus distance from shore within the Pal-LTER grid area for gridlines 200 through 600.

were 2222 and 2219 μmol kg^{-1} respectively (Fig 4.4A). Values were within the range of 2134 to 2259 μmol kg^{-1}. During the 1994 annual austral summer cruise, the median and mean n35DIC concentrations were 2208 and 2210 μmol kg^{-1} respectively. Overall, concentrations were within the range of 2071 to 2272 μmole kg^{-1}.

During the 1993 annual austral summer cruise, the median and mean n35TA concentrations were 2392 and 2390 μmol kg^{-1} respectively (Fig 4.4B). Overall, concentrations were within the range of 2262 to 2428 μmol kg^{-1}. During the February to March 1993 cruise, the median and mean n35TA concentrations were 2360 and 2365 μmol kg^{-1} respectively (Fig 4.4B). Values were within the range of 2352 and 2422 μmol kg^{-1}. During the August 1993 austral winter cruise, the mean and median n35 DIC concentrations were 2426 and 2429 μmol kg^{-1} respectively. Values were within the range of 2363 and 2537 μmol kg^{-1}. During the 1994 annual austral summer cruise, the median and mean n35TA concentrations were 2393 and 2394 μmol kg^{-1} respectively (Fig 4.4B). Overall, concentrations were within the range of 2202and 2498 μmol kg^{-1}.

During the 1993 annual austral summer cruise, the median and mean n35N concentrations were 19.29 and 19.06 μmol kg^{-1} respectively (Fig 4.5A). Overall, concentrations were within the range of 8.30 and 31.63 μmol kg^{-1}. During the February to March 1993 cruise, the median and mean n35N concentrations were 28.26 and 28.18 μmol kg^{-1} respectively (4.5A). Values were within the range of 27.12 and 29.22 μmol kg^{-1}. During the Aug 1993 austral winter cruise, the mean and median n35DIC concentrations

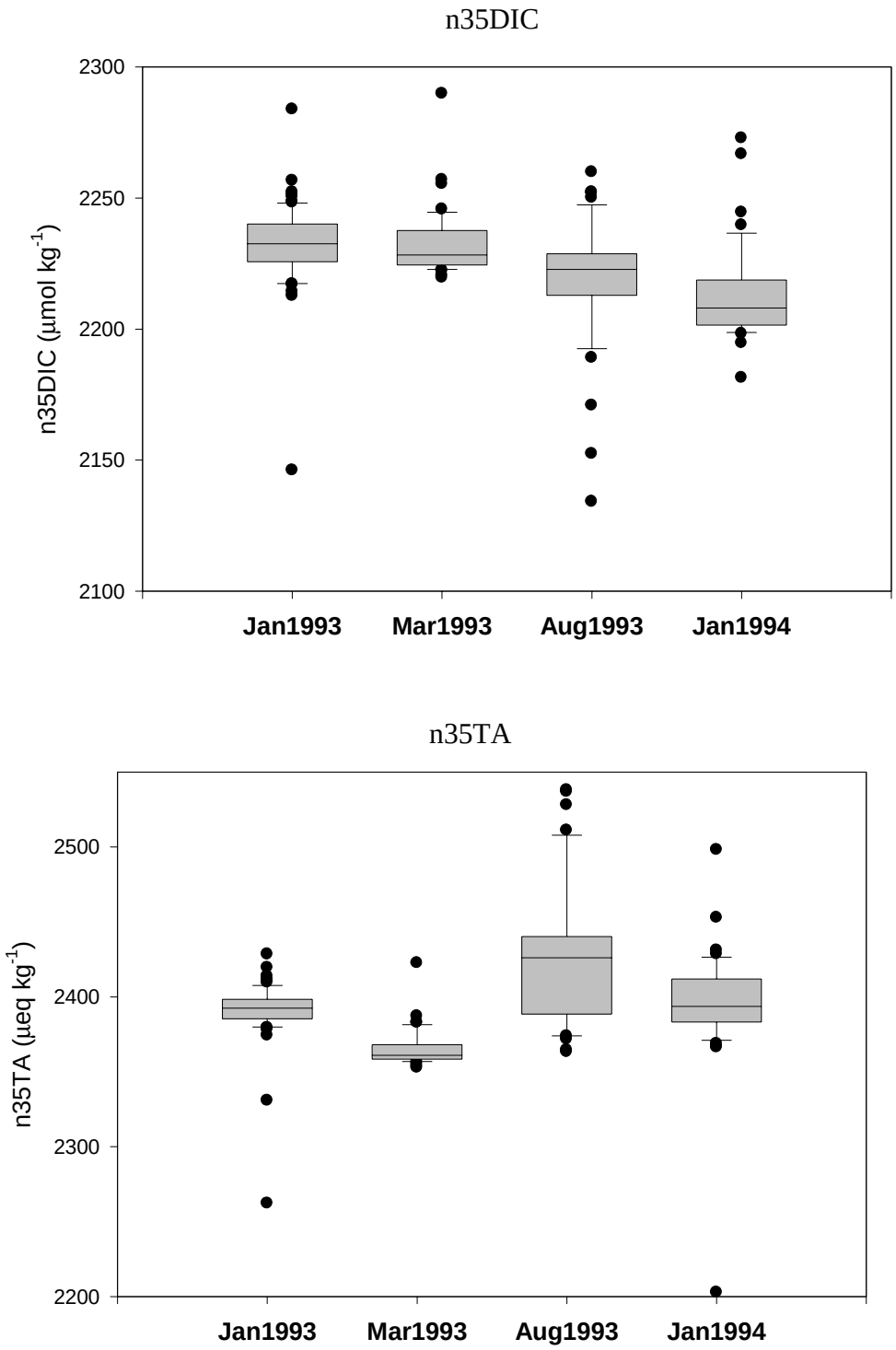

Figure 4.4 A) Boxplots of n35DIC B) Boxplots of n35TA

were 29.95 and 28.72 μmole kg^{-1} respectively (Fig 4.5A). Values were within the range of 19.51 and 33.44 μmole kg^{-1}. During the 1994 annual austral summer cruise, the median and mean n35N concentrations were 24.94 and 25.25 μmole kg^{-1} respectively. Overall, concentrations were within the range of 22.61 and 33.21 μmole kg^{-1}.

During the 1993 annual austral summer cruise, the median and mean n35P concentrations were 1.43 and 1.56 μmol kg^{-1} respectively (Fig 4.5B). Overall, concentrations were within the range of 1.03 and 2.58 μmole kg^{-1}. During the February to March 1993 cruise, the median and mean n35P concentrations were 1.93 and 1.99 μmole kg^{-1} respectively (Fig 4.5B). Values were within the range of 1.66 and 2.62 μmole kg^{-1}. During the Aug 1993 austral winter cruise, the mean and median n35 DIC concentrations were 1.95 and 2.04 μmol kg^{-1} respectively. Values were within the range of 1.47 and 3.34 μmole kg^{-1}. During the 1994 annual austral summer cruise, the median and mean n35P concentrations were 1.67 and 1.68 μmol kg^{-1} respectively (Fig 4.5B). Overall, concentrations were within the range of 1.46 and 2.22 μmol kg^{-1}.

Discussion

Geographic Variability

Comparisons of the geographical variability of DIC and salinity highlight areas where fresher waters dilute DIC concentrations. During the January-1993 austral summer cruise, DIC concentrations exhibited a wide range of values within the Pal-LTER grid

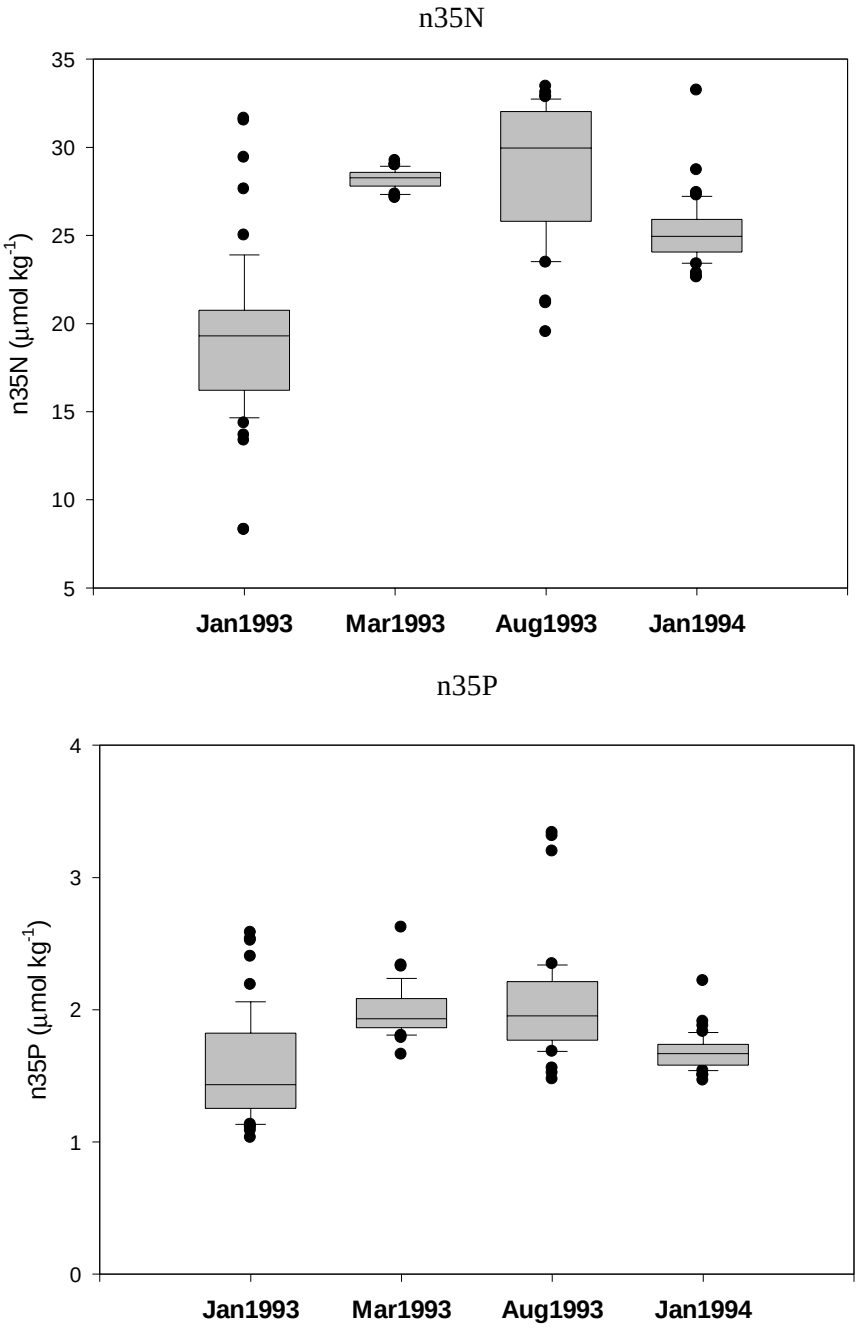

Figure 4.5 A) Boxplots of n35N B) Boxplots of n35P

area (Fig 4.2A). Depletions within the southern inshore region of the grid (200 and 300 lines) were correlated with fresher waters, suggesting dilution of DIC concentrations by ice melt and precipitation (Fig 4.5A and B). Within the northern region (500 and 600 lines), DIC concentrations and salinity remained relatively constant (± 5 μmol kg^{-1} and ± 0.1 respectively) when compared to the southern lines. After normalizing DIC to a salinity of 35 (n35DIC = DIC*35/salinity), the geographical distribution reflects concentrations that have been corrected for freshwater input (Fig 4.3A). Normalized-35DIC concentrations on the 200, 400 and 600 lines displayed offshore gradients with relatively higher n35DIC concentrations shoreward (40 to 80 km from shore) compared to lower n35DIC concentrations seaward (160 to 200 km from shore; Fig 4.3A).

The spatial variability of n35DIC is a function of many processes such as air-to-sea exchange, temperature, horizontal advection, upwelling, photosynthesis, and respiration. These processes affect n35DIC concentrations over varying spatial and temporal scales. Comparing spatially varying n35DIC concentrations to n35N and n35P concentrations shows the effects of photosynthesis and respiration. Depletions of n35N and n35P correlate to depletions of n35DIC if the removal of these elements is constant with phytoplankton growth. During the RACER field program, the mean N:P assimilation ratio of 15 was very close to the Redfield ratio of 16 (Fig 4.6A) within coastal areas. Overall, values within the Pal-LTER grid compare with the regression (Model II) of N:P calculated during the RACER project (Fig 4.6). Seven values from the 400 to 600 gridlines are located below the regression line at n35N concentrations greater then 20 μmol kg^{-1}. During RACER, the molar C:N relationship of 6.3 was very close to the Redfield ratio of 6.6, but the molar C:P relationship (94.2) was less than the expected

Redfield ratio of 106 (Fig 4.7A and B; Redfield et al. 1963). Normalized-35DIC values within the Pal-LTER grid area are decoupled with n35N and n35P concentrations (Fig 4.7). Therefore, processes (i.e. photosynthesis and respiration) controlling n35N and n35P concentrations do not necessarily control n35DIC concentrations.

Seasonal Variability

The central tenet of the Pal-LTER program states that the timing and magnitude of sea ice growth and ablation control the distributions and concentrations of the chemical properties of surface seawaterand ultimately, system productivity. Surface waters are subject to seasonal fluctuations of temperature, salinity, ice formation and ablation (Klink 1998). Ice cover within the LTER region generally develops rapidly and then declines slowly with peak ice cover in August (Stammerjohn and Smith, 1996). This cycle is different from other regions of the Southern Ocean, where ice advance is slower and then declines rapidly, with the peak ice cover in September (Stammerjohn et al. submitted).

As air temperatures increase from winter to summer, sea-ice ablates and surface waters freshen, stratify, and warm from solar heating. The quantity and timing of ice melt determine the broad range of temperature and salinity ratios during the summer season (Fig 4.8). Between summer and winter, surface waters cool, and ice formation begins. As air temperatures decrease from summer to winter, surface seawater temperatures decrease (Fig 4.8). Sea-ice growth begins, and brine drainage into the sub-ice water increases the salinity (Fig 4.8). This saline water sinks and combined with storm activity, mixed layers deepen with water temperature

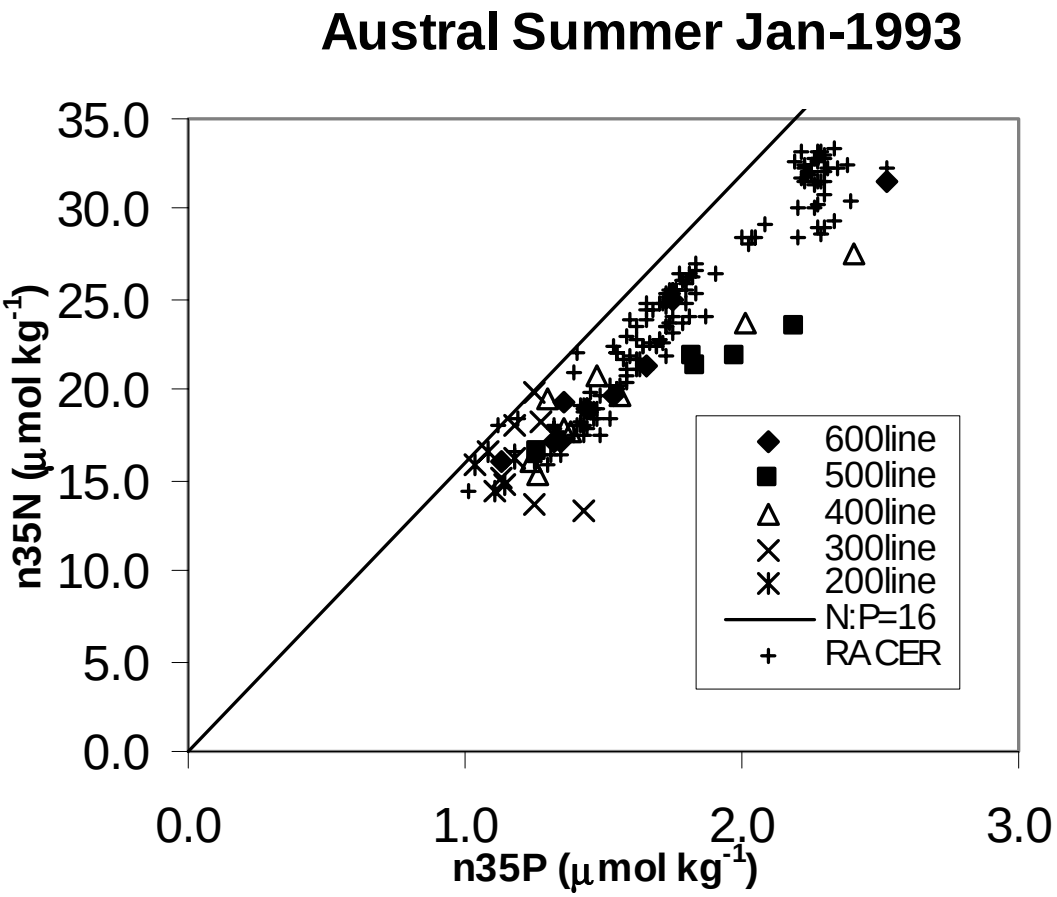

Figure 4.6 n35N versus n35P. Solid regression line represents a N:P relationship of n35N = n35P*16 + 0.

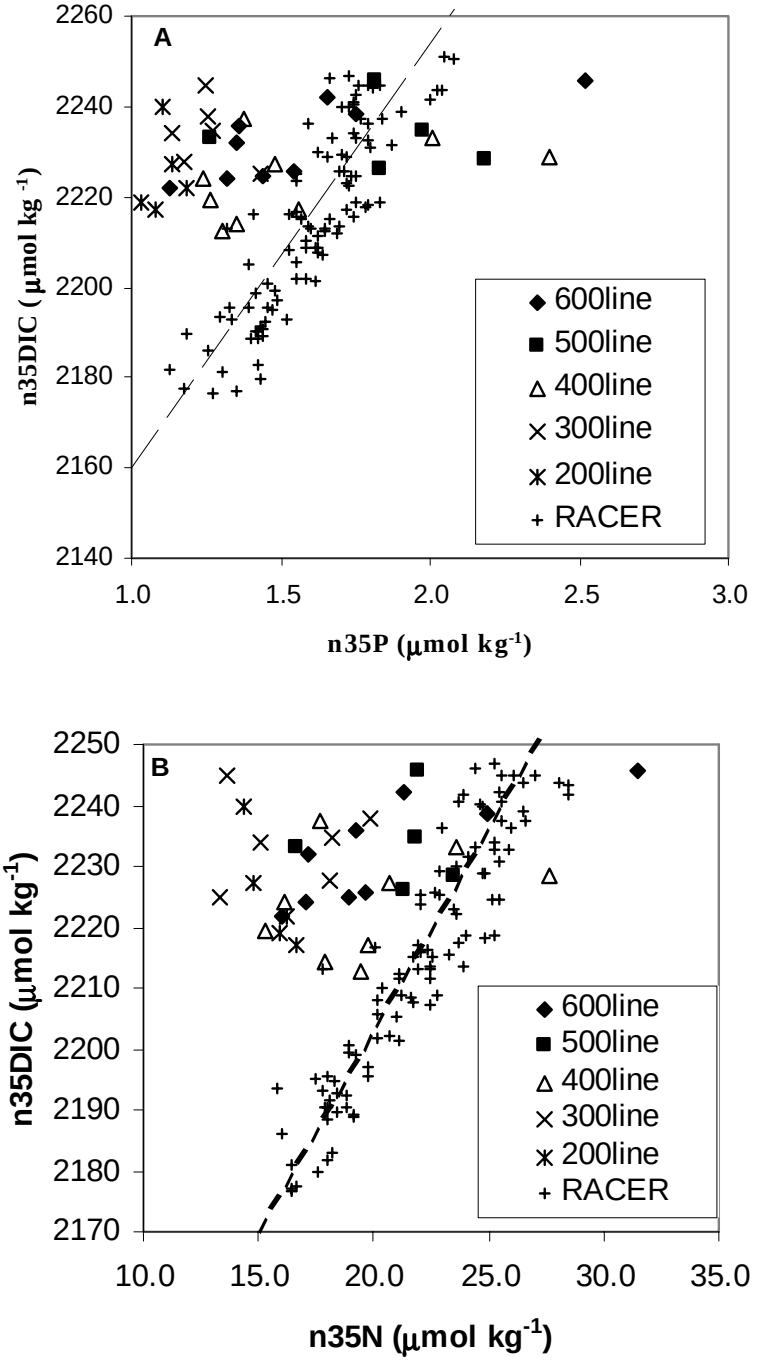

Figure 4.7 A) n35P versus n35DIC. Dashed regression line represents a relationship (Model II) of n35DIC = n35P*94.2 + 2063.5 fit to the RACER data B) n35N versus n35DIC. Dashed regression line represents a relationship (Model II) of n35DIC = n35N*6.3 + 2075.4 fit to the RACER data.

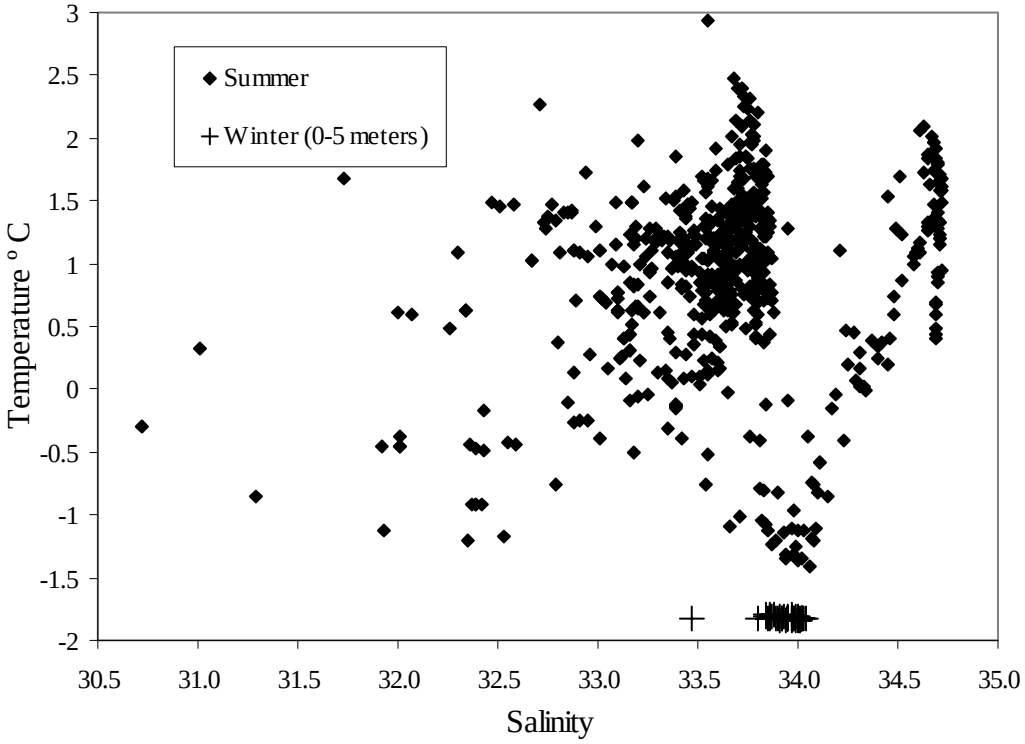

Figure 4.8 Salinity versus temperature within the Pal-LTER grid area.

very near freezing. Winter waters are generally relatively colder, saltier and more uniform than summer surface waters with respect to salinity and sea surface temperature (Fig 4.8).

As surface waters freshen and warm during spring and summer, surface ocean DIC concentrations are predicted to decrease because of dilution by melt-water. Phytoplankton blooms can further decrease DIC, N and P concentrations. As surface waters cool during fall and winter, sea ice formation begins and DIC and nutrient concentrations are predicted to increase as mixed layers cool and deepen during fall and winter seasons (Fig 4.9 A and B; Carrillo and Karl, 1999; Gibson et al. 1999). Normalized N and n35P displayed seasonal cycles consistent with the seasonal physical hydrography (Fig 4.5A and B). Concentrations increased between January and March as mixed layers deepened (Fig 4.5A and B and 4.9).

Within the Pal-LTER grid area (40 to 200 km offshore between the 200 and 600 lines) spatially variable n35DIC concentrations complicate seasonal interpretations. For example, n35DIC concentrations decreased from January 1993 to August 1993 by as much as 83 μmol kg^{-1} in some areas and increased 25 μmol kg^{-1} in other areas relative to the preceding austral summer (January, 1993). Normalized-35DIC concentrations in the winter are similar, if not slightly lower than the preceding summer values (Fig 4.4A). Low n35DIC concentrations relative to summer values are consistent with observations in the Weddell Sea and Prydz Bay during the austral winter but contrary to high n35DIC concentrations observed in the Gerlache Strait (Hoppema et al. 1995; Carrillo and Karl 1999).

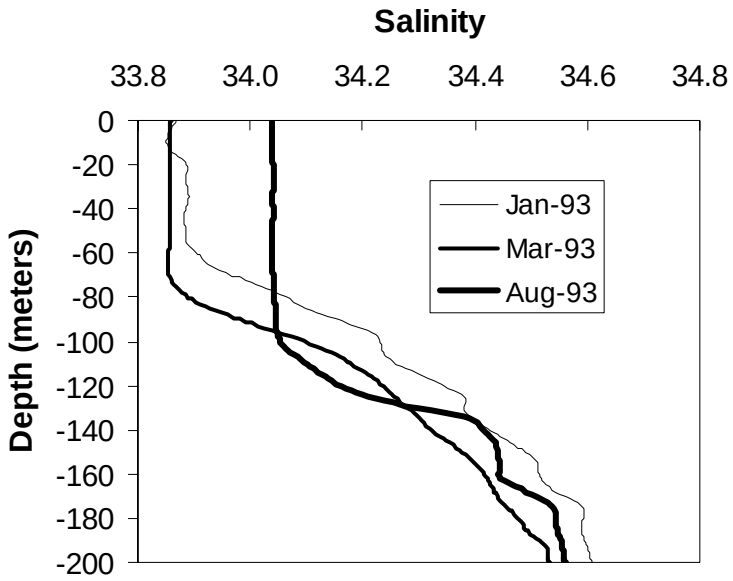

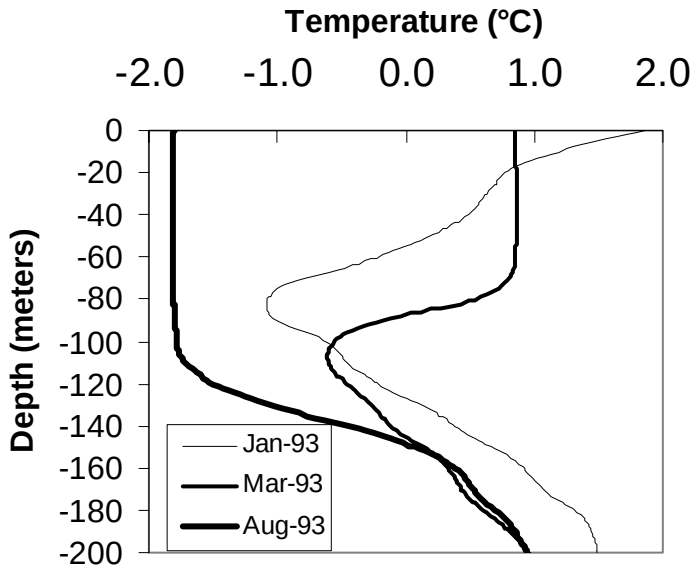

Figure 4.9 A) Depth dependent profiles of salinity within the Pal-LTER areas. B) Depth dependent profiles of temperature within the Pal-LTER area.

Differences between the Pal-LTER grid area and coastal areas like Gerlache Strait are highlighted through the inorganic carbon dynamics. Depletions of n35DIC were encountered in coastal fjords and embayments such as Gerlache Strait and Marguerite Bay (Carrillo and Karl 1999). Depletions of n35DIC (up to 100 μmol kg^{-1}) were greater than expected based solely on changes in solubility and are attributed to CO_2 uptake by phytoplankton. Summertime depletions of DIC or fCO_2 (or pH increases) by photosynthesis have also been observed in the Weddell Sea, Prydz Bay, Author Harbor and Marguerite Bay (Gibson et al. 1999, Carrillo and Karl 1999, Hoppema et al. 1999 and Shabica 1977). Within Gerlache Strait, DIC and n35DIC concentrations increase from summer to winter as mix-layers deepen, photosynthesis-to-respiration ratios decreases and air-to-sea exchanges of CO_2 combine to replace inorganic carbon (Carrillo and Karl 1999, Carrillo 1996).

The seasonal Pal-LTER n35DIC depletions were decoupled from nutrient dynamics. A comparison of the seasonal C:N:P removals between the RACER (coastal inshore) and Pal-LTER regions (offshore 40 to 200 km) shows similarities between N:P ratios and differences between C:N and C:P ratios (Fig 4.10 and Fig 4.11). During the RACER program, seasonal depletions of n35DIC correlate with reductions of nitrate and phosphate with an overall C:N:P ratio of 94:15:1. Between January and August, 1993 (austral summer to winter) LTER seasons, n35DIC is decoupled from reductions of nitrate and phosphate (Fig 4.11). The seasonal decoupling of C:N is a function of the geographical distributions of nutrients and n35DIC. Overall, n35DIC concentrations in

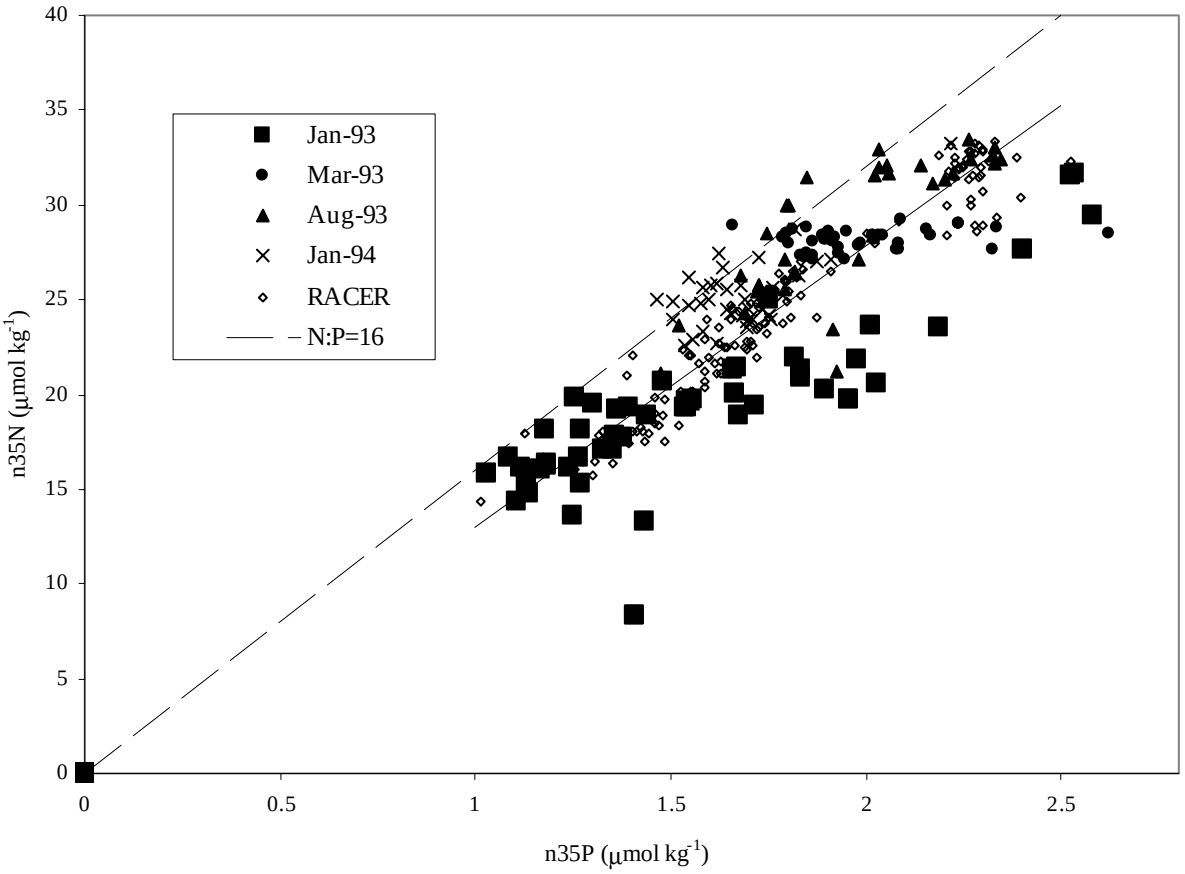

Figure 4.10 n35P versus n35N. The solid line represents the regression analysis (Model II) and yielded a relationship (Model II) n35N= 14.86(n35P) –1.88. The dashed line represents a N:P relationship of n35N=n35P*16 + 0.

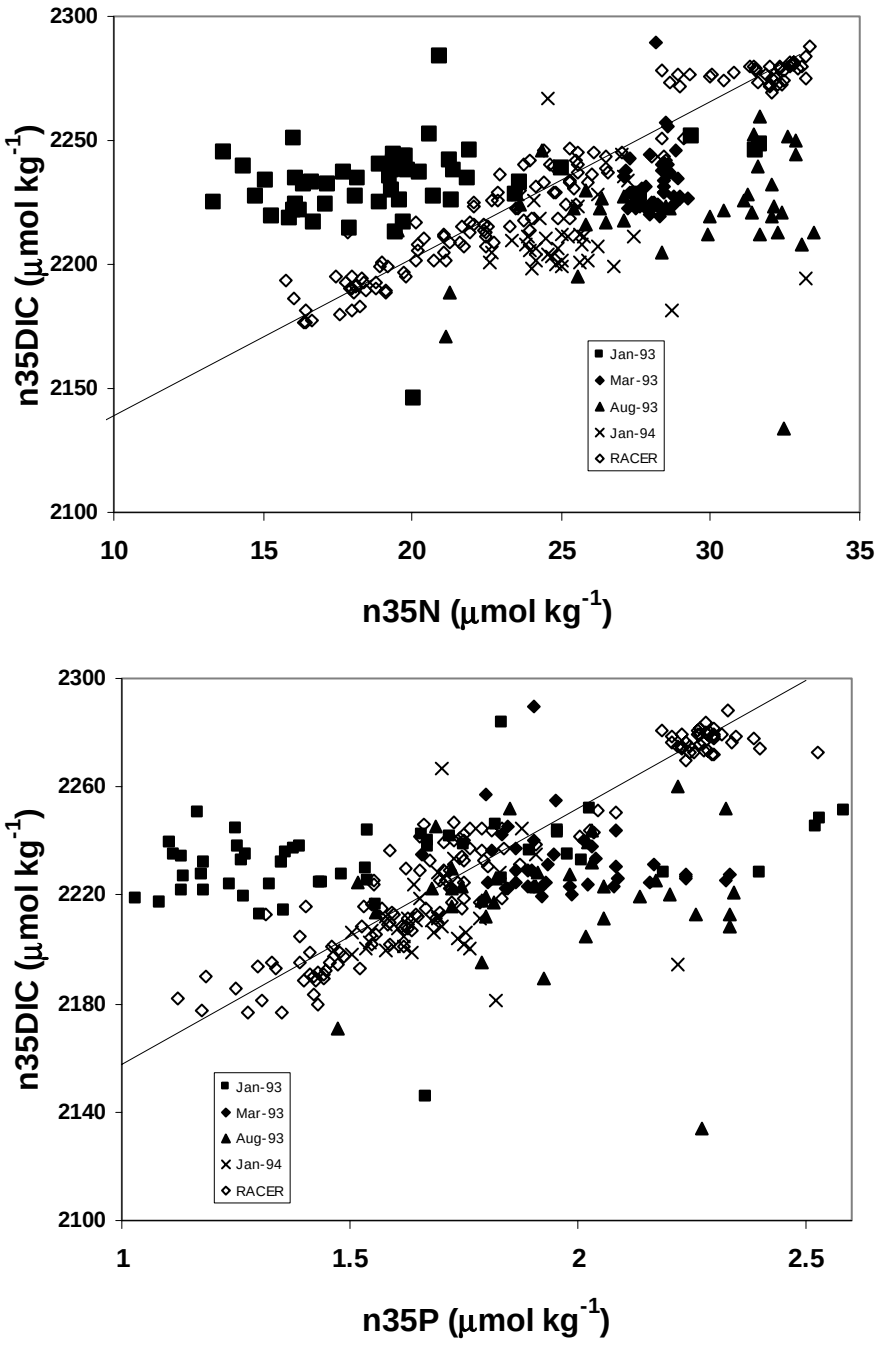

Figure 4.11 A) n35N versus n35DIC. The regression analysis (Model II) yielded n35DIC= 6.3(n35N) +2075.4 B) n35P versus n35DIC. The regression analysis (Model II) yielded n35DIC= 94.2(n35P) + 2063.5

surface waters are constant (2231.7 ± 15.3 μmol kg^{-1}) between January 1993 and August 1993 (Fig 4.9B). During the austral winter season, the Pal-LTER study region shows a wider range of nitrate and phosphate concentrations of 20-34 μmol kg^{-1} and 1.5 to 2.4 μmol kg^{-1} respectively relative to the Gerlache Strait.

Consistent or decreasing surface water n35DIC concentrations are inconsistent with observations of deeper mixing during the austral fall to winter seasons. Profiles of temperature and salinity show that as mixed layers deepen from approximately 40 to 100 meters, n35DIC concentrations should increase in proportion to nitrate and phosphate. Between January 1993 and March 1993, mixed layer depths deepened from approximately 35 meters to 70 meters based on changes in temperature and salinity (Fig 4.9). As mixed layer depths deepen, nitrate + nitrite and phosphate increase as higher nutrient water is mixed upward (Fig 4.9). Between March 1993 and August 1993, mixed layer depths increased an additional 40 meters from approximately 70 to 110 meters. Based on mixed layer depths, nitrate and phosphate concentrations, n35DIC should increase to 2280 μmol kg^{-1}; a 40 μmol kg^{-1} deficit.

Processes controlling DIC concentrations with respect to nitrate and phosphate may differ between austral summer and winter seasons. Growth rates during the summer may be slow enough that air-to-sea exchange of CO_2 replenishes inorganic carbon concentrations. During the winter, lower n35DIC and significantly higher n35TA concentrations may be the result of two independent processes; calcium carbonate ($CaCO_3$) precipitation and dissolution and under-ice algal productivity. Calcium carbonate has been reported to precipitate rapidly at the salinity and temperature in sea

ice brine and can be trapped in the ice matrix or expelled into the water through channels (Richardson 1976). Subsequently, the dissolution of $CaCO_3$ in waters just below the ice may subsequently increase TA and DIC. The increase in DIC could be offset by the uptake of DIC by ice algae.

Annual Variability

Relatively larger geographical and seasonal changes of sea surface temperature, salinity, n35DIC and fCO_2 make it difficult at this time to place confidence in annual trends despite an 8 year time series (Fig 4.12). Normalized-35DIC and fCO_2 are positively correlated to changes in temperature and salinity, implying that hydrographic variations may control the annual concentrations measured during each January cruise.

Conclusions

Within the Pal-LTER grid area, geographic studies of DIC show spatial variability that results primarily from the freshening of surface water from ice melt and precipitation. Geographic studies of n35DIC also show spatial variability. Areas of relatively low n35DIC concentrations were coupled with depletions of nitrate and phosphate and were mostly in coastal fjords and bays. Areas of relatively higher n35DIC concentrations occurred off the shelf and were decoupled from depletions of nitrate and phosphate. Within the Pal-LTER grid area, seasonal studies of n35DIC are not consistent with the seasonal cycle of physical hydrography, n35N or n35P. However, n35DIC measurements within Gerlache Strait are correlated with n35N and n35P. Annual changes of sea surface temperature, salinity, n35DIC and fCO_2 are difficult to interpret at this time

despite an 8 year time series because of larger geographical and seasonal variability (Fig 4.12).

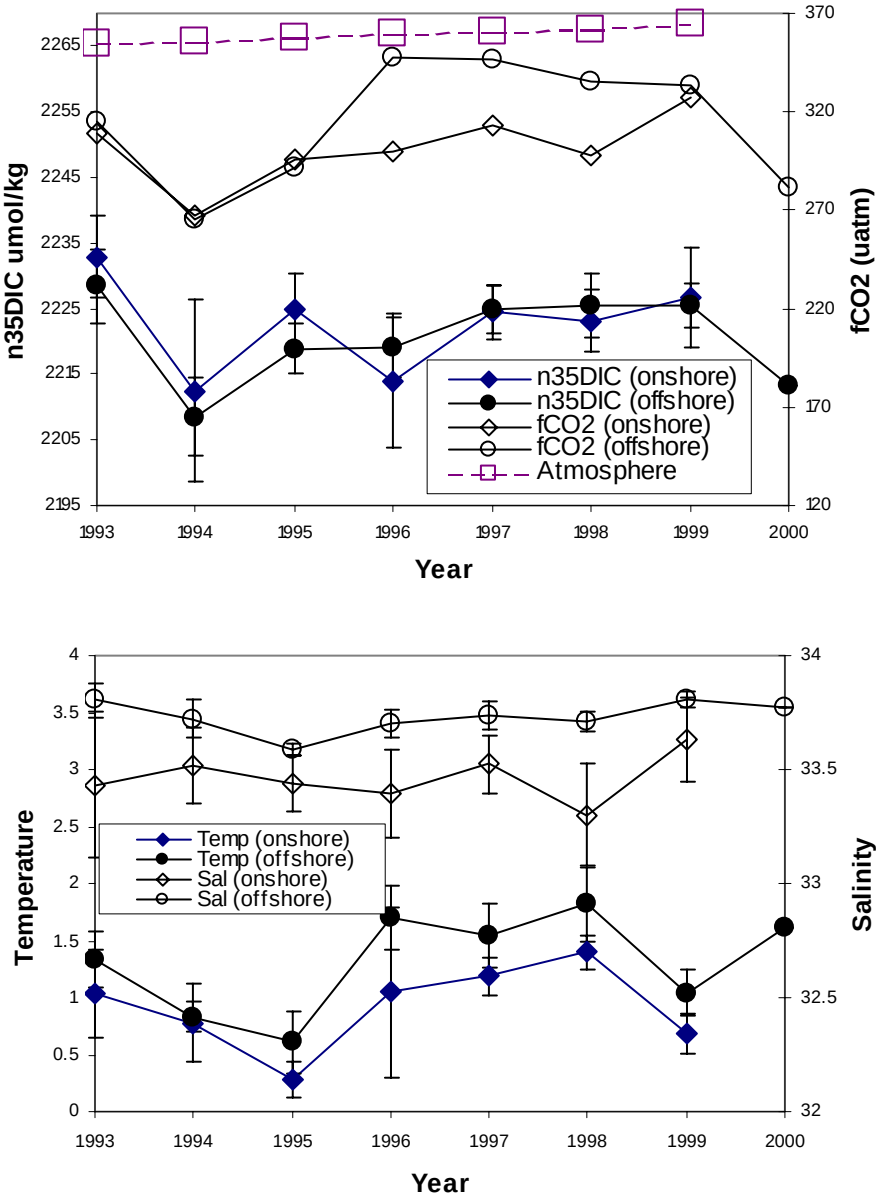

Figure 4.12 A) Annual changes of n35DICconcentration and fCO_2 pressure. B) Annual changes of temperature and salinity within the Pal-LTER study area

Appendix A Internal Consistency

The internal consistency of carbon system parameters was calculated using the program of Lewis and Wallace (1995). This BASIC program can be obtained from the CDIAC website (http://www.cdiac.esd.ornl.gov). The program calculates the carbon system parameters based on user-selected constants of K_1 and K_2. Any two of the four measurable carbon system parameters (DIC,TA, pH or fCO_2), temperature, salinity, phosphate, and silicate are required to calculate the other two carbon system parameters. Calculations can be performed as single input or batch modes.

Between 1996 and 1999, fCO_2, DIC and TA were measured during the annual Pal-LTER cruises in the area west of the Antarctic Peninsula. Using the constants of Mehrbach et al. (1973) refit by Dickson and Millero (1987), the estimated internal consistency between parameters is $3.2 \pm 4.2\%$ fCO_2, $-0.3 \pm 0.3\%$ DIC, $0.3 \pm 0.4\%$ TA (Table 4.1). Using the constants of Roy et al (1993, 1994, 1996), the estimated internal consistency between parameters is $2.6 \pm 4.3\%$ fCO_2, $-0.2 \pm 0.4\%$ DIC, $0.2 \pm 0.4\%$ TA (Table 4.2).

Profiles of salinity, DIC, n35DIC and TA as a function of depth within the Pal-LTER region have similar shapes (Fig 4.2, 4.3, 4.4, and 4.5). Salinity, DIC, n35DIC and TA are lower in the surface water and increase with depth to approximately 500 meters (Fig 4.2, 4.3, 4.4, and 4.5). Below 500 meters, there is very little change to the sea floor. Values range from 31.0 to 34.7, 1850 to 2264 $\mu mol\ kg^{-1}$, 2028 to 2284 $\mu mol\ kg^{-1}$, and 2106 to 2360 $\mu eq\ kg^{-1}$ respectively (Fig 4.2, 4.3, 4.4, and 4.5). TA normalized to a salinity of 35 is higher in surface waters and decreases with depth to approximately 100

meters (Fig 4.5). Below 150 meters, there is very little change to the seafloor.

Concentrations range from 2375 to 2541μeq kg^{-1} (Fig 4.5).

Table 4.1. Internal Consistency of carbon system parameters measured in the region west of the Antarctic Peninsula using the apparent dissociation constants of Roy et al. (1993, 1994, 1996).

Parameter Pair	ΔTA	ΔDIC	ΔfCO_2
fCO_2-TA		-0.2 ± 0.4%	
fCO_2-DIC	0.2 ± 0.4%		
DIC-TA			2.6 ± 4.3%

Table 4.2. Internal Consistency of carbon system parameters measured in the region west of the Antarctic Peninsula using the apparent dissociation constants of Mehrbach et al. (1973) refit by Dickson and Millero (1987).

Parameter Pair	ΔTA	ΔDIC	ΔfCO_2
fCO_2-TA		-0.3 ± 0.3%	
fCO_2-DIC	0.3 ± 0.4%		
DIC-TA			3.2 ± 4.2%

The apparent thermodynamic equilibrium constants are measured as a function of salinity and temperature. Few estimates are determined at temperatures common in Antarctic surface waters (< 0 ºC), especially during the winter. A comparison of the internal consistency between the parameters TA, DIC, and fCO_2 reveals no significant differences between the apparent constants of Mehrbach et al. (1973) refit by Dickson and Millero (1987), and those of Roy et al. (1993, 1994, 1996; Table 4.1 & 4.2). The variability observed between measured and calculated values may originate from one of two reasons. First, the Pal-LTER program region includes numerous habitats with a wide range of DIC, TA, and fCO_2 values, and hence, variable TA/DIC ratios. Second, in many of the highly productive areas, mixed-layer depths are shallow (<10 m), and sampling

coherence between the underway system and the CTD is not exact. Spatial scales of variability are enhanced by heterogeneous hydrography and patchy phytoplankton blooms.

CHAPTER V

CROSS-SITE COMPARISON OF THE INORGANIC CARBON DYNAMICS AT THE HAWAII OCEAN TIME-SERIES AND PALMER LONG TERM ECOLOGICAL RESEARCH SITES

Abstract

The ocean carbon pumps are processes that maintain surface ocean depletions of dissolved inorganic carbon relative to deeper waters. The relative importance of each pump in maintaining the gradient of DIC is estimated by comparing the working strengths of the individual pumps; solubility, carbonate and soft tissue. The potential of each pump to modify carbon fluxes is contingent upon the environmental variables that characterize strengths and efficiencies. At Station ALOHA, the soft tissue pump explains 93% of the observed gradient of n35DIC between the surface and deep water and is working at 97% efficiency. The potential of this pump to increase carbon fluxes to the deep ocean would require fundamental changes in the standing stocks of microorganisms and nutrient pathways. Within the Pal-LTER region, the soft tissue pump explains 100% of the observed gradient of n35DIC between the surface and deep water and is working at 50 to 100% efficiency. The solubility pump at Station ALOHA explains 7% of the gradient of n35DIC but has the potential to explain 57% of the gradient of n35DIC. Within the Pal-LTER region the solubility pump does not exist and has little potential to alter carbon fluxes.

Introduction

The processes controlling carbon dioxide in the ocean have been described for two environments; the North Pacific Subtropical Gyre and the region west of the

Antarctic Peninsula (Chapters 2, 3, & 4). These two ecosystems represent contrasting regions of the world's oceans. The HOT program site (Station ALOHA) is characterized by sea surface water temperatures ranging from 23 to 27 ºC and sub-micromolar inorganic nutrient ([nitrate+nitrite] and phosphate) concentrations (N ≤ 10 nM, P ≤ 100 nM), typical of subtropical marine environments. Low stocks of phototrophic microoganisms (chlorophyll *a* concentration ≤ 0.1 $\mu g\ l^{-1}$) are dominated by photosynthetic picoplankton and typically export 0.8 to 1.0 mol C $m^{-2}\ yr^{-1}$. On the other hand, relatively cold surface waters ranging from -1.8 to 3.0 ºC and relatively high inorganic nutrient concentrations (nitrate ≤ 33 $\mu mol\ kg^{-1}$, phosphate ≤ 2.5 $\mu mol\ kg^{-1}$) characterize the western Antarctic Peninsula Palmer- Long Term Ecological Research (Pal-LTER) region.

The potential of these and other oceanic ecosystems to sequester carbon dioxide and respond to climate variation will depend on the response of the individual processes controlling the fluxes of carbon between the atmosphere and deep ocean. Models may over-simplify the description of the oceans, yet are exceedingly complex in their treatment of the controls on dissolved CO_2 concentrations. Additionally, model comparison between contrasting ecosystems are sometimes difficult when model variables are tailored to fit certain regions. The only goal of this chapter is to compare and contrast these two study sites, which have been discussed in this dissertation with a finite set of fundamental processes that describe the vertical gradients of n35TA and n35DIC.

For example, what role does the solubility pump play in controlling n35DIC concentrations at Station ALOHA, and within the Pal-LTER region? Would a larger role

be expected at Station ALOHA where the range of surface to deep water temperature change is 6 times that of the Pal-LTER region. What role does the biological pump play in describing the profiles of n35DIC as a function of depth between these two regions?

The equilibration of CO_2 between the atmosphere and surface ocean via air-to-sea exchange of CO_2 does not necessarily represent a net sink for CO_2. Ultimately, the enhanced transfer of carbon via the solubility and biological pumps governs the removal of carbon (Volk and Hoffert 1985). In their paper, Volk and Hoffert describe six equations describing 3 processes. The results were compared to more complicated general circulation models. I chose this method because these equations are as valid today as they were in 1985 in describing the basic properties of the carbon pumps. These "pumps" maintain the vertical gradient of DIC observed in the oceans. The solubility pump refers to the change of CO_2 driven by solubility differences of warm and cold water. The biological pump is subdivided into two components; the soft tissue and carbonate pump (Volk and Hoffert 1985). The soft tissue pump describes the process of photosynthesis at the ocean surface removing inorganic carbon and essential macronutrients, and producing organic matter, some of which is exported to depths beneath the euphotic zone. The carbonate pump refers to a process similar to the soft tissue pump except that $CaCO_3$ is precipitated in surface waters by microorganisms and mesozooplankton. A portion of this $CaCO_3$ is transported to depth where it dissolves or is buried (depending on ocean depth).

In any ocean system where the solubility, carbonate, and soft tissue pumps are working, the strength and efficiency of the soft tissue and solubility pump is estimated from knowledge of DIC, TA, HPO_4 (or NO_3), C/P (or C/N), salinity, and temperature.

The strength of each pump is defined as the concentration difference created between the surface and deep water. The efficiency is defined as the ratio of the actual working strength to the maximum working strength. The pump efficiency is useful for comparing the pump to its maximum potential, and the pump strength is useful for comparing environments.

Data

Profiles of n35DIC concentrations at Station ALOHA and the LTER study region have fundamentally similar depth-dependent features where n35DIC concentrations are low in surface waters and high in deep waters (Fig 5.1). For example, both regions have minimum n35DIC concentrations in the near-surface water (HOT = 1960-1970 μmol kg^{-1} versus LTER = 2025 – 2340 μmol kg^{-1}), and concentrations increase with depth. The slope of the gradient and the depth of the maximum concentrations vary considerably (Fig 5.1). Maximum concentrations at Station ALOHA of 2400 μmol kg^{-1} occur at approximately 1000 meters and are relatively unchanged to 2000 meters. Below 2000 meters, n35DIC concentrations decrease slightly to approximately 2350 μmol kg^{-1} at 4500 meters. Within the LTER study region, maximum n35DIC concentrations of only 2285.0 μmol kg^{-1} are displaced upward (~200 m) and remain unchanged to at least 3500 meters (Fig 5.1).

Depth dependent n35TA profiles at Station ALOHA and the LTER study region have dissimilar shapes (Fig 5.2). At Station ALOHA, n35TA concentrations range from 2288.3 to approximately 2329.1 μeq kg^{-1} between 0 and 400 meters (Fig 5.2). Below 400

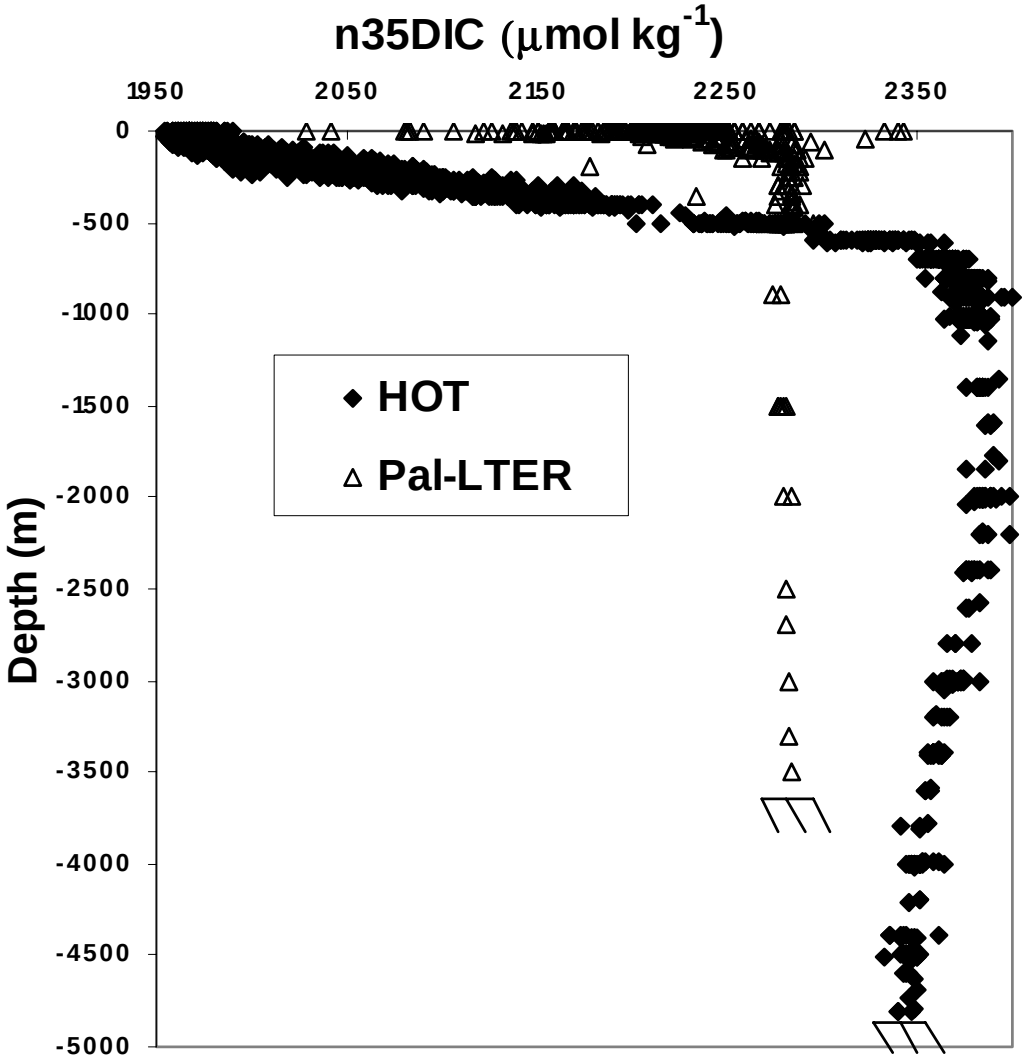

Figure 5.1 Depth dependent profile of n35DIC at Station ALOHA and within the Pal-LTER region

meters n35TA concentrations increase to approximately 2450 μeq kg^{-1} at 2000 meters and remain unchanged to 4500 meters. Within the LTER study region, surface water n35TA concentrations range from 2350 to 2550 μeq kg^{-1}. Below the surface, n35TA concentration decrease with depth to approximately 500 meters. Below 500 meters, n35TA concentrations are relatively constant at 2375.6 μeq kg^{-1} (Fig 5.2).

Depth dependent profiles of temperature have dissimilar shapes. At Station ALOHA, temperature ranges from 23 to 26 °C in surface waters (0-70m). Temperature decreases with depth to a minimum of 1.46 °C at 400 meters (Fig 5.3). Within the Pal-LTER region, surface temperature ranges from –1.8 to 3.0 °C (0-10 meters). For waters with surface temperatures above –1.8 °C, temperature deceases with depth to minimum of -1.8 to –1.6 °C at 60 to 120 meters. Below 120 meters, temperatures increase to approximately 2 °C at 350 to 500 meters. Below 500 meters, temperature slightly decreases to 0.4 °C at 3500 meters.

Profiles of N concentrations at Station ALOHA and the LTER study region have fundamentally similar depth-dependent features where N concentrations are low in surface waters and high in deep waters (Fig 5.4). For example, both regions have minimum n35N concentrations in the near surface water (HOT 0 μmol kg^{-1} versus LTER = 0-40 μmol kg^{-1}), and concentrations increase with depth. The slope of the gradient and the depth of the maximum concentrations vary considerably (Fig 5.4). Maximum concentrations at Station ALOHA of 43 μmol kg^{-1} are at approximately 1000

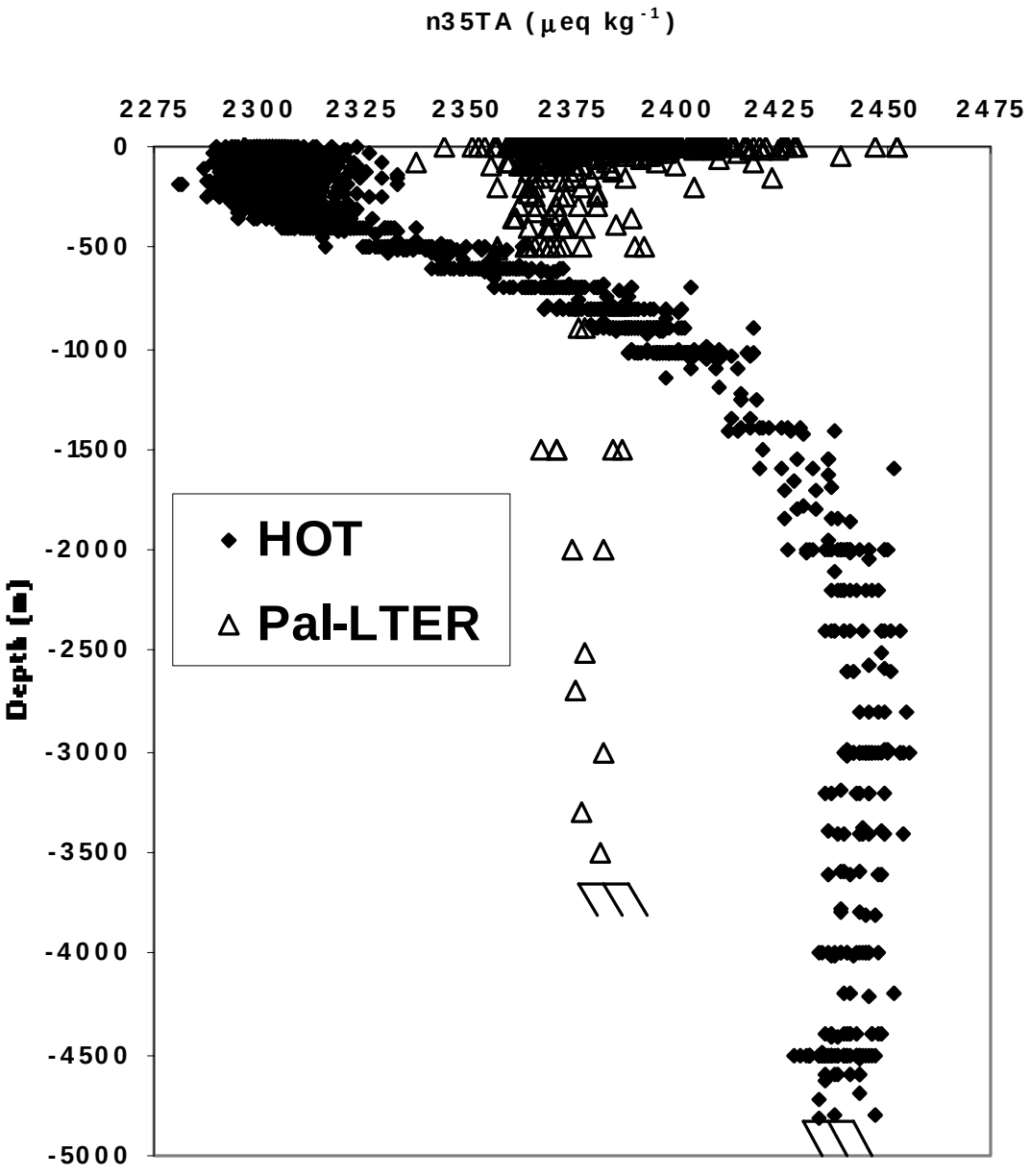

Figure 5.2 Depth dependent profile of n35TA at Station ALOHA and within the Pal-LTER region

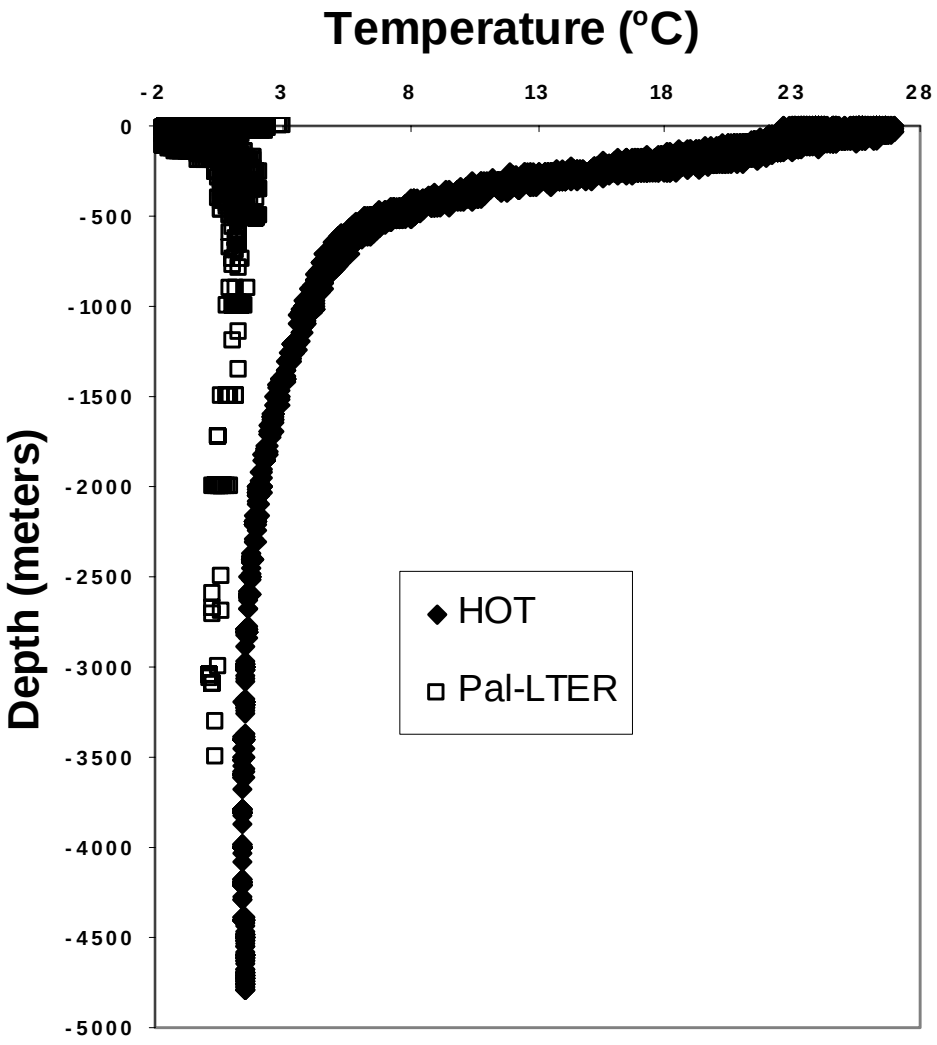

Figure 5.3 Depth dependent profile of temperature at Station ALOHA and within the Pal-LTER region

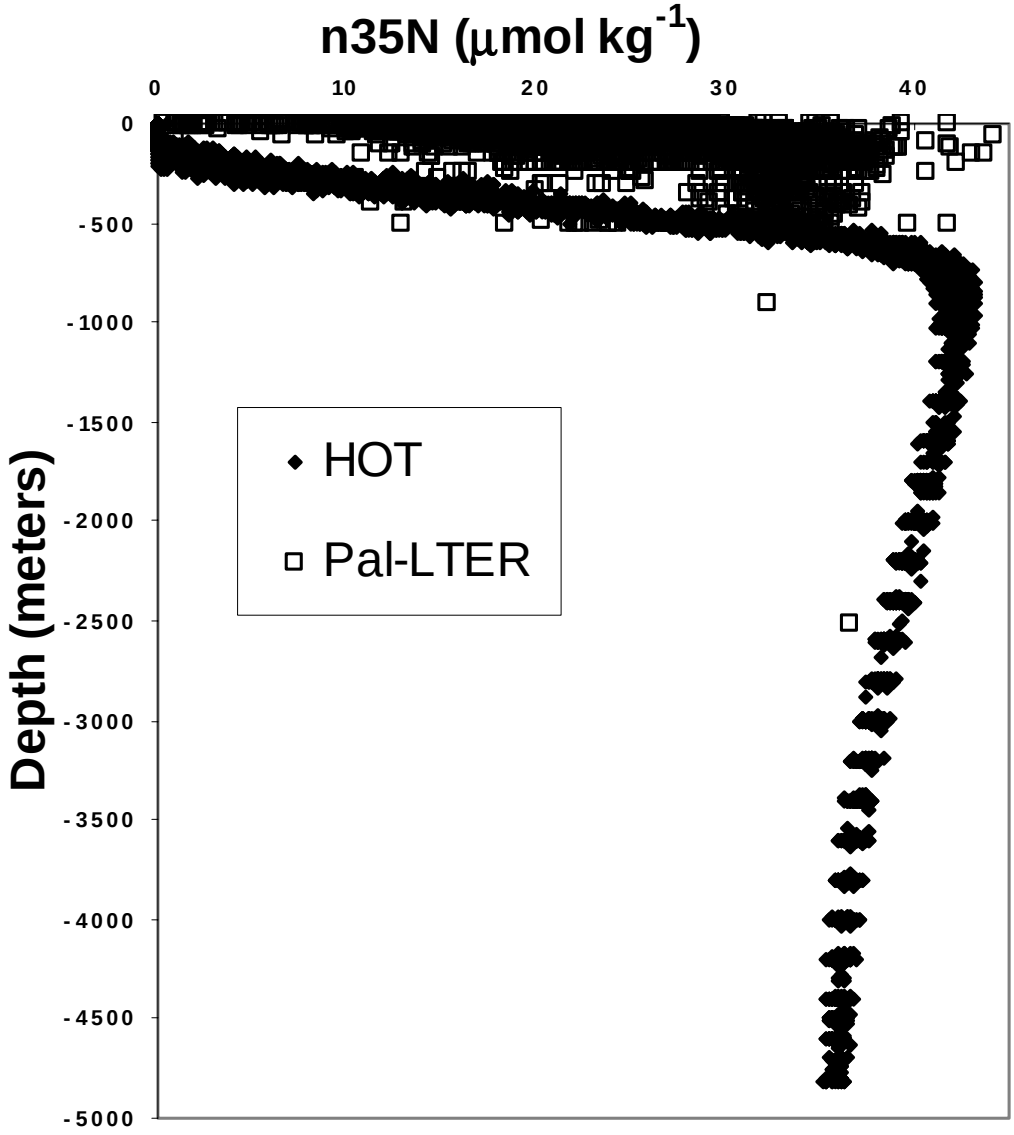

Figure 5.4 Depth dependent profile of n35N at Station ALOHA and within the Pal-LTER region

meters and decrease slightly with depth. Below 1000 meters, N concentrations decrease slightly to approximately 35 μmol kg^{-1} at 4500 meters. Within the LTER study region, maximum N concentrations of only 43 μmol kg^{-1} are displaced upward (~800 m). Typically, maximum N concentrations are variable between 0 and 500 meters (Fig 5.4).

Discussion

By quantifying the efficiency and strength of the individual inorganic carbon pumps, the processes responsible for maintaining the depth-dependent gradients of n35DIC are compared between the two marine environments.

Carbonate Pump

Although the treatment of the carbonate pump is primarily to correct DIC concentrations, it represents a fundamental difference between sites. The changes of n35DIC caused by the precipitation and dissolution of $CaCO_3$ rely on the difference between deep and mixed layer n35TA concentrations. The depth-dependent profile of n35TA at station ALOHA represents a "typical" profile to estimate carbonate pump strengths. Shallow n35TA and n35DIC concentrations are depleted by the precipitation of calcareous tests (Fig 5.2). As the tests sink, n35TA and n35DIC concentrations increase through the dissolution of $CaCO_3$. After correcting n35DIC concentrations (Appendix A; equation 4) for the precipitation of $CaCO_3$ in surface waters and dissolution of $CaCO_3$ in deep waters, a depth-dependant profile of n35DIC represents the soft tissue and solubility pump processes (Fig 5.5).

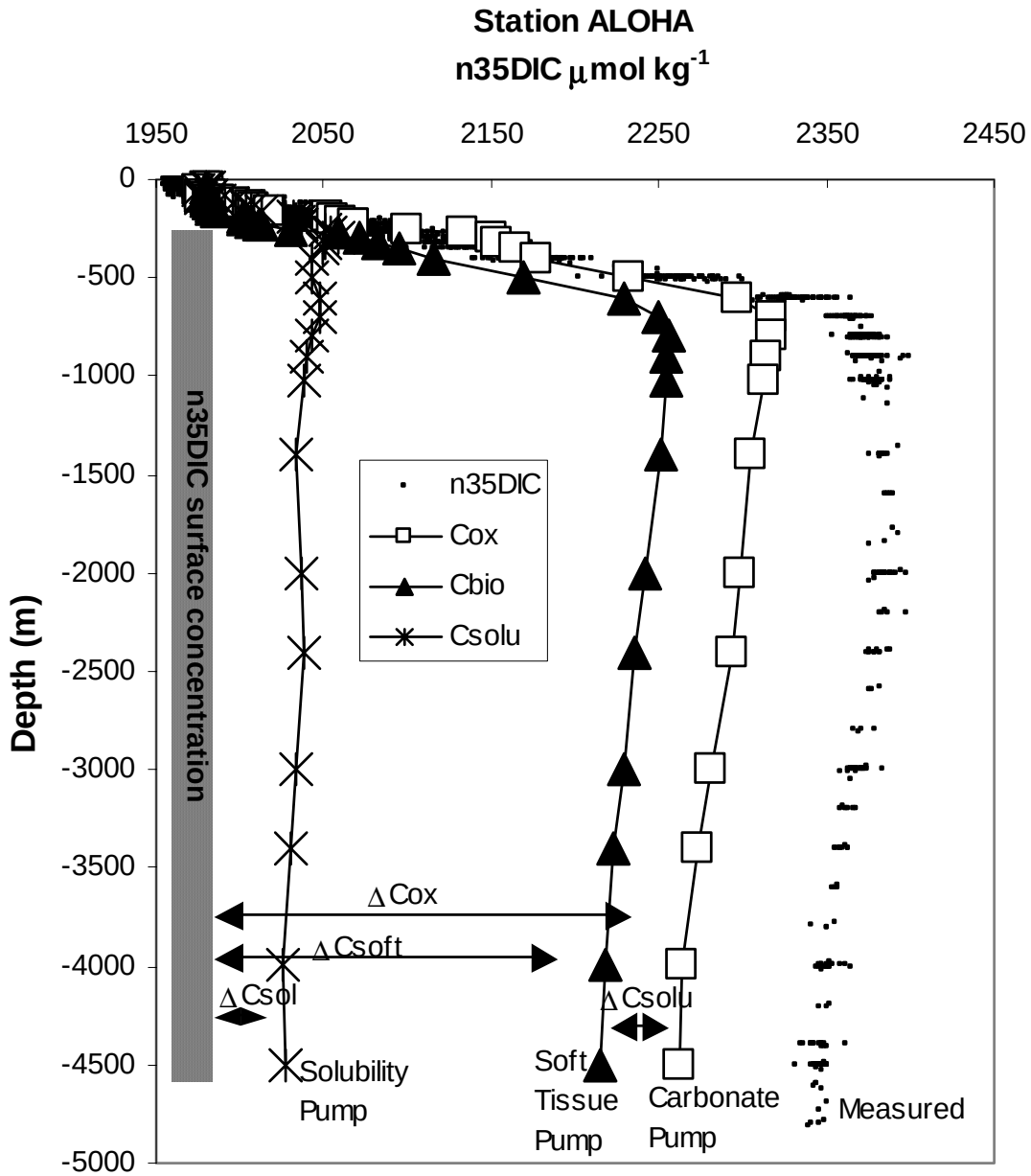

Figure 5.5 Depth dependent profile of n35DIC and model-generated profiles of n35DIC at Station ALOHA.

Within, the LTER study region, a typical carbonate pump is not working. If anything, a "reverse" carbonate pump best describes the observed depth dependent profile of n35TA (higher n35TA observed in shallow waters and relatively lower n35TA observed in deep waters). Normalized-35TA was not corrected for the uptake of N by phytoplankton. Therefore, surface values may be lower by as much as 40 umol kg^{-1} (Goldman and Brewer 1980). Inorganic carbon is not transported from deep to shallow waters by the formation, sinking and dissolution of $CaCO_3$. The cause of slightly higher n35TA observed in surface waters is unknown. The precipitation and subsequent dissolution of $CaCO_3$ by the freezing and thawing of sea ice or the growth and remineralization of calcerous phytoplankton could explain these observations. The timing of $CaCO_3$ precipitation and dissolution events alter seasonal surface water n35TA concentrations, but this does not represent a vertical transport of carbon.

Soft Tissue Pump

Model estimates of the soft tissue pump strength show it to be one of the primary controls of n35DIC concentrations as a function of depth at Station ALOHA (Table 5.1; Fig 5.5). It explains 93% of the observed gradient of n35DIC. The pump strength is a function of the C/P or C/N ratio multiplied by the difference between deep and surface nutrient concentrations (Appendix A, equation 3a and 3b). Therefore, variations of the C/N and C/P ratios have a direct effect on the estimation of ΔCsoft (soft tissue strength;

Table 5.1 Station ALOHA and Pal-LTER data analysis

Property	Depth	HOT	Pal-LTER	Notes
PO_4 (μmol kg^{-1})	m	0.1	1.3	
	d	3	2.4	
NO_3 (μmol kg^{-1})	m	0.01	20	
	d	40	33	
n35TA	m	2305	2450	
	d	2450	2375	
n35DIC (μmol kg^{-1})	m	1970	2225	
	d	2390	2280	
C_{ox} (μmol kg^{-1})	m	1970	2215	Equation 4
	d	2298	2301	Equation 4
ΔC_{ox} (μmol kg^{-1})		328	86	Equation 5
$\Delta C_{solumax}$ (μmol kg^{-1})		187	0	
ΔC_{soft} (μmol kg^{-1})		305	86	Equation 3a
n_{soft}		97%	39%	Equation 2a
ΔC_{solu} (μmol kg^{-1})		23	0	Equation 6b
n_{solu}		12%	0%	Equation 1

Karl et al. 2001). The efficiency of the soft pump is a function of surface and deep nutrient concentrations (Appendix A, equation 2a and 2b). At Station ALOHA, surface nutrient concentration are sub-micromolar compared to micromolar deep-water concentrations. Therefore, the efficiency is approximately 97%.

Within the LTER region, model estimates of the soft tissue pump show it to be the control of n35DIC concentrations as a function of depth. It explains 100% of the observed gradient of n35DIC. Because surface water nutrient concentrations are not fully

utilized, estimated efficiency is only approximately 39%. Within coastal areas pump efficiency and strengths are much higher because of the complete depletion of nutrients.

Solubility Pump

The solubility pump strength is determined as the difference between the carbonate and soft tissue pump strength (ΔC_{soft}; Equation 6). The solubility pump potential is governed by the temperature gradient between surface and deep water. The working strength is a function of the strengths of the biological and carbonate pumps. At Station ALOHA, the strength of the solubility pump is only responsible for less then ~ 5% of the observed gradient of n35DIC. It has the potential to explain 57% of the gradient of n35DIC (187/328*100) because of the approximately 25 °C temperature difference between the surface and deep water (Fig 5.3).

In comparison, the solubility pump does not exist within the LTER study region. The seasonal heating and cooling of surface water spans the vertical range of temperature (Fig 5.3) Therefore, the solubility pump explains 0% of the gradient of n35DIC.

Cross-site Comparison

Overall, the analysis has shown the importance of the soft tissue pump at Station ALOHA and within the Pal-LTER region. Pump strengths can explain >97% of the observed vertical gradient of n35DIC at these two contrasting sites. Because the soft tissue pump explains such a large portion of the n35DIC signal, the solubility pump remains unimportant in both regions. The solubility pump has the potential to explain 57% of the n35DIC signal at Station ALOHA if the soft tissue pump were to decrease. The solubility pump has no potential to alter fluxes of carbon within the LTER region

unless there were changes in the vertical temperature structure. Differences occur in the strength of the carbonate pumps. Station ALOHA represents a typical open ocean area where n35TA is relatively low in surface waters compared to higher values within deeper waters. The reverse profile is observed within the LTER region. High n35TA is observed in surface waters relative to lower vales within deeper waters.

The importance of the soft tissue pump at Station ALOHA supports the hypothesis in Chapter 2 that the mean annual 13 μatm fCO_2 undersaturation was explained by the uptake of CO_2*aq by phytoplankton (Appendix B end of dissertation). These results suggest primary production as the cause for fCO_2 undersaturations. Within the Pal-LTER region, n35DIC was not correlated with depletions of n35N or n35P suggesting that primary production does not control the distributions of n35DIC.

Conclusions

Overall, the analysis has quantified the importance of the soft tissue pump in maintaining the gradient of n35DIC at both sites. A comparison between soft tissue pump strength and efficiency show that Station ALOHA has a much stronger and more efficient soft tissue pump. Analysis of the carbonate pump shows that Station ALOHA has a typical carbonate pump while the LTER region does not maintain a carbonate pump. The solubility pumps are unimportant at both sites.

Appendix A Model

All calculations and notation are taken from Volk and Hoffert (1985). The solubility pump efficiency is defined as

$$n_{solu} = (\Delta C_{solu} / \Delta C_{solumax}) \quad (1)$$

where ΔC_{solu} and $\Delta C_{solumax}$ are the measured and maximum surface-to-deep DIC differences due only to temperature-driven solubility changes. The $\Delta C_{solumax}$ is estimated by determining the change of DIC due to the temperature change between the surface and deep water with an initial DIC concentration in equilibrium with the atmosphere. The program of Lewis and Wallace (1995) with the constants (K_1 and K_2) of Mehrbach (1973) refit by Dickson and Millero (1987) were used to determine these changes. The efficiency and strength of the soft tissue pump is connected to the utilization of nutrients (P or N) for growth and the C/P or C/N ratio. The soft tissue pump efficiency is defined by

$$n_{soft} = 1- P_m / P_d \qquad (2a)$$

or

$$n_{soft} = 1- N_m / N_d \qquad (2b)$$

where the subscripts m and d represent mixed layer and deep concentrations. The soft tissue pump strength is defined as

$$\Delta C_{soft} = C/P*(P_d – P_m) \qquad (3a)$$

$$\Delta C_{soft} = C/P*(N_d – N_m) \qquad (3b)$$

where C/P or C/N represent the C to P or the C to N ratios and the subscripts d and m represent deep and mixed layer concentrations.

The efficiency and strength of the carbonate pump are not directly calculated but corrected for in the measured DIC data. A term, Cox is the residual leftover from subtracting away the $CaCO_3$ contributionto the DIC profile. The correction is connected to changes in TA by

$$Cox = DIC - 0.5(TA - TAm + NO_3 - NO3m) \quad (4)$$

where the subscript m represents the mixed layer concentration. A depth-dependent profile of Cox only contains the signals from the solubility and soft tissue pumps. A variable (overall strength) is defined

$$\Delta C_{ox} = Cox,d - Cox,m \quad (5)$$

where the subscripts d and m represent deep and mixed layer concentrations. The overall strength is defined in terms of the soft tissue and solubility pumps, so that

$$\Delta Cox = \Delta Csolu + \Delta Csoft \quad (6a)$$

or solving for ΔCsolu

$$\Delta Csolu = \Delta Cox - \Delta Csoft \quad (6b)$$

Therefore, an ocean containing all three pumps, the strength and efficiencies of the soft tissue and solubility pump can be calculated from temperature, DIC, TA, N (or P) and C/N (or C/P).

CHAPTER VI

KINETICS OF THE INORGANIC CARBON SYSTEM IN A CONTINUOUS CULTURE

Abstract

Inorganic carbon system chemistry was studied in two continuous culture systems (chemostats). A chemostat was inoculated with *Phaeodactylum tricornutum* (referred to as the biological chemostat) and another chemostat was abiotic (i.e. was not inoculated) and is referred to as the control chemostat. Measurements of dissolved inorganic carbon (DIC), total alkalinity (TA) and pCO_2 were internally consistent, and thermodynamic equilibrium calculations were adequate to describe CO_2 chemistry in the control chemostat. Within the biological chemostat, equilibrium calculations were not adequate to describe measured CO_2 system parameters and therefore could not be used to calculate the speciation of the inorganic carbon system (i.e. CO_2*(aq), HCO_3^- and CO_3^{2-}). Gas-solution equilibrium was never achieved between the pCO_2 pressure of the gas being bubbled through the chemostat and measured pCO_2 pressure of the growth medium. A steady state model was developed to explain observed differences between measured pCO_2 of the gas leaving the chemostat, calculated pCO_2 of the growth medium (from DIC and TA) and pCO_2 of the gas being bubbled through the chemostat. The flux of CO_2 gas between the growth medium and bubbling of gas through the chemostat is governed by the hydration-dehydration reactions of CO_2*(aq), pH and growth rate of phytoplankton.

Introduction

The role of the biological pump in transporting carbon dioxide to the deep ocean ultimately relies on the growth of marine phytoplankton. The growth of marine phytoplankton is regulated by their ability to utilize both inorganic and organic pools of nutrients, including carbon dioxide. An understanding of inorganic carbon chemistry in seawater is important for the study of phytoplankton growth and physiology, especially studies investigating their preference for bicarbonate (HCO^-_3) or aqueous carbon dioxide (CO_2*(aq)). Laboratory evidence for the utilization of the individual carbon species by selected groups of phytoplankton relies not only on precise and accurate measurements of the carbon system parameters but also on the derivation of the concentrations of individual carbon species calculated from these measurements. For example, the determination of CO_2(aq) in solution relies on accurate and precise measurements of DIC, TA and the proper apparent equilibrium constants K_1 and K_2 of carbonic acid in sea water.

The individual species of the carbon dioxide system cannot be directly measured but rather are derived from any two of the four measured variables that constitute the inorganic carbon parameters of seawater, namely: dissolved inorganic carbon (DIC), total alkalinity (TA), pH, and the fugacity of CO_2 (fCO_2). The fugacity of CO_2 accounts for the non-ideal nature of the gas, and numerically it is 0.3 to 0.4% lower then the partial pressure of CO_2 (pCO_2). The partial pressure of CO_2 is the product of the mole fraction of CO_2 and total pressure. These measurable parameters are linked by a specific set of chemical reactions describing the three pools of CO_2 dissolved in seawater. Carbon dioxide gas dissolved in seawater exists as a variety of species in equilibrium with each

other; [$CO_{2(aq)}$], [H_2CO_3], [HCO^-_3] and [$CO^{=}_3$]. Since it is impossible to distinguish between [$CO_{2(aq)}$] and [H_2CO_3] by analytical means, the combined species is referred to as [$CO2^*_{(aq)}$] (i.e. [$CO_2{}^*_{(aq)}$] = [$CO_{2(aq)}$] + [H_2CO_3]).

A complete description of the inorganic carbon system at equilibrium is obtained with any 2 carbon parameters, the apparent thermodynamic equilibrium constants, temperature, salinity, pressure, phosphate, and silicate concentrations. Unfortunately, error propagation through the equations places constraints on the accuracy of the calculations. For example, calculated pCO_2 differences (from DIC and alkalinity) can result from errors related to the apparent equilibrium constants and variables used in the calculations (Goyet et al.1991; Millero 1995).

Inherent in these formulations is the assumption of chemical equilibrium. The internal consistency of the carbon system parameters can be assessed if any three or all four inorganic carbon parameters are measured. Usually, it is best to measure a particular parameter directly rather than calculate it from other measurements. Biological processes are rarely at equilibrium, and the derivations describing these processes are very different.

The fields of marine CO_2 chemistry and phytoplankton physiology remain far apart but have much to gain form each other. Marine chemists rarely appreciate the difficulties of studying biological systems, and phytoplankton physiologists rarely have an understanding of the analytical techniques of marine chemists (Crawford and Harrison 1997). For instance, marine chemists have the resources to measure accurate and precise pCO_2, DIC, pH and TA values, but rarely apply these techniques outside their field. On the other hand, phytoplankton physiologists have not attempted to use these current

approaches, but continue to use dated and sometimes questionable analysis (Crawford and Harrison 1997).

Understanding the relationship between the uptake of CO_2 by phytoplankton and the carbon chemistry of seawater requires an understanding of how basic chemical principles of chemical equilibrium apply to biological metabolism. The application of equilibrium calculations without a complete understanding of the timescales or assumptions is always dangerous. An appreciation of biological pathways and effects upon chemical kinetics is essential to understanding a system. For example, timescale of approximately 90 seconds is required to establish chemical equilibrium of the carbonate system in seawater (Zeebe et al. 1999). When time scales of less then 90 seconds are encountered, application of equilibrium models is inconsistent with the disequilibrium state of the carbonate chemistry. Time-dependent (kinetic) models are essential for a complete description of the system.

In this chapter, the chemical thermodynamic equilibria of the inorganic carbon system were investigated between 2 continuous cultures (chemostats) using an equilibrium and steady-state model. One chemostat was inoculated with *Phaeodactylum tricornutum* (referred to as the "biological" chemostat), and a second chemostat was not inoculated; the second abiotic chemostat is referred to as the control chemostat. Measurements of pCO_2, DIC and TA were analyzed to determine the validity of describing the CO_2 system with an equilibrium model. The equilibrium model accurately describes the inorganic carbon system within the control chemostat but fails to describe the speciation of carbon in the biological chemostat.

Methods

Chemostats

Phaeodactylum tricornutum was grown (0.3 d^{-1}) in a nitrate (NO_3^-)-limited chemostat system at a temperature of 16 ºC and a salinity of 34.8 (Laws and Bannister 1980). The growth medium was prepared using Station ALOHA surface seawater obtained from the Hawaii Ocean Time-series (HOT) program supplemented with 100 µM nitrate, 40 µM phosphate and essential trace metals and vitamins. Another chemostat was operated next to the biological chemostat and represented the control. All environmental conditions were the same for each chemostat.

An infrared gas analyzer, LI-COR model 6262, was attached to the chemostat outflow to determine the mole fraction of CO_2 in dry air. The gas was dried using a magnesium perchlorate scrubber that was changed daily. The LI-COR 6262 was configured in "absolute mode" using a 0 uM M^{-1} CO_2 reference gas (N_2). The mole fraction of CO_2 was converted to the pCO_2 in wet (100% water saturated) air using the total pressure measured by a Setra pressure transducer and water vapor correction of Ambrose and Lawrenson (1972). Although the calibration coefficients supplied by LI-COR Inc. were used to calculate the mole fraction of CO_2, these coefficients were checked daily using a primary gas standard of 374.8 µatm supplied by the World Meteorological Organization. Analytical precision of 1 uM M^{-1} was assessed over a 24 hour period by making multiple (every 10 min) measurements of a secondary standard gas standard.

The attachment of the gas analyzer required a modification to the outflow of the chemostat system. A double U-connector was employed to allow growth medium to drain

while keeping the chemostat system uncontaminated by atmospheric lab air (Fig 6.1). Varying CO_2 mole fractions from 0 to 2459 uM M^{-1} were bubbled through the chemostat and monitored. Once gas concentrations were observed constant (< ± 5 μatm change over 12 hr), replicate samples of DIC and TA were taken in 300 ml Pyrex glass bottles. Samples were poisoned with 100-200 μl of saturated mercuric chloride and stored at 4 ºC in the dark. Samples were typically analyzed within 24 to 72 hours. DIC was measured on a Single Operator Metabolic Mutiparameter Analyzer (SOMMA) system (Johnson et al 1998). The system was calibrated with high purity CO_2 and traceable to Certified Reference Materials (CRMs). Total alkalinity was determined in an open cell by a potentiometric titration with calibrated HCl, and analyzed using a modified Gran plot as recommended by Department of Energy (1994). Both systems have been in use for more then 10 years in the HOT and Pal-LTER programs making high precision measurements from the Pacific and Southern Oceans.

Equilibrium Model

The assumption of thermodynamic equilibrium was tested by comparing the internal consistency of measured versus calculated pCO_2 and pH from DIC and TA. Although there are at least five sets of apparent thermodynamic dissociation constants in the literature, we will compare only those of Mehrbach et al. (1973), refit by Dickson and Millero (1987) with those of Roy et al. (1993, 1994, 1996). The program of Lewis and Wallace (1995) was used for these calculations. This program can be obtained at CDIAC

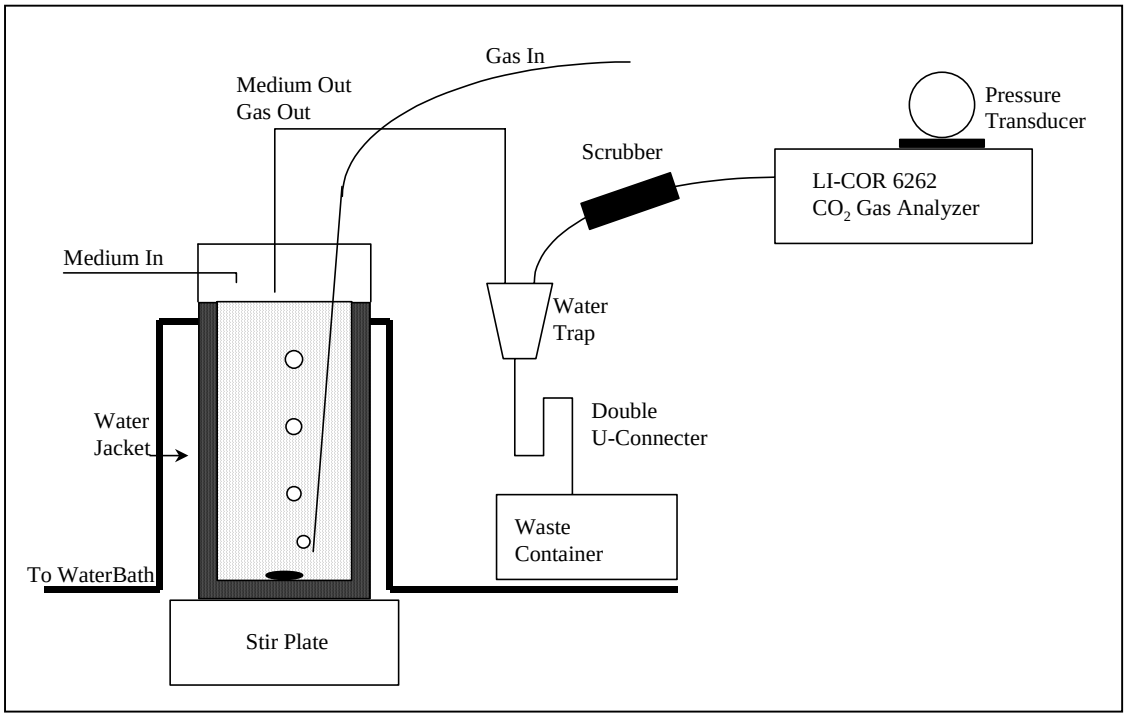

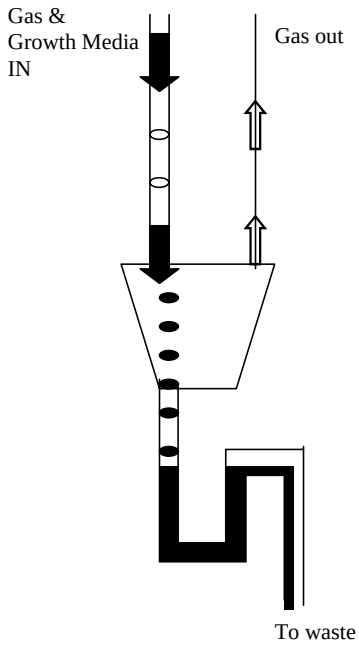

Fig 6.1 Schematic of the chemostat system. Bottom figure is a enlargement showing the double U-joint connecter that allowed growth media to drain from the system while keeping the system uncontaminated with lab air.

(http://www.cdiac.esd.ornl.gov). Additionally, the CO_2 system speciation (CO2*(aq), HCO_3^-, CO_3^{2-}), pH on the total and NBS scales, and pCO_2 were determined for a range of DIC concentrations at a constant TA and a temperature of 16 °C.

Steady State Model

Using DIC, TA and pCO_2 measurements from the biological chemostat, a steady-state model was developed to investigate the conditions of the inorganic carbon system within the chemostat. Specifically, the model was used to investigate changes of CO_2*(aq) concentrations. The model is described by the following equation;

$$\frac{\Delta CO2}{\Delta t} = \left(\frac{\Delta CO2}{\Delta t}\right)_{MediaIn} + \left(\frac{\Delta CO2}{\Delta t}\right)_{GasFlux} + \left(\frac{\Delta CO2}{\Delta t}\right)_{CS} - \left(\frac{\Delta CO2}{\Delta t}\right)_{Prod} - \left(\frac{\Delta CO2}{\Delta t}\right)_{MediaOut} \quad (1)$$

where Δt is one second. The terms $(\Delta CO_2/\Delta t)_{MediaIn}$ and $(\Delta CO_2/\Delta t)_{MediaOut}$ describe the flux of CO_2 from the addition and loss of growth medium. The term $(\Delta CO_2/\Delta t)_{GasFlux}$ describes the flux of CO_2 from the bubbling of CO_2 gas through the chemostat. The term $(\Delta CO_2/\Delta t)_{CS}$ describes the flux of CO_2 from the hydration and dehydration of CO_2*(aq) and HCO_3^- within the carbon system. Finally, $(\Delta CO_2/\Delta t)_{Prod}$ represents the flux of CO_2 from the growth of phytoplankton.

The air-to-medium exchange of inorganic carbon is described by:

$$\left(\frac{\Delta CO2}{\Delta t}\right)_{GasFlux} = kS\Delta pCO2 \quad (2)$$

k = piston velocity coefficient (cm hr^{-1})
S= solubility (mol kg^{-1} μatm^{-1})
ΔpCO_2 = the difference in CO_2 gas between medium and gas (μatm)

This equation was used to determine the efficiency of CO_2 gas transfer between the growth medium and gas bubbled through the chemostats.

The rate law and rate constants describing the hydration and dehydration of CO_2 were taken from equation 6 of Johnson (1987).

$$\frac{\Delta CO_2}{\Delta t} = -(k_{CO_2} + \frac{k_{OH}K_W}{a_H})[CO_{2*aq}] + (k_d aH + k_{HCO_3})[HCO_3^-] \quad (3)$$

aH = hydrogen activity

$kCO_2 = k_{31} + k_{32}$

$k_{OH}Kw = [HCO_3]/[[CO_2*(aq)]aH$

$kd = k_{13} + k_{23}/K'H_2CO_3$

$k_{HCO3} = [CO_2*(aq)][OH]k_{OH}/HCO_3$

The subscripts $k_{\#\#}$ refer to the rate constants for the mechanism of direct hydration and dehydration of carbon dioxide with seawater, and $K'H_2CO_3$ represents the true apparent dissociation constant of carbonic acid (Eigen et al 1961)

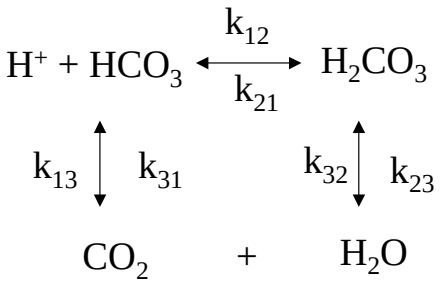

(4)

Rate Constants	**16 ºC 34.8 salinity**
k_{CO2}	1.6×10^{-3}
$k_{OH}Kw$	4.627×10^{-11}
k_d	1.781×10^{4}
k_{HCO3}	5.172×10^{-4}

Results

Within the control chemostat, equilibrium between gas and solution was always attained with mole fractions ≥98 uM M^{-1}. Average differences were 0.1 ± 0.2%; Table 6.1). Calculated pCO_2 (from DIC and TA) using the constants of Mehrbach et al.(1973) refit by Dickson and Millero (1987), differed from measured pCO_2 by –1.0 ± 1.2% (Table 6.1). In comparison, calculated pCO_2 using the constants of Roy (1993, 1994, 1996) differed from measured values by –6.8 ± 2.0%. Within the biological chemostat gas-solution equilibration was never attained. Measured values of CO_2 gas concentrations were less then the concentration of CO_2 gas being bubbled through the chemostat. Calculated values (from DIC and TA) were even less than measured values. Typically, the mole fraction of CO_2 measured in the chemostat was 36 ± 13% less then the mole fraction of gas being bubbled through it. For example, CO_2 concentrations of 188 uM M^{-1} were measured with the gas analyzer when a gas with a CO_2 concentration of 296 uM M^{-1} was bubbled through the chemostat. Calculated pCO_2 differed by as much as 72.9 ± 15.6% when compared to measured values regardless of which set of dissociation constants used (Table 6.1). Calculated gas concentrations differed by over 100% when compared to the gas concentration being bubbled through the growth medium (Table 6.1).

Discussion

Equilibration Model

A chemostat functions as both a growth chamber for phytoplankton and as an equilibrator for gases dissolving in solution. At gas-solution equilibrium, the pCO_2 in seawater growth medium corresponds to the pCO_2 of gas bubbling through it.

Furthermore, chemical equilibrium can be confirmed by comparing measured and calculated values of the four measured carbon system parameters; DIC, TA, pH and pCO_2. This is called the internal consistency of the carbon system.

The calculation of the individual inorganic carbon species in seawater relies not only on the use of proper apparent dissociation constants in seawater for carbonic acid, K_1 and K_2, but on the assumption of chemical equilibrium. The errors associated with calculating the internal consistency of the carbon system will depend on the accuracy and precision of the measured carbon parameters, and the errors associated with the apparent thermodynamic constants K_1 and K_2 (Millero 1995). DIC and TA accuracy are determined by the use of primary standards: pure CO_2 gas for a Single Operator Mutiparameter Metabolic Analyzer (SOMMA) system and standardization of acid titrant for TA titrations. Certified Reference Materials (CRMs) are also available as secondary "check" standards. Finally the measurement of pCO_2 has no secondary standard, but most investigators standardize the analyzer with a set of primary gases; few, if any investigators routinely assess equilibrator efficiency.

Within the control chemostat, the internal consistency of the carbon system parameters suggests the carbon system was in chemical thermodynamic equilibrium. The internal consistency determined using the apparent constants of Mehrbach et al. (1973) refit by Dickson and Millero(1987) exhibit a 6% better fit then the internal consistency calculated using the constants of Roy et al. (1993, 1994, 1996). Our results agree with the

Table 6.1 Inorganic carbon dioxide data from the chemostat experiments

Control

Mole Fraction CO_2 Air (uM M^{-1})	Mole Fraction CO_2Chemo (uM M^{-1})	Diff	%Diff	Meas pCO_2 (µatm)	DIC (µM kg^{-1})	TA (µM kg^{-1})	Mehrbach pCO_2calc (µatm)	Meas Diff	% diff from Meas	Roy pCO_2calc (µatm)	Meas Diff	% diff
0	22	-22		22	1481.0	2222.6	44	-22	-103.3%	47	-25	-117.2%
0	29	-29		29	1531.6	2213.6	56	-27	-95.5%	60	-31	-109.1%
98	98	0.2	0.2%	96	1668.4	2227.1	96	-1	-0.5%	103	-7	-7.7%
250	250	0	0.0%	245	1889.9	2237.9	248	-3	-1.4%	266	-21	-8.6%
251	251	0	0.0%	248	1888.4	2232.3	252	-4	-1.7%	270	-22	-8.8%
305	305	0	0.0%	299	1926.9	2240.2	296	3	0.9%	317	-18	-6.0%
408	407	1	0.2%	399	1980.9	2235.6	403	-4	-0.9%	430	-31	-7.8%
857	858	-1	-0.1%	841	2093.0	2229.7	853	-12	-1.4%	901	-61	-7.2%
1192	1195	-3	-0.3%	1174	2137.7	2230.6	1188	-14	-1.2%	1246	-72	-6.1%
1725	1720	5	0.3%	1668	2187.0	2233.0	1720	-52	-3.1%	1784	-116	-6.9%
2459	2457	2	0.1%	2382	2230.1	2234.4	2372	10	0.4%	2435	-53	-2.2%
	Avg		0.1%				**Avg**		**-1.0%**			**-6.8%**
	SD		0.2%				**SD**		**1.2%**			**2.0%**

Biotic

296	188	108	36.5%	184	1336.55	2279.2	18.4	166	90.0%	19.6	164	89.3%
580	446	134	23.1%	436	1794.27	2283.9	134.3	302	69.2%	144	292	67.0%
1176	598	578	49.1%	586.9	1939.86	2304.6	237.8	349	59.5%	254.9	332	56.6%
	Avg		36.2%				**Avg**		**72.9%**			**71.0%**
	SD		13.0%				**SD**		**15.6%**			**16.8%**

detailed study of Lueker et al (2000), who compared the internal consistency of the carbon system parameters by applying various sets of apparent equilibrium constants to surface seawater from Station ALOHA.

These results also demonstrate that the addition of nutrients, vitamins and trace metals to seawater did not have any effect on the selection of apparent constants. Filtered surface seawater from Station ALOHA was used to make the growth medium for the chemostats. Because the apparent equilibrium constants depend on the seawater matrix, the addition of nutrient salts and trace metals could have an effect on the seawater matrix. However, the internal consistency between our measured and calculated values using the same constants as Lueker (2000) shows that the addition of nutrient salts and trace metals did not change the seawater matrix.

In comparison, the biological chemostat showed large differences between the calculated pCO_2 (from DIC and TA), measured pCO_2 (with the gas analyzer) and pCO_2 of air (from the gas bubbled through the chemostat) regardless of which sets of dissociation constants were used. Although the chemostat was sampled after many days when measured pCO_2 values had remained relatively constant (±5 μatm), calculated versus measured values suggest the chemostat system was in steady state, but not in gas-solution or chemical thermodynamic equilibrium with respect to the carbon system. Gas equilibration between the chemostat medium and air bubbled through it was never attained. Concentrations measured in the chemostat were always lower than the concentrations bubbled through it (pCO_2air > pCO_2measured). Calculated values of pCO_2 were even lower than the measured values within the chemostat, suggesting [CO_2*aq]

was lower than that calculated from Henry's law (pCO_2air > pCO_2measured > pCO_2calculated). Although an outside observer might initially suspect leaks, the chemostat was checked numerous times. There were no differences observed when secondary standards were run during the day and night periods when pCO_2 in the lab differed by >3000 μatms. Additionally, by flowing only gas through the system at a positive pressure (no growth medium), the chemostat was checked to determine if seals were secure.

The speciation of the CO_2 system (CO_2*aq, HCO_3^- and CO_3^{2-}), pH (on the total and NBS scale) and pCO_2 were calculated from a range of DIC concentrations (1900 to 2400 μmol kg^{-1}), constant TA (2300 μeq kg^{-1}) phosphate (34 μmol kg-1), silicate (100 μmol kg-1), salinity (35), apparent equilibrium constants of Merbach (1973) refit by Dickson and Millero (1987) and K_o from Weiss(1974) using the program of Lewis and Wallace (1995; Fig 6.2 and 6.3). These calculations represent the speciation concentrations and values of measured parameters at a variety of DIC, pCO_2 and pH at the temperature and salinity of the chemostat system. These calculations will be referred to as the equilibrium model.

Because the control chemostat displayed excellent internal consistency between measured parameters, calculated pH(total scale) matched with pH(total scale) from the equilibrium model. Within the biological chemostat, measured DIC and TA were used to calculate pH(total scale) and then compared to the equilibrium model to determine if DIC, TA and pCO_2 were accurate measurements. Values of pH(total scale) were comparable between the model and biological chemostat suggesting that the measurement of pCO_2 was in error. This is not the case. In the next section, I will show

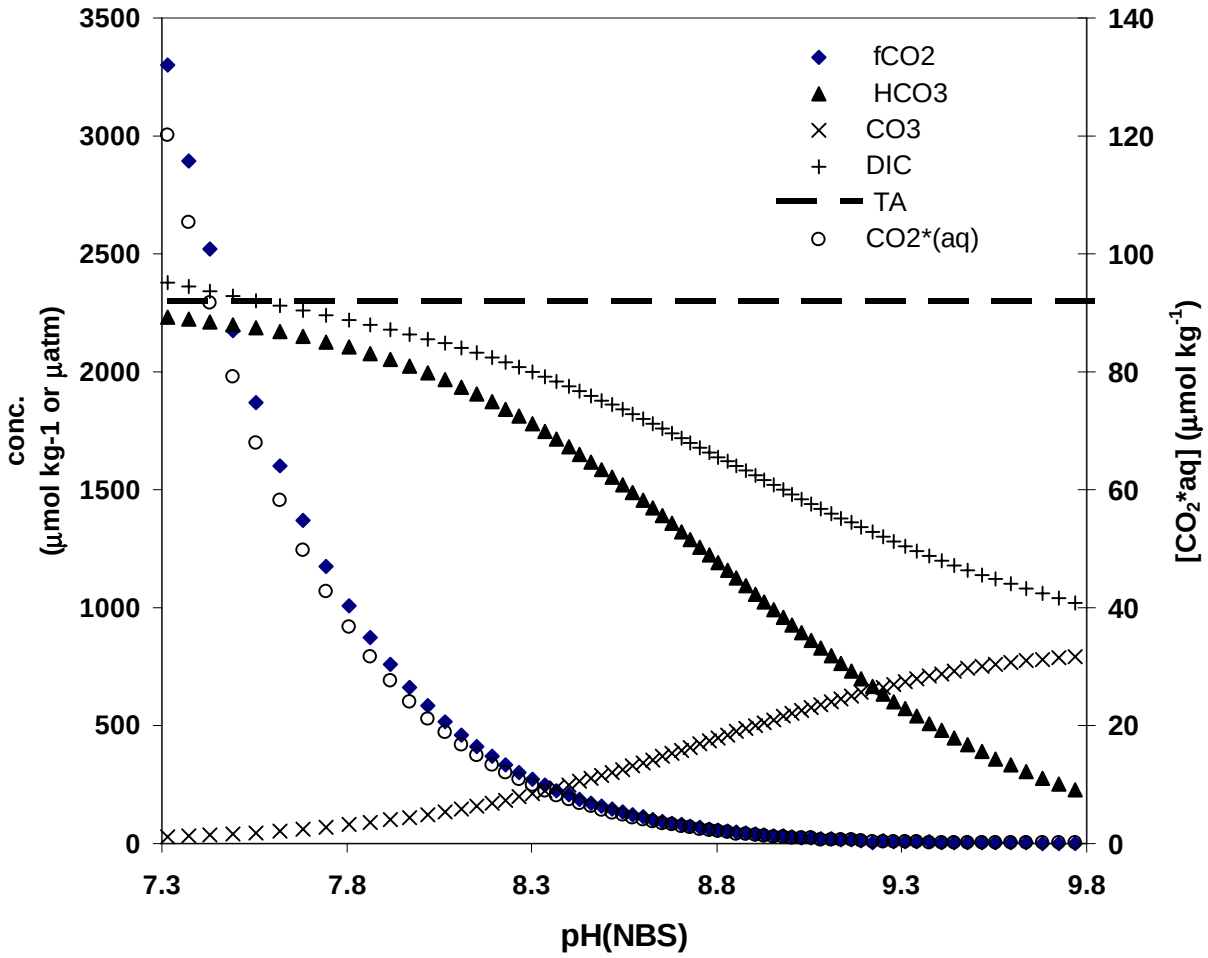

Figure 6.2 pH (NBS scale) versus fCO_2, DIC and the inorganic carbon system species; CO_2*aq, HCO_3, CO_3. The speciation of the CO2 system (CO2*aq, HCO3 and CO3), pH (on the total and NBS scale) and pCO were calculated from a range of DIC concentrations (1900 to 2400 µmol kg^{-1}), constant TA (2300) phosphate (34 µM kg-1), silicate (100 µM kg-1), salinity (35), apparent equilibrium constants of Merbach (1973) refit by Dickson and Millero (1987) and Ko from Weiss(1974) using the program of Lewis and Wallace (1995; Fig 6.2 and 6.3). These calculations represent the speciation concentrations and values of the measured parameters at a variety of DIC, fCO2 and pH for the temperature and salinity of the chemostat system. These calculations will be referred to as the equilibrium model.

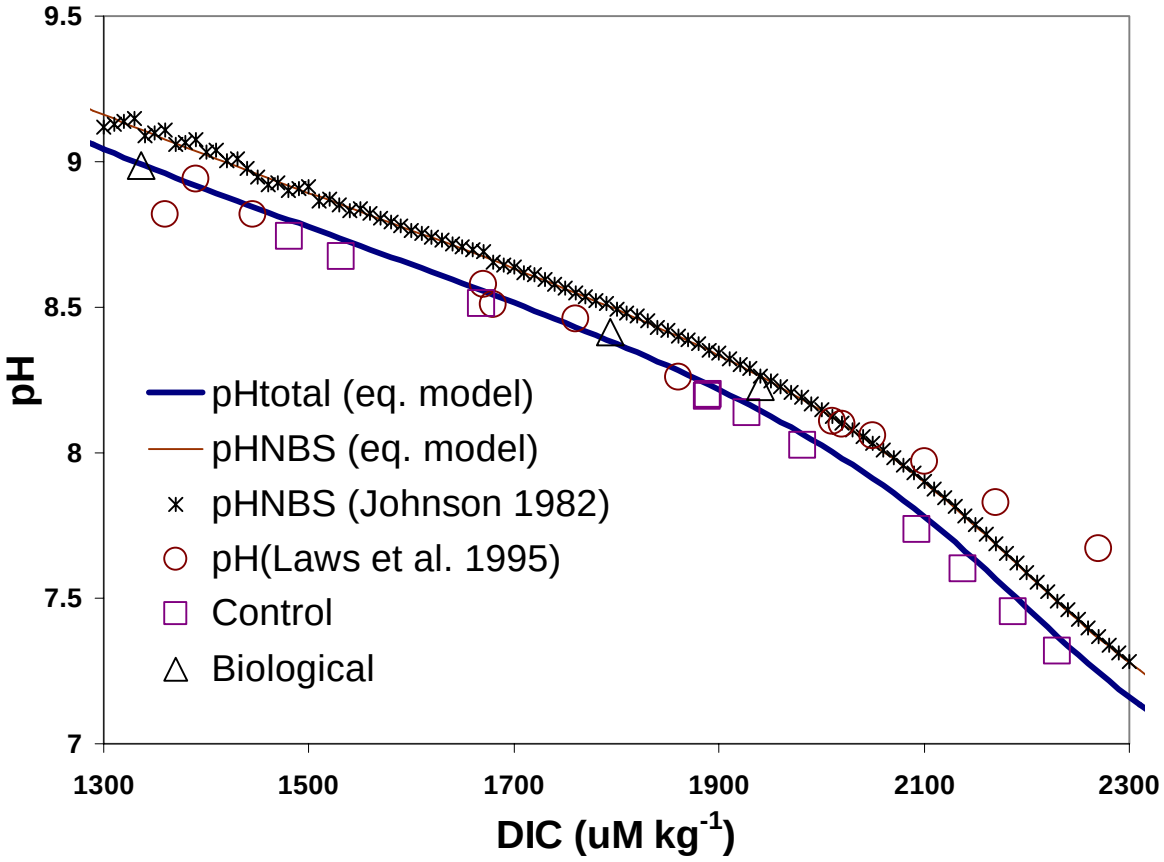

Figure 6.3 DIC versus pH on the total and NBS scale calculated from the equilibrium model (see text and Fig 6.2) Also shown are pH on the NBS scale from the equations of Johnson(1982), pHs reported in Laws (et al. 1995), calculated pHs on the total scale from the control and biological chemostat experiments.

that the measurement of pCO_2 is correct because equilibrium calculations cannot be applied to systems in disequilibria.

Laws et al. (1995) operated a similar chemostat and reported DIC, [CO_2*aq] and pH values that we can compare with the equilibrium model. Unfortunately, Laws et al. (1995) did not report the pH scale or whether pH was measured or calculated. More than likely, pH was on the total scale because the constants of Roy et al. (1993, 1994, 1996) were used to calculate [CO_2*(aq)]. The apparent equilibrium constants of Roy et al. (1993, 1994, 1996) were measured on the total scale. Either way (measured or calculated), the pH values reported by Laws et al. (1995) match pH(total) values calculated assuming the equilibrium model at high pH (8.5; low DIC) but not at low pH (7.5; high DIC; Fig 6.3). Differences were as great as 0.42 ph units.

Laws et al. (1995) reports that gas concentrations were determined by mixing a tank of 2% CO_2 in air using mass flow controllers. These same types of mass flow controllers were used to mix high CO_2 gas concentrations in the control chemostat and have temperature dependence. As lab temperature increased, measured CO_2 concentrations in the chemostat also increased, suggesting the mass flow controllers were not maintaining constant mixtures of CO_2. During our experiments, excessive care was taken when sampling the control chemostat only during periods of constant lab temperature to ensure consistent gas mixtures. Future experiments should include thermostatically controlled mixing of gasses to ensure consistent gas concentrations. Additionally, it is recommended that single tanks of premixed CO_2 in air be used to alleviate this problem.

Steady State Model

A steady state model was developed to understand the disequilibrium between calculated and measured pCO_2 within the biological chemostat. Within the following sub-sections, each term of the steady state model is described.

Medium In, Net Organic Matter Production and Medium Out

The rate of addition of medium controls the growth rate of phytoplankton in a chemostat vessel. Nutrients needed for growth are added in excess except for one that limits development. The rate at which the limiting nutrient is added to the chemostat then regulates the growth of phytoplankton. It is generally assumed that inorganic carbon is not limiting within the growth medium. The concentration of CO_2*(aq), HCO^-_3 and $CO^=_3$ in seawater at a salinity of 35, temperature of 25 ºC and saturated with respect to atmospheric CO_2 (360 μatm) are 10, 1800 and 190 μM respectively. At a growth rate of approximately 0.38 per day, approximately 1.0 liter of medium is added to the chemostat in one day. This corresponds to approximately 0.0002 μM sec^{-1} of CO_2*(aq) and 0.022 μM sec^{-1} HCO^-_3.

The uptake of CO_2*(aq) by phytoplankton is set by the uptake of nitrate that is present at limiting concentrations of 100 μM. A growth rate of approximately 0.3 d^{-1} corresponds to the uptake of approximately 0.007μM C sec^{-1} using a C:N ratio of 6.6. Although C:N ratios can vary depending on growth conditions, small deviations will not make a significant difference to this analysis. For instance, C:N ratios ranging from 5 to 8 equate to a range of 0.006 to 0.009 μM C sec^{-1}.

Because chemostats are operated at a constant volume, the addition of growth medium must be balanced by the reduction of medium. Phytoplankton cells and excess non-limiting nutrients are removed from the chemostat at the same rate growth medium is added. Since the chemostats in this study were nitrate limited, the concentration of nitrate in the waste stream was near zero. The concentration of the inorganic carbon species are generally greater then zero but regulated by other factors such as the hydration and dehydration of CO_2, gas flux and growth rate. As an example, at low DIC concentrations (1400 μmol kg^{-1}), the calculated removal rates are very low; <0.000001 uM sec^{-1} CO_2 *(aq) and 0.008 uM sec^{-1} HCO^-_3.

Gas Flux

The flux of CO_2 from the exchange of air bubbled into the chemostat is modeled using equation 2 by fitting a piston velocity coefficient to match the observed changes of pCO_2 within the control chemostat. The exchange of CO_2 between the air and solution is a function of the piston velocity coefficient, solubility and the pCO_2 difference between the air bubbled into the chemostat and the growth medium within the chemostat. The solubility is a function of temperature and salinity (Weiss 1974). Therefore, solubility was constant in the chemostat experiments because the chemostat vessels were kept at constant temperature, and the inflowing medium had a constant salinity.

The piston velocity coefficient describes the rate of gas transfer from the air to the medium and is usually determined as a function of wind speed. Gas transfer through the air to water interface is regulated by turbulence, viscosity and the diffusion coefficient of the gas. Other factors that can influence the gas transfer rate are chemical enhancement and bubble entrainment. The chemical enhancement effect occurs by the reaction of

CO_2*(aq) with hydroxide ions that have a greater influence at high pH. Bubbles increase the surface area for gas exchange.

Barring these uncertainties and using the control chemostat as the model, a piston velocity coefficient was determined by fitting modeled fluxes of CO_2 to observed changes (Fig 6.4). The medium pump was turned off so the only factor affecting CO_2 in the chemostat was the bubbling of air. The pCO_2 within the chemostat was monitored during a period of 3 to 4 days until gas-solution equilibration was achieved. Flux estimates were converted to pCO_2 using a Revelle factor of 10 and a DIC concentration of 1980 μmol kg^{-1} (Takahashi et al. 1980). Results of these calculations show that a piston velocity coefficient of approximately 40 cm hr^{-1} describes the rate of gas transfer within these chemostats (Fig 6.4).

Chemostat systems should be individually calibrated to determine the efficiency of gas transfer. This model shows the efficiency of gas transfer is determined by the piston velocity coefficient (Fig 6.5). For example, if an air stone were used to bubble air through the chemostat (rather than a tube which discharges single bubbles), the quantity and size of bubbles would determine the efficiency of gas transfer. Hence, the piston velocity coefficient would be higher. On the other hand, if the flow rate of gas is lowered (i.e. fewer bubbles), then a smaller piston velocity coefficient might be appropriate (Fig 6.5). At this point in time, the value describing the efficiency and rate of gas transfer cannot be calculated but must be experimentally derived for each chemostat system.

Once the piston velocity coefficient of the chemostat system is known, then the pCO_2 difference between the gas bubbling through the chemostat and the growth medium determines the flux of CO_2. The greater the difference, the higher the flux (Fig 6.5).

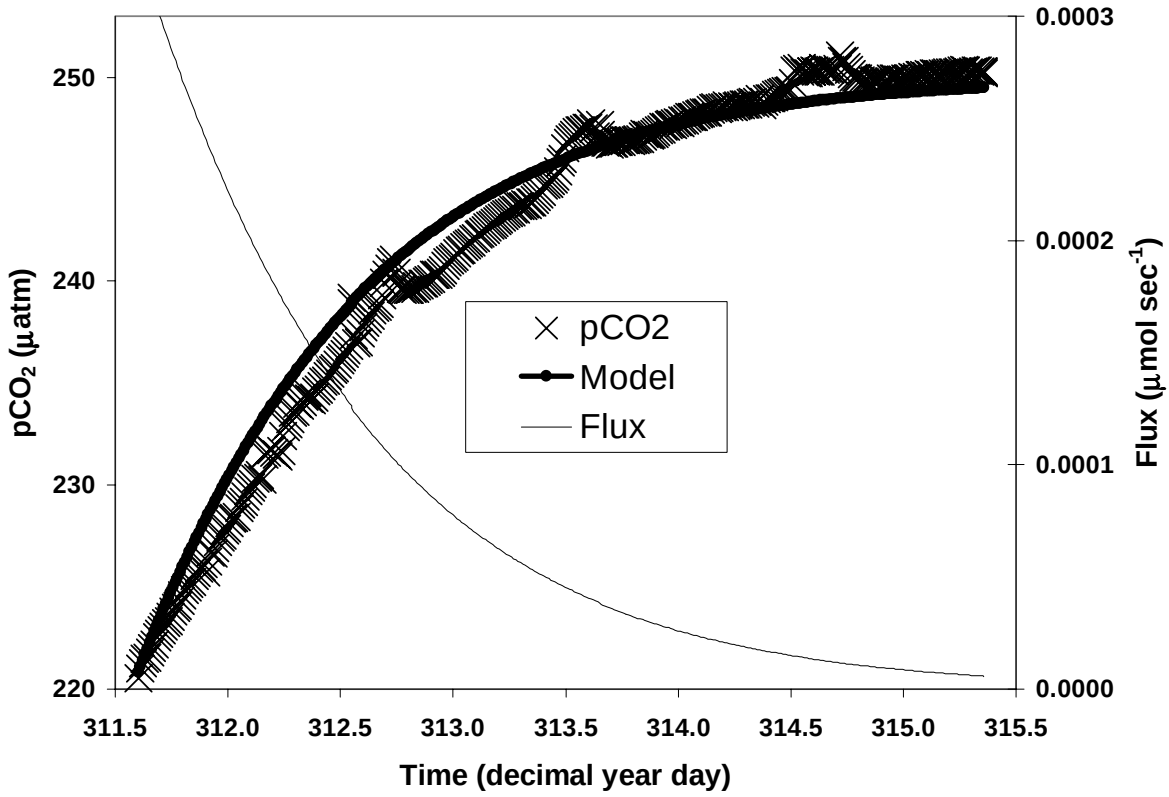

Figure 6.4 Measured pCO_2 pressures during four days. A gas was bubbled through the chemostat to determine the time for gas-solution equilibration. A gas-solution flux model was fit to the data to calibrate the efficiency of the chemostat for gas exchange

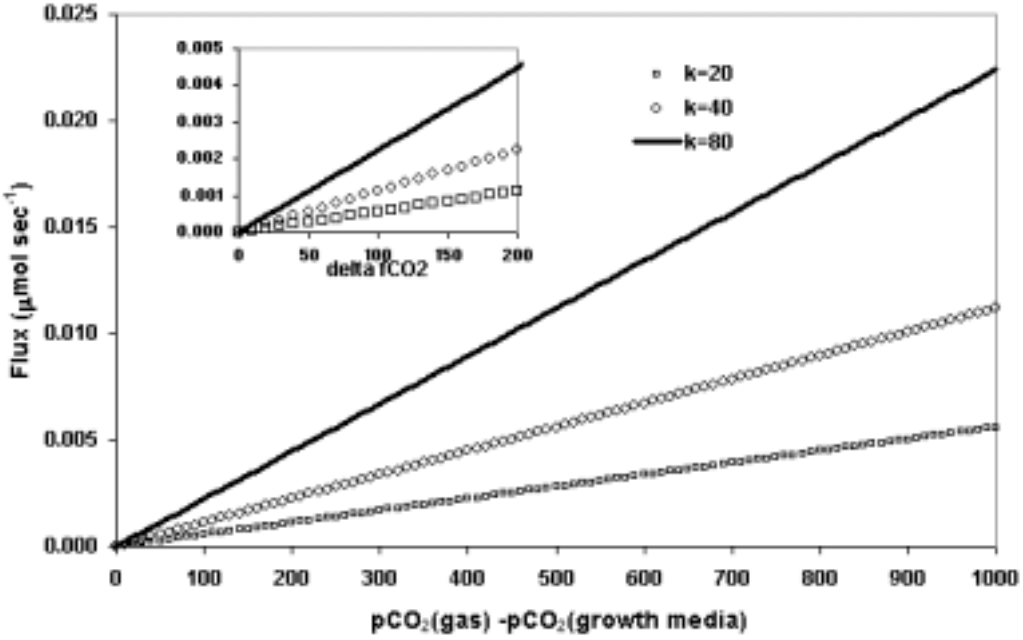

Figure 6.5 The change in pCO_2 versus the flux for 3 piston velocity coefficients within the chemostat experiments

Within the biological chemostat, pCO_2 differences were approximately 100 μatm at air concentrations of less then 600 μatm. Using the experimentally derived piston velocity coefficient of 40 cm hr^{-1}, the flux of CO_2 from the air to the medium is about 0.001 μM sec^{-1}. If the rate of gas transfer were 2 times greater, then values could be as high as 0.003 μM sec^{-1}.

Hydration/Dehydration

The rate law of Eigen (1961) describes the hydration and dehydration of CO_2 as a function of pH, [CO_2*(aq)] and [HCO^-_3]. The most recent determination of the rate constants was estimated by Johnson (1982) using a pH-stat method (Magid and Turbeck 1968). The rate constants were determined between pH values of 7.2 and 8.6 on a NBS scale. Therefore, measured pH values should also be on the NBS scale when using the rate law and constants of Eigen (1961) and Johnson (1982). At equilibrium, the rate law can be set equal to zero and solved for pH. The relative accuracy of the rate constants and rate law can be determined by comparing pH_{NBS} values generated from the rate law with pH_{NBS} generated using the equilibrium model. Additionally, the accuracy of the rate constants can be assessed beyond the pH limits at which they were determined by extending the comparison beyond the measured values of Johnson (1982).

Using values of CO_2*(aq) and HCO^-_3 generated by the equilibrium model, pH_{NBS} was determined by solving the rate law at equilibrium (equation 3; rate = 0).

$$\frac{1}{2[HCO3]kd} * ([CO2]kCO2 - [HCO3]kHCO3 + \sqrt{[CO2]2kCO22 - 2[CO2]kCO2[HCO3]kHCO3 + HCO32kHCO32 + 4[HCO3]kd[CO2]kOHKw} \quad (3)$$

Between DIC concentrations of 1700 and 2380 μmol kg^{-1}, pH_{NBS} values determined from the rate law are slightly greater by 0.005 ± 0.002 than pH(NBS) values generated using the equilibrium model (Fig 6.3). Between DIC concentrations of 1300 and 1700 μmol kg^{-1}, pH_{NBS} values determined from the rate law tend to be slightly lower by –0.025 ± 0.115 but not significantly different from zero (Fig 6.3). The variability at lower DIC concentrations is an artifact of the calculations and is a function of the resolution at which CO_2*(aq) concentrations are reported from the equilibrium calculations. Overall, the rate law and equilibrium model compare very well.

The rates of hydration and dehydration of CO_2 are examined by perturbing the CO_2 system at equilibrium concentrations of pH, [CO_2*(aq)] and [HCO_3]. Although disequilibrium of the CO_2 system can be achieved by changing any one, two or all three concentrations, initially only changes of [CO_2*(aq)] will be examined. For simplification, rates will be calculated at representative high pH_{NBS} value of 9.1 (relatively low CO_2*(aq)) and a low pH_{NBS} value of 7.9 (relatively high CO_2*(aq)). These pH values correspond to equilibrium DIC concentrations of 1380 and 2180 μmol kg^{-1} respectively.

The rate law is a linear function of ΔCO_2 with a slope determined by (kOH Kw/aH; Fig 6.6). The rate law predicts the removal of [CO_2*(aq)] (i.e. uptake by phytoplankton) will produces a positive rate of CO_2 formation (Fig 6.6). The addition of [CO_2*(aq)] produce a negative rate or [CO_2*(aq)] removal (Fig 6.6). The rate of CO_2 formation is greater at higher pH values then at lower pH values for a given change of [CO_2*(aq)]. The overall effect at high pH, is a 0.13 μM decrease of [CO_2*aq], which is

enough to supply 0.007 μM C sec^{-1} to balance growth rate of phytoplankton within the chemostat. At low pH values, a relatively larger change of [CO_2*(aq)] is needed.

A change of CO_2 corresponds to a change in pH (Fig 6.2 and 6.3). As CO_2*aq is removed from the medium, pH increases. Changes of pH have the opposite effect compared to changes of CO_2*(aq) (Fig 6.7). An increase of pH produces a negative rate or CO_2*(aq) removal (Fig 6.7). A decrease in pH produces a positive rate of CO_2*(aq) formation. [CO_2*(aq)] produced will balance the system and equilibrate the carbon system. The rate of CO_2*(aq) formation is greater at lower pH values than at higher pH values for a given change of pH.

Although the changes of pH and CO_2*(aq) offset each other, control of the hydration and dehydration of CO_2*(aq) depends on the non linear relationship between pH and CO_2*(aq) (Fig 6.2). At high pH (low CO_2*(aq)) changes in CO_2*(aq) control the rate of hydration and dehydration, while at low pH (high CO_2*(aq)) changes in pH control the rate of hydration and dehydration. Practical application of the Eigen (1961) rate law using the Johnson (1982) rate constants is difficult to imagine. First of all, potentiometric pH measurements are troublesome at best. Accuracy and precision are reported to be 0.004 and 0.003 pH units, but this is rarely, if ever, achieved (Crawford and Harrison 1998). NBS calibrating buffers are only accurate to 0.02 pH units, and this error alone can cause large biases in the rate calculations. Spectrophotometric pH measurements could offer hope in resolving pH issues, but this method would be difficult to implement.

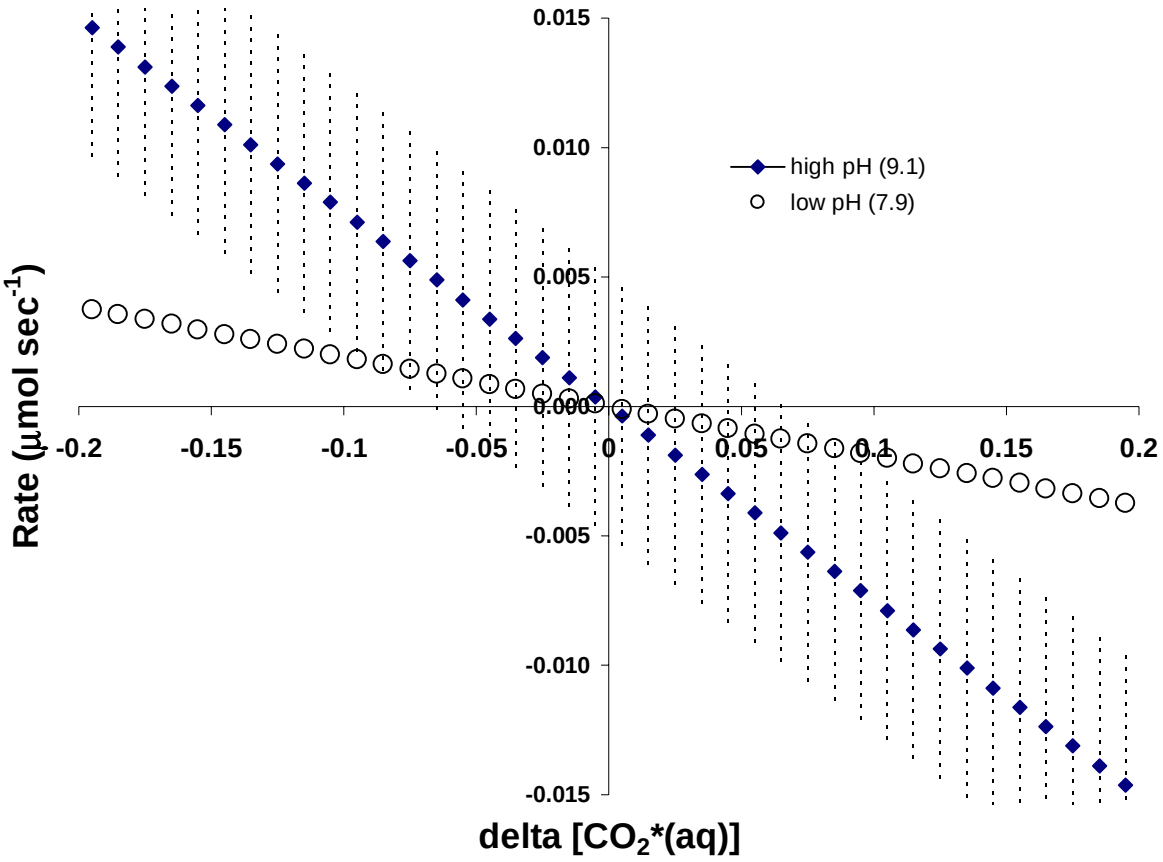

Figure 6.6 Changes of CO_2*(aq) versus rate of hydration and dehydration using the rate constants of Johnson (1982) and rate equation of Eigen et al. (1961). The vertical dashed lines represent the error in the rate estimation based on the error in the rate constants from Johnson (1982).

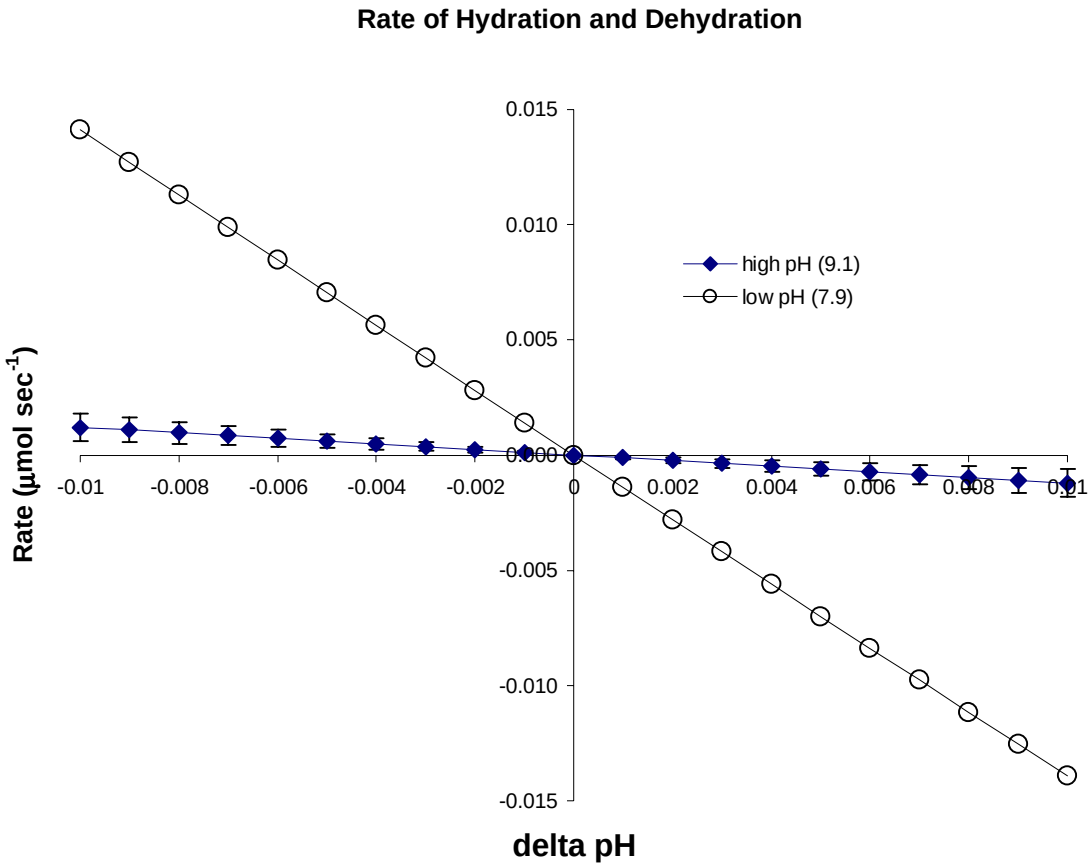

Figure 6.7 Changes of pH versus rate of hydration and dehydration using the rate constants of Johnson (1982) and rate equation of Eigen et al. (1961). The vertical dashed lines represent the error in the rate estimation based on the error in the rate constants from Johnson (1982).

Spectrophotometric pH relies on the absorbance measurement at specific wavelengths, and interference from phytoplankton cells degrades the precision and accuracy of this method. Second, the rate law is a function of CO_2*(aq) and HCO^-_3, which cannot be measured. Therefore, these species must be calculated. It is inconsistent to determine the rate of hydration and dehydration of CO_2*(aq) from concentrations calculated from an equilibrium model, when the system is not at equilibrium.

Combining the terms describing the inorganic carbon system in a continuous culture can now solve the steady-state model. The terms describing the Medium In and Out are dropped because they represent less then 1% of the CO_2*(aq) added or removed at the time scale being investigated. At steady-state, the rate law can be set equal to zero and solved in terms of the gas flux, carbon system and production.

$$\left(\frac{\Delta CO2}{\Delta t}\right)_{GasFlux} + \left(\frac{\Delta CO2}{\Delta t}\right)_{CS} = \left(\frac{\Delta CO2}{\Delta t}\right)_{\mathrm{Pr}\,od}$$

Within the biological chemostat, phytoplankton continuously deplete CO_2*(aq) at a rate equal to the addition of nitrate. This continuous removal of CO_2*(aq) drives the inorganic system out of chemical thermodynamic equilibrium. The inorganic carbon system will try to re-establish equilibrium by the addition of carbon through gas-solution (growth medium) exchange and/or by the redistribution of CO_2 species through the hydration and dehydration reactions.

The results from the steady-state model can now be used to explain the observations of CO_2 within the biological chemostat. The differences between the concentration of pCO_2 in air bubbled into the chemostat and pCO_2 pressure measured by

the LI-COR infrared gas analyzer is a function of the gas transfer efficiency and the degree to which the hydration and dehydration reactions can supply CO_2*(aq) for growth. The degree to which the inorganic carbon system can supply CO_2*(aq) is a function of pH and CO_2*(aq). At high pH (9.1; low CO_2) the hydration and dehydration reactions can supply most of the carbon needed for growth. The rate of CO_2*(aq) formation is driven by the depletion of CO_2*(aq) concentrations by the growth of phytoplankton. Therefore, gas flux supplies less carbon (<15%; 0.001 $\mu M\ s^{-1}$) of that needed to sustain growth (0.007 uM sec^{-1} at a growth rate of 0.38 per day). Therefore, the difference between gas concentrations between the gas bubbled through the chemostat and growth medium are relatively less then that compared at low pH (7.9; high CO_2). At low pH (7.9; high CO_2), the hydration and dehydration of CO_2 cannot supply the carbon needed for growth. The gas flux provides >50% (0.004 $\mu M\ sec^{-1}$) of the carbon needed to sustain growth. The rate of CO_2*(aq) formation is controlled mainly by changes in pH. As pH decreases, the air-to-medium CO_2 flux will supply CO_2*(aq) required for growth. Hence, the difference between gas concentrations is greater relative to high pH (9.1; low CO_2).

Therefore, all measured and calculated values associated with the biological chemostat are accurate. Each value is an indicator for each term in the steady state model. The measured pCO_2 (from the gas analyzer) determines the flux of CO_2 needed to balance the hydration and dehydration reactions and the uptake by phytoplankton. The calculated pCO_2 pressure (from DIC and TA) is an indicator of the flux of CO_2*(aq) from the hydration and dehydration reactions to balance the air to media flux and uptake by phytoplankton. These reactions are a function of pH and CO_2*(aq).

Conclusions

The internal consistency of the carbon system parameters was investigated in two continuous cultures using an equilibrium and steady state models. The equilibrium model combined with the apparent constants of Mehrbach et al. (1973) refit by Dickson and Millero (1987) accurately describes the carbon system within the control chemostat. A steady state model consisting of the terms for air-to-medium gas exchange, phytoplankton production and the hydration and dehydration of CO_2 can accurately describe the CO_2 system in the "biological " chemostat. The rates of air-to-medium exchange and the hydration and dehydration of CO_2 are dependent on the efficiency of gas transfer within the chemostat system and the pH of the culture. At pHs of approximately 9.1 the dehydration and hydration reactions supply CO_2*(aq) needed for growth. At pHs of approximately 7.1, the air-to-medium exchange supplies the CO_2*(aq) needed for growth.

CHAPTER 7

CONCLUSIONS

The observed variability of the measured carbon system parameters within the North Pacific Subtropical Gyre was investigated over seasonal, annual and long-term (>10 years) time scales. At Station ALOHA, the seasonal cycle of fCO_2 and n35DIC were correlated to sea surface temperature, demonstrating the thermodynamic control on the solution chemistry of CO_2 in seawater. The thermodynamic control is manifest through changes in the apparent equilibrium constants for carbonic acid in seawater. The mean annual fCO_2 undersaturation (with respect to the atmosphere) of 13 μatm is due to the uptake of CO_2 by phytoplankton or the cooling and horizontal advection of water. Although the depth dependent analysis of n35DIC showing the soft tissue pump as the major control of inorganic carbon concentrations supports the uptake of CO_2 by phytoplankton, a spatially resolved analysis of fCO_2 gradients would confirm this.

During annual timescales, the marked increase of n35DIC between 1995 and 1999 is correlated to a marked decrease of annual sea surface temperature, illustrating the thermodynamic control of the solution chemistry in seawater. Finally, Long-term (20-year) trends of fCO_2 are consistent with the rise of atmospheric CO_2. Although the long-term trends suggest the changes of fCO_2 are controlled by atmospheric input of CO_2, variability of n35DIC suggest changes in the TA pool actually control fCO_2 over long-term timescales.

Within the Pal-LTER study region, net organic matter production is a large source of O_2 and sink for CO_2, yet is observed only within coastal, inshore areas of the Pal-LTER grid. Additionally, areas of relatively low n35DIC concentrations were coupled with depletions of n35N and n35P and were found in coastal fjords and bays, supporting the conclusion that net organic matter production controls measured carbon system parameters within these areas

Heating and cooling of surface waters are relatively small sources and sinks (± 10 to 15%) of O_2 and CO_2 in the Pal-LTER grid area (40 to 200 kilometers from shore). The spatial distribution of $O_{2\{Sat\}}$:$fCO_{2\{Sat\}}$ values centered around atmospheric equilibrium account for 80% of the Pal-LTER grid surveyed in January. Geographic studies of dissolved inorganic carbon (DIC) show spatial variability that results primarily from the freshening of surface water from ice melt and precipitation. Geographic studies of n35DIC also show spatial variability and were decoupled with depletions of n35N and n35P. Seasonal studies of n35DIC are not consistent with the seasonal cycle of physical hydrography, n35N or n35P. Although, n35DIC does not show any correlation to n35N and n35P, the soft tissue pump explains 100% of the observed gradient of n35DIC between the surface and deep water, and is working at 50 to 100% efficiency. Since the potentials of the solubility and carbonate pumps to explain depth-dependant gradients of n35DIC are small to nonexistent, it is an enigma to understand the decoupling of n35DIC from n35N and n35P.Annual changes of sea surface temperature, salinity, n35DIC and fCO_2 are difficult to interpret at this time despite an 8-year time series because of larger geographical and seasonal variability.

Although the chemostat study was originally planned as an investigation of phytoplankton metabolism, it became an analysis of the inorganic carbon system at disequilibrium. The internal consistency of the carbon system parameters was investigated in two continuous cultures using an equilibrium and steady state models. The equilibrium model combined with the apparent constants of Mehrbach et al. (1973) refit by Dickson and Millero (1987) accurately describes the carbon system within the control chemostat. A steady state model consisting of the terms for air-to-medium gas exchange, phytoplankton production and the hydration and dehydration of CO_2 can accurately describe the CO_2 system in the "biological " chemostat. The rates of air to medium exchange and the hydration and dehydration of CO_2 are dependent on the efficiency of gas transfer within the chemostat system and the pH of the culture. At pHs of approximately 9.1 the dehydration and hydration reactions supply CO_2*(aq) needed for growth. At pHs of approximately 7.1, the air-to-medium exchange supplies the CO_2*(aq) needed for growth.

The processes that control CO_2 in seawater have been investigated over various temporal and spatial scales. The interactions of these processes create a variety of observations of the measured carbon parameters within the ecosystems studied. Without a full understanding of the solution chemistry in seawater, incorrect conclusions result from the observed changes of the measured carbon system parameters.

References

Ackley, S.F. and W., S.C., 1994. Physical controls on the development and characteristics of Antarctic sea ice biological communities-a review and synthesis. Deep sea research, 41: 1583-1604.

Alvarez, M., Fernandez, E. and Perez, F.F., 1999. Air-sea CO_2 fluxes in a coastal embayment affected by upwelling: physical versus biological control. Oceanologica acta, 22: 499-515.

Ambrose, D. and Lawrenson, I.J., 1972. The vapour pressure of water. Journal Chemical Thermodynamics, 4: 755-761.

Anderson, J.W. and Beardall, J., 1991. Molecular activities of plant cells: an introduction to plant biochemistry. Blackwell Scientific Publications, Boston, 185-194 pp.

Anderson, L.A. and Sarmiento, J.L., 1994. Redfield ratios of remineralization determined by nutrient data analysis. Global Biogeochemical Cycles, 8: 65-80.

Aristegui, J. and Montero, M., 1995. Plankton community respiration in Bransfield Strait (Antarctic Ocean) during austral spring. Journal of Plankton Research, 17: 1647-1659.

Bakker, D.C.E., de Barr, H.J.W. and de Wilde, H.P.J., 1996. Dissolved carbon dioxide in Dutch coastal waters. Marine Chemistry, 55: 247-263.

Bates, N.R., Hansell, D.A. and Carlson, C.A., 1998a. Distribution of CO_2 species, estimates of net community production, and air-sea CO_2 exchange in the Ross Sea polynya. Journal of Geophysical Research, 103: 2883-2896.

Bates, N.R., Knap, A.H. and Michaels, A.F., 1998b. Contribution of hurrianes to local and global estimates of air-sea exchange of CO_2. Nature, 395: 58-61.

Bates, R.G. and Culberson, C.H., 1977. Hydrogen ions and the thermodynamic state of marine systems. In: N.R. Anderson and A. Malahoff (Editors), The Fate of Fossil Fuel CO2 in the Oceans. Plenum, New York.

Bellerby, R.G.J., Turner, D.R. and Robertson, J.E., 1995. Surface pH and pCO_2 distributions in the Bellingshausen Sea, Southern Ocean, during the early Austral summer. Deep sea research II, 42: 1093-1107.

Bender, M., Ellis, T., Tans, P., Francey, R. and Lowe, D., 1996. Variability in the O_2/N_2 ratio of southern hemisphere air, 1991-1994: Implications for the carbon cycle. Global Biogeochemical Cycles, 10(1): 9-21.

Bidigare, R.R., Fluegge, A., Freeman, K.H., Hanson, K.L., Hayes, J.M., Hollander, D., Jasper, J.P., King, L.L., Laws, E.A., Milder, J., Millero, F.J., Pancost, R., Popp, B.N., Steinberg, P.A. and Wakeham, S.G., 1997. Consistent fractionation of ^{13}C in nature and in the laboratory: Growth-rate effects in some haptophyte algae. 11: 279-292.

Bird, D.F. and Karl, D.M., 1999. Uncoupling of bacteria and phytoplankton during the austral spring bloom in Gerlache Strait, Antarctic Peninsula. Aquatic Microbial Ecology, 19: 13-27.

Bjork, V.O., 1948. Brain perfusions in dogs with artificially oxygenated blood. Acta Chir Scand suppl., 96(137): 9-122.

Blight, S.B., Bentley, T.L., Lefevre, D., Robinson, C., Rodrigues, R., Rowlands, J. and Williams, P.J.l., 1995. Phasing of autotrophic and heterotrophic plankton metabolism in a temperate coastal ecosystem. Marine Ecology Progress Series, 128: 61-75.

Boehme, S.E., Sabine, C.L. and Reimers, C.E., 1998. CO_2 fluxes from a coastal transect: a time-series approach. Marine Chemistry, 63: 49-67.

Brewer, P.G., 1983. Carbon dioxide in the oceans., Changing climate: Report of the carbon dioxide assessment committee. National Academy Press, Washington DC, pp. 188-215.

Brewer, P.G. and Goldman, J.C., 1976. Alkalinity changes generated by phytoplankton growth. Limnology and Oceanography, 21: 108-117.

Broecker, W.S., 1982. Ocean chemistry during glacial time. Geochimica et cosmochimica acta, 46: 1689-1705.

Broecker, W.S. and Peng, T.-H., 1982. Tracers in the sea. Lamont-Doherty Geological Observatory, New York.

Broecker, W.S. and Peng, T.-H., 1989. The cause of the glacial to interglacial atmospheric CO_2 change: A polar alkalinity hypothesis. Global Biogeochemical Cycles, 3: 215-239.

Buch, K., 1938. New determination of the second dissociation constant of carbonic acid in seawater. Acta Acad. Aeboensis Mat. Phys., 11: 18.

Buch, K., 1951. Kohlensauregleichgewichtssystem im meerwasser. Havsforshkn Inst. Skr., 151.

Buch, K., Harvey, H.W., Wattenberg, H. and S., G., 1932. Uber das kohlensauresystem im meerwasser. Reun Cons perm int Explor Mer, 79: 1-70.

Calderia, K. and Philip, D.B., 2000. The role of the Southern Ocean in uptake and storage of anthropogenic carbon dioxide. Science, 287(5433): 620.

Cao, M.K. and Woodward, F.I., 1998. Dynamic responses of terrestrial ecosystem carbon cycling to global climate change. Nature, 393: 249-252.

Carpenter, S.R., Cole, J.J., Essington, T.E., Hodgson, J.R., Houser, J.N., Kitchell, J.F. and Pace, M.L., 1998. Evaluting alternative explanations in ecosystem experiments. Ecosystems, 1: 335-344.

Carrillo, C.J. and Karl, D.M., 1999. Dissolved inorganic carbon pool dynamics in northern Gerlache Strait, Antarctica. Journal of Geophysical Research, 104: 15,873-15,884.

Chen, C.-T.A., 1982. On the distribution of anthropogenic CO_2 in the Atlantic and Southern oceans. Deep sea research, 29: 563-580.

Chen, C.-T.A., 1993. Carbonate chemistry of the wintertime Bering Sea marginal ice zone. Continental Shelf Research, 13: 67-87.

Chipman, D.M., Marra, J. and Takahashi, T., 1993. Primary production at 47 N and 20 W in the North Atlantic Ocean: a comparison between the 14C incubation method and the mixed layer carbon budget. Deep sea research II, 40: 151-169.

Clayton, T.D., Byrne, R.H., Breland, J.A., Feely, R.A., Millero, F.J., Campbell, D.M., Murphy, P.P. and Lamb, M.F., 1995. The role of pH measurements in modern oceanic CO_2-system characterizations: Precision and thermodynamic consistency. Deep-Sea Research, 42: 411-429.

Copin-Montegut, C., 1988. A new formula for the effect of temperature on the partial pressure of CO_2 in seawater. Marine Chemistry, 25: 29-37.

Copin-Montegut, C. and Copin-Montegut, G., 1983. Stoichiometry of carbon, nitrogen, and phosphorous in marine particulate matter. Deep sea research, 30: 31-46.

Crawford, D.W. and Harrison, P.J., 1997. Direct measurement of pCO_2 in cultures of marine phytoplankton: how good is the estimate from pHNBS and a single point titration of alkalinity. Marine Ecology Progress Series, 158: 61-74.

Cross, F.S., Berne, R.M., Hirose, Y., Jones, R.D. and Kay, E.B., 1956. Evaluation of a rotating type reservoir-oxygenator. Proceedings Society of Experimental Biology and Medicine, 93: 210-214.

Culberson, C.H., 1981. Direct potentiometry. In: M. Whitfield and D. Jagner (Editors), Marine Electrochemistry. Wiley, pp. 187-261.

Deacon, G.E.R., 1982. Physical and biological zonation in the Southern Ocean. Deep-Sea Research, 29(1A): 1-15.

DeGrandpre, M.D., Hammar, T.R., Smith, S.P. and Sayles, F.L., 1995. In situ measurements of seawater pCO_2. Limnology and Oceanography, 40: 969-975.

DeGrandpre, M.D., Hammar, T.R., Wallace, D.W.R. and Wirick, C.D., 1997. Simultaneous mooring-based measurements of seawater CO_2 and O_2 off Cape Hatteras, North Carolina. Limnology and Oceanography, 42(1): 21-28.

DeGrandpre, M.D., Hammar, T.R. and Wirick, C.D., 1998. Short-term pCO_2 and O_2 dynamics in California coastal waters. Deep-Sea Research II, 45: 1557-1575.

Dickson, A.G., 1981. An exact definition of total alkalinity and a procedure for the estimation of alkalinity and total inorganic carbon from titration data. Deep sea research, 28A: 609-623.

Dickson, A.G., 1984. pH scales and proton-transfer reactions in saline media such as sea water. Geochimica et cosmochimica acta, 48: 2299-2308.

Dickson, A.G., 1991. Measuring oceanic CO_2: Progress on quality control. U. S. JGOFS News, 3: 4.

Dickson, A.G., 1993. The measurement of sea water pH. Marine Chemistry, 44: 131-142.

Dickson, A.G. and Millero, F.J., 1987. A comparison of the equilibrium constants for the dissociation of carbonic acid in seawater media. Deep-Sea Research, 34: 1733-1743.

DOE, 1994. Handbook of methods for the analysis of the various parameters of the carbon dioxide system in seawater; version 2. ORNL/CDIAC-74.

Dore, J.E., Carrillo, C.J., Hebel, D.H. and Karl, D.M., 2001. Carbon cycle observations at the Hawaii Ocean Time-series Station ALOHA. In: Y. Nojiri and R.A. Feely (Editors), Proceedings of the PICES North Pacific CO2 data synthesis symposium.

Edmond, J.M. and Gieskes, T.M., 1970. On the calculation of the degree of saturation of seawater with respect to calcium carbonate under in situ conditions. Geochim. Cosmochim. Acta, 34: 1261-1291.

Eigen, M., Kustin, K. and Maass, G., 1961. Die Geschwindigkeit der Hydration von SO_2 in wasseriges. Losung. Z. Physik. Chem. (N. F.), 30(130-136).

Emerson, S., Quay, P.D., Karl, D., Winn, C., Tupas, L. and Landry, M., 1997. Experimental determination of organic carbon flux from open-ocean surface waters. Nature, 389: 951-954.

Emerson, S., Quay, P.D., Stump, C., Wilbur, D. and Schudlich, R., 1995. Chemical tracers of productivity and respiration in the subtropical Pacific Ocean. Journal of Geophysical Research, 100: 15873-15887.

Fan, S., Gloor, M., Mahlman, J., Pacala, S., Sarmiento, J., Takahashi, T. and Tans, P., 1998. A large terrestial carbon sink in north america implied by atmospheric and oceanic carbon dioxide data and models. Science, 282: 442-446.

Feely, R.A., 2001. Uptake and Storage of Carbon Dioxide in the Ocean: The Global CO_2 Survey. Oceanography, 14: 18-32.

Feely, R.A., Wanninkhof, R., Takahashi, T. and Tans, P., 1999. Influence of El Nino on the equatorial Pacific contribution to atmospheric CO_2 accumulation. Nature, 398: 597-601.

Francey, R.J., Tans, P., Allison, C.E., Enting, C.E., White, J.W.C. and Trolier, M., 1995. Changes in oceanic and terrestrial carbon uptake since 1982. Nature, 373: 326-330.

Fraser, W.R., Trivelpiece, W.Z., Ainley, D.G. and Trivelpiece, S.G., 1992. Increases in Antarctic penguin populations: reduced competition with whales or a loss of sea ice due to environmental warming. Polar Biology, 11: 525-531.

Frost, T. and Upstill-Goddard, R.C., 1999. Air-sea gas exchange into the millennium: progress and uncertainties. In: A.D. Ansell, R.N. Gibson and M. Barnes (Editors), Oceanography and Marine Biology: an Annual Review. Taylor and Francis, pp. 1-45.

Garcia, H.E. and Gordon, L.I., 1992. Oxygen solubility in seawater: better fitting equations. Limnology and Oceanography, 37(6): 1307-1312.

Gibson, J.A.E. and W., T.T., 1999. Annual cycle of fCO_2 under sea-ice and in open water in Prydz Bay, East Antarctica. Marine Chemistry, 66: 187-200.

Gieskes, J., 1973. In: J. Berkowitz (Editor), Marine Electrochemistry. Electrochemical Society, Princeton.

Gleitz, M., Kukert, H., Riebesell, U. and Dieckmann, G.S., 1996. Carbon acquisition and growth of Antarctic sea ice diatoms in closed bottle incubations. Marine Ecology Progress Series, 135: 169-177.

Gleitz, M., v.d. Loeff, M.R., Thomas, D.N., Dieckmann, G.S. and Millero, F.J., 1995. Comparison of summer and winter inorganic carbon, oxygen and nutrient concentrations in Antarctic sea ice brine. Marine Chemistry, 51: 81-91.

Goldman, J.C., 1999. Inorganic carbon availability and the growth of large marine diatoms. Marine Ecology Progress Series, 180: 81-91.

Goldman, J.C. and Brewer, P.G., 1980. Effect of nitrogen source and growth rate on phytoplankton-mediated changes in alkalinity. Limnology and Oceanography, 25: 352-357.

Gordon, A.L. and Huber, B.A., 1990. Southern Ocean winter mixed layer. Journal of Geophysical Research, 95(C7): 11655-11672.

Goyet, C., Beauverger, C., Brunet, C. and Poisson, A., 1991. Distribution of carbon dioxide partial pressure in surface waters of the Southwest Indian Ocean. Tellus, 43B: 1-11.

Goyet, C., Metzl, N., Millero, F.J., Eischeid, G., O'Sullivan, D. and Poisson, A., 1998. Temporal variation of the sea surface CO_2/ carbonate properties in the Arabian Sea. Marine Chemistry, 63: 69-79.

Goyet, C., Millero, F.J., Poisson, A. and Shafer, D.K., 1993. Temperature dependance of CO_2 fugacity in seawater. Marine Chemistry, 44: 205-219.

Goyet, C. and Poisson, A., 1989. New determination of carbonic acid dissociation constants in seawater as afunction of temperature and salinity. Deep sea research, 36: 1635-1654.

Hansson, I., 1973a. A new set of acidity constants for carbonic acid and boric acid in seawter. Deep-Sea Research, 20: 661-678.

Hansson, I., 1973b. A new set of pH-scales and standard buffers for sea water. Deep sea research, 20: 479-491.

Haywood, J.M., Stouffer, R.J., Wetherald, R.T., Manabe, S. and Ramaswamy, V., 1997. Transient response of a coupled model to estimate changes in greenhouse gas and sulfate concentrations. Geophysical Research Letters, 24: 1335-1338.

Heimann, M. and Maier-Reimer, E., 1996. On the relations between the oceanic uptake of CO_2 and its carbon isotopes. Global Biogeochemical Cycles, 10: 89-110.

Hein, M. and Sand-Jensen, K., 1997. CO_2 increases oceanic primary production. Nature, 388: 526-527.

Hofmann, E.E., Klinck, J.M., Lascara, C.M. and Smith, D.A., 1996. Water mass distribution and circulation west of the Anarctic Peninsula and including Bransfield Strait. In: R.M. Ross, E.E. Hofmann and L.B. Quetin (Editors), Foundations for ecological research west of the Antarctic Peninsula. American Geophysical Union, Washington, pp. 61-80.

Holm-Hansen, O. and Mitchell, B.G., 1991. Spatial and temporal distribution of phytoplankton and primary production in the western Bransfield Strait region. Deep-Sea Research, 38: 961-980.

Holm-Hansen, O., Mitchell, B.G., Hewes, C.D. and Karl, D.M., 1989. Phytoplankton blooms in the vicinity of Palmer Station, Antarctica. Polar Biology, 10: 49-57.

Hoppema, J.M.J., 1991. The seasonal behaviour of carbon dioxide and oxygen in the coastal north sea along the Netherlands. Netherlands Journal of Sea Research, 28: 167-179.

Hoppema, M., Fahrbach, E., Schroder, M., Wisotzki, A. and de Baar, H.J.W., 1995. Winter-summer differences of carbon dioxide and oxygen in the Weddell Sea surface layer. Marine Chemistry, 51: 177-192.

Houghton, R.A., Boone, R.D., Fruci, J.R., Hobbie, J.E., Melillo, J.M., Palm, C.A., Peterson, B.J., Shaver, G.R., Woodwell, G.M., Moore, B., Skole, D.L. and N., M., 1987. The flux of carbon from terrestrial ecosystems to the atmosphere in 1980 due to changes in land use: geographic distribution of the global flux. Tellus, 39B: 122-139.

Huntley, M., Karl, D.M., Niiler, P. and Holm-Hansen, O., 1991. Research on Antarctic Coastal Ecosystem Rates (RACER): an interdisciplinary field experiment. Deep sea research, 38: 911-942.

Inoue, H.Y., Matsueda, H., Ishii, M., Fushimi, K., Hirota, M., Asanuma, I. and Takasugi, Y., 1995. Long-term trend of the partial pressure of carbon dioxide (pCO2) in surface waters of the western North Pacific, 1984-1993. Tellus, 47B: 391-413.

Ishii, M., Inoue, H.Y., Matsueda, H. and Tanoue, E., 1998. Close coupling between seasonal biological production and dynamics of dissolved inorganic carbon in the Indian Ocean sector and the western Pacific Ocean sector of the Antarctic Ocean. Deep sea research I, 45: 1187-1209.

Jahnke, R.A. and Craven, D.B., 1995. Quantifing the role of heterotrophic bacteria in the carbon cycle: A need for respiration rate measurements. Limnology and Oceanography, 40: 436-441.

Jannasch, H.W., 1997. Small is Powerful: Recollections of a Microbiologist and Oceanograpgher. Annu. Rev. Microbiol, 51: 1-45.

Jenkins, W.J. and Goldman, J.C., 1985. Seasonal oxygen cycling and primary production in the Sargasso Sea. Journal of Marine Research, 43: 465-491.

Johnson, K.M., 1982. Carbon dioxide hydration and dehydration kinetics in seawater. Limnology and Oceanography, 27: 849-855.

Johnson, K.M., Dickson, A.G., Eischeid, G., Goyet, C., Guenther, P., Key, R.M., Millero, F.J., Purkerson, D., Sabine, C.L., Schottle, R.G., Wallace, D.W.R., Wilke, R.J. and Winn, C., 1998. Coulometric total carbon dioxide aanalysis for marine studies: assessment of the quality of total inorganic carbon measurements made during the US Indian Ocean CO2 survey 1994-1996. Marine Chemistry, 63: 21-37.

Johnson, K.M., leB Williams, P.J., Brandstorm, L. and Siebburth, J.M., 1987. Coulometric TCO_2 analysis for marine studies: Automation and calibration. Marine Chemistry, 21: 117-133.

Johnson, K.M., Pytkowicz, R.M. and Wong, C.S., 1979. Biological production and the exchange of oxygen and carbon dioxide across the sea surface in Stuart Channel, British Columbia. Limnology and Oceanography, 24: 474-482.

Johnston, J., 1916. The determination of carbonic acid, combined and free, in solution, particularly in natural waters. Journal Amercan Chemical Society, 38: 947-975.

Jones, E.P., Coote, A.R. and Levy, E.M., 1983. Effect of sea ice meltwater on the alkalinity of seawater. Journal of Marine Research, 41: 43-52.

Kanwisher, J., 1963. On the exchange of gases between the atmosphere and the sea. Deep-Sea Research, 10: 195-207.

Karl, D., Letelier, R., Tupas, L., Dore, J., Christian, J. and Hebel, D., 1997. The role of nitrogen fixation in biogeochemical cycling in the subtropical North Pacific Ocean. Nature, 388: 533-538.

Karl, D.M., 1999. A sea of change: biogeochemical variability in the North Pacific Subtropical gyre. Ecosystems, 2: 181-224.

Karl, D.M., Bates, N.R., Emerson, S., Harrison, P.J., Jeandel, C., Llinas, O., Liu, K.K., Marty, J.-C., Michaels, A.F., Miquel, J.C., Neuer, S., Nojiri, Y. and Wong, C.S., 2002. Temporal studies of biogeochemical processes determined from ocean time-series observations during the JGOFS era.

Karl, D.M. and Bird, D.F., 1993. Bacterial-agal interactions in Antarctic coastal ecosystems. In: G. E. and Pedros-Alio (Editors), Trends in microbial ecology, sixth international symposium on microbial ecology, pp. 37-40.

Karl, D.M., Christian, J.R., Dore, J.E. and Letelier, R.M., 1996. Microbiological oceanography in the region west of the Antarctic peninsula: microbial dynamics, nitrogen cycle and carbon flux. In: R.M. Ross, E.E. Hofmann and L.B. Quetin (Editors), Foundations for ecological research west of the Antarctic Peninsula. American Geophysical Union, Washington, pp. 303-332.

Karl, D.M., Dore, J.E., Lukas, R., Michaels, A.F., Bates, N.R. and Knap, A., 2001. The U. S. JGOFS Time-Series Observation Programs. Oceanography, 14: 6-17.

Karl, D.M., Holm-Hansen, O., Taylor, G.T., Tien, G.T. and Bird, D.F., 1991. Microbial biomass and productivity in the western Bransfield Strait, Antarctica during the 1986-87 austral summer. Deep Sea Research, 38: 1029-1055.

Karl, D.M. and Lukas, R., 1996. The Hawaii Ocean Time-series (HOT) program: background, rationale and field implementation. Deep Sea Research, 43: 129-156.

Keeling, R.F., Najjar, R.P., Bender, M.L. and Tans, P.P., 1993. What atmospheric oxygen measurements can tell us about the global carbon cycle. Global Biogeochemical Cycles, 7(1): 37-67.

Keeling, R.F. and Shertz, S.R., 1992. Seasonal and interannual variations in atmospheric oxygen and implications for global carbon cycle. Nature, 358: 723-727.

Kelly, C.A., Pakulski, J.D., Sandvik, S.L.H., Coffin, R.B., Downer Jr, R.C., Aas, P., Lyons, M.M. and Jeffrey, W.H., 1999. Phytoplanktonic and bacterial carbon pools and productivities in the Gerlache Strait, Antarctica, during early austral spring. Microbial Ecology, 38: 296-305.

Klinck, J.M., 1998. Heat and salt changes on the continential shelf west of the Antarctic Peninsula between January 1993 and January 1994. Journal of Geophysical Research, 103(C4): 7617-7636.

Larsson, A.-M. and Svansson, A., 1992. Fluxes of gases in an ice related ecosystem in the north-western Weddell Sea. Polar Biology, 12: 183-188.

Laws, E.A., 1991. Photosyntheic quotients, new production and net community production in the open ocean. Deep Sea Research, 38(1): 143-167.

Laws, E.A. and Bannister, T.T., 1980. Nutrient- and light-limited growth of Thalassiosira fluiatilis in continuous coulture, with implications for phytoplankton growth in the ocean. Limnology and Oceanography, 25: 457-473.

Laws, E.A., Bidigare, R.R. and Popp, B.N., 1997. Effect of growth rate and CO_2 concentration on carbon isotopic fraction by the marine diatom Phaeodactylum tricornutum. Limnology and Oceanography, 42: 1552-1560.

Laws, E.A., Popp, B.N., Bidigare, R.R., Kennicutt, M.C. and Macko, S.A., 1995. Dependence of phytoplankton carbon isotopic composition on growth rate and $[CO_2]$aq: Theoretical considerations and experimental results. Geochimica et cosmochimica acta, 59: 1131-1138.

leB Williams, P.J., 1993. On the definition of plankton production terms. ICES Mar. Sci. Symp., 197: 9-19.

Lee, K., 2001. Global net community production estimated from the annual cycle of surface water total dissolved inorganic carbon. Limnology and Oceanography, 46: 1287-1297.

Lee, K. and Millero, F.J., 1995. Thermodynamic studies of the carbonate system in seawater. Deep-Sea Research, 42: 2035-2061.

Lee, K., Millero, F.J., Byrne, R.H., Feely, R.A. and Wanninkhof, R., 2000. The reccommended dissociation constants for carbonic acid in seawater. Geophysical Research Letters, 27(2): 229-232.

Lee, K., Millero, F.J. and Campbell, D.M., 1996. The reliability of the thermodynamic constants for the dissociation of carbonic acid in seawater. Marine Chemistry, 55: 233-245.

Lee, K., Millero, F.J. and Wanninkhof, R., 1997. The carbon dioxide system in the Atlantic Ocean. Journal of Geophysical Research, 102: 15693-15707.

Lee, K., Wanninkhof, R., Takahashi, T., Doney, S.C. and Feely, R.A., 1998. Low interannual variability in recent oceanic uptake of atmospheric carbon dioxide. Nature, 396: 155-159.

Lewis, E.R. and Wallace, W.R., 1995. Basic programs for the CO_2 system in seawater. Data Report, BNL-61827. Brookhaven National Lab, Upton, New York.

Liss, P.S., 1973. Processes of gas exchange across an air-water interface. Deep Sea research, 20: 221-238.

Liss, P.S. and Merlivat, L., 1986. Air-sea gas exchange rates: Introduction and synthesis. The role of air-sea exchange in geochemical cycling. D. Reidel, Hingham, Mass, 113-129 pp.

Longhurst, A.R., 1991. Role of the marine biosphere in the global carbon cycle. Limnology and Oceanography, 36: 1507-1526.

Lueker, T.J., Dickson, A.G. and Keeling, C.D., 2000. Ocean pCO_2 calculated from dissolved inorganic carbon, alkalinity, and equations for K_1 and K_2: validation based on laboratory measurements of CO_2 in gas and seawater at equilibrium. Marine Chemistry, 70: 105-119.

Lyman, J., 1956. Buffer mechanism of seawater, Univ. of calif. Los Angeles.

Marland, G., J., A.R. and Boden, T.A., 1994. Global, regional, and national CO_2 emissions. In: T.A. Boden, D.P. Kaiser, R.J. Sepanski and R.W. Stoss (Editors), Trends 93. Carbon dioxide information center, Oak Ridge National Laboratory, TN, pp. 505-581.

Martinson, D.G. and Iannuzzi, R.A., 1998. Antarctic Ocean-ice interaction: Implications from ocean bulk property distributions in the Weddell Gyre, Antarctic Research Series:Antarctic Sea Ice: Physical processes, interactions and variability. American Geophysical Union, pp. 243-271.

McElligott, S., Byrne, R.H., Lee, K., Wanninkhof, R., Millero, F.J. and Feely, R.A., 1998. Discrete water column measurements of CO_2 fugacity and pHT in seawater: A comparison of direct measurements and thermodynamic calculations. Marine Chemistry, 60: 63-73.

McNeil, C.L. and Merlivat, L., 1996. The warm oceanic surface layer: Implications for CO_2 fluxes and surface gas measurements. Geophysical Research Letters, 23: 3575-3578.

Mehrbach, C., Culberson, C.H., Hawley, J.E. and Pytkowicz, R.M., 1973. Measurement of the apparent dissociation constants of carbonic acid in seawater at atmospheric pressure. Limnology and Oceanography, 18: 897-907.

Metzl, N., Beauverger, C., Brunet, C., Goyet, C. and A., P., 1991. Surface water pCO_2 in the western Indian sector of the southern ocean: A highly variable CO_2 surce sink region during the austral summer. Marine Chemistry, 35: 85-95.

Metzl, N., Louanchi, F. and Poisson, A., 1998. Seasonal and interannual variations of sea surface carbon dioxide in the subtropical Indian Ocean. Marine Chemistry, 60: 131-146.

Michaels, A.F., Bates, N.R., Buesseler, K.O., Carlson, C.A. and Knap, A.H., 1994. Carbon-cycle imbalances in the Sargasso Sea. Nature, 372: 537-540.

Michaels, A.F., Karl, D.M. and Knap, A.H., 2000. Temporal studies of biogeochemical dynamics in oligotrophic oceans. In: R.B. Hanson, H.W. Ducklow and J.G. Field (Editors), The Changing Ocean Carbon Cycle. Cambridge University Press, Cambridge, UK, pp. 392-413.

Miller, L.A., Chierici, M., Johannessen, T., Noji, T.T., Rey, F. and Skjelvan, I., 1999. Seasonal dissolved inorganic carbon variations in the Greenland Sea and implications for atmospheric CO2 exchange. Deep sea research II, 46: 1473-1496.

Millero, F.J., 1995. Thermodynamics of the carbon system in the oceans. Geochimica et Cosmochimica Acta, 59: 661-677.

Millero, F.J., Byrne, R.H., Wanninkhof, R., Feely, R., Clayton, T., Murphy, P. and Lamb, M.F., 1993. The internal consistency of CO_2 measurements in the equatorial Pacific. Marine Chemistry, 44: 269-280.

Millero, F.J., Dickson, A.G., Eischeid, G., Goyet, C., Guenther, P., Johnson, K.M., Key, R.M., Lee, K., Purkerson, D., Sabine, C.L., Schottle, R.G., Wallace, D.W.R., Lewis, E. and Winn, C., 1998a. Assessment of the quality of the shipboard measurements of total alkalinity on the WOCE Hydrographic Program Indian Ocean CO2 survey cruises 1994-1996. Marine Chemistry, 63: 9-20.

Millero, F.J., Lee, K. and Roche, M., 1998b. Distribution of alkalinity in the surface waters of the major oceans. Marine Chemistry, 60: 111-130.

Mitchell, G.B., Brody, E.A., Holm-Hansen, O., McClain, C. and Bishop, J., 1991. Light limitation of phytoplankton biomass and macronutrient utilization in the Southern Ocean. Limnology and Oceanography, 36: 1662-1677.

Moore, J.K., Abott, M.R., Richman, J.R., Smith, W.O., Cowles, T.J., Coale, K.H., Gardner, W.D. and Barber, R.T., 1999. SeaWiFS satellite ocean color data from the Southern Ocean. Geophysical Research Letters, 26(10): 1465-1468.

Morse, J.W. and Mackenzie, F.T., 1990. Geochemistry of Sedimentray Carbonates. Elsevier, New York.

Najjar, R.G. and Keeling, R.F., 2000. Mean annual cycle of the air-sea oxygen flux: A global view. Global Biogeochemical Cycles, 14: 573-584.

Oechel, W.C., Vourlitis, G.L., Hastings, S.J., Zulueta, R.C., Hinzman, L. and Kane, D., 2000. Acclimation of ecosystem CO_2 exchange in the Alaskan Arctic in response to decadal climate warming. Nature, 406: 978-981.

Ohshima, K.I., Kazumasa, Y., Haruhito, S., Masaaki, W., Tatsuo, E. and Fukuchi, M., 1998. Relationship between the upper ocean and sea ice during the Antarctic melting season. Journal of Geophysical Research, 103(C4): 7601-7615.

Peng, T.-H., Key, R.M. and Ostlund, H.G., 1998a. Temporal varations of bomb radiocarbon inventory in the Pacific Ocean. Marine Chemistry, 60: 3-13.

Peng, T.-H., Wanninkhof, R., Bullister, J.L., Feely, R.A. and Takahashi, T., 1998b. Quantification of decadal anthropogenic CO_2 uptake in the ocaen based on dissolved inorganic carbon measurements. Nature, 396: 560-563.

Platt, T. and Harrison, W.G., 1985. Biogenic fluxes of carbon and oxygen in the ocean. Nature, 318: 55-57.

Poisson, A., Metzl, N., Brunet, C., Schauer, B., Bres, B., Ruiz-Pino, D. and Louanchi, F., 1993. Variability of sources and sinks of CO_2 in the western Indian and Southern

Oceans during the year 1991. Journal of Geophysical Research, 98(c12): 22,759-22,778.

Poisson, A., Metzl, N., Danet, X., Louanchi, F., Brunet, C., Schauer, B., Bres, B. and Ruiz-Pino, D., 1994. Air-sea CO_2 fluxes in the Southern Ocean between 25E and 85E, The polar Oceans and their role in shaping the global environment. American Geophysical Union.

Pomeroy, L.R., 1974. The ocean's food web, a changing paradigm. Bioscience, 24: 499-504.

Popp, B.N., Laws, E.A., Bidigare, R.R., Dore, J.E., Hanson, K.L. and Wakeham, S.G., 1998. Effect of phytoplankton cell geometry on carbon isotopic fractionation. Geochimica et cosmochimica acta, 62: 69-77.

Quay, P.D., Tilbrook, B. and Wong, C.S., 1992. Oceanic uptake of fossil fuel CO_2: Carbon-13 evidence. Science, 256: 74-78.

Rakestraw, N.W., 1949. The conception of alkalinity or excess base of sea water. Journal of Marine Research, 8: 14-20.

Redfield, A.C., Ketchum, B.H. and A., R.F., 1963. The influence of organisms on the composition of sea water. In: M.N. Hill (Editor), The Sea. Interscience, New York, pp. 26-77.

Revelle, R. and Suess, H.E., 1957. Carbon dioxide exchange between the atmosphere and ocean and the question of an increase of atmospheric CO_2 during the past decades. Tellus, 9: 18-27.

Richardson, C., 1976. Phase relationships in sea ice as a function of temperature. J. Glaciology, 17: 507-519.

Robertson, J.E. and Watson, A.J., 1995. A summertime sink for atmospheric carbon dioxide in the Southern Ocean between 88 deg W and 80 deg E. Deep-Sea Research Part II, 42: 1081-1091.

Robertson, J.E., Watson, A.J., Langdon, C., Ling, R.D. and Wood, J.W., 1993. Diurnal variation in surface pCO^2 and O_2 at 60 N, 20 W in the North Atlantic. Deep sea research II, 40: 409-422.

Robinson, C., Archer, S.D. and le B. Williams, P.J., 1999. Microbial dynamics in coastal waters of East Antarctica: plankton production and respiration. Marine Ecology Progress Series, 180: 23-36.

Roy, R.N., Roy, L.N., Vogel, K.M., P., M.C., Pearson, T., Good, C.E., Millero, F.J. and Campbell, D.M., 1993. The dissociation constants of carbonic acid in seawater at salinities 5 to 45 and temperatures 0 to 45 oC. Marine Chemistry, 44: 249-267.

Roy, R.N., Roy, L.N., Vogel, K.M., P., M.C., Pearson, T., Good, C.E., Millero, F.J. and Campbell, D.M., 1994. The dissociation constants of carbonic acid in seawater at salinities 5 to 45 and temperatures 0 to 45 oC. Marine Chemistry, 45: 337.

Roy, R.N., Roy, L.N., Vogel, K.M., P., M.C., Pearson, T., Good, C.E., Millero, F.J. and Campbell, D.M., 1996. The dissociation constants of carbonic acid in seawater at salinities 5 to 45 and temperatures 0 to 45 oC. Marine Chemistry, 52: 183.

Rubin, S.I., Takahashi, T., Chipman, D.M. and Goddard, J.G., 1998. Primary productivity and nutrient utilization ratios in the Pacific sector of the Southern Ocean based on seasonal changes in seawater chemistry. Deep sea research I, 45: 1211-1234.

Sabine, C.L. and Key, R.M., 1998. Controls on fCO_2 in the South Pacific. Marine Chemistry, 60: 95-110.

Sabine, C.L., Key, R.M., Johnson, K.M., Millero, F.J., Poisson, A., Sarmiento, J.L., Wallace, D.W.R. and Winn, C.D., 1999. Anthropogenic CO_2 inventory of the Indian Ocean. Global Biogeochemical Cycles, 13(1): 179-198.

Sabine, C.L., Mackenzie, F.T., Winn, C. and Karl, D.M., 1995. Geochemistry of carbon dioxide in seawater at the Hawaii Ocean Time series station ALOHA. Global Biogeochemical Cycles, 9: 637-651.

Sarmiento, J.L., Hughes, T.M.C., Stouffer, R.J. and Manabe, S., 1998. Simulated response of the ocean carbon cycle to anthropogenic climate warming. Nature, 393: 245-249.

Sarmiento, J.L. and Sundquist, E.T., 1992. Revised budget for the oceanic uptake of anthropogenic carbon dioxide. Nature, 356: 589-593.

Sarmiento, J.L. and Wofsy, S.C. (Editors), 1999. A U.S. carbon cycle science plan. U.S. Global Change Research Program, Washington DC, 69 pp.

Sasai, Y., Ikeda, M. and Tanaka, N., 2000. Changes of total CO_2 and pCO_2 in the surface ocean during the mixed layer development in the northern North Pacific. Journal of Geophysical Research, 105: 3465-3481.

Schink, D.R., Sigalove, J.J., Charnell, R.L. and Guinasso Jr., N.L., 1970. Use of Rn/Ra ratios to determine air/sea gas exchange and vertical mixing in the sea, a final technical report. Office of Naval Research, Palo Alto.

Seyler, C., 1897. The estimation of carbonic acid in natural waters. Analyst, 22: 312.

Shabica, S.V., Hedgpeth, J.W. and Park, P.K., 1977. Dissolved oxygen and pH increases by primary production in surface water of Arther Harbor, Antarctica, 1970-1971.

In: G.A. Llano (Editor), Adaptations within Antarctic Ecosystems. Smithsonian Institution, pp. 83-97.

Sherr, E.B. and Sherr, B.F., 1996. Temporal offset in oceanic production and respiration processes implied by seasonal changes in atmospheric oxygen: the role of heterotrophic microbes. Aquatic Microbial Ecology, 11: 91-100.

Sigman, D.M. and Boyle, E.A., 2000. Glacial/interglacial variations in atmospheric carbon dioxide. Nature, 407: 859-869.

Simpson, J.J., 1985. Air-sea exchange of carbon dioxide and oxygen induced by phytoplankton. In: A. Zirino (Editor), Mapping Strategies in Chemical Oceanography. American Chemical Society, Washington DC, pp. 409-450.

Skjelvan, I., Johannessen, T. and Miller, L.A., 1999. Interannual variability of fCO_2 in the Greenland and Norwegian Seas. Tellus, 51B: 477-489.

Smith, D.A., Hofmann, E.E., Klinck, J.M. and Lascara, C.M., 1999a. Hydrography and circulation of the West Antarctic Peninsula Continental Shelf. Deep-Sea Research, 46: 925-949.

Smith, R.C., Ainley, D., Baker, K., Domack, E., Emslie, S., Fraser, B., Kennett, J., Leventer, A., Mosley-Thompson, E., Stammerjohn, S. and Vernet, M., 1999b. Marine Ecosystem Sensitivity to climate change. Bioscience, 49(5): 393-404.

Smith, R.C., Baker, K.s., Fraser, W.R., Hofmann, E.E., Karl, D.M., Klinck, J.M., Quetin, L.B., Prezelin, B.B., Ross, R.M., Trivelpiece, W.Z. and Vernet, M., 1995. The Palmer LTER: A long-term ecological research program at Palmer Station, Antarctica. Oceanography Magazine, 8: 77-86.

Smith, R.C., Baker, K.S., Fraser, W.R., Trivelpiece, W.Z., Hofmann, E.E., Klinck, J.M., Karl, D.M., Quetin, L.B., Ross, R.M. and Vernet, M., 1996a. The Western Antarctic Peninsula region: summary of environmental and ecological processes. In: R.M. Ross, E.E. Hofmann and L.B. Quetin (Editors), Foundations for Ecological Research West of the Antarctic Peninsula. American Geophysical Union, Washington D.C., pp. 437-448.

Smith, R.C., Baker, K.S. and P., D., 1981. Fluorometric techniques for the measurement of oceanic chlorophyll in the support of remote sensing. 81-17, Scripps Inst. Oceanogr.

Smith, R.C., Baker, K.S. and Stammerjohn, S.E., 1998. Exploring sea ice indexes for polar ecosystem studies. Bioscience, 48: 83-93.

Smith, R.C., Booth, C.R. and Star, J.L., 1984. Oceanographic bio-optical profiling system. Applied Optics, 23: 2791-2797.

Smith, R.C., Dierssen, H.M. and Vernet, M., 1996b. Phytoplankton biomass and productivity in the western Antarctic Peninsula Region. In: R.M. Ross, E.E. Hofmann and L.B. Quetin (Editors), Foundations for Ecological Research West of the Antarctic Peninsula. American Geophysical Union, Washington D.C., pp. 333-356.

Smith, S.V., 1985. Physical, chemical and biological characteristics of CO_2 gas flux across the air-water interface. Plant, Cell and Environment, 8: 387-398.

Smith, W.O. and Nelson, D.M., 1985. Phytoplankton bloom produced by a receding ice edge in the Ross Sea: Spatial coherence with the density field. Science, 227: 163-166.

Stammerjohn, S.E. and Smith, R.C., 1996. Spatial and temporal variability in the weat Antarctic Peninsulasea ice coverage. In: R.M. Ross, E.E. Hofmann and L.B. Quetin (Editors), Foundations for ecological research west of the Antarctic Peninsula. American Geophysical Union, Washington, pp. 81-104.

Stammerjohn, S.E. and Smith, R.C., 1997. Opposing southern ocean climate patterns as revealed by trends in regional sea ice coverage. Climatic Change: 1-19.

Stephens, B.B. and Keeling, R.F., 2000. The influence of Antarctic sea ice on glacial-interglacial CO_2 variations. Nature, 404: 171-174.

Sunquist, E.T., 1993. The global carbon dioxide budget. Science, 259: 934-941.

Sweeney, C., Hansell, D.A., Carlson, C.A., Codispoti, L.A., Gordon, L.I., Marra, J., Millero, F.J., Smith, W.O. and Takahashi, T., 2000. Biogeochemical regimes, net community production and carbon export in the Ross Sea, Antarctica. Deep sea research II, 47: 3369-3394.

Takahashi, T., Broecker, W.S., Werner, S.R. and Brainbridge, A.E., 1980. Carbonate chemistry of the surface waters of the world oceans. In: E.D. Goldberg, Y. Horibe and K. Saruhashi (Editors), Isotope Marine Chemistry. Uchida Rokakuko, Tokyo, pp. 291-325.

Takahashi, T., Feely, R.A., Weiss, R.F., Wanninkhof, R.H., Chipman, D.M., Sutherland, S.C. and Takahashi, T., 1997. Global air-sea flux of CO_2: An estimate based on measurements of sea-air pCO_2 difference. Proc. Natl. Acad. Sci., 94: 8292-8299.

Takahashi, T., Olafsson, J., Goddard, J.G., W., C.D. and Sutherland, S.C., 1993. Seasonal variation of CO_2 and nutrients in high latitude surface oceans: A comparative study. Global Biogeochemical Cycles, 7: 843-878.

Takahashi, T., Weiss, R.F., Culberson, C.H., Edmond, J.M., E., H.D., S., W.C., Li, Y. and Brainbridge, A.E., 1970. A carbonate chemistry profile at the 1969 Geosecs intercalibration station in the Eastern Pacific Ocean. Journal of Geophysical Research, 75(36): 7648-7666.

Tan, F.C., Dyrssen, D. and Strain, P.M., 1983. Sea-ice meltwater and excess alkalinity in the east Greenland current. Oceanologica acta, 6: 283-288.

Tans, P.P., Fung, I.Y. and Takahashi, T., 1990. Observational constraints on the global atmospheric CO_2 budget. Science, 247: 1431-1438.

Thompson, T.G. and Anderson, D.H., 1940. The determination of the alkalinity of sea water. Journal of Marine Research, 3: 224-229.

Toggweiler, J.R. and Sarmiento, J.L., 1985. Glacial to interglacial changes in atmospheric carbon dioxide: the critical role of ocean surface water in high latitudes. In: S.E. T. and W.S. Broecker (Editors), Natural Varations Archean to Present. American Geophysical Union, Washington D.C., pp. 163-184.

Tolbert, N.E., 1997. The C_2 oxidative photosynthetic carbon cycle. Annual Review Physiology Plant Molecular biology, 48: 1-25.

Tomczak, M. and Godfrey, S.J., 1994. Regional Oceanography: An Introduction. Pergamon.

van Geen, A., Takesue, R.K., Goddard, J., Takahashi, T., A., B.J. and R.L., S., 2000. Carbon and nutrient dynamics during coastal upwelling off Cape Blanco, Oregon. Deep Sea research II, 47: 975-1002.

Volk, T. and Hoffert, M.I., 1985. Ocean carbon pumps: analysis of relative sterengths and efficiencies in ocean-driven atmospheric CO2 changes. Natural Variations

Archean to Present, 32. American Geophysical Union, Washington D. C., 99-110 pp.

Wallace, D.W.R., 2001. Storage and transport of excess CO_2 in the oceans: The JGOFS/WOCE Global CO_2 Survey. In: G. Siedler, J. Church and J. Gould (Editors), Circulation and Climate Observing and Modeling the Global Ocean. Academic Press, San Diego, pp. 489-521.

Wanninkhof, R., 1992. Relationship between wind speed and gas exchange over the ocean. Journal of Geophysical Research, 97(C5): 7373-7382.

Wanninkhof, R. and Feely, R.A., 1998. fCO_2 dynamics in the Atlantic, South Pacific and South Indian oceans. Marine Chemistry, 60: 15-31.

Wanninkhof, R., Feely, R.A., Atwood, D.K., Berberian, G., Wilson, D., Murphy, P.P. and Lamb, M.F., 1995. Seasonal and lateral variations in carbon chemistry of surface water in the eastern equatorial Pacific during 1992. Deep Sea Research II, 42: 387-409.

Wanninkhof, R., Lewis, E., Feely, R.A. and Millero, F.J., 1999. The optimal carbonate dissociation constants for determining surface pCO_2 from alkalinity and total inorganic carbon. Marine Chemistry, 65: 291-301.

Waters, K.J. and Smith, R.C., 1992. Palmer LTER: A Sampling Grid for the Palmer LTER program. Antarctic Journal of the United States, 27: 236-239.

Watson, A.J., Robertson, J.E. and Ling, R.D., 1993. Air-sea exchange of CO_2 and its relationship to primary production. In: R. Wollast, F.T. Mackenzie and L. Chou (Editors), Interactions of C, N, P and S Biogeochemical Cycles and Global Change. Springer, Verlag Berlin Heidelberg.

Watson, A.J., Robinson, C., Robinson, J.E., le B. Williams, P.J. and Fasham, M.J.R., 1991. Spatial variability in the sink for atmospheric carbon dioxide in the North Atlantic. Nature, 350: 50-53.

Weiss, R.F., 1970. The solubility of nitrogen, oxygen and argon in water and seawater. Deep-Sea Research, 17: 721-735.

Weiss, R.F., 1974. Carbon dioxide in water and seawater: the solubility of a non-ideal gas. Marine Chemistry, 2: 203-215.

Weiss, R.F., Jahnke, R.A. and Keeling, C.D., 1982. Seasonal effects of temperature and salinity on the partial pressure of CO_2 in seawater. Nature, 300: 511-513.

Weiss, R.F., Ostlund, H.G. and Craig, H., 1979. Geochemical studies of the Weddell Sea. Deep sea research, 26A: 1093-1120.

Wenk, T. and Siegenthaler, U., 1985. The high latitude ocaen as a control of atmospheric CO_2. In: S.E. T. and W.S. Broecker (Editors), Natural Varations Archean to Present. American Geophysical Union, Washington D.C., pp. 185-194.

Winn, C.D., Li, Y.H., Mackenzie, F.T. and Karl, D.M., 1998. Rising surface ocean dissolved inorganic carbon at the Hawaii Ocean Time-series site. Marine Chemistry, 60: 33-47.

Winn, C.D., Mackenzie, F.T., Carrillo, C.J., Sabine, C.L. and Karl, D.M., 1994. Air-sea carbon dioxide exchange in the North Pacific Subtropical Gyre: Implications for the global carbon budget. Global Biogeochemical Cycles, 8: 157-163.

Wolf-Gladrow, D.A. and Riebesell, U., 1977. Diffusion and reactions in the vicinity of plankton: A refined model for inorganic carbon transport. Marine Chemistry, 59: 17-34.

Wong, C.S., Chan, Y.-H. and Page, J.S., 1995a. Geographical, seasonal and interannual variations of air-sea CO_2 exchange in the subtropical Pacific surface waters during 1983-1988 (II). Air-sea CO_2 fluxes with skin-temperature adjustments. Tellus, 47B: 431-446.

Wong, C.S., Chan, Y.-H., Page, J.S., Bellegay, R.D. and Iseki, K., 1995b. Geographical, seasonal and interannual variations of air-sea CO_2 exchange in the subtropical Pacific surface waters during 1983-1988 (I). Variabilities of oceanic fCO_2. Tellus, 47B: 414-430.

Wood, R.A., Keen, A.B., Mitchell, J.F.B. and Gregory, J.M., 1999. Changing spatial structure of the thermohaline circulation in response to atmospheric CO2 forcing in a climate model. Nature, 399: 572-575.

Wyrtki, K., 1962. The oxygen minima in relation to ocean circulation. Deep Sea Research, 9: 11-23.

Yager, P.L., Wallace, D.W.R., Johnson, K.M., Smith, W.O., Minnett, P.J. and Deming, J.W., 1995. The Northest water polyna as an atmospheric CO_2 sink: A seasonal rectification hypothesis. Journal of Geophysical Research, 100: 4389-4398.

Zeebe, R.E., Wolf-Gladrow, D.A. and Jansen, H., 1999. On the time required to establish chemical and isotopic equilibrium in the carbon dioxide system in seawater. Marine Chemistry, 65: 135-153.

Zhang, J.-Z., 2000. The use of pH and buffer intensity to quantify the carbon cycle in the ocean. Marine Chemistry, 70: 121-131.

Zwally, J.H., Parkinson, C.L. and Comiso, J.C., 1983. Variability of Antarctic sea ice and changes in carbon dioxide. Science, 220: 1005-1012.

Appendix A Data Pal-LTER Summer/Winter 1993

	Station	Salinity	DIC µmol/kg	n35DIC	TA µeq/kg	n35TA	n35P (µmol/kg)	n35N (µmol/kg)
Jan-93	600.200	33.839	2151	2224.8	2323.3	2403.0	1.4	18.9
	600.180	33.816	2156.6	2232.1	2305.8	2386.6	1.4	17.1
	600.160	33.843	2148.5	2222.0	2313.4	2392.5	1.1	16.1
	600.140	33.811	2148.4	2224.0	2318.2	2399.7	1.3	17.1
	600.120	33.71	2153.4	2235.8			1.4	19.2
	600.100	33.413	2124.7	2225.6	2287.5	2396.2	1.5	19.6
	600.080	33.706	2159.2	2242.1	2305.2	2393.7	1.7	21.3
	600.060	33.539	2145.1	2238.5	2306.1	2406.6	1.8	25.0
	600.040	33.547	2152.4	2245.6	2297.6	2397.2	2.5	31.5
	500.180	33.547	2162.9	2256.6	2310.5	2410.6		
	500.160	33.853	2159.9	2233.1	2309.8	2388.0	1.3	16.6
	500.140	33.863	2162.2	2234.8	2309.6	2387.1	2.0	21.9
	500.120	33.834	2154.2	2228.4	2318.4	2398.3	2.2	23.5
	500.100	33.806	2150.2	2226.1	2311.7	2393.3	1.8	21.3
	500.080	33.79	2152.2	2229.3	2335.8	2419.5		
	500.060	33.671	2160.5	2245.8	2315.5	2406.9	1.8	21.9
	400.200	33.819	2138	2212.7	2299.1	2379.4	1.3	19.5
	400.180	33.855	2144.4	2216.9	2303.9	2381.9	1.6	19.7
	400.160	33.816	2139.3	2214.2	2303.6	2384.2	1.4	17.9
	400.140	33.772	2141.5	2219.4	2306.9	2390.8	1.3	15.3
	400.120	33.779	2146.4	2224.0	2302.0	2385.2	1.2	16.1
	400.100	33.745	2147.5	2227.4	2301.8	2387.4	1.5	20.7
	400.080	33.617	2148.9	2237.3	2306.0	2400.9	1.4	17.7
	400.060	33.587	2138.6	2228.6	2302.7	2399.6	2.4	27.6
	400.040	33.056	2109	2233.0	2277.7	2411.6	2.0	23.6
	300.200	33.857	2166.8	2240.0	2314.7	2392.9		
	300.180	33.827	2159.9	2234.8	2302.1	2382.0	1.3	18.2
	300.160	33.834	2163.3	2237.9			1.3	19.8
	300.140	33.841	2170.5	2244.8	2301.1	2379.9	1.3	13.7
	300.100	33.851	2154.6	2227.7	2301.1	2379.2	1.2	18.1
	300.080	33.238	2121.2	2233.6	2273.3	2393.8		
	300.060	33.668	2140.3	2225.0	2295.5	2386.4	1.4	13.3
	300.040	33.23	2121.1	2234.1	2267.4	2388.1	1.1	15.1
	200.200	33.789	2142.1	2218.9	2297.8	2380.2	1.0	15.9
	200.160	33.83	2143	2217.1	2298.8	2378.3	1.1	16.7
	200.120	33.64	2135.5	2221.8	2293.3	2386.1	1.2	16.3
	200.080	33.555	2135.3	2227.3	2296.5	2395.4	1.1	14.7
	200.040	33.053	2115.1	2239.7	2255.9	2388.8	1.1	14.3

	Station	Salinity	DIC µmol/kg	n35DIC	TA µeq/kg	n35TA	n35P (µmol/kg)	n35N (µmol/kg)
Aug-93	600.160	33.912	2103.34	2170.8	2314.1	2388.3	1.5	21.1
	600.140	33.878	2142.72	2213.7	2308.4	2384.9	1.6	19.5
	600.120	33.858	2148.61	2221.1	2365.6	2445.4	2.3	32.4
	600.100	33.933	2149.59	2217.2	2477.6		1.8	26.5
	600.080	33.951	2163.31	2230.2	2344.4	2416.8	1.7	25.8
	600.060	34.114	2139.35	2194.9	2368.1	2429.6	1.8	25.6
	600.040	33.47	2153.72	2252.2			1.8	31.5
	500.200	34.016	2155.76	2218.1	2359.2	2427.5	1.8	27.1
	500.180	33.978	2140.43	2204.8	2363.1	2434.2	2.0	28.3
	500.160	33.972	2124.69	2189.0	2341.6	2412.4	1.9	21.3
	500.140	33.969	2158.85	2224.4	2437	2511.0	1.5	23.6
	500.120	33.975	2178.25	2244.0	2304.7	2374.2	2.0	32.9
	500.100	33.955	2172.73	2239.6	2293.8	2364.4	2.0	31.6
	500.080	33.89	2174.37	2245.6	2298.4	2373.7	1.7	24.3
	500.060	33.842	2145.92	2219.3	2360	2440.8	1.8	30.0
	400.200	33.996	2156.89	2220.6	2309.6	2377.8	2.2	31.4
	400.180	33.992	2155.82	2219.7	2404.9	2476.2	2.1	32.0
	400.160	33.923	2153.2	2221.6	2363.4	2438.4	3.3	30.4
	400.140	33.864	2155.24	2227.5	2422	2503.3	2.0	27.1
	400.120	33.842	2152.04	2225.7	2352.3	2432.8	2.2	31.1
	400.100	33.874	2154.65	2226.3	2446.6	2528.0	1.8	26.3
	400.080	33.856	2150.11	2222.8	2313.5	2391.7	1.7	26.3
	400.060	33.846	2149.63	2222.9	2342.5	2422.4	1.9	28.6
	400.040	33.802	2155.63	2232.0	2342.1	2425.1	2.0	32.0
	300.200	33.917	2143.96	2212.4	2359.3	2434.6	1.8	29.9
	300.180	34.002	2159.77	2223.2	2348.8	2417.7	2.1	32.1
	300.160	34.022	2161.4	2223.5	2360.5	2428.4	1.7	28.5
	300.140	34.013	2150.42	2212.8			2.3	32.2
	300.120	34.019	2165.78	2228.2	2340.1	2407.6	1.9	23.4
	300.100	34.018	2150.66	2212.7	2358.1	2426.2	2.3	33.4
	300.080	34.027	2160.93	2222.7	2366.6	2434.3	1.7	25.4
	300.060	33.99	2147.96	2211.8	2341.7	2411.3	2.1	31.6
	300.040	33.903	2188.96	2259.8	2297.3	2371.6	2.2	31.6
	200.160	34.036	2075.39	2134.2	2369.6	2436.7	2.3	32.5
	200.140	33.974	2164.54	2229.9	2462.5	2536.9		
	200.120	34.006	2091.32	2152.4	2315.2	2382.9		
	200.100	34.008	2145.58	2208.2	2414.1	2484.5	2.3	33.1
	200.080	33.971	2183.96	2250.1	2293.8	2363.3	3.3	32.8
	200.060	33.943	2183.85	2251.9	2304	2375.7	2.3	32.6
	200.040	33.912	2158.78	2228.0	2459	2537.9	3.2	31.2

Pal-LTER Seasonal Summary

	n35P				n35N			
	Jan-93	**Mar-93**	**Aug-93**	**Jan-94**	**Jan-93**	**Mar-93**	**Aug-93**	**Jan-94**
Max	2.58	2.6215	3.3	2.2169	31.6	29.2	33.4	33.20925
Min	1.03019	1.6585	1.5	1.4631	8.3	27.1	19.5	22.61055
Median	1.43261	1.9298	2.0	1.6682	19.3	28.3	30.0	24.93977
Mean	1.55555	1.9884	2.0	1.6774	19.1	28.2	28.7	25.24964
StdDev	0.40055	0.1831	0.4	0.1372	4.5	0.6	3.8	1.919932

	n35TA				n35DIC			
	Jan-93	**Mar-93**	**Aug-93**	**Jan-94**	**Jan-93**	**Mar-93**	**Aug-93**	**Jan-94**
Max	2428.34	2422.5	2537.93	2498.2	2283.7	2289.731	2259.788	2272.774
Min	2262.16	2352.7	2363.29	2202.6	1993.3	2219.628	2134.171	2071.545
Median	2392.31	2360.9	2426.15	2393.7	2232.6	2228.274	2222.722	2208.016
Mean	2390.1	2365.4	2429.08	2394.7	2226.6	2232.411	2219.067	2210.19
StdDev	21.1461	12.298	48.5152	38.509	39.679	12.75305	24.18726	28.33482

RACER 3

	Station	Sal	T	n35P	n35N	DIC	n35DIC	TA	n35TA
Date				**µmol/kg**	**µmol/kg**	**µmol/kg**	**µmol/kg**	**µmol/kg**	**µmol/kg**
15-Dec-1991	1	33.941	0.26	1.7	25.3	2179.1	2247.0	2318.0	2390.3
	2	33.890	0.52	1.5	22.0				
	3	33.848	0.08	1.6	22.0	2150.6	2223.7	2304.7	2383.1
	4	33.613	-0.13	1.6	21.7	2127.4	2215.2	2286.3	2380.6
	5	33.545	0.40	1.4	19.2	2107.5	2198.9	2290.4	2389.7
	6	33.373	0.69	1.3	17.8	2110.2	2213.1	2328.1	2441.6
	7	33.645	0.68	1.3	18.0	2110.4	2195.4	2297.5	2390.1
	8	33.921	0.08	1.7	25.6	2171.5	2240.5	2311.7	2385.2
	9	33.948	-0.07	1.7	24.6	2172.8	2240.2	2302.2	2373.6
	24	34.004	0.15	1.7	25.3	2170.5	2234.1		
	25	34.050	0.00	1.8	26.0	2175.5	2236.2	2305.3	2369.6
	26	33.998	-0.03	1.7	25.4			2326.8	2395.3
	28	34.010	0.20	1.8	25.4	2167.8	2230.9	2308.6	2375.8
	29	34.058	0.20	1.8	25.5	2164.7	2224.5	2307.4	2371.2
	30	34.025	0.04	1.8	25.5	2182.3	2244.9	2312.3	2378.6
	31	34.078	0.17	1.7	25.3	2174.1	2232.9	2313.4	2376.0
	32	34.071	0.06	1.8	26.1	2185.3	2244.8	2310.1	2373.0
	34	33.690	0.77	1.6	23.0	2152.6	2236.3	2302.0	2391.5
	35	33.414	0.82	1.3	17.8	2093.6	2193.0	2275.4	2383.4
	37	33.915	-0.06	1.8	26.4			2304.0	2377.7
						2174.4			
	39	33.488	1.39			2132.6	2228.9		
	40	33.675	0.25						
	41	33.963	-0.02	1.4	22.0	2150.2	2215.9	2259.2	2328.2

	42	33.656	0.11	1.7	24.4	2159.9	2246.2	
	43	33.980	-0.16	1.7	24.4	2167.9	2233.0	2313.7	2383.2
	44	33.850	0.15	1.6	23.6	2156.8	2230.0	2307.8	2386.1
	45	33.818	0.72	1.6	22.1	2150.2	2225.3	2306.3	2386.9
	46	33.978	0.04	1.7	24.8	2174.3	2239.8	2311.5	2381.0
	47	33.939	-0.06	1.7	25.1	2157.1	2224.5	2287.1	2358.6
	48	33.976	-0.15	1.8	25.6	2172.0	2237.4	2299.2	2368.5
	49	33.994	-0.26						
	50	34.024	-0.30	1.8	27.0	2182.3	2244.9	2313.7	2380.0
	51	34.037	-0.25						
	52	34.048	-0.16	1.8	26.5	2182.9	2243.9	2308.3	2372.9
	53	34.042	-0.06						
	54	34.004	0.20						
	55	34.083	-0.10	1.8	26.5	2178.7	2237.3	2306.2	2368.3
	56	34.051	0.04	1.8	26.2				
	57	33.988	-0.20	1.8	25.9	2168.2	2232.7	2305.6	2374.2
	58	34.068	0.08	1.7	24.8	2169.6	2229.0	2310.5	2373.8
	59	34.064	0.10	1.8	25.5	2182.4	2242.3	2313.0	2376.5
	60	33.985	-0.14	1.7	23.9	2176.9	2241.9	2307.9	2376.9
21-Dec-1991	1	33.613	0.82	1.4	18.1	2104.6	2191.5	2281.0	2375.1
	2	33.775	0.92	1.7	22.4	2136.2	2213.7	2290.1	2373.1
	3	33.588	0.95	1.4	18.0	2100.2	2188.5	2286.5	2382.6
	4	33.827	0.02	1.9	24.1	2156.9	2231.7	2295.0	2374.6
	5	33.294	0.65	1.6	20.4	2102.4	2210.1	2271.9	2388.3
	6	33.572	1.02	1.4	17.6	2090.8	2179.8	2262.0	2358.3
	7	33.669	0.82	1.3	16.5	2093.9	2176.7	2295.5	2386.3
	24	34.130	-0.04	2.0	28.4	2187.7	2243.5	2350.2	2410.1
	25	34.024	0.50	1.8	25.3	2156.9	2218.7		
	26	34.036	0.74	1.8	24.0	2157.6	2218.7	2325.7	2391.6
	28	34.212	-0.03	2.1	29.1	2200.0	2250.6	2352.5	2406.6
	29	33.928	0.89	1.6	22.5	2139.6	2207.2	2329.3	2402.9
	30	33.866	0.98	1.6	21.1	2130.0	2201.3	2325.2	2403.1
	33	33.784	1.41	1.5	17.6			2307.3	2390.4
	34	33.594	1.07	1.3	16.4	2089.5	2177.0	2280.3	2375.7
	35	33.363	1.19	1.5	18.3	2092.1	2194.7	2268.6	2379.9
	37	33.965	-0.14	1.7	24.7	2163.0	2228.9	2306.2	2376.5
	38	33.548	0.46	1.7	22.8	2133.2	2225.5	2293.9	2393.2
	39	33.743	0.98	1.6	20.2	2126.5	2205.7	2295.2	2380.6
	40	33.864	0.68						
	41	33.919	-0.06	1.2	18.4	2122.0	2189.7	2300.7	2374.0
	42	33.816	0.11	1.5	22.4	2141.1	2216.1	2296.3	2376.7
	43	33.850	0.22	1.7	21.9	2144.4	2217.2	2307.9	2386.3
	45	33.640	1.03	1.4	18.8	2107.3	2192.5	2293.5	2386.3
	46	33.754	1.18	1.6	21.1	2132.7	2211.5		
	47	33.546	1.40	1.5	20.2	2116.4	2208.1	2290.8	2390.1
	48	33.694	1.34	1.7	22.6	2142.5	2225.5	2301.1	2390.3

	49	33.830	1.24			2158.0	2232.6		
	50	33.969	0.69	1.8	24.1			2329.8	2400.5
	51	33.957	0.51						
	52	33.988	0.58	1.8	23.7	2153.5	2217.6	2347.8	2417.7
	53	33.935	0.72						
	54	34.047	0.68						
	55	34.164	-0.04	2.0	28.0	2190.2	2243.8	2342.0	2399.4
	56	34.161	0.05	2.0	28.4	2197.2	2251.2	2334.9	2392.2
	57	34.176	-0.06			2193.3	2246.1	2358.9	2415.7
	58	33.920	0.91	1.6	21.9	2144.8	2213.1	2336.8	2411.2
26-Dec-1991	1	33.871	0.94	1.7	22.5	2140.3	2211.6	2334.7	2412.5
	2	33.859	0.71	1.7	21.1	2140.3	2212.4	2307.2	2384.9
	3	33.677	1.28	1.5	19.8	2112.5	2195.4	2316.9	2407.9
	4	33.062	1.23	1.7	23.7	2116.6	2240.7	2269.1	2402.1
	5	33.649	1.20	1.5	20.1	2131.2	2216.7	2300.6	2392.9
	6	33.312	1.67	1.3	15.8	2087.7	2193.5	2287.8	2403.8
	7	33.786	0.61	1.4	18.2	2107.4	2183.1	2314.7	2397.9
	8	34.010	0.07	2.0	28.5	2178.3	2241.7	2308.9	2376.1
	9	33.944	1.04	1.9	26.5	2171.4	2238.9	2338.5	2411.2
	24	33.980	0.91	1.7	22.5	2150.7	2215.3	2313.3	2382.8
	25	33.946	1.12	1.7	22.8	2162.0	2229.1	2322.8	2394.9
	26	33.987	0.69	1.8	24.9	2154.0	2218.2	2324.9	2394.2
	28	33.978	1.06	1.6	21.6	2144.0	2208.5		
	29	33.860	1.17	1.5	20.1	2130.1	2201.7	2307.3	2384.9
	30	33.756	1.39	1.4	19.1	2111.3	2189.1	2332.2	2418.1
	31	33.860	1.19	1.7	23.4	2150.4	2222.8	2303.7	2381.3
	32	33.771	1.42	1.4	18.8	2113.4	2190.3	2303.1	2386.9
	33	33.752	1.74	1.3	16.0	2108.0	2185.9		
	34	33.630	1.44	1.5	19.0	2114.6	2200.8	2295.5	2389.1
	35	33.427	1.20	1.5	18.9	2100.4	2199.2	2282.6	2390.0
	37	34.003	0.38	1.6	23.9	2150.5	2213.6	2315.0	2382.9
	38	33.835	1.02	1.5	18.4	2119.7	2192.8	2312.4	2392.1
	39	33.539	1.72	1.4	17.4	2103.6	2195.3	2300.4	2400.6
	40	33.979	0.60	1.0	14.3				
	41	33.940	0.55	1.1	18.0	2115.7	2181.8	2315.6	2387.9
	42	33.675	1.28	1.2	16.7	2094.9	2177.3	2301.2	2391.7
	43	33.976	0.87	1.6	22.7	2144.1	2208.7	2314.0	2383.7
	44	33.838	1.08	1.4	21.0	2131.9	2205.2	2315.6	2395.1
	45	33.522	1.16	1.4	18.0	2097.9	2190.5	2307.7	2409.4
	46	33.765	1.81	1.4	17.9	2113.3	2190.6	2326.2	2411.3
	47	33.868	1.74	1.5	18.5				
	48	33.938	1.16	1.6	21.7	2140.5	2207.5	2319.8	2392.4
	49	33.974	1.51						
	50	33.920	1.57	1.6	20.7	2134.0	2202.0	2329.4	2403.6
	51	33.886	1.36						
	52	33.941	0.89	1.7	23.2	2148.5	2215.5	2340.0	2413.0

	53	33.941	1.04						
	54	33.945	1.01						
	55	33.975	0.95	1.6	21.2	2144.2	2208.9	2311.0	2380.7
	56	33.986	0.97	1.6	22.5	2149.1	2213.2	2316.4	2385.5
	57	33.984	0.77	1.7	23.6	2157.8	2222.3	2318.4	2387.7
	58	33.652	1.74	1.3	16.4	2097.1	2181.1	2293.7	2385.6
	59	33.744	1.54	1.5	19.7	2118.3	2197.1	2301.8	2387.5
	60	33.757	1.35	1.4	19.1	2111.1	2188.8	2294.5	2379.0
Jul-92	1	34.131	-1.51	2.3	32.4	2216.1	2272.5	2309.9	2368.6
	2	34.123	-1.59	2.3	31.5	2222.0	2279.2	2313.2	2372.7
	3	34.148	-1.24	2.3	32.3	2224.0	2279.5	2321.5	2379.4
	4	34.094	-1.16	2.3	33.3	2229.0	2288.2	2318.4	2380.0
	5	34.083	-1.38	2.3	32.8	2221.7	2281.5	2318.5	2380.8
	6	34.108	-1.43	2.3	33.1	2221.9	2280.0	2315.8	2376.3
	7	34.073	-1.47	2.3	33.2	2223.6	2284.1	2312.1	2375.0
	8	34.103	-1.32	2.2	33.2	2216.3	2274.6	2314.3	2375.2
	9	34.147	-1.63	2.3	31.3	2224.0	2279.6	2323.3	2381.4
	24	34.147	-1.70	2.2	32.0	2214.2	2269.5	2320.6	2378.5
	25	34.120	-1.77	2.3	29.0	2214.9	2272.0	2320.2	2380.0
	26	34.120	-1.75	2.3	28.9	2219.2	2276.4		
						2236.0		2356.9	
	29	34.130	-1.75	2.2	32.0	2216.2	2272.7	2324.9	2384.1
	30	34.129	-1.74	2.3	30.0	2218.9	2275.6		
	31	34.129	-1.74		32.0	2223.3	2280.1	2336.5	2396.2
	32	34.140	-1.65	2.2	32.6	2225.0	2281.1	2330.4	2389.1
	33	34.079	-1.59	2.3	32.9	2219.1	2279.0	2313.1	2375.6
	34	34.088	-1.40	2.3	32.8	2221.9	2281.3	2317.4	2379.4
	35	34.022	-1.64	2.3	32.8	2217.3	2281.0	2305.6	2371.8
	37	34.079	-1.46	2.3	30.3			2346.3	2409.8
	38	34.109	-1.58	2.3	30.8	2219.7	2277.7	2311.4	2371.7
	39	34.095	-1.57	2.3	32.6	2220.7	2279.7	2312.6	2374.0
	40	34.084	-1.31	2.3	32.7	2220.7	2280.4	2309.7	2371.7
	41	34.041	-1.39	2.3	32.0	2209.8	2272.1	2309.0	2374.1
	42	34.110	-1.28			2217.4	2275.2	2311.1	2371.4
	43	34.114	-1.34	2.4	30.4	2216.7	2274.2	2314.7	2374.8
	44	34.110	-1.31	2.4	32.5	2219.9	2277.8	2317.7	2378.1
	45	34.121	-1.53	2.3	32.3	2221.5	2278.7	2318.0	2377.7
	46	34.142	-1.58	2.2	30.0	2220.6	2276.4	2320.9	2379.2
	47	34.132	-1.70	2.2	32.0	2218.2	2274.6	2317.7	2376.6
	48	34.130	-1.68	2.3	31.5	2221.9	2278.5	2367.3	2427.6
						2218.9		2360.7	#DIV/0!
	50	34.100	-1.77	2.2	31.9	2217.8	2276.3	2320.7	2382.0
	51	34.097	-1.78	2.2	31.5	2220.7	2279.6	2317.0	2378.4
	53	34.121	-1.76	2.2	32.2	2218.1	2275.2		
	54	34.139	-1.73	2.3	28.6	2217.2	2273.2	2316.2	2374.6
	55	34.137	-1.70	2.3	31.6	2217.2	2273.2	2324.9	2383.7

56	34.166	-1.46	2.2	31.8				
57	34.268	-1.28	2.2	28.3	2230.9	2278.6	2348.5	2398.7
58	34.132	-1.75	2.2	32.5	2217.8	2274.2	2321.4	2380.4
59	34.152	-1.72	2.5	32.3	2217.7	2272.8	2323.5	2381.2
60	34.131	-1.72	2.3	29.3	2219.8	2276.3	2322.6	2381.7

Pal-LTER Data

Year	Station	Depth meters	Salinity	Temperature °C	DIC µmol/kg	TA µeq/kg	n35DIC µmol/kg	n35TA µmol/kg
93	2.000	-1	33.362	1.18	2142.4	2293.7	2247.6	2406.4
93	2.000	-1	33.369	0.96	2137.3	2285.6	2241.8	2397.3
93	3.000	-2	33.531	1.04	2139.1	2286.6	2232.8	2386.7
93	4.000	-2	33.601	0.90	2141.0		2230.1	
93	5.000	-1.5	33.434	1.59	2140.7	2284.6	2241.0	2391.6
93	6.000	-1.4	33.438	1.36	2143.9	2278.2	2244.0	2384.6
93	7.000	-1	33.478	1.27	2139.6	2284.0	2236.9	2387.8
93	8.000	-1.4	33.552	0.83	2146.3	2291.0	2238.9	2389.8
93	9.000	-1	33.605	0.71	2056.1	2312.5	2141.5	2408.5
93	10.000	-1	33.572	1.16	2137.8	2294.4	2228.7	2392.0
93	600.040	-1	33.436	0.28	2157.3	2292.9	2258.2	2400.1
93	600.040	-1	33.359	0.41	2138.2	2287.0	2243.4	2399.5
93	600.060	-1	33.539	1.20	2145.1	2306.1	2238.5	2406.5
93	600.080	-1	33.704	1.19	2159.2	2305.1	2242.2	2393.7
93	600.100	-1	33.428	1.11	2124.7	2287.4	2224.6	2395.0
93	600.120	-1	33.710	1.00	2153.4		2235.8	
93	600.140	-1	33.811	1.28	2148.4	2318.1	2224.0	2399.6
93	600.160	-1	33.843	1.35	2148.5	2313.3	2222.0	2392.4
93	600.180	-1	33.816	1.79	2156.6	2305.8	2232.1	2386.5
93	600.200	-1	33.838	1.73	2151.0	2323.3	2224.9	2403.0
93	600.180	-2	33.852	1.40	2158.5	2304.9	2231.7	2383.1
93	600.180	-2	33.852	1.33	2156.6	2311.1	2229.7	2389.5
93	600.180	-2	33.857	1.35	2157.1	2317.5	2229.9	2395.8
93	600.180	-2	33.855	1.33	2155.7	2304.1	2228.6	2382.0
93	600.180	-1	33.946	1.29	2155.3	2319.7	2222.2	2391.7
93	600.180	-1	33.852	1.24	2155.7	2314.1	2228.8	2392.6
93	500.180	-2	33.679	0.93	2162.9	2310.5	2247.7	2401.1
93	500.160	-2	33.853	0.73	2159.9	2309.7	2233.1	2387.9
93	500.140	-1	33.863	0.72	2162.2	2309.5	2234.8	2387.0
93	500.120	-1	33.835	0.77	2154.2	2318.3	2228.4	2398.1
93	500.100	-1	33.805	0.87	2150.2	2311.6	2226.2	2393.3
93	500.080	-1	33.799	0.79	2158.3	2310.0	2235.0	2392.1
93	500.060	-1	33.671	0.75	2160.5	2315.4	2245.8	2406.8
93	500.060	-1		1.00	2155.1	2295.0		
93	600.040	-1	33.562	0.87	2145.1	2282.5	2237.0	2380.3
93	600.040	-1	33.574	0.92	2152.4	2297.6	2243.8	2395.1
93	600.040	-2	33.576	1.20	2140.7	2289.3	2231.5	2386.3
93	10.000	-1	33.484	1.23	2146.4		2243.6	
93	9.000	-1	33.550	0.92	2153.7	2299.9	2246.8	2399.3

93	5.000	-1	33.694	0.98	2198.0	2337.1	2283.2	2427.7
93	2.000	-1	33.206	1.00	2133.0	2268.2	2248.2	2390.8
93	5.000	-1	33.414	1.43	2141.0	2278.9	2242.6	2387.1
93	600.040	-1	33.565	1.31	2128.6	2273.2	2219.6	2370.4
93	500.080	-1	33.789	1.05	2152.9	2299.1	2230.1	2381.5
93	500.080	-1		1.00	2154.8	2318.5		
93	500.080	-1		1.00	2152.2	2335.8		
93	400.040	-1	33.072	1.00	2109.0	2277.6	2231.9	2410.4
93	400.060	-5	33.604	1.36	2138.6	2302.6	2227.4	2398.3
93	400.080	-1	33.617	1.24	2148.9	2306.0	2237.3	2400.8
93	400.100	-3	33.748	1.02	2147.5	2301.8	2227.2	2387.2
93	400.120	-2	33.778	1.00	2146.4	2302.0	2224.1	2385.2
93	400.140	-1	33.772	1.11	2141.5	2306.8	2219.4	2390.7
93	400.180	-1	33.854	1.36	2141.3	2307.6	2213.8	2385.7
93	400.160	-1	33.816	1.68	2139.3	2303.5	2214.2	2384.1
93	400.180	-1		1.00	2144.4	2303.9		
93	400.200	-1	33.819	1.63	2138.0	2299.0	2212.7	2379.3
93	300.200	-1.7	33.857	1.30	2155.5	2304.2	2228.3	2382.0
93	300.200	-1.7		1.00	2166.8	2314.7		
93	300.180	-1	33.827	1.56	2159.9	2302.1	2234.8	2381.9
93	300.160	-1	33.834	1.74	2163.3		2237.9	
93	-9.000	-1		1.00	2162.8	2315.2		
93	300.140	-1	33.841	1.90	2170.5	2301.0	2244.8	2379.8
93	300.120	-1	33.685	1.28	2162.6	2304.4	2247.0	2394.4
93	300.120	-1		1.00	2147.7	2301.8		
93	300.100	-1	33.850	1.69	2154.6	2301.0	2227.8	2379.2
93	300.080	-1	33.288	1.20	2121.2	2273.2	2230.3	2390.1
93	300.060	-1	33.668	1.38	2140.3	2295.5	2225.0	2386.3
93	300.040	-1	33.230	1.62	2121.1	2267.3	2234.1	2388.1
93	200.200	-1	33.788	1.69	2142.1	2297.8	2218.9	2380.2
93	200.200	-1		1.00	2135.3	2299.4		
93	200.160	-1	33.830	1.79	2143.0	2298.7	2217.1	2378.2
93	200.120	-1	33.634	1.07	2135.5	2293.3	2222.2	2386.4
93	200.080	-1	33.539	1.36	2135.3	2296.4	2228.3	2396.5
93	200.040	-1	33.103	0.73	2115.1	2255.8	2236.3	2385.1
93	200.000	-1	32.008	-0.38	2044.0	2178.3	2235.1	2381.9
93	-1.000	-1		1.00	1948.8	2211.6		
93	-1.000	-1		1.00	2009.9	2278.7		
94	500.060	-1	33.566	0.66				
94	500.080	-1	33.591	1.16	2114.6	2319.7	2203.3	2417.0
94	500.100	-1	33.630	0.63	2114.4	2302.2	2200.5	2396.0
94	500.120	-1	33.683	0.61	2130.7	2310.2	2214.0	2400.5
94	500.120	-676		1.00	2245.9	2361.5		
94	500.120	-600		1.00	2242.3	2383.2		
94	500.120	-495		1.00	2233.4	2399.2		
94	500.120	-398		1.00	2235.5	2393.5		
94	500.120	-301		1.00	2239.5	2390.4		
94	500.120	-201	34.523	0.86		2371.2		2404.0
94	500.120	-151	34.399	0.34	2219.2	2381.4	2258.0	2423.0
94	500.120	-102		1.00	2180.9	2367.2		

94	500.120	-72	33.977	-0.96	2176.5	2347.4	2242.0	2418.1
94	500.120	-30	33.791	0.51	2129.1	2331.2	2205.3	2414.6
94	500.120	-10		1.00	2125.1	2329.6		
94	500.140	-1	33.785	0.63	2134.3	2315.1	2211.1	2398.4
94	500.160	-1	33.690	0.67	2128.1		2210.8	
94	500.180	-1	33.756	0.82	2130.9	2309.5	2209.4	2394.6
94	500.200	-1		1.00	2125.3	2310.0		
94	600.200	-1	33.786	0.81	2123.0	2306.0	2199.3	2388.9
94	600.180	-1	33.818	0.95	2125.5	2346.4	2199.8	2428.4
94	600.160	-1	33.822	0.85	2137.4	2304.0	2211.8	2384.2
94	600.140	-1	33.525	1.03	2111.3	2349.4	2204.2	2452.8
94	600.120	-1	33.656	1.18	2121.7	2293.1	2206.4	2384.7
94	600.100	-1	33.613	1.18	2114.5	2298.1	2201.8	2392.9
94	600.080	-1	33.665	1.29	2121.9	2333.7	2206.0	2426.2
94	600.040	-1	33.389	0.30	2132.4	2265.4	2235.3	2374.7
94	600.060	-1	33.643	1.24	2122.8	2319.5	2208.4	2413.1
94	4.000	-1	33.383	0.98	2097.6	2299.2	2199.2	2410.6
94	10.000	-1	33.323	1.18	2103.2	2271.6	2209.0	2385.9
94	620.015	-1		1.00	2131.5	2298.9		
94	602.017	-1	33.007	-0.39	2101.2	2256.5	2228.1	2392.8
94	585.010	-1	32.427	-0.49	2057.2	2198.3	2220.4	2372.7
94	595.013	-1		1.00	2050.2	2265.5		
94	575.010	-1	32.363	-0.45	2095.9		2266.7	
94	550.005	-1	31.293	-0.85	1959.2	2146.2	2191.3	2400.4
94	510.000	-1	31.006	0.33	2074.8	2206.1	2342.1	2490.3
94	440.015	-1	31.935	-1.12	2032.5	2206.3	2227.6	2418.1
94	382.010	-1		1.00	2000.3	2224.1		
94	375.020	-1	32.355	-1.21	2056.0	2201.1	2224.1	2381.0
94	400.040	-1	33.305	0.62	2104.2	2277.9	2211.3	2393.8
94	400.060	-1	33.439	0.82	2119.7	2261.5	2218.7	2367.1
94	400.080	-1	33.656	1.08	2122.9	2292.9	2207.7	2384.5
94	400.100	-1	33.647	1.03	2119.4	2309.7	2204.6	2402.6
94	400.120	-1	33.669	0.88	2127.7	2290.5	2211.8	2381.0
94	400.140	-1	33.663	0.86	2138.8	2275.9	2223.7	2366.3
94	400.160	-1	33.769	0.72	2123.9	2296.6	2201.3	2380.3
94	400.180	-1	33.799	0.87	2135.6	2315.1	2211.5	2397.4
94	400.200	-1	33.830	0.38	2158.9	2289.6	2233.6	2368.8
94	300.200	-1	33.782	0.96	2124.9	2288.9	2201.5	2371.4
94	300.180	-1	33.803	0.89	2123.7	2302.1	2198.9	2383.6
94	300.160	-1		1.00	2113.9	2302.6		
94	300.140	-1		1.00	2117.7	2318.5		
94	300.120	-1	33.636	1.05	2120.3	2299.0	2206.3	2392.2
94	300.100	-1	33.638	0.99	2121.2	2302.9	2207.1	2396.1
94	300.080	-1	33.604	0.78	2125.5	2297.7	2213.8	2393.2
94	300.060	-1	32.945	-0.25	2139.2	2235.1	2272.6	2374.5
94	300.040	-1	33.354	0.45	2101.0	2271.1	2204.7	2383.2
95	600.080	9		1.00	2099.3	2252.4		
95	2.000	-1	32.906	1.09	2099.8	2239.1	2233.4	2381.6
95	5.000	-2	33.007	0.73	2105.9	2234.7	2233.1	2369.7
95	500.060	-1	33.355	0.08	2117.8	2267.4	2222.2	2379.2

95	500.080	-1	33.341	0.15	2111.8	2276.6	2216.9	2389.9
95	500.100	-2	33.527	0.22	2115.4	2285.1	2208.3	2385.5
95	500.120	-5	33.573	0.24	2121.9	2288.3	2212.1	2385.6
95	500.140	-2	33.588	0.39	2113.5	2281.4	2202.3	2377.3
95	500.140	-2	33.565	0.42	2112.2	2283.0	2202.5	2380.7
95	500.160	-3	33.605	0.21	2246.1	2354.6	2339.3	2452.3
95	500.180	-2	33.607	0.16	2125.1	2292.4	2213.2	2387.4
95	500.200	-2	33.602	0.69	2122.7	2303.4	2211.0	2399.2
95	600.200	-2	33.625	0.69	2123.8	2288.6	2210.6	2382.2
95	600.180	-3	33.641	0.95	2122.8	2270.6	2208.6	2362.4
95	600.160	-1	33.613	0.35	2127.9	2279.1	2215.7	2373.2
95	600.140	-2	33.641	0.49	2123.6	2293.5	2209.4	2386.1
95	600.040	-1	33.128	0.41	2093.2	2265.3	2211.5	2393.3
95	600.080	-1	33.233	0.61	2097.7	2254.2	2209.2	2374.1
95	600.080	-1	33.233	0.61	2098.1	2264.4	2209.7	2384.8
95	600.100	-2	33.541	0.78	2119.8	2277.8	2212.0	2376.9
95	600.120	-7		1.00	2134.0	2302.7		
95	2.000	-1	32.885	1.11	2075.9	2227.8	2209.4	2371.1
95	5.000	-1	33.007	0.73	2089.0	2283.7	2215.1	2421.6
95	500.140	-2	33.565	0.42	2124.2	2279.9	2215.0	2377.4
95	620.040	-1	33.261	1.29	2092.0	2259.0	2201.4	2377.1
95	615.038	-1		1.00	2104.8	2254.5		
95	610.035	-1	33.191	1.20	2095.6	2255.4	2209.8	2378.4
95	605.033	-1		1.00	2119.7	2250.3		
95	600.030	-1	33.168	0.51	2133.0	2256.9	2250.8	2381.5
95	600.040	-1	33.128	0.41	2113.5	2248.0	2232.9	2375.0
95	595.038	-1		1.00	2105.3	2251.2		
95	590.035	-1	32.958	0.28	2097.9	2238.4	2227.9	2377.1
95	585.030	-1		1.00	2087.0	2229.8		
95	600.080	-1	33.174	1.48	2104.3	2253.7	2220.1	2377.8
95	600.060	-2	33.300	1.21	2096.9	2264.8	2203.9	2380.4
95	600.040	-1	33.038	0.69	2103.1	2240.8	2228.0	2373.9
95	620.015	-1	34.450	0.19	2140.5	2260.8	2174.7	2296.9
95	-1.000	-1		1.00	2065.8	2236.7		
95	595.014	-1	32.884	0.13	2147.1	2228.2	2285.3	2371.6
95	585.010	-1	32.001	0.61	2048.3	2198.6	2240.3	2404.7
95	575.010	-1	32.295	1.10	2058.4	2204.5	2230.8	2389.1
95	550.005	-1	30.718	-0.30	1975.4	2106.1	2250.8	2399.7
95	550.005	-1	30.718	-0.30	1978.7	2111.3	2254.5	2405.7
95	550.005	-1		1.00	1979.0	2112.6		
95	530.005	-1	32.815	1.09	2091.8	2227.9	2231.1	2376.3
95	510.000	-1	31.919	-0.46	2067.2	2182.9	2266.7	2393.6
95	5.000	-1	33.103	0.77	2052.6	2234.0	2170.2	2362.0
95	2.000	-1	32.885	1.11	2056.3	2240.4	2188.6	2384.4
95	2.000	-1	32.885	1.11	2078.3	2268.1	2212.0	2413.9
95	5.000	-1	33.103	0.77	2090.8	2272.7	2210.6	2403.0
95	600.060	-1	33.286	1.29	2109.9		2218.5	
95	630.030	-1	33.091	1.15	2072.8	2275.1	2192.4	2406.4
95	610.035	-1	33.191	1.20	2118.1	2266.2	2233.5	2389.8
95	600.040	-1	33.038	0.69	2116.4	2263.6	2242.1	2398.0

95	605.040	-1	33.180	0.83	2118.2	2260.2	2234.4	2384.2
95	600.050	-9	33.200	0.83	2118.9	2260.3	2233.8	2382.9
95	605.060	-1	33.286	1.17	2102.6	2272.4	2210.9	2389.5
95	2.000	-1	33.163	0.84	2049.9	2238.4	2163.5	2362.3
95	5.000	-1	32.775	1.47	2082.4	2271.9	2223.8	2426.1
95	400.200	-3		1.00	2133.1	2283.3		
95	400.160	-2		1.00	2139.6	2286.3		
95	400.140	-2	33.523	0.56	2136.0	2286.9	2230.1	2387.6
95	400.120	-2	33.562	0.59	2138.9		2230.6	
95	400.100	-1	33.485	0.43	2136.8	2277.5	2233.4	2380.6
95	400.080	-2	33.517	0.43	2140.6	2282.7	2235.3	2383.7
95	400.060	-2	33.482	0.35	2137.1	2278.0	2234.0	2381.3
95	400.060	-2	33.478	0.35	2138.6	2276.5	2235.9	2380.0
95	400.060	-2		1.00	2138.1	2279.0		
95	400.040	-2	33.143	0.09	2103.5	2263.4	2221.4	2390.2
95	300.040	-2	33.507	0.11	2136.5	2277.9	2231.7	2379.4
95	300.060	-1	33.596	0.15	2158.3	2295.7	2248.5	2391.6
95	300.080	-1	33.613	0.35		2286.6		2380.9
95	300.100	-9	33.645	0.63		2299.2		2391.8
95	300.120	-2	33.639	0.66	2132.5	2296.6	2218.8	2389.5
95	300.140	-1	33.605	0.71	2131.1	2294.0	2219.6	2389.3
95	300.160	-1	33.617	0.77	2134.1	2303.1	2221.9	2397.9
95	300.180	-1	33.644	0.82	2140.6	2296.8	2226.9	2389.4
95	300.200	-2	33.530	1.30	2124.6	2285.4	2217.7	2385.6
95	200.200	-1	33.523	0.84	2125.1	2287.2	2218.7	2388.0
95	200.180	-2	33.531	0.67	2132.3	2289.0	2225.7	2389.2
95	200.160	-3	33.560	0.63	2135.2	2283.8	2226.8	2381.8
95	200.140	-2		1.00	2135.4	2281.5		
95	200.120	-2	33.547	0.14	2135.0	2285.1	2227.5	2384.1
95	200.100	-2	33.469	0.10	2129.4	2290.0	2226.8	2394.8
95	200.080	-2	33.545	0.11	2135.0	2285.6	2227.6	2384.8
95	200.060	-1	33.505	0.03	2131.9	2288.9	2227.0	2391.0
95	200.040	-500	34.690	1.35	2258.4	2369.1	2278.6	2390.3
95	200.040	-200	34.475	0.60	2250.0	2341.6	2284.3	2377.2
95	200.040	-105	33.934	-1.15	2201.2	2308.7	2270.3	2381.3
95	200.040	-80	33.714	-1.01	2171.5	2307.3	2254.3	2395.3
95	200.040	-55	33.422	-0.39	2136.1	2283.5	2237.0	2391.3
95	200.040	-27	33.389	-0.15	2119.4	2285.2	2221.7	2395.5
95	200.040	-21	33.388	-0.14	2121.1	2280.9	2223.5	2391.1
95	200.040	-15	33.388	-0.14	2124.1	2293.2	2226.7	2403.9
95	200.040	-9	33.388	-0.14	2114.1	2288.0	2216.2	2398.5
95	200.040	-4	33.388	-0.13	2117.1	2280.5	2219.3	2390.6
95	200.040	-2	33.388	-0.13	2113.0		2215.0	
95	200.040	-1	33.388	-0.12	2121.2	2279.9	2223.6	2390.0
95	200.000	9		1.00		2275.6		
95	360.010	-1	32.419	-0.91	2057.9	2215.5	2221.7	2391.9
95	360.010	-1	32.392	-0.91	2056.3	2205.6	2221.9	2383.2
95	360.010	-1	32.392	-0.91	2055.0	2205.4	2220.5	2383.0
95	380.010	-1	32.586	-0.44	2095.8	2221.7	2251.1	2386.3
95	400.015	-1	32.427	-0.17	2028.4	2232.2	2189.3	2409.4

95	420.015	-500	34.654	1.29	2258.8	2349.3	2281.4	2372.8
95	420.015	-250	34.594	1.09	2256.0	2344.5	2282.5	2372.1
95	420.015	-125	34.290	0.07	2233.9	2321.2	2280.2	2369.3
95	420.015	-70	33.903	-0.82	2197.0	2297.7	2268.1	2372.0
95	420.015	-50	33.550	-0.52	2165.8	2284.8	2259.4	2383.5
95	420.015	-25	33.254	-0.04	2112.7	2264.7	2223.6	2383.6
95	420.015	-20	33.203	-0.05	2111.1	2272.1	2225.4	2395.0
95	420.015	-15	33.159	-0.09	2096.3	2253.6	2212.7	2378.8
95	420.015	-9	32.910	-0.25	2074.0	2237.6	2205.7	2379.7
95	420.015	-4	32.549	-0.43	2053.7	2215.2	2208.3	2382.1
95	420.015	-1	32.386	-0.47	2049.2		2214.6	
95	440.015	-1	32.797	0.37	2057.1	2230.4	2195.3	2380.2
95	600.060	-185		1.00	2250.4	2342.7		
95	600.060	-125	34.372	0.39	2240.0	2341.7	2280.9	2384.5
95	600.060	-100	34.246	0.20	2199.9	2311.4	2248.3	2362.3
95	600.060	-80	34.245	0.47	2160.7	2287.4	2208.3	2337.9
95	600.060	-60	33.950	-0.08	2225.8	2338.1	2294.6	2410.4
95	600.060	-40	33.471	0.97	2221.0	2332.7	2322.5	2439.3
95	600.060	-30	33.507	0.85	2137.6	2276.2	2232.8	2377.6
95	600.060	-20	33.431	1.09	2120.1	2270.4	2219.6	2377.0
95	600.060	-15	33.413	1.08	2113.9	2268.7	2214.3	2376.5
95	600.060	-11	33.354	1.09	2115.7	2264.7	2220.1	2376.5
95	600.060	-5	33.331	1.22	2117.2	2268.9	2223.2	2382.5
95	600.060	-2	33.319	1.22	2112.4	2266.8	2219.0	2381.2
95	600.040	9		1.00	2115.4	2261.6		
95	5.000	-1	32.828	1.41	2055.9	2234.3	2191.9	2382.2
95	5.000	-1	33.244	1.19	2058.3	2235.7	2167.0	2353.8
95	5.000	-1	33.244	1.19	2056.3	2233.0	2164.9	2351.0
95	2.000	-5	32.950	1.05	2056.6	2237.6	2184.6	2376.8
96	2.000	-1.2	32.342	0.63	2025.8		2192.3	
96	5.000	-1.5	33.179	0.82	2051.5	2260.4	2164.1	2384.5
96	500.060	-1.3	33.183	-0.51	2130.8	2263.1	2247.5	2387.0
96	500.080	-1.7	33.346	0.85	2120.6	2281.3	2225.8	2394.5
96	500.080	-1.7	33.346	0.85	2116.9	2261.9	2221.9	2374.1
96	500.080	-1.7			2115.1	2266.9		
96	500.100	-1.8	33.537	0.71	2127.3	2273.7	2220.1	2372.9
96	500.120	-2.2			2132.5	2285.3		
96	500.140	-2.7	33.719	1.34	2156.0	2308.1	2237.9	2395.8
96	500.160	-1.3	33.689	1.84	2134.7	2284.6	2217.8	2373.5
96	500.180	-385	34.696	1.40	2264.5	2364.8	2284.3	2385.5
96	500.180	-337	34.678	1.47	2262.5	2350.3	2283.5	2372.1
96	500.180	-1.8	33.777	1.41	2136.5	2288.1	2213.9	2370.9
96	500.200	-400			2255.1	2343.2		
96	500.200	-1.1	33.757	1.43	2132.3	2291.9	2210.8	2376.3
96	600.200	-301	34.625	1.72	2256.8	2350.9	2281.2	2376.4
96	600.200	-1.4	33.779	1.51	2137.5	2291.7	2214.8	2374.5
96	600.180	-299	34.661	1.63	2259.4	2339.4	2281.5	2362.3
96	600.180	-1.8	33.803	1.44	2142.5	2295.4	2218.4	2376.7
96	600.180	-1.8	33.803	1.44	2142.4	2297.9	2218.3	2379.3
96	600.180	-1.8			2141.5	2298.7		

96	600.160	-390		1.00	2264.7	2360.6		
96	600.140	-2.4	33.599	0.91	2122.7	2278.2	2211.2	2373.2
96	600.120	-1.4	33.389	1.06	2102.2	2271.2	2203.6	2380.8
96	600.100	-2		1.00	2050.5	2268.7		
96	600.080	-1.4	33.201	1.98	2027.4	2274.7	2137.3	2398.0
96	600.060	-1.1	33.095	1.48	2062.8	2268.3	2181.5	2398.9
96	600.040	-504.6	34.654	1.33	2257.0	2333.7	2279.5	2357.0
96	600.040	-342	34.597	1.12	2258.3	2342.6	2284.6	2369.9
96	600.040	-175	34.485	0.74	2247.6	2338.3	2281.2	2373.2
96	600.040	-100	34.310	0.29	2231.7	2325.3	2276.6	2372.1
96	600.040	-50	33.807	-0.79	2200.8	2311.5	2278.5	2393.1
96	600.040	-18	33.196	0.65	2042.7	2271.6	2153.7	2395.0
96	600.040	-13	33.196	0.66	2037.7	2265.3	2148.4	2388.4
96	600.040	-9	33.198	0.66	2044.2	2271.3	2155.2	2394.6
96	600.040	-4	33.194	0.66	2037.6	2266.7	2148.5	2390.0
96	600.040	-1.6	33.193	0.66	2040.1	2267.6	2151.2	2391.0
96	2.000	-1	32.342	0.63	2058.7	2261.7	2227.9	2447.6
96	5.000	-1	33.126	0.97	2061.5	2268.3	2178.1	2396.6
96	600.035	-1	33.119	0.26	2043.3	2237.6	2159.3	2364.7
96	605.035	-1	33.163	0.44	2045.8	2269.6	2159.1	2395.3
96	605.035	-1	33.162	0.44	2042.6	2274.6	2155.8	2400.7
96	605.035	-1	33.162	0.44	2043.9	2266.0	2157.2	2391.6
96	610.035	-2	33.165	0.31	2051.0	2270.2	2164.5	2395.8
96	615.035	-2	33.168	0.63	2043.3	2267.6	2156.2	2392.8
96	620.035	-2	33.264	0.93	2068.6	2271.9	2176.6	2390.5
96	620.035	-1.5	33.263	0.94	2050.3	2287.2	2157.4	2406.6
96	610.035	-1	33.162	0.31	2026.3		2138.6	
96	600.035	-1	33.108	0.25	2042.7	2258.4	2159.4	2387.5
96	5.000	-1	33.126	0.97	2021.6	2268.1	2136.0	2396.4
96	-1.000	-2		1.00	2054.4	2263.6		
96	-1.000	-1		1.00	2061.4	2264.6		
96	2.000	-1	33.023	0.72	2072.0	2250.7	2196.0	2385.4
96	5.000	-1	33.104	0.61	2067.8	2265.4	2186.2	2395.1
96	-1.000	-1			2075.8	2271.7		
96	595.014	-1			2002.2	2232.6		
96	585.010	-1	32.374	-0.91	2002.1	2223.7	2164.5	2404.1
96	575.010	-1	32.531	-1.17	2048.8	2217.4	2204.3	2385.7
96	550.005	-1			2083.3	2220.0		
96	-1.000	-1			2070.8			
96	-1.000	-1			2069.6	2213.3		
96	-1.000	-1			2071.4	2215.9		
96	-1.000	-1			2092.8	2262.4		
96	-1.000	-1			2088.6	2259.7		
96	-1.000	-1			2062.9	2249.7		
96	2.000	-1	33.023	0.72	2069.9	2266.8	2193.8	2402.5
96	5.000	-1	33.100	0.62	2072.3	2262.5	2191.3	2392.4
96	400.200	-1	33.712	1.41	2142.7	2296.9	2224.6	2384.7
96	400.180	-500	34.719	1.59	2262.7	2348.9	2281.0	2367.9
96	400.180	-1	33.711	1.69	2138.4	2289.7	2220.2	2377.3
96	400.160	-1	33.712	1.75	2140.9	2288.3	2222.7	2375.7

96	400.140	-1	33.709	1.64	2139.2	2282.4	2221.1	2369.8
96	400.120	-1	33.643	1.29	2139.1	2289.0	2225.4	2381.3
96	400.100	-1	33.649	1.21	2136.9	2286.2	2222.7	2378.0
96	400.080	-1	33.616	0.93	2131.3	2284.0	2219.0	2378.0
96	400.060	-1	33.567	0.86	2130.5	2276.3	2221.5	2373.5
96	400.040	-1	32.794	-0.75	2084.1	2241.3	2224.3	2392.1
96	300.040	-1	33.209	0.23	2110.9	2258.3	2224.7	2380.1
96	300.060	-1	33.548	1.02	2131.5	2295.9	2223.8	2395.3
96	300.060	-1		1.00	2135.4	2279.4		
96	300.060	-1		1.00	2136.1	2280.4		
96	300.080	-1	33.591	1.91	2135.3	2281.6	2224.9	2377.3
96	300.100	-1	33.551	2.94	2130.7	2283.7	2222.7	2382.3
96	300.120	-1	33.528	1.66	2128.6	2282.6	2222.1	2382.8
96	300.140	-1	33.590	1.75	2136.7	2283.5	2226.4	2379.4
96	300.160	-1	33.707	1.95	2134.8	2283.9	2216.7	2371.5
96	300.180	-500	34.714	1.66	2277.1	2344.9	2295.9	2364.2
96	300.180	-350	34.695	1.80	2213.8	2341.1	2233.3	2361.7
96	300.180	-200	34.522	1.24	2246.5	2325.2	2277.6	2357.4
96	300.180	-125	34.331	0.02	2229.4	2319.4	2272.8	2364.6
96	300.180	-75	33.997	-1.37	2201.4	2296.8	2266.3	2364.6
96	300.180	-53	33.823	-1.05	2174.8	2296.7	2250.5	2376.6
96	300.180	-44	33.759	-0.38	2161.3	2294.7	2240.8	2379.1
96	300.180	-27	33.664	1.27	2136.5	2305.8	2221.3	2397.3
96	300.180	-20	33.677	1.60	2131.4	2279.8	2215.1	2369.4
96	300.180	-9	33.675	2.01	2132.7	2274.6	2216.6	2364.1
96	300.180	-1	33.680	2.47	2130.0	2279.6	2213.5	2368.9
96	300.200	-1	33.756	3.03	2137.7	2278.8	2216.5	2362.8
96	300.200	-910		1.00	2249.7	2343.5		
96	200.200	-1	33.766	2.03	2138.9	2287.0	2217.1	2370.6
96	200.180	-1	33.758	1.76	2141.2	2278.6	2220.0	2362.4
96	200.160	-1	33.685	2.14		2277.4		2366.3
96	200.140	-1	33.549	1.62		2285.5		2384.3
96	200.120	-3	33.550	1.68	2123.9	2279.5	2215.7	2378.0
96	200.100	-1		1.00		2286.7		
96	200.080	-1	33.460	1.44		2284.6		2389.7
96	200.060	-1	33.438	1.38	2120.8	2272.8	2219.9	2379.0
96	200.040	-1	33.439	0.99	2115.8	2280.2	2214.6	2386.6
96	1001.100	-1			2020.2	2215.9		
96	1001.300	-200			2254.8	2340.0		
96	1001.300	-100			2213.8	2292.5		
96	1001.300	-75			2193.6	2304.8		
96	1001.300	-50			2191.2	2260.2		
96	1001.300	-20			2144.2	2286.0		
96	1001.300	-17			2138.7	2285.5		
96	1001.300	-10			2111.4	2215.4		
96	1001.300	-7			2097.0	2251.2		
96	1001.300	-3			2116.9	2254.0		
96	1001.400	-1			2019.5	2219.0		
96	1001.300	-1			1849.5	2220.2		
96	1001.500	-1			2012.7	2086.8		

96	1001.600	-1			1984.2	2198.5		
96	1001.700	-90			2159.6	2260.2		
96	1001.700	-30			2157.3	2258.6		
96	1002.200	-1			1995.0	2234.6		
96	1002.400	-60			1984.4	2239.0		
96	1002.400	-1			1974.7	2233.3		
96	1002.300	-1			1920.8			
96	1002.600	-1			1895.4	2198.8		
96	-1.000	-1			2092.8	2246.5		
96	400.015	-1			2082.4	2245.1		
96	420.015	-1			2078.8	2251.3		
96	2.000	-1	33.049	0.17	1974.1	2254.5	2090.6	2387.6
96	5.000	-1	33.100	0.62	1968.3	2248.2	2081.3	2377.3
97	2.000	-1	33.005	1.11	2103.3	2271.3	2230.4	2408.6
97	5.000	-1	33.472	1.49		2276.5		2380.5
97	8.000	-1	33.543	1.57	2114.1	2271.0	2205.9	2369.7
97	10.000	-1	33.448	1.47	2106.0	2277.1	2203.8	2382.8
97	500.060	-1	33.577	1.10	2128.4	2284.9	2218.6	2381.7
97	500.080	-1	33.586	0.81	2141.0	2287.9	2231.2	2384.2
97	500.100	-1	33.719	0.81	2140.4	2289.8	2221.7	2376.8
97	500.120	-1	33.728	0.98	2146.8	2288.2	2227.7	2374.5
97	500.140	-1	33.752	0.94	2148.7	2306.9	2228.1	2392.1
97	500.160	-1	33.724	1.14	2150.3	2296.3	2231.6	2383.2
97	500.180	-1	33.770	1.18	2149.0	2293.1	2227.3	2376.6
97	500.200	-500			2255.3	2349.2		
97	500.200	-300	34.677	1.83	2256.1	2349.7	2277.1	2371.5
97	500.200	-200			2255.9	2336.5		
97	500.200	-150	34.494	1.27	2249.3		2282.3	
97	500.200	-100	34.230	-0.41	2221.7	2324.8	2271.6	2377.1
97	500.200	-81	34.074	-1.19	2192.6	2301.5	2252.2	2364.0
97	500.200	-48			2154.1	2292.3		
97	500.200	-24			2148.2	2289.4		
97	500.200	-9	33.825	1.22	2148.1	2288.2	2222.7	2367.7
97	500.200	-5	33.827	1.25	2148.1	2283.0	2222.6	2362.2
97	500.200	-1			2149.5	2285.2		
97	500.200	-1			2149.9	2285.9		
97	500.200	-1500			2260.3	2365.3		
97	500.200	-1000			2256.9	2362.5		
97	500.200	-750			2234.4	2329.0		
97	500.200	-500			2255.6	2334.2		
97	600.040	-1300			2250.0	2344.8		
97	600.040	-1	33.626	1.17	2134.9	2288.2	2222.2	2381.7
97	600.040	-1	33.626	1.17	2135.4	2292.8	2222.6	2386.5
97	600.040	-1	33.162	1.24	2135.1	2285.0	2253.5	2411.6
97	600.060	-1	33.341	1.52	2112.0	2262.5	2217.1	2375.1
97	600.080	-1	33.486	1.22	2120.6	2275.0	2216.4	2377.8
97	600.100	-1	33.598	1.20	2134.4	2280.7	2223.5	2375.9
97	600.120	-1	33.580	1.21	2132.3	2280.2	2222.4	2376.6
97	600.140	-1	33.808	1.11	2149.0	2282.5	2224.7	2363.0
97	600.160	-1	33.817	1.07	2151.5	2287.7	2226.7	2367.7

97	600.180	-1	33.817	1.52	2152.1	2287.7	2227.4	2367.8
97	600.200	-1	33.783	1.76	2138.9	2274.1	2215.9	2356.0
97	2.000	-1	33.005	1.11	2080.0	2222.7	2205.8	2357.1
97	4.000	-1	33.387	1.53	2122.1	2267.8	2224.6	2377.3
97	10.000	-1	33.448	1.47	2108.5	2262.7	2206.3	2367.7
97	600.040	-1			2111.6	2255.9		
97	600.040	-1			2112.2	2260.5		
97	600.040	-1			2112.1			
97	550.010	-100	34.190	-0.04	2233.6	2316.4	2286.5	2371.2
97	550.010	-79	34.046	-0.37	2222.3		2284.6	
97	550.010	-60	33.828	-0.81	2191.0	2293.9	2266.9	2373.4
97	550.010	-41	33.543	-0.76	2168.2	2273.1	2262.4	2371.8
97	550.010	-24	33.353	-0.32	2140.0	2265.4	2245.6	2377.3
97	550.010	-12			2112.0	2261.1		
97	550.010	-7	32.890	0.71	2096.6	2252.7	2231.1	2397.2
97	550.010	-1	32.672	1.02	2052.9	2222.1	2199.2	2380.5
97	550.010	-1	32.672	1.02	2056.7	2236.8	2203.2	2396.2
97	400.040	-1	33.563	1.22	2134.3	2278.2	2225.7	2375.7
97	400.060	-1	33.495	1.16	2131.2	2275.1	2227.0	2377.3
97	400.080	-1	33.717	1.38	2146.9	2286.8	2228.6	2373.8
97	400.100	-1	33.734	1.53	2149.4	2289.8	2230.1	2375.7
97	400.120	-1	33.697	1.50	2145.7	2293.6	2228.7	2382.2
97	400.140	-1	33.733	1.35	2148.5	2285.5	2229.2	2371.4
97	400.160	-1	33.755	1.49	2145.0	2284.5	2224.1	2368.7
97	400.180	-1	33.779	1.57	2147.7	2279.2	2225.3	2361.6
97	400.200	-1	33.721	2.10	2136.7	2280.0	2217.8	2366.5
97	300.200	-1	33.783	2.02	2147.0	2283.2	2224.4	2365.4
97	300.200	-1	33.783	2.02	2147.2	2291.7	2224.6	2374.3
97	300.200	-1			2145.5	2285.6		
97	300.180	-1	33.767	1.96	2145.7	2281.9	2224.1	2365.2
97	300.160	-1	33.777	1.99	2144.5	2281.5	2222.2	2364.1
97	300.140	-1	33.751	1.83				
97	300.120	-1	33.699	1.60	2139.0	2289.4	2221.6	2377.8
97	300.100	-1	33.672	1.48	2140.0	2278.4	2224.4	2368.2
97	300.080	-1	33.411	1.25	2123.9	2268.3	2224.9	2376.2
97	300.060	-1	33.558	1.35	2138.1	2271.1	2230.0	2368.7
97	300.040	-1	33.267	1.11	2113.4	2253.1	2223.5	2370.5
97	200.200	-1	33.781	2.11	2143.0	2278.9	2220.3	2361.2
97	200.180	-1	33.746	2.24	2139.3	2280.4	2218.8	2365.1
97	200.160	-1	33.739	1.86	2144.0	2286.7	2224.1	2372.1
97	200.140	-1	33.553	1.30	2140.8	2284.1	2233.2	2382.6
97	200.120	-1	33.628	1.26	2140.6	2281.1	2227.9	2374.2
97	200.100	-1	33.649	1.43	2141.7	2284.2	2227.7	2376.0
97	200.080	-1	33.429	1.21	2126.8	2270.9	2226.8	2377.6
97	200.060	-1	33.236	1.06	2117.0	2265.1	2229.3	2385.3
97	200.040	-1	33.271	0.96	2115.4	2262.9	2225.4	2380.5
97	200.020	-1	33.409	1.02	2111.4	2426.2	2212.0	2541.8
97	200.000	-1	33.443	1.17	2119.1	2275.8	2217.8	2381.7
97	-200.020	-1	33.450	1.09	2118.4	2270.1	2216.6	2375.2
97	-200.040	-1	32.786	1.35	1988.3	2239.9	2122.6	2391.2

97	-200.040	-1	32.745	1.29	1988.8	2241.7	2125.7	2396.1
97	-200.060	-1	32.257	0.49	1869.4	2212.2	2028.4	2400.3
97	-200.060	-1	32.070	0.60	1870.6	2214.0	2041.5	2416.3
97	380.010	-1	32.011	-0.46	1984.7		2170.0	
97	380.010	-1	32.011	-0.46	1984.1		2169.3	
97	2.000	-1	33.450	1.12	2078.5		2174.9	
97	5.000	-1	33.472	1.49	2100.5		2196.4	
97	600.040	-500	34.656	1.32	2253.8		2276.2	
97	600.040	-300	34.602	1.12	2250.4		2276.3	
97	600.040	-100	34.173	-0.16	2214.1		2267.7	
97	600.040	-50	33.811	-0.41	2185.6		2262.5	
97	600.040	-22	33.631	1.17	2117.4		2203.6	
97	600.040	-6	33.404	1.18	2115.9	2299.3	2217.0	2409.2
97	600.040	-1			2119.1	2286.3		
98	600.040	-1	32.511	1.46	2080.0	2238.0	2239.3	2409.3
98	600.060	-1			2084.1			
98	600.100	-1	33.574	1.67	2130.2	2295.9	2220.7	2393.4
98	600.120	-1	33.649	1.79	2143.0	2286.6	2229.1	2378.4
98	600.140	-1	33.728	1.68	2142.9	2285.4	2223.7	2371.7
98	600.160	-1	33.756		2146.3	2280.2	2225.5	2364.3
98	600.180	-1	33.759	2.14	2141.6	2293.5	2220.3	2377.8
98	600.200	-1	33.764	2.32	2145.5	2283.7	2224.0	2367.3
98	500.180	-1	33.741	1.52	2139.8	2303.0	2219.7	2388.9
98	500.160	-1	33.727	1.43	2132.4		2212.8	
98	500.140	-1	33.743	1.47	2145.0	2287.3	2224.9	2372.5
98	500.120	-1	33.657	1.39	2139.2	2281.2	2224.5	2372.2
98	500.100	-1	33.575	1.45	2132.9	2276.4	2223.4	2373.0
98	500.080	-1	33.516	1.69	2127.4	2284.8	2221.6	2386.0
98	500.060	-1	33.391	1.85	2111.2	2286.3	2212.9	2396.4
98	400.060	-1	33.179	1.20	2104.3	2258.5	2219.8	2382.4
98	400.100	-1	33.378	1.50	2114.0	2271.9	2216.8	2382.4
98	400.140	-1	33.647	1.39	2136.5	2307.3	2222.5	2400.1
98	400.180	-1	33.734	2.25	2147.7	2285.9	2228.3	2371.7
98	300.180	-1	33.758	1.97	2151.3	2295.4	2230.5	2379.9
98	300.140	-1	33.707	1.86	2143.2	2306.7	2225.4	2395.2
98	300.100	-1	33.701	1.64	2159.8	2303.4	2243.1	2392.2
98	300.060	-1	33.187	1.30	2107.6		2222.7	
98	200.200	-1	33.705	2.39	2141.0	2275.1	2223.3	2362.5
98	200.180	-500	34.679	1.96	2254.5	2342.2	2275.4	2363.9
98	200.180	-500	34.679	1.96	2248.5	2359.0	2269.3	
98	200.180	-350	34.632	2.09	2252.9	2336.3	2276.8	2361.1
98	200.180	-225	34.513	1.70	2250.9	2347.6	2282.7	2380.7
98	200.180	-150	34.276	0.46	2221.5	2330.0	2268.4	2379.2
98	200.180	-105	34.108	-0.59	2203.3	2323.1	2260.9	2383.8
98	200.180	-85	34.003	-1.13	2186.3	2293.1	2250.4	2360.4
98	200.180	-65	33.937	-1.34	2177.0	2294.7	2245.1	2366.5
98	200.180	-54	33.892	-1.20	2174.4	2313.9	2245.5	2389.6
98	200.180	-25	33.725	2.33	2139.3	2281.8	2220.2	2368.0
98	200.180	-12	33.724	2.39	2138.5	2282.0	2219.4	2368.3
98	200.180	-1	33.723	2.39	2143.2	2295.8	2224.3	2382.7

98	200.180	-1	33.722	2.39	2141.3	2284.9	2222.4	2371.5
98	200.160	-1	33.781	2.11	2151.7	2284.8	2229.3	2367.3
98	200.140	-1	33.677	1.43	2138.5	2277.8	2222.5	2367.3
98	200.120	-410	34.706	1.32	2265.6	2353.8	2284.8	2373.7
98	200.120	-410	34.706	1.32	2264.8	2358.3	2284.0	2378.3
98	200.120	-250	34.608	1.10	2257.0	2339.3	2282.6	2365.8
98	200.120	-176	34.424	0.38	2247.0	2332.7	2284.7	2371.7
98	200.120	-125	34.154	-0.85	2221.7	2318.6	2276.7	2376.0
98	200.120	-90	33.994	-1.25	2203.3	2297.2	2268.4	2365.1
98	200.120	-77			2188.2	2295.4		
98	200.120	-41	33.733	0.75	2156.8	2300.9	2237.8	2387.3
98	200.120	-31	33.693	1.19	2143.3	2288.5	2226.4	2377.3
98	200.120	-17	33.673	1.33	2141.6	2285.8	2226.0	2375.8
98	200.120	-10	33.677	1.37	2141.3		2225.4	
98	200.120	-1	33.678	1.36	2140.6		2224.7	
98	200.120	-1	33.677	1.37	2142.0	2292.7	2226.2	2382.8
98	200.100	-1	33.677	1.30	2144.8	2291.3	2229.0	2381.3
98	200.808	-1			2141.3	2282.0		
98	200.060	-1	33.476	1.16	2126.7	2274.0	2223.5	2377.5
98	200.040	-500	34.700	1.35	2262.2	2357.0	2281.7	2377.4
98	200.040	-500	34.700	1.35	2262.2	2349.8	2281.7	2370.1
98	200.040	-350	34.660	1.31	2261.3	2365.8	2283.5	2389.1
98	200.040	-200	34.344	-0.01	2239.4	2318.9	2282.2	2363.2
98	200.040	-185			2205.0	2308.9		
98	200.040	-88	33.849	-1.13	2188.0	2288.4	2262.4	2366.2
98	200.040	-64	33.652	-0.03	2155.9	2289.3	2242.3	2381.0
98	200.040	-38	33.553	0.67	2138.4	2279.1	2230.6	2377.4
98	200.040	-27	33.473	0.95	2128.9	2270.7	2226.0	2374.3
98	200.040	-15	33.441	1.11	2126.5	2268.0	2225.7	2373.7
98	200.040	-8	33.438	1.13	2121.8	2274.7	2220.9	2380.9
98	200.040	-1	33.434	1.14	2126.1	2281.6	2225.7	2388.4
98	200.040	-1			2126.0	2267.0		
98	200.020	-1	33.439	0.95	2125.3	2267.1	2224.5	2372.9
98	200.000	-1	33.511	0.93	2130.2	2273.3	2224.9	2374.3
98	-200.020	-1	33.424	0.81	2121.9	2270.4	2222.0	2377.4
98	-200.040	-410			2264.9	2347.3		
98	-200.040	-410	34.698	1.35	2264.7	2351.9	2284.4	2372.4
98	-200.040	-250	34.662	1.29	2263.7	2357.8	2285.7	2380.7
98	-200.040	-150	34.310	0.02	2245.6	2319.4	2290.8	2366.0
98	-200.040	-75	33.867	-1.24	2206.0	2292.9	2279.8	2369.6
98	-200.040	-50	33.658	-1.09	2178.3	2302.1	2265.2	2393.9
98	-200.040	-27	33.478	0.59	2129.9	2283.7	2226.7	2387.5
98	-200.040	-18	33.422	0.83	2117.1	2315.1	2217.1	2424.4
98	-200.040	-12	33.403	0.97	2106.0	2307.1	2206.7	2417.4
98	-200.040	-9	33.348	1.21	2113.4	2276.7	2218.0	2389.4
98	-200.040	-1	33.170	1.48	2038.6	2270.4	2151.1	2395.7
98	-200.040	-1	33.170	1.48	2059.6	2221.5	2173.2	2344.0
98	-200.060	-225	34.583	0.99	2261.2	2336.3	2288.5	2364.5
98	-200.060	-150	34.310	0.17	2236.2	2340.5	2281.2	2387.6
98	-200.060	-76	33.841	-1.07	2190.7	2304.4	2265.7	2383.4

98	-200.060	-25	33.374	0.06	2128.7	2266.9	2232.4	2377.3
98	-200.060	-18	33.182	1.16	2070.6	2271.9	2184.0	2396.4
98	-200.060	-14	32.993	1.30	2028.7	2256.4	2152.2	2393.6
98	-200.060	-10	32.872	1.41	2002.3	2262.1	2131.9	2408.5
98	-200.060	-8	32.854	1.41	1987.2	2271.9	2117.0	2420.3
98	-200.060	-5	32.874	1.43	1978.7	2274.0	2106.7	2421.1
98	-200.060	-1	32.751	1.37	1947.3	2253.2	2081.0	2408.0
98	-200.060	-1	32.730	1.33	1947.7	2248.5	2082.8	2404.4
98	380.010	-1	32.577	1.47	2047.5	2219.4	2199.8	2384.4
98	420.015	-1	32.711	2.27	2036.5	2251.9	2179.0	2409.4
98	500.000	-1	31.728	1.68	2008.0	2165.1	2215.0	2388.4
98	550.005	-1	31.785	1.94	2036.1	2202.4	2242.0	2425.2
98	595.015	-1			2110.7	2254.2		
98	600.040	-1	32.472	1.48	2058.3	2222.2	2218.5	2395.2
98	5.000	-1	32.937	1.72	2093.6	2242.0	2224.7	2382.5
99	5.000	-1	33.580	0.62	2120.4	2282.6	2210.1	2379.1
99	510.000	-1	32.850	-0.11	2111.5	2221.9	2249.7	2367.4
99	530.005	-1	33.300	0.14	2108.5	2267.7	2216.2	2383.5
99	500.006	-1	33.790	0.42	2148.2	2308.1	2225.1	2390.7
99	500.080	-1	33.790	0.40	2149.4	2284.6	2226.4	2366.5
99	500.100	-1	33.860	0.44	2155.7	2296.6	2228.3	2374.0
99	500.120	-1	33.880	0.61	2154.9	2303.7	2226.2	2379.8
99	500.140	-1	33.870	0.71	2149.9	2299.4	2221.6	2376.1
99	500.160	-1	33.870	0.77	2153.1	2294.7	2224.9	2371.2
99	500.180	-1	33.860	0.83	2152.8	2305.4	2225.3	2383.0
99	500.200	-1	33.870	1.04	2156.0	2296.5	2227.9	2373.1
99	500.220	-1	33.830	1.26	2146.7	2291.4	2221.0	2370.7
99	500.220	-1	34.710	1.16	2261.2	2358.3	2280.0	2378.0
99	500.220	-1	34.700	1.80	2258.7	2353.0	2278.2	2373.3
99	500.220	-1	34.650	1.84	2257.4	2340.4	2280.2	2364.0
99	500.220	-1	34.070	-0.74	2198.4	2301.5	2258.4	2364.3
99	500.240	-1	34.720	1.49	2263.2	2373.3	2281.5	2392.4
99	500.240	-1	34.610	2.05	2259.3	2341.6	2284.7	2368.0
99	500.240	-1	34.100	-0.82	2203.5	2299.6	2261.7	2360.3
99	500.240	-1	33.830	1.09	2147.0	2286.9	2221.3	2366.0
99	300.180	-85	34.020	-1.34	2189.0	2304.8	2252.1	2371.2
99	300.180	-1	33.840	0.80	2255.2	2339.6	2332.5	2419.8
99	300.180	-1500	34.720	0.95	2259.3	2352.6	2277.5	2371.5
99	300.180	-400	34.680	1.74	2254.7	2342.9	2275.5	2364.5
99	300.180	-250	34.650	1.86	2260.1	2349.9	2282.9	2373.7
99	300.160	-1	33.830	0.70	2146.8	2309.9	2221.0	2389.8
99	300.140	-1	33.790	0.54	2147.8	2286.9	2224.8	2368.8
99	300.120	-1	33.850	0.82	2151.7	2301.9	2224.8	2380.1
99	300.100	-1	33.800	0.70	2144.2	2287.7	2220.3	2368.9
99	300.080	-1	33.790	0.72	2172.7	2284.8	2250.5	2366.6
99	300.060	-1	33.800	0.60	2145.2	2294.6	2221.4	2376.1
99	300.040	-1	33.430	0.09	2128.6	2270.9	2228.6	2377.6
99	600.040	-1	33.670	0.86	2139.8	2306.6	2224.3	2397.7
99	600.060	-1	33.600	0.87	2137.7	2282.3	2226.8	2377.4
99	600.080	-1	33.650	0.78	2144.0	2291.7	2230.0	2383.7

99	600.100	-1	33.690	0.87	2143.9	2297.5	2227.3	2386.9
99	600.120	-1	33.700	0.97	2138.0	2291.5	2220.4	2379.9
99	600.140	-1	33.790	1.14	2143.8	2293.1	2220.6	2375.2
99	600.160	-1	33.800	2.20	2146.9	2290.6	2223.2	2371.9
99	600.220	-2000	34.690	0.69	2264.4	2361.0	2284.6	2382.1
99	600.220	-500	34.690	1.92	2258.9	2345.2	2279.1	2366.2
99	600.220	-90	34.110	-0.59	2204.0	2308.5	2261.5	2368.7
99	600.220	-1	33.830	1.35	2146.9	2298.1	2221.2	2377.6
99	600.200	-1500	34.700	0.90	2257.9	2364.0	2277.4	2384.4
99	600.200	-500	34.690	1.73	2258.1	2350.0	2278.2	2371.0
99	600.200	-100	34.080	-0.76	2225.0	2305.6	2285.1	2367.9
99	600.180	-900	34.710	1.20	2259.2	2358.4	2278.1	2378.1
99	600.180	-500	34.710	1.59	2258.6	2372.7	2277.4	2392.5
99	600.180	-100	34.210	1.10	2249.8	2345.4	2301.7	2399.5
99	600.180	-5	33.850	1.36	2151.7	2294.2	2224.8	2372.2
99	595.014	-1	32.880	-0.26	2117.2	2242.6	2253.7	2387.2
99	5.000	-1	33.580	0.67	2142.7		2233.4	
99	400.200	-1500	34.700	0.84	2261.2	2366.7	2280.8	2387.1
99	400.200	-500	34.710	1.70	2259.2	2350.0	2278.1	2369.6
99	400.200	-325	34.690	1.84	2258.6	2345.3	2278.8	2366.2
99	400.200	-100	34.060	-1.41	2203.4	2307.3	2264.3	2371.0
99	400.200	-5	33.800	0.98	2169.2	2297.4	2246.2	2379.0
99	400.180	-1	33.820	1.06	2165.0	2283.3	2240.5	2363.0
99	400.160	-1	33.850	1.04	2155.2	2312.3	2228.4	2390.9
99	400.140	-1	33.850	1.09	2154.8	2294.4	2228.0	2372.4
99	400.120	-1	33.840	1.02	2157.7	2301.9	2231.7	2380.8
99	400.100	-1	33.820	1.03	2155.1	2287.0	2230.3	2366.8
99	400.080	-1	33.830	0.93	2153.6	2292.4	2228.0	2371.7
99	400.060	-1	33.790	0.92	2155.9	2282.6	2233.1	2364.4
99	400.040	-1	33.460	0.74	2126.7	2271.0	2224.5	2375.6
99	200.040	-500	34.690	1.31	2265.0	2342.9	2285.2	2363.9
99	200.040	-400	34.680	1.33	2264.2	2347.7	2285.1	2369.3
99	200.040	-300	34.650	1.27	2267.0	2357.3	2289.9	2381.1
99	200.040	-200	34.580	1.06	2260.5	2337.9	2287.9	2366.3
99	200.040	-150	34.460	0.40	2249.8	2331.1	2285.1	2367.6
99	200.040	-95	34.090	-1.11	2210.0	2305.8	2269.0	2367.3
99	200.040	-45	33.840	-0.12	2165.4	2296.6	2239.6	2375.3
99	200.040	-23	33.670	0.52	2135.4	2287.8	2219.8	2378.2
99	200.040	-17	33.670	0.53	2136.5	2290.1	2220.9	2380.6
99	200.040	-8	33.670	0.66	2133.3	2297.4	2217.6	2388.1
99	200.040	-3	33.660	0.75	2130.9	2278.9	2215.7	2369.7
99	200.040	-1	33.660	0.79	2129.1	2284.3	2213.8	2375.2
99	200.020	-1	33.650	0.91	2128.8	2280.5	2214.2	2372.0
99	200.000	-1	33.690	1.09	2131.7	2283.7	2214.6	2372.5
99	-200.020	-152	34.400	0.25	2248.5	2334.4	2287.7	2375.1
99	-200.020	-100	34.030	-1.12	2215.9	2310.0	2279.1	2375.8
99	-200.020	-80	33.960	-9.75	2186.0	2295.1	2252.9	2365.4
99	-200.020	-40	33.740	0.49	2142.6	2289.9	2222.6	2375.4
99	-200.020	-22	33.660	0.63	2134.1	2277.6	2219.1	2368.3
99	-200.020	-1	33.610	0.79	2126.2	2273.1	2214.2	2367.1

99	200.080	-1	33.660	1.01	2140.6	2262.9	2225.8	2353.0
99	200.100	-1	33.650	1.16	2140.4	2278.3	2226.2	2369.7
99	200.120	-400	34.700	1.29	2269.0	2349.4	2288.6	2369.7
99	200.120	-300	34.670	1.35	2262.8	2344.3	2284.3	2366.6
99	200.120	-200	34.610	1.17	2260.8	2338.0	2286.3	2364.3
99	200.120	-75	34.080	-1.21	2205.9	2301.8	2265.4	2363.9
99	200.120	-58	33.970	-1.11	2179.2	2300.8	2245.3	2370.5
99	200.120	-1	33.710	1.12	2138.8	2282.2	2220.7	2369.5
99	200.140	-1	33.610	1.03	2133.7	2274.1	2221.9	2368.1
99	200.160	-1	33.790	1.38	2148.2	2278.7	2225.1	2360.3
99	200.180	-1500	34.710	1.21	2261.2	2348.3	2280.1	2367.9
99	200.180	-900	34.720	1.68	2255.2	2357.6	2273.4	2376.6
99	200.180	-80	33.940	-1.32	2175.1	2287.6	2243.0	2359.1
99	200.180	-1	33.730	1.17	2143.1	2275.3	2223.8	2361.0
99	200.200	-1	33.750	1.34	2142.5	2281.1	2221.9	2365.6
99	200.200	-3500	34.690	0.41	2264.4	2360.7	2284.6	2381.8
99	200.200	-3300	34.690	0.43	2261.8	2355.9	2282.0	2377.0
99	200.200	-3000	34.690	0.49	2262.0	2361.3	2282.2	2382.4
99	200.200	-2700	34.690	0.59	2261.3	2354.5	2281.5	2375.6
99	200.200	-2500	34.690	0.68	2261.1	2356.6	2281.4	2377.6
99	200.200	-2000	34.700	0.93	2260.2	2354.9	2279.7	2375.2
99	200.200	-1500	34.710	1.23	2258.3	2351.5	2277.2	2371.2
99	200.200	-100	34.720	1.61	2254.6	2344.5	2272.8	2363.4
99	200.200	-500	34.670	2.02	2255.7	2335.1	2277.2	2357.3
99	200.200	-200	34.450	1.54	2143.7	2281.1	2177.9	2317.5
99	200.200	-100	33.980	-1.32	2184.1	2287.1	2249.6	2355.7
99	200.200	-5	33.740	1.25	2141.2	2275.3	2221.2	2360.2
99	300.120	-1	33.600	1.35	2138.6	2274.3	2227.7	2369.1
99	300.100	-1	33.650	1.12	2141.6	2275.8	2227.5	2367.1
99	300.080	-1	33.720	1.34	2139.7	2283.1	2220.9	2369.7
99	300.060	-1	33.760	1.30	2142.2	2288.7	2220.8	2372.8
99	300.040	-1	33.530	0.82	2130.4	2268.3	2223.8	2367.7
99	300.040	-1	33.580	1.09	2133.3	2275.1	2223.5	2371.3
99	400.000	-1	33.260	0.74	2116.6	2253.2	2227.3	2371.0
99	500.100	-1	33.820	1.36	2149.2	2287.1	2224.2	2366.9
99	500.160	-1	33.840	1.22	2151.5	2283.3	2225.3	2361.6
99	600.200	-1	33.820	1.71	2149.6	2280.1	2224.7	2359.6
99	600.180	-1	33.820	1.57	2149.2	2283.4	2224.2	2363.1
99	600.160	-1	33.780	1.46	2146.5	2285.0	2224.1	2367.5
99	600.140	-1	33.750	1.41	2143.2	2285.0	2222.5	2369.6
99	600.120	-1	33.700	1.37	2140.9	2279.0	2223.5	2366.9
99	600.100	-1	33.610	1.43	2134.3	2276.6	2222.5	2370.8
99	600.080	-1	33.720	1.47	2144.2	2282.7	2225.6	2369.4
99	5.000	-1	33.620	1.26	2138.0	2277.3	2225.7	2370.8
99	600.060	-1	33.610	1.17	2140.2	2272.7	2228.7	2366.7
99	600.040	-1	33.520	0.79	2141.7	2272.1	2236.3	2372.5

Appendix B MATLAB model

```
% Ed Laws created this MATLAB model April 20, 2002. It was used to
%investigate the interactions of the carbon system parameters with
%temperature, air-to-sea exchange and export production.

clf;
% temperature of seawater by month beginning in January
t=[24 23.5 23.5 23.6 24.1 25.1 25.5 26 26.5 26.2 25.3 24.7 24];
T=[22 24 26 28];

% Export production at ALOHA in micromoles per liter per month
%export=[1.17 1.34 1.61 1.45 1.6 1.58 1.56 1.38 1.31 1.21 0.91 0.93];
%export=zeros(size(export));

% export production forced to match change in DIC during summer
export=[0 0 0 0 4 5 3 1 1 1 0 0];

% Henry's law constant converts atmospheric ppm to micro-moles per liter
KH=[313 297 281 265]/10000;
TT=[20 25 30];

% first and second equilibrium constants for CO2 system
pK1=[6.02 6 5.98];
pK2=[9.17 9.1 9.02];

% Boric acid dissociation constant
pKB=[8.75 8.71 8.67];

% boric acid concentration in micromoles per liter
BA=400;

% piston is the change in CO2 concentration (micro-moles per liter per month)
caused by a 1.0 ppm %difference  in fCO2 between atmosphere and ocean
piston=0.1;

% assume system is initially at equilibrium in January
% with TA concentration of 2305 micromoles per liter
tem=t(1);
kh=interp1(T,KH,tem);
pk1=interp1(TT,pK1,tem);
pk2=interp1(TT,pK2,tem);
pkb=interp1(TT,pKB,tem);
k1=10^(-pk1);
k2=10^(-pk2);
kb=10^(-pkb);
```

```
% calculate pH
micro=10^(-6);
b=BA*micro;
ta=2305*micro;
kw=10^(-14);
co2=338.5*kh*micro;
for k=1:1000;
   ph=8+k/2000;
   h=10^(-ph);
   f(k)=co2*k1*(1+2*k2/h)/h-ta+kb*b/(kb+h)+kw/h-h;
end;
[y,j]=min(abs(f));
pH=8+j/2000;
ah=10^(-pH);

% calculate carbonate alkalinity in microequivalents per liter
ca=(2305-BA*kb/(kb+ah))+(ah-kw/ah)/micro;
dic=ca*(1+k2/ah+ah/k1)/(1+2*k2/ah);

% This is CO2 concentration in micro-moles per liter
co2=340*kh;

yearend=20;
gasflux=0;efflux=0;
for years=1:yearend;
        for k=1:12;

        % calculate atmospheric pCO2
        pco2=340+3*cos((k-5)*2*pi/12);

        % Calculate influx or efflux of CO2
        tem=t(k);
        kh=interp1(T,KH,tem);

        % convert present CO2 concentration to equivalent ppm
        ppmco2=co2/kh;
        if years==yearend;
        subplot(2,2,1);
        plot((years-1)*12/(yearend-1)-12+k,ppmco2,'*k');
        set(gca,'xlim',[0 13]);
        hold on;
        ylabel('fCO_2 (ppm)');
        subplot(2,2,2);
        plot((years-1)*12/(yearend-1)-12+k,co2,'vk');
```

```
set(gca,'xlim',[0 13]);
hold on;
ylabel('CO_2 (\muM)');
subplot(2,2,3);
plot((years-1)*12/(yearend-1)-12+k,dic,'^k');
ylabel('DIC (\muM)');
xlabel('Month');
set(gca,'xlim',[0 13]);
hold on;
subplot(2,2,4);
plot((years-1)*12/(yearend-1)-12+k,pH,'+k');
ylabel('pH');
xlabel('Month');
set(gca,'xlim',[0 13]);
hold on;
end;

dic=dic+piston*(pco2-ppmco2)-export(k);

if years==yearend;
        gasflux=gasflux+piston*(pco2-ppmco2);
        efflux=efflux+export(k);
        disp([piston*(pco2-ppmco2) export(k)]);
end;
tem=t(k+1);
pk1=interp1(TT,pK1,tem);
pk2=interp1(TT,pK2,tem);
pkb=interp1(TT,pKB,tem);
k1=10^(-pk1);
k2=10^(-pk2);
kb=10^(-pkb);


% calculate pH
for k=1:1000;
         ph=8+k/2000;
        ah=10^(-ph);
           f(k)=dic-(1+k2/ah+ah/k1)/(1+2*k2/ah)*((2305-BA*kb/(kb+ah))+(ah-
        kw/ah)/micro);
end;
[y,j]=min(abs(f));
pH=8+j/2000;
ah=10^(-pH);
F=(1+k2/ah+ah/k1)/(1+2*k2/ah);
ca=dic/F;
```

```
        co2=ca*ah/(k1*(1+2*k2/ah));
        end;
end;

hold off;
disp([gasflux efflux]);
%print -deps chris02;
```

A model was developed to study the interaction between the CO_2 system, temperatures, air-to-sea exchange of CO_2 and export production at Station ALOHA over seasonal to annual timescales. The model was initiated using a constant TA of 2305 ueq $kg^{-1}$and a pCO_2 of 340 ppm, and allowed to run until a cyclic steady state was obtained. The apparent equilibrium constants (pK_1 and pK_2) for carbonic acid in seawater of Riley and Chester (Marine Chemistry) were used to calculate the measured carbon system parameters. pH was estimated on the NBS scale. The model was iterated every month for 20 years with a constant piston velocity coefficient of 0.1 μmol $liter^{-1}$ $month^{-1}$.

Changes to the carbon system were determined by altering DIC concentrations based on temperature, air-to-sea flux and export production. The air-to-sea flux was determined by multiplying the piston velocity coefficient (0.1 μmol $liter^{-1}$ $month^{-1}$) by the difference between atmospheric concentration (340 ppm) and calculated pCO_2. The changes of CO_2 based on temperature were determined through the temperature effects on the apparent equilibrium constants. Finally, export production was estimated from the sediment traps at 150 meters or that the drawdown of DIC concentrations between May and October was equated to export production during that time.

Although the model can be altered to investigate many types of scenarios, only two will be discussed for illustrative purposes. The model was initially run with export production set to 0 so changes in the carbon system parameters are a function of temperature and air-to-sea exchange (Fig B.1). The fugacity of CO_2 increased from February to September, and decreased from September to February with values ranging from 315 to 368 ppm. DIC concentrations increased from December to June, and decreased from June to November with concentrations ranging from 1967 to 1977 μM.

The model was run again with export production forced to match changes in DIC concentrations during the summer. This situation would simulate the effect of biological production on the CO2 system. The fugacity of CO2 increased from February to September, and decreased from September to February with a range of values between 308 and 349 ppm. DIC concentrations increased from November to May, and decreased from May to November with values ranging from 1957 to 1973 μM.

The initial run of the model illustrates the effect of temperature and air-to-sea exchange on the seasonal cycle of DIC and fCO_2. Although fCO2 values oscillate around atmospheric concentrations, they are generally higher then those observed at Station ALOHA (Fig 2.4 Chapter 2 and Fig B.1). Additionally, DIC concentrations oscillate, but are higher then observed values. Once export production is added (forced to the observed DIC removals between spring and summer) model estimates match observed estimates of DIC and fCO_2 (Fig 2.4 Chapter 2 and Fig B.2). This model illustrates that the removal of inorganic carbon by phytoplankton is a plausible explanation for the mean annual fCO_2 undersaturation with respect to the atmosphere.

An important feature concerning the output of this model is that the drawdown of DIC may be equal to export production during the six-month stratification period (Lee 2001, Karl et al. 2001). The results are consistent with the assumptions made by others that the drawdown of DIC is biologically mediated, yet they do not prove the assumptions are correct. If they are right, the result is a bit fortuitous because there are other mechanisms that can produce similar results without requiring that export production equal the drawdown of DIC. The observation that the seasonal, cyclic cycles of fCO_2 and DIC are out of phase is counter-intuitive if the drawdown in DIC is due to

biological uptake. The shift in fCO_2 and DIC can be explained by the annual cycle of seawater temperature annual undersaturation of fCO_2 (which may be attributed to export production) and the sluggishness of the air-sea exchange.

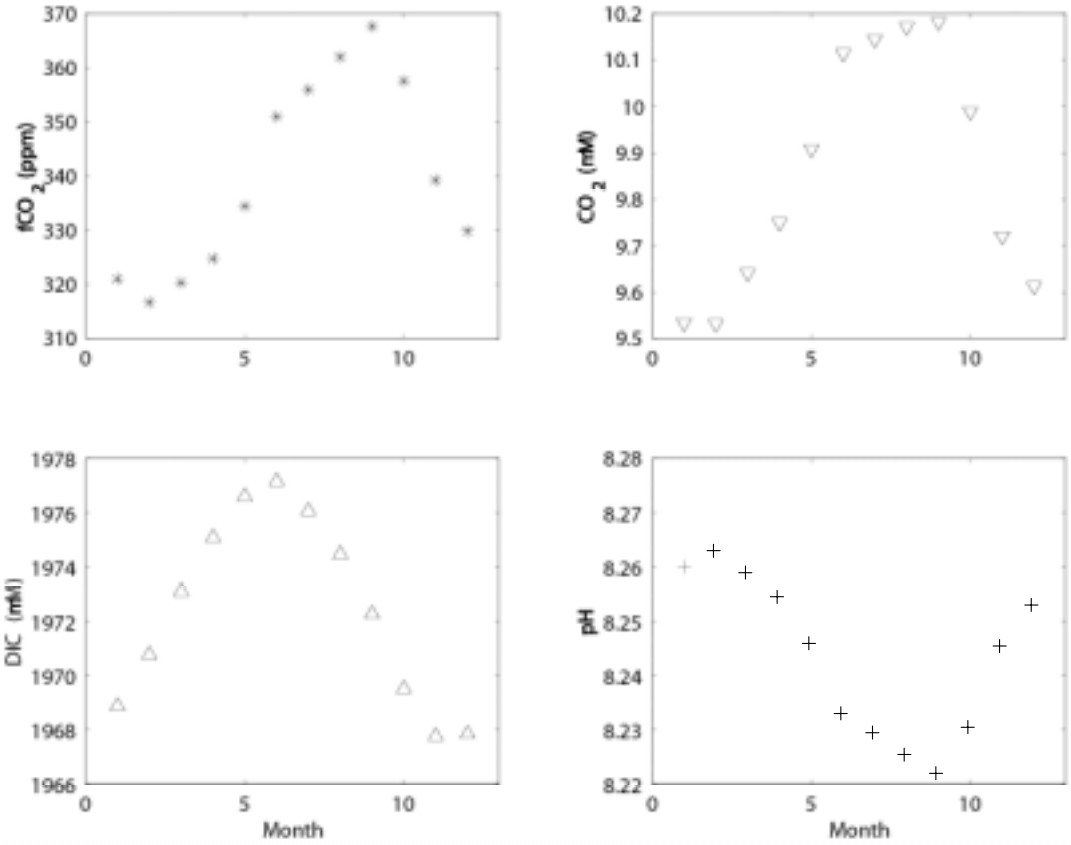

Figure B.1 Model output of A) fCO_2 (ppm) B) CO_2 (µM) C) DIC (µM) and D) pH. These values were estimated using the relationship on line 104 of dic=dic+piston*(340-ppmco2), which calculates DIC based on temperature and the air-to-sea flux.

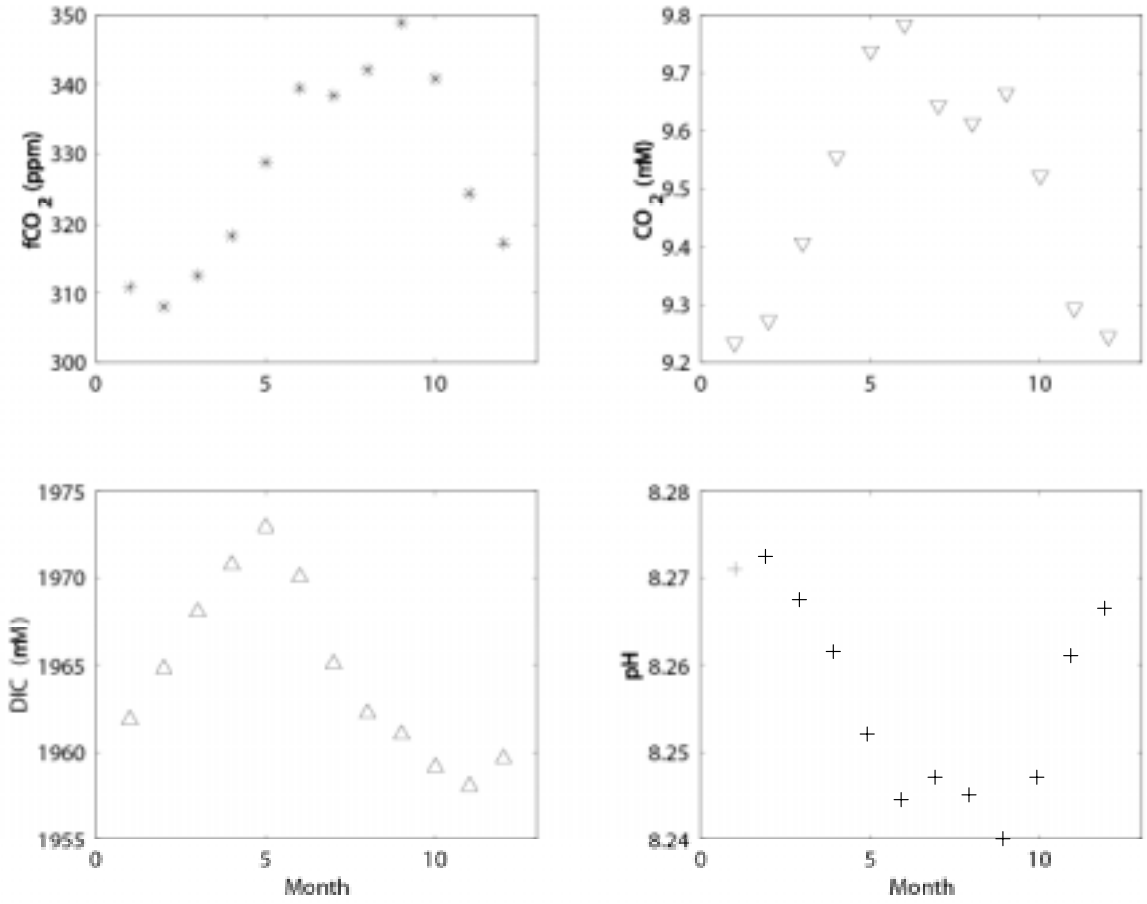

Figure B.2 Model output of A) fCO_2 (ppm) B) CO_2 (μM) C) DIC (μM) and D) pH. These values were estimated using the relationship on line 104 of dic=dic+piston*(340-ppmco2)-export(k), which calculates DIC based on temperature, the air-to-sea flux and export production. The export production was forced to match the observed DIC decrease during summer.